# Dynamics of electrons in 2D materials

Sami Siraj-Dine

# Dynamics of electrons in 2D materials

Sami SIRAJ-DINE[1,2,3]
Directors: Eric CANCES[1,2], Clotilde FERMANIAN-KAMMERER[3],
Supervisor: Antoine LEVITT[2].

[1] CERMICS, École des Ponts ParisTech,
[2] MATHERIALS, Inria Paris,
[3] LAMA, Université Paris-Est.

December 17, 2020

# Contents

# Chapter 1

# Introduction

## 1.1 General framework and notation

### 1.1.1 Quantum mechanics of electrons

In this section, we give an introduction to the quantum behavior of electrons. Let us first define some mathematical notation. We consider the general case of a $d$ dimensional space $\mathbb{R}^d$, where $d = 1, 2$ or 3.

Let $L^2(\mathbb{R}^d; \mathbb{C})$ be the vector space of (equivalence classes according to the Lebesgue-almost-everywhere equality relation of) Lebesgue measurable functions from $\mathbb{R}^d$ to $\mathbb{C}$ that are square integrable, *i.e.* $f \in L^2(\mathbb{R}^d; \mathbb{C})$ if $\int_{\mathbb{R}^d} |f|^2 < \infty$.

The Sobolev spaces $H^k(\mathbb{R}^d; \mathbb{C})$, for integer $k$, are defined as the vector spaces of $L^2(\mathbb{R}^d; \mathbb{C})$ functions with weak derivatives up to order $k$ are also in $L^2(\mathbb{R}^d; \mathbb{C})$.

For a self-adjoint operator $T$ on a Hilbert space $\mathcal{H}$ with domain $\mathcal{D}$, we recall that its spectrum $\sigma(T)$ is the set of scalars $\lambda \in \mathbb{C}$ such that $(H - \lambda I)$ does not admit a bounded inverse, where $I$ denotes the identity operator on $\mathcal{H}$. Moreover, the scalar $\lambda$ is called an eigenvalue if $H - \lambda I$ is not injective. The spectrum $\sigma(T)$ can be decomposed into the disjoint union of the discrete spectrum $\sigma_{\mathrm{d}}(T)$, of isolated eigenvalues with finite multiplicity, and the essential spectrum $\sigma_{\mathrm{ess}}(T) = \sigma(T) \backslash \sigma_{\mathrm{d}}(T)$.

**Principles of quantum mechanics** This paragraph introduces some fundamental terminology for the quantum description of electrons.

In quantum theory, the pure states of a system are represented by the unit sphere of a Hilbert space $\mathcal{H}$. More precisely, a pure state is identified with a *wave function* $\psi \in \mathcal{H}$, of unit norm, up to a phase. This means that $\psi$ and $\mathrm{e}^{i\alpha}\psi$ represent the same physical state, a fact of importance for later developments. We denote the scalar product of $\psi, \phi \in \mathcal{H}$ by $\langle \psi, \phi \rangle$, and the associated norm by $\|\psi\|^2 = \langle \psi, \psi \rangle$.

In the simple case of a *single electron without spin*, in the configuration space $\mathbb{R}^d$ (describing the position of the particle), in motion between the initial time $t = 0$ and the time horizon $t = T$, we can choose the position representation

$$\begin{aligned} \psi : \ \mathbb{R}^d \times [0, T] &\to \mathbb{C} \\ (\mathbf{x}, t) \quad &\mapsto \psi(\mathbf{x}, t), \end{aligned}$$

where the Hilbert space considered is the set of complex-valued, square-integrable functions $L^2(\mathbb{R}^d; \mathbb{C})$, such that $\|\psi(\cdot, t)\| = 1, \ \forall t$. In fact, there is an additional discrete degree of freedom, the *spin*, which is an intrinsic type of angular momentum, whose value is characterized by the *spin quantum number*, an integer multiple of $\frac{1}{2}$, but we will omit it here in order to simplify the notation.

The Copenhagen interpretation gives a physical meaning to $\psi$ in this representation: the function $\mathbf{x} \mapsto |\psi(\mathbf{x}, t)|^2$ represents the probability density of finding the particle at the point $\mathbf{x}$ at the time $t$.

*Scalar observables* are self-adjoint operators $A$ on $\mathcal{H}$, which represent experimentally measurable quantities. When performing a quantum experiment, the result is not deterministic in general, but probabilistic, and its probability density function is determined by $A$ and $\psi$. In particular, the expectation value of the observable $A$ for the state $\psi \in \mathcal{D}(A)$, where $\mathcal{D}(A)$ is the domain of $A$, is given by the scalar product $\langle \psi, A\psi \rangle = \langle \psi A, \psi \rangle$. One can also define *vector observables* $\mathbf{A}$ (we restrict ourselves to $d$ dimensional vectors here), by linear combination of the scalar observables $\{A_i\}_{i=1}^d$, *i.e.* $\mathbf{A} = \sum_{i=1}^d A_i \mathbf{e}_i$, where $\{\mathbf{e}_i\}_{i=1}^d$ denotes the canonical orthonormal basis of $\mathbb{R}^d$.

A *measurement* of an observable $A$ has an impact on the state of the system, and returns a value, which is an element of the spectrum of $A$. The action of a measurement is to project the wavefunction of the system to a spectral subspace of the observable $A$, and the value of the measurement will be the associated spectrum element. This projection is called the *collapse of the wavefunction*, and it implies that, if the same measurement is made again very shortly after, the result will be the same with a high probability. In the case of a scalar observable $A$ with pure point spectrum, if we denote $\forall n,\ A\phi_n = a_n \phi_n$, the normalized eigenvectors and eigenvalues of $A$, according to the *Born rule*, the probability of measuring the value $a_n$ will be given by $|\langle \phi_n, \psi \rangle|^2$.

Two important observables are the *position* and *momentum* operators, denoted $\widehat{\mathbf{x}}$ and $\widehat{\mathbf{p}}$, with hats to distinguish them from the variables, defined for a regular and localized function $\psi$ as

$$(\widehat{\mathbf{x}}\psi)(\mathbf{x}) = \mathbf{x}\psi(\mathbf{x}), \quad (\widehat{\mathbf{p}}\psi)(\mathbf{x}) = -i\hbar\nabla\psi(\mathbf{x}), \quad \forall \mathbf{x} \in \mathbb{R}^d,$$

where the reduced Planck constant $\hbar$ is set to 1 in atomic units. They do not commute, but satisfy the *canonical commutation relation*,

$$[\widehat{x}_j, \widehat{p}_k] = i\hbar\delta_{jk} I = i\delta_{jk} I, \quad \forall 1 \leq j, k \leq d.$$

where $I$ denotes the identity operator, and $\delta_{jk}$ is the Kronecker symbol.

The *Heisenberg uncertainty principle* states that, for two non-commuting observables, like $\mathbf{x}$ and $\mathbf{p}$, one cannot find a state in which both observables are determined. In algebraic terms, this corresponds to the fact that two non-commuting operators cannot be co-diagonalized. Indeed, the result of a measurement is determined if the wavefunction of the system is in an eigenstate of the observable operator. Further, for two non-commuting observables $A, B$ satisfying $[A, B] = iI$, the standard deviations of the observables, defined by $\sigma_A = \sqrt{\langle \psi, A^2\psi \rangle - (\langle \psi, A\psi \rangle)^2}$ satisfy the Heisenberg uncertainty relation $\sigma_A \sigma_B \geq \frac{1}{2}$.

**Schrödinger equation** We are now ready to describe the dynamics of a system of a single electron, which is given by the partial differential equation known as the *Schrödinger equation*. Assuming the system is in the state $\psi_0 \in L^2(\mathbb{R}^d; \mathbb{C})$ at time $t = 0$, it will evolve according to

$$\begin{cases} i\partial_t \psi(t) = H\psi(t) \\ \psi(0) = \psi_0, \end{cases}$$

where $H$ is the *Hamiltonian operator* of the system, that is, the observable corresponding to the energy. It is easily checked that for any $t \geq 0$, the solution $\psi(t)$ has same norm $\|\psi(t)\| = \|\psi_0\|$ and the same energy $\langle \psi(t), H\psi(t) \rangle = \langle \psi_0, H\psi_0 \rangle$ as the initial data $\psi_0$. Formally, the solution is

$$\psi(t) = \exp(-itH)\psi_0, \quad \forall t,$$

where the meaning of $(\exp(-itH))_{t\in\mathbb{R}}$ and its differentiation $\partial_t$ can be made rigorous [84]. Moreover, the Schrödinger equation admits stationary solutions, for which all observable properties are constant in time. In this case, the system is stationary, but since the wavefunction is physically meaningful only up to the phase factor, the solution to the Schrödinger equation can have a time-varying global phase. These states satisfy *the time-independent Schrödinger equation*:

$$H\phi = \varepsilon\phi, \quad \|\phi\| = 1,$$

where $H$ is the Hamiltonian operator, and $\varepsilon$ is the energy of the state. Note that this equation is an eigenvalue problem for the Hamiltonian, and accordingly, the state $\phi$ is called an eigenstate. It follows that the solution to the time-dependent Schrödinger equation, with an eigenstate as initial condition, is simply

$$\psi(t) = \exp(-it\varepsilon)\phi, \quad \forall t$$

that is, the wavefunction undergoes only a change of phase, corresponding to the same pure state. We have now completed our description of single-electron systems. The following paragraphs generalize these notions to systems containing multiple electrons.

**$N$-particle wavefunctions** A quantum system with $N$ spinless electrons is described by a wavefunction

$$\psi : (\mathbf{x}_1, \dots, \mathbf{x}_N) \mapsto \psi(\mathbf{x}_1, \dots, \mathbf{x}_N).$$

satisfying the antisymmetry conditions

$$\psi(\mathbf{x}_1, \dots, \mathbf{x}_i, \dots, \mathbf{x}_j, \dots, \mathbf{x}_N) = -\psi(\mathbf{x}_1, \dots, \mathbf{x}_j, \dots, \mathbf{x}_i, \dots, \mathbf{x}_N), \quad \forall i \neq j.$$

In the Copenhagen interpretation, $|\psi(\mathbf{x}_1, \dots, \mathbf{x}_N)|^2$ corresponds to the probability density of finding the $N$ electrons at positions $(\mathbf{x}_1, \dots, \mathbf{x}_N)$. The antisymmetry condition explains in particular the Pauli exclusion principle: if two electrons, labeled $i$ and $j$, are at the same position $\mathbf{x}_i = \mathbf{x}_j$, the wavefunction is zero.. Therefore, having two electrons at the same position is an event of probability 0. We refer the reader to [48] for more information.

**Many-body Schrödinger equation** We now consider a system with $M$ nuclei, located at $\mathbf{R}_\alpha$, of charges $Z_\alpha$, and $N$ electrons, located at $\mathbf{x}_i$, of charges $-1$. The *Born-Oppenheimer approximation* states that, due to the large difference in mass of the nuclei and the electrons, it is sufficient to describe the nuclei classically, and to consider their positions fixed when studying the quantum behavior of the electrons. Under the Born-Oppenheimer approximation, and neglecting the spin degrees of freedom, we describe the system by an antisymmetric wavefunction in $L^2(\mathbb{R}^{dN}; \mathbb{C})$, which satisfies the many-body Schrödinger equation with the Hamiltonian

$$H = \sum_{1\leq i\leq N} \left( -\frac{1}{2}\Delta_{\mathbf{x}_i} - \sum_{1\leq\alpha\leq M} \frac{Z_\alpha}{|\mathbf{x}_i - \mathbf{R}_\alpha|} \right) + \sum_{1\leq i<j\leq N} \frac{1}{|\mathbf{x_i} - \mathbf{x_j}|},$$

where the coordinate-specific Laplacian $\Delta_{\mathbf{x}_i}$ denotes $\sum_{j=1}^{d} \frac{\partial^2}{\partial x_{i,j}^2}$. We will denote the interaction potential of one electron with the nuclei by

$$v(\mathbf{x}) = -\sum_{1\leq\alpha\leq M} \frac{Z_\alpha}{|\mathbf{x} - \mathbf{R}_\alpha|}.$$

When studying a physical system with a given Hamiltonian, the first and most important step is to determine the ground state, that is, the wavefunction $\psi$ that minimizes the energy $\langle\psi, H\psi\rangle$. Hence, we want to solve the constrained minimization problem

$$E_0 = \inf_{\|\psi\|=1} \langle\psi, H\psi\rangle.$$

However, the full problem is almost impossible to solve numerically, even for simple systems with a dozen of electrons, given the high dimensionality of the space $\mathbb{R}^{dN}$. It is therefore required to devise simpler models that can be solved using reasonable computing power, which is the topic of the following paragraphs.

**Hartree-Fock** The core idea of the Hartree-Fock method is to reduce the variational space in the minimization problem, assuming that the solution can be expressed by a single Slater determinant, that is, an antisymmetric function $\psi$ that is constructed as follows. Let $\{\chi_i\}_{i=1}^N$ be one-electron orthonormal orbitals, that is, $\chi_1, \dots \chi_N \in L^2(\mathbb{R}^d; \mathbb{C})$, such that

$$\forall 1 \leq i, j \leq N, \quad \langle \chi_i, \chi_j \rangle = \delta_{ij}.$$

Then one defines $\psi$ as the matrix determinant

$$\psi(\mathbf{x}_1, \mathbf{x}_2, \dots, \mathbf{x}_N) = \frac{1}{\sqrt{N!}} \begin{vmatrix} \chi_1(\mathbf{x}_1) & \chi_2(\mathbf{x}_1) & \cdots & \chi_N(\mathbf{x}_1) \\ \chi_1(\mathbf{x}_2) & \chi_2(\mathbf{x}_2) & \cdots & \chi_N(\mathbf{x}_2) \\ \vdots & \vdots & \ddots & \vdots \\ \chi_1(\mathbf{x}_N) & \chi_2(\mathbf{x}_N) & \cdots & \chi_N(\mathbf{x}_N) \end{vmatrix}.$$

The Slater determinant is a simple way to construct an antisymmetric function in $L^2(\mathbb{R}^{dN}; \mathbb{C})$ (with $d \times N$ variables) with $N$ functions in $L^2(\mathbb{R}^d; \mathbb{C})$ (with $d$ variables only). In what follows, we denote

$$\bigwedge^N L^2(\mathbb{R}^d; \mathbb{C})$$

the vector space of antisymmetric functions in $L^2(\mathbb{R}^{dN}; \mathbb{C})$, *i.e.* the space generated by linear combination of Slater determinants with orbitals in $L^2(\mathbb{R}^d; \mathbb{C})$. A similar notation

$$\bigwedge^N H^1(\mathbb{R}^d; \mathbb{C})$$

will be used for the vector subspace of $H^1(\mathbb{R}^{dN}; \mathbb{C})$ generated by Slater determinants of orbitals in $H^1(\mathbb{R}^d; \mathbb{C})$.

**Density Functional Theory** *Density Functional Theory* is a widely used computational method in quantum chemistry and solid-state physics. Rather than computing the wavefunction of a system, a function on $\mathbb{R}^{dN}$, it characterizes the system by its *single-electron density*, a function on $\mathbb{R}^d$ only, and produces approximations of this density. By performing such a reduction however, one loses the linearity of the equation to solve, transforming it into a minimization problem involving a non-linear functional of the density (hence the name of the method), which is not known analytically. In what follows, we give a brief formalization of the method and describe a commonly used approximation scheme, the *Kohn-Sham method*.

Let us define the single-electron density $\rho_\psi$ of $\psi$,

$$\rho_\psi(\mathbf{x}) = N \int_{\mathbf{x}_2 \in \mathbb{R}^d} \dots \int_{\mathbf{x}_d \in \mathbb{R}^d} |\psi(\mathbf{x}, \mathbf{x}_2, \dots, \mathbf{x}_d)|^2 \, d\mathbf{x}_2 \dots d\mathbf{x}_d.$$

One can rewrite the minimization problem considered in terms of densities, as

$$E_0 = \inf \left( F(\rho) + \int_{\mathbb{R}^d} \rho v, \quad \rho \geq 0, \quad \sqrt{\rho} \in H^1(\mathbb{R}^d; \mathbb{R}), \quad \int_{\mathbb{R}^d} \rho = N \right),$$

where $F$ is the so-called Levy-Lieb functional which depends only on the number of electrons in the system, and not on the particular configuration it is in. It is defined, for $H^0$ the Hamiltonian $H$ without the interaction with the nuclei, *i.e.* $v = 0$, by

$$F(\rho) = \inf \left( \langle \psi, H^0 \psi \rangle, \quad \psi \in \bigwedge^N H^1(\mathbb{R}^d; \mathbb{C}), \quad \rho = \rho_\psi \right).$$

It is not obvious that the condition $\sqrt{\rho} \in H^1(\mathbb{R}^d; \mathbb{R})$ is equivalent to the existence of $\psi$ in the domain of $H^0$, hence that the variational spaces are equivalent. The interested reader can find out more in the seminal paper [62].

In practice, when simulations are performed, the computational cost of the Levy-Lieb functional is too high, and approximations are required. A widely used scheme is the Kohn-Sham method, which gives rise to equations of the form

$$\left( -\frac{1}{2}\Delta + v_{\text{eff}}[\rho] \right) \chi_i(\mathbf{x}) = \varepsilon_i \chi_i(\mathbf{x}), \quad \forall\, 1 \leq i \leq N,$$

$$\text{where } \rho(\mathbf{x}) = \sum_{i=1}^{N} |\chi_i(\mathbf{x})|^2, \quad \int \chi_i \chi_j = \delta_{ij}, \quad \forall 1 \leq i, j \leq N.$$

for almost every $\mathbf{x} \in \mathbb{R}^d$ (in the sense of the Lebesgue measure), and where $v_{\text{eff}}[\rho]$ is an effective potential depending on the density $\rho$ whose definition is beyond the scope of this manuscript (see [55]).

The important consequence of this approximation is that the system of $N$ coupled electrons, interacting with each other through the electrostatic potential, has been effectively decoupled into $N$ independent electrons (not interacting with each other), evolving in the effective external potential $v_{\text{eff}}[\rho]$. Hence, in what follows, we will consider only the behavior of independent electrons in an external potential.

### 1.1.2 Electrons in periodic crystals

In this section, we aim to give an introduction to the description of the behaviour of electrons in a periodic crystal within the framework of the Born-Oppenheimer approximation.

#### Crystal structure

A perfect *crystal* is a periodic arrangement of particles (atoms, ions, molecules) that is assumed to be infinite in all directions.

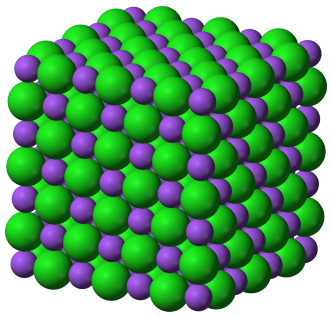

Figure 1.1: Crystal structure of Sodium Chloride, source [3]

**Bravais lattice, reciprocal lattice, Brillouin Zone** Perfect crystals are invariant by translations of a period along their principal axes. Hence, one can represent their structure as a *lattice*, informally defined as a repetition of a small building block called the unit cell. The geometry of this unit cell is described using $d$ vectors $\mathbf{a}_1, \dots, \mathbf{a}_d$, where $d \leq 3$ is the dimension of the crystal, which form an independent set of vectors. They are called the *primitive vectors* of the lattice.

More formally, a *Bravais lattice* $\mathcal{R}$ is a discrete set of points obtained by translations of the origin along integer linear combinations of the basis of *primitive vectors* $\mathbf{a}_1, \dots \mathbf{a}_d$

$$\mathbf{R} = n_1\mathbf{a}_1 + \cdots + n_d\mathbf{a}_d, \quad n_1, \dots, n_d \in \mathbb{Z}.$$

We define the (centered) *unit cell* $\Omega$ of $\mathcal{R}$ as

$$\Omega = \left\{ \sum_{i=1}^{d} \alpha_i \mathbf{a}_i,\ \{\alpha_i\}_{i=1}^{d} \in \left[-\frac{1}{2}, \frac{1}{2}\right)^d \right\}.$$

One can associate a dual object to the Bravais lattice $\mathcal{R}$ (generated by the basis $\{\mathbf{a}_i\}_{i=1}^{d}$ ). We call the *reciprocal lattice* of $\mathcal{R}$ the lattice $\mathcal{R}'$ generated by the unique set of primitive vectors $\{\mathbf{b}_i\}_{i=1}^{d}$ satisfying

$$\mathbf{a}_i \cdot \mathbf{b}_j = 2\pi\delta_{ij}.$$

It is well defined, as one can find the $\mathbf{b}_j$ by solving the well-posed matrix equation

$$[\mathbf{b}_1 \dots \mathbf{b}_d] = 2\pi[\mathbf{a}_1 \dots \mathbf{a}_d]^{-T},$$

where $[\mathbf{a}_1 \dots \mathbf{a}_d]$ is the matrix of columns $\mathbf{a}_i$, invertible because the primitive vectors form a basis.

The reciprocal lattice $\mathcal{R}'$ is the support of the Fourier transforms of $\mathcal{R}$-periodic functions. To explain this, we introduce some notation: for a multi-index $\boldsymbol{\alpha} \in \mathbb{N}^d$, a smooth function $f$, and $\mathbf{x} \in \mathbb{R}^d$, we define

$$\mathbf{x}^{\boldsymbol{\alpha}} = \prod_{i=1}^{d} x_i^{\alpha_i}, \quad (\partial_{\boldsymbol{\alpha}} f)(\mathbf{x}) = (\partial_{\alpha_1}\partial_{\alpha_2} \dots \partial_{\alpha_d} f)(\mathbf{x}).$$

Let $\mathcal{S}(\mathbb{R}^d;\mathbb{C})$ denote the Schwartz space of rapidly decreasing smooth functions, *i.e.*

$$\mathcal{S}(\mathbb{R}^d;\mathbb{C}) = \left\{ f \in C^\infty(\mathbb{R}^d;\mathbb{C}) \;\middle|\; \forall \alpha, \beta \in \mathbb{N}^d,\ \sup_{\mathbf{x}\in\mathbb{R}^d} |\mathbf{x}^{\boldsymbol{\alpha}}\partial_\beta f(\mathbf{x})| < \infty \right\}.$$

We define the Fourier Transform of a Schwartz function $\psi \in \mathcal{S}(\mathbb{R}^d;\mathbb{C})$ as the function $\widehat{\psi} \in \mathcal{S}(\mathbb{R}^d;\mathbb{C})$ that verifies

$$\widehat{\psi}(\boldsymbol{\xi}) = \int_{\mathbb{R}^d} \psi(\mathbf{x}) \mathrm{e}^{-i\boldsymbol{\xi}\cdot\mathbf{x}}\, d\mathbf{x}, \quad \forall \boldsymbol{\xi} \in \mathbb{R}^d.$$

The Fourier Transform $\widehat{T}$ of a *tempered distribution* $T$ in $\mathcal{S}'(\mathbb{R}^d;\mathbb{C})$ is given by $\langle \widehat{T}, \varphi\rangle_{\mathcal{S}',\mathcal{S}} = \langle T, \widehat{\varphi}\rangle_{\mathcal{S}',\mathcal{S}}, \quad \forall \varphi \in \mathcal{S}(\mathbb{R}^d;\mathbb{C})$, where $\langle\cdot,\cdot\rangle_{\mathcal{S}',\mathcal{S}}$ denotes the duality bracket.

We can now get back to our point. Let $f$ be a $C^\infty$ $\mathcal{R}$-periodic function, such that for $\mathbf{x} \in \mathbb{R}^n$, and $\mathbf{R} \in \mathcal{R}$, $f(\mathbf{x}+\mathbf{R}) = f(\mathbf{x})$. Denoting $\mathbf{K}$ the points of $\mathcal{R}'$ with integer coordinates in the basis $\{\mathbf{b}_j\}_{j=1}^{d}$, and using $\mathbf{a}_i \cdot \mathbf{b}_j = 2\pi\delta_{ij}$, $f$, which can be identified with a tempered distribution, can be expanded in a Fourier series,

$$f(\mathbf{x}) = \sum_{\mathbf{K}\in\mathcal{R}'} c_{\mathbf{K}} \mathrm{e}^{i\mathbf{K}\cdot\mathbf{x}},$$

and the Fourier transform of $f$ in the sense of distributions on $\mathbb{R}^d$ is $\sum_{\mathbf{K}\in\mathcal{R}'} c_{\mathbf{K}}\delta_{\mathbf{K}}$, where $\delta_{\mathbf{K}}$ is the Dirac delta of support $\mathbf{K}$.

The first *Brillouin Zone* $\mathcal{B}$ is the Voronoï cell of the reciprocal lattice containing the origin, that is, the locus of the points that are closer to the origin than to any other point in the lattice $\mathcal{R}'$.

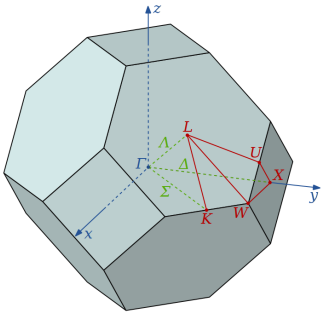


Figure 1.2: First Brillouin zone of face centred cubic structure, source [1]

Abusing notation, in what follows, we will also call Brillouin Zone the primitive cell

$$\mathcal{B} = \left\{ \sum_{j=1}^{d} \beta_j b_j,\ \{\beta_j\}_{j=1}^{d} \in [0,1)^d \right\}.$$

The definition of the primitive cell is a convention, as many choices are possible. However, this particular choice is convenient in our context.

### Electronic band structure theory

$L^2_{\text{per}}(\mathbb{R}^d;\mathbb{C})$ is defined as the space of $\mathcal{R}$-periodic functions $v$ that verify $\int_\Omega v^2 < \infty$, where $\Omega$ is the centered unit cell of the lattice $\mathcal{R}$. $L^2_{\text{per}}(\mathbb{R}^d;\mathbb{R})$ is defined similarly for real-valued functions.

**Description of the system** From here on, we work under the following assumptions:

- The electrons are independent from each other,
- Each electron is subjected to a $L^2_{\text{per}}(\mathbb{R}^d;\mathbb{R})$ scalar potential $V$.

Hence, we will consider wavefunctions $\mathbb{R}^d \ni \mathbf{x} \mapsto \psi(\mathbf{x})$, with a single position variable, and restrict ourselves to a Hamiltonian operator with the following explicit form, in atomic units,

$$(H\psi)(\mathbf{x}) = \left(-\frac{1}{2}\Delta + V(\mathbf{x})\right)\psi(\mathbf{x}),$$

for almost every $\mathbf{x} \in \mathbb{R}^d$.

To properly define the Hamiltonian operator, its explicit form has to be completed by the definition of the domain of the operator, that is, a dense subset of $\mathcal{H}$. According to the Kato-Rellich theorem, with these assumptions, the Hamiltonian is a self-adjoint operator on $L^2(\mathbb{R}^d;\mathbb{C})$ with domain $\mathcal{D} = H^2(\mathbb{R}^d;\mathbb{C})$. By the spectral theorem, the spectrum of $H$ is real. However, it does not consist of eigenvalues. In contrast, it is in fact purely (absolutely) continuous. To characterize the spectrum in a more precise way, we first introduce a set of functions, the Bloch waves, that play a particular role in the study of such Hamiltonians.

**Bloch waves** In what follows, we derive formally a convenient basis of generalized (*i.e.* non-normalized) eigenfunctions of $H$, the Bloch waves, without consideration for the well-posedness of such a problem. However, this "physicist's" approach is useful to give some intuition for the more rigorous presentation done in later paragraphs.

Let us define the translation operator $\tau_{\mathbf{R}}$, for $\mathbf{R} \in \mathcal{R}$, and $f$ a smooth function as

$$\left(\tau_{\mathbf{R}} f\right)(\mathbf{x}) = f(\mathbf{x} - \mathbf{R}), \quad \forall \mathbf{x} \in \mathbb{R}^d.$$

The translation operators satisfy $\tau_{\mathbf{R}}\tau_{\mathbf{R}'} = \tau_{\mathbf{R}'}\tau_{\mathbf{R}}$, and $\tau_{\mathbf{R}}^* = \tau_{-\mathbf{R}} = \tau_{\mathbf{R}}^{-1}$, where $\tau_{\mathbf{R}}^*$ denotes the adjoint with respect to the $L^2(\mathbb{R}^d;\mathbb{C})$ scalar product. Then the periodicity of the potential can be seen as a commutation relation, as

$$\tau_{\mathbf{R}}\left(V\psi\right)(\mathbf{x}) = V(\mathbf{x}+\mathbf{R})\psi(\mathbf{x}+\mathbf{R}) = V(\mathbf{x})\psi(\mathbf{x}+\mathbf{R}) = \left(\left(V\tau_{\mathbf{R}}\right)\psi\right)(\mathbf{x}).$$

Of course, the same applies to the Laplacian operator $\Delta$, and so we conclude that the Hamiltonian commutes with translations by vectors of the lattice $\mathcal{R}$,

$$\tau_{\mathbf{R}}\left(H\psi\right) = H\left(\tau_{\mathbf{R}}\psi\right).$$

In analogy with the finite-dimensional case, where commutation between matrices implies that the matrices are co-diagonalizable, the commuting operators $H$ and the set $\{\tau_{\mathbf{R}}\}_{\mathbf{R}\in\mathcal{R}}$ are formally co-diagonalizable. Consider a function $\psi \neq 0$ satisfying

$$\begin{aligned} H\psi &= \varepsilon\psi \\ \tau_{\mathbf{R}}\psi &= \lambda(\mathbf{R})\psi, \quad \forall \mathbf{R} \in \mathcal{R}. \end{aligned}$$

A natural property of the translation operator is that for all $\mathbf{R}, \mathbf{R}' \in \mathcal{R}$,

$$\tau_{\mathbf{R}}\tau_{\mathbf{R}'} = \tau_{\mathbf{R}'}\tau_{\mathbf{R}} = \tau_{\mathbf{R}+\mathbf{R}'},$$

implying that the eigenvalues $\lambda(\mathbf{R})$ of the translation operator $\tau_{\mathbf{R}}$ satisfy

$$\lambda(\mathbf{R})\lambda(\mathbf{R}') = \lambda(\mathbf{R}+\mathbf{R}').$$

Moreover, we have $\lambda(\mathbf{0}) = 1$, and $|\lambda(\mathbf{R})| = 1$ because a translation along $\mathbf{0}$ is the identity, and translation operators are unitary, hence have spectrum included in the unit circle of the complex plane. Along each primitive vector $\mathbf{a}_j$, we then have

$$\lambda(\mathbf{a}_j)^n = \lambda(n\mathbf{a}_j),$$

which means that we can choose numbers $\{k_j\}_{j=1}^d$ in $[0,1)^d$, such that $\lambda(\mathbf{a}_j) = \mathrm{e}^{2\pi i k_j}$. We recall that $\mathbf{a}_j \cdot \mathbf{b}_i = 2\pi\delta_{ij}$, so, for any lattice vector $\mathbf{R} = \sum_{j=1}^d n_j\mathbf{a}_j$, denoting $\mathbf{k} = \sum_{i=1}^d k_i\mathbf{b}_i$,

$$\lambda(\mathbf{R}) = \prod_{j=1}^d \lambda(\mathbf{a}_j)^{n_j} = \exp\left(\sum_{j=1}^d 2\pi i k_j n_j\right) = \mathrm{e}^{i\mathbf{k}\cdot\mathbf{R}}.$$

It follows that the eigenstate $\psi$ is such that

$$\psi(\mathbf{x}+\mathbf{R}) = \mathrm{e}^{i\mathbf{k}\cdot\mathbf{R}}\psi(\mathbf{x}), \quad \forall \mathbf{x} \in \mathbb{R}^d, \forall \mathbf{R} \in \mathcal{R}.$$

Let us now define, for $\mathbf{x} \in \mathbb{R}^d$,

$$u(\mathbf{x}) = \mathrm{e}^{-i\mathbf{k}\cdot\mathbf{x}}\psi(\mathbf{x}),$$

and notice that this function is $\mathcal{R}-$periodic.

To recap, we have formally shown that a *Bloch wave* is an eigenfunction of the translation operators $\{\tau_{\mathbf{R}}\}_{\mathbf{R}\in\mathcal{R}}$, that is, a function of the form

$$\psi_{\mathbf{k}}(\mathbf{x}) = \mathrm{e}^{i\mathbf{k}\cdot\mathbf{x}} u_{\mathbf{k}}(\mathbf{x}),$$

where $u_{\mathbf{k}}$ is a $\mathcal{R}$-periodic function.

Rigorously, Bloch waves are not in the domain of the Hamiltonian operator. For this reason, they are not actual eigenfunctions, and we will call them *Bloch eigenstates*. However, they can be recombined to give elements of the domain. This is similar to the Fourier decomposition, in which one "diagonalizes" the Laplacian operator on the Fourier basis, which are then recombined to give elements of the proper domain, which is legitimate because the Fourier Transform is a unitary operator. In the same way, the results of these formal calculations will be made rigorous by the introduction of the Bloch Transform in the next paragraph.

We now consider the action of the Hamiltonian on Bloch waves. Hence, we use the *Ansatz* of the Bloch eigenstates of $H$: they are of the form $\mathrm{e}^{i\mathbf{k}\cdot\mathbf{x}}u(\mathbf{x})$, for some $\mathbf{k}\in\mathcal{B}$, where $u$ is $\mathcal{R}$-periodic.

$$\begin{aligned} H\left(\mathrm{e}^{i\mathbf{k}\cdot\mathbf{x}}u_{\mathbf{k}}(\mathbf{x})\right) &= -\frac{1}{2}\Delta\left(\mathrm{e}^{i\mathbf{k}\cdot\mathbf{x}}u_{\mathbf{k}}(\mathbf{x})\right) + V(\mathbf{x})\left(\mathrm{e}^{i\mathbf{k}\cdot\mathbf{x}}u(\mathbf{x})\right) \\ &= \mathrm{e}^{i\mathbf{k}\cdot\mathbf{x}}\left(-\frac{1}{2}\Delta - i\mathbf{k}\cdot\nabla + \frac{|\mathbf{k}|^2}{2}\right)u_{\mathbf{k}}(\mathbf{x}) + \mathrm{e}^{i\mathbf{k}\cdot\mathbf{x}}\left(V(\mathbf{x})u_{\mathbf{k}}(\mathbf{x})\right). \end{aligned}$$

Hence, it is natural to define the family of operators

$$H_{\mathbf{k}} = \frac{1}{2}(-i\nabla + \mathbf{k})^2 + V, \quad \forall \mathbf{k}\in\mathcal{B},$$

acting on the $\mathcal{R}$-periodic part of Bloch waves, the function $u$. We have therefore reduced the problem of determining Bloch eigenstates on the whole space to determining eigenfunctions of a modified operator on the primitive cell $\Omega$ for each $\mathbf{k}$.

**Bloch Transform** To motivate the definition of the Bloch Transform, we start by a formal calculation showing its relationship to the Fourier Transform. Recall that the Fourier Transform of a Schwartz function $\psi\in\mathcal{S}(\mathbb{R}^d;\mathbb{C})$ is the function $\widehat{\psi}\in\mathcal{S}(\mathbb{R}^d;\mathbb{C})$ that verifies

$$\widehat{\psi}(\boldsymbol{\xi}) = \int_{\mathbb{R}^d}\psi(\mathbf{x})\mathrm{e}^{-i\boldsymbol{\xi}\cdot\mathbf{x}}\,d\mathbf{x}, \quad \forall\boldsymbol{\xi}\in\mathbb{R}^d.$$

It satisfies the reciprocal Fourier identity

$$\psi(\mathbf{x}) = \frac{1}{|\mathcal{B}|}\int_{\mathbb{R}^d}\widehat{\psi}(\boldsymbol{\xi})\mathrm{e}^{i\boldsymbol{\xi}\cdot\mathbf{x}}\,d\boldsymbol{\xi}, \quad \forall\mathbf{x}\in\mathbb{R}^d.$$

In our case, the space is endowed with a Bravais lattice $\mathcal{R}$, and the frequency space with the reciprocal lattice $\mathcal{R}'$. Hence, a natural decomposition for $\boldsymbol{\xi}$ is

$$\boldsymbol{\xi} = \mathbf{k} + \mathbf{K}, \quad \mathbf{k}\in\mathcal{B}, \ \ \mathbf{K}\in\mathcal{R}'.$$

Substituting into the reciprocal Fourier identity, one obtains

$$\psi(\mathbf{x}) = \frac{1}{|\mathcal{B}|}\sum_{\mathbf{K}\in\mathcal{R}'}\int_{\mathbf{k}\in\mathcal{B}}\mathrm{e}^{i\mathbf{k}\cdot\mathbf{x}}\widehat{\psi}(\mathbf{k}+\mathbf{K})\mathrm{e}^{i\mathbf{K}\cdot\mathbf{x}}\,d\mathbf{k}, \quad \forall\mathbf{x}\in\mathbb{R}^d.$$

By exchanging sum and integral, we can group together the dependence in $\mathbf{K}$,

$$\psi(\mathbf{x}) = \frac{1}{|\mathcal{B}|}\int_{\mathbf{k}\in\mathcal{B}} \mathrm{e}^{i\mathbf{k}\cdot\mathbf{x}} \sum_{\mathbf{K}\in\mathcal{R}'} \widehat{\psi}(\mathbf{k}+\mathbf{K})\mathrm{e}^{i\mathbf{K}\cdot\mathbf{x}}\, d\mathbf{k}, \quad \forall \mathbf{x}\in\mathbb{R}^d.$$

Let us now define the *Bloch Transform* $(u_{\mathbf{k}})_{\mathbf{k}\in\mathbb{R}^d}$ of $\psi$, and the Bloch wave $(\psi_{\mathbf{k}})_{\mathbf{k}\in\mathbb{R}^d}$,

$$u_{\mathbf{k}}(\mathbf{x}) = \sum_{\mathbf{K}\in\mathcal{R}'} \widehat{\psi}(\mathbf{k}+\mathbf{K})\mathrm{e}^{i\mathbf{K}\cdot\mathbf{x}}, \quad \psi_{\mathbf{k}}(\mathbf{x}) = \mathrm{e}^{i\mathbf{k}\cdot\mathbf{x}}u_{\mathbf{k}}(\mathbf{x}), \quad \forall \mathbf{x}\in\mathbb{R}^d, \mathbf{k}\in\mathbb{R}^d.$$

Let us remark that the $(u_{\mathbf{k}})_{\mathbf{k}\in\mathbb{R}^d}$ satisfy the $\mathcal{R}'$-quasi-periodicity relation in $\mathbf{k}\in\mathbb{R}^d$

$$u_{\mathbf{k}+\mathbf{K}}(\mathbf{x}) = \mathrm{e}^{-i\mathbf{K}\cdot\mathbf{x}}u_{\mathbf{k}}(\mathbf{x}), \quad \forall \mathbf{K}\in\mathcal{R}', \mathbf{x}\in\mathbb{R}^d,$$

and that the Bloch wave $\mathbf{k}\mapsto\psi_{\mathbf{k}}$ is $\mathcal{R}'$-periodic. Hence, one can restrict the $(u_{\mathbf{k}})_{\mathbf{k}\in\mathbb{R}^d}$ to $\mathbf{k}\in\mathcal{B}$ without loss of information.

One can also express the Bloch Transform in terms of $\psi$ and not of its Fourier Transform, through the Poisson summation formula. Let $f\in\mathcal{S}(\mathbb{R}^d;\mathbb{C})$, we then have

$$\sum_{\mathbf{R}\in\mathcal{R}} f(\mathbf{R}) = \sum_{\mathbf{K}\in\mathcal{R}'} \widehat{f}(\mathbf{K}).$$

Applying this formula for the Schwartz function defined by $f:\mathbf{r}\mapsto \mathrm{e}^{-i\mathbf{k}\cdot(\mathbf{x}+\mathbf{r})}\psi(\mathbf{x}+\mathbf{r})$, for some $\mathbf{k},\mathbf{x}\in\mathbb{R}^d$, with Fourier transform at $\mathbf{K}\in\mathcal{R}'$, $\widehat{f}(\mathbf{K}) = \mathrm{e}^{i\mathbf{K}\cdot\mathbf{x}}\widehat{\psi}(\mathbf{K}+\mathbf{k})$, it follows that

$$u_{\mathbf{k}}(\mathbf{x}) = \sum_{\mathbf{K}\in\mathcal{R}'} \widehat{\psi}(\mathbf{k}+\mathbf{K})\mathrm{e}^{i\mathbf{K}\cdot\mathbf{x}} = \sum_{\mathbf{R}\in\mathcal{R}} \mathrm{e}^{-i\mathbf{k}\cdot(\mathbf{x}+\mathbf{R})}\psi(\mathbf{x}+\mathbf{R}).$$

To summarize, we have decomposed $\psi$ as a continuous collection (indexed by $\mathbf{k}\in\mathcal{B}$) of periodic functions $u_{\mathbf{k}}$. The *inverse Bloch Transform* is defined by the relation

$$\psi(\mathbf{x}) = \frac{1}{|\mathcal{B}|}\int_{\mathbf{k}\in\mathcal{B}} \mathrm{e}^{i\mathbf{k}\cdot\mathbf{x}}u_{\mathbf{k}}(\mathbf{x})d\mathbf{k} = \frac{1}{|\mathcal{B}|}\int_{\mathbf{k}\in\mathcal{B}} \psi_{\mathbf{k}}(\mathbf{x})d\mathbf{k}, \quad \forall \mathbf{x}\in\mathbb{R}^d.$$

Like the Fourier Transform, we can extend the Bloch Transform to the space of square-integrable functions, and it is then a unitary operator from $L^2(\mathbb{R}^d;\mathbb{C})$ to $L^2(\mathcal{B};L^2_{\mathrm{per}}(\mathbb{R}^d;\mathbb{C}))$.

**Decomposition of the Hamiltonian $H$ into the $(H_{\mathbf{k}})_{\mathbf{k}}$** For a potential $V\in L^2_{\mathrm{per}}(\mathbb{R}^d;\mathbb{R})$ and $d\leq 3$, let us define the self-adjoint operator on $L^2(\mathbb{R}^d;\mathbb{C})$ with domain $H^2(\mathbb{R}^d;\mathbb{C})$,

$$H = -\frac{1}{2}\Delta + V,$$

and the family of operators on $L^2_{\mathrm{per}}(\mathbb{R}^d;\mathbb{C})$, with a common domain $\mathcal{D} = H^2_{\mathrm{per}}(\mathbb{R}^d;\mathbb{C})$,

$$H_{\mathbf{k}} = \frac{1}{2}(-i\nabla+\mathbf{k})^2 + V, \quad \forall \mathbf{k}\in\mathcal{B}.$$

For all $\mathbf{k}\in\mathcal{B}$, the operators $H_{\mathbf{k}}$ are self-adjoint on $\mathcal{D}$, and if $\lambda$ is not in the spectrum of $H_{\mathbf{k}}$, the resolvent $(H_{\mathbf{k}}-\lambda I)^{-1}$ is a compact operator. Since for all $\mathbf{k}\in\mathcal{B}$, $H_{\mathbf{k}}$ has compact resolvent, it is bounded below, and its spectrum is a sequence of eigenvalues diverging to $+\infty$, *i.e.* there exists $\lambda_0 > -\infty$, such that

$$\sigma(H_{\mathbf{k}}) = \sigma_{\mathrm{d}}(H_{\mathbf{k}}) \subset [\lambda_0, +\infty).$$

Let us order the eigenvalues and denote them by

$$\varepsilon_1(\mathbf{k}) \leq \varepsilon_2(\mathbf{k}) \leq \ldots, \quad \forall \mathbf{k} \in \mathcal{B},$$

where the dependence in $\mathbf{k}$ is denoted functionally, for the eigenvalues have good properties as functions of $\mathbf{k}$. Indeed, for all $n$, $\varepsilon_n(\mathbf{k})$ is Lipschitz in $\mathbf{k}$ and $\mathcal{R}'$-periodic. Moreover,

$$\varepsilon_n(\mathbf{k}) \xrightarrow[n\to+\infty]{} +\infty, \text{ where the limit is uniform in } \mathbf{k}.$$

Then $H$ is decomposed by the Bloch Transform into the $(H_\mathbf{k})_{\mathbf{k}\in\mathcal{B}}$, that is, for $\psi \in \mathcal{S}(\mathbb{R}^d;\mathbb{C})$, and its Bloch Transform $(u_\mathbf{k})_{\mathbf{k}\in\mathcal{B}}$,

$$(H\psi)(\mathbf{x}) = \frac{1}{|\mathcal{B}|}\int_{\mathbf{k}\in\mathcal{B}} \mathrm{e}^{i\mathbf{k}\cdot\mathbf{x}} (H_\mathbf{k} u_\mathbf{k})(\mathbf{x}) d\mathbf{k}, \quad \forall \mathbf{x} \in \mathbb{R}^d,$$

and the spectrum of $H$ is the union of the spectra of the $H_\mathbf{k}$ for all $\mathbf{k} \in \mathcal{B}$. That is,

$$\sigma(H) = \{\varepsilon_n(\mathbf{k}) \mid \mathbf{k} \in \mathcal{B},\ n \in \mathbb{N}\}.$$

For a proof of these results, we refer the reader to [86].

**Band Structure** The behavior of the eigenvalues of $H_\mathbf{k}$, which we previously denoted $\varepsilon_n(\mathbf{k})$, contains some meaningful physical information. Thus, it is useful to plot their variation with $\mathbf{k}$. The $\mathbf{k} \mapsto \varepsilon_n(\mathbf{k})$ are usually plotted in 1D, even if we are considering a system of greater dimension, and this plot is called a band structure diagram. This is done by choosing an appropriate path in the Brillouin zone, and representing the value of each band along this path. The structure of the bands determines some physical properties. An important feature is their position with respect to the *Fermi level* $\varepsilon_F$, which verifies the following relation to the number of electrons $N$ in the unit cell

$$N = \frac{1}{|\mathcal{B}|}\sum_n \int_\mathcal{B} \mathbb{1}(\varepsilon_n(\mathbf{k}) \leq \varepsilon_F)\, d\mathbf{k}.$$

The significance of the Fermi level in the context of solid-state physics is that the electrons in their ground state are in the eigenstates corresponding to the bands below the Fermi level.

For example, if the Fermi level is in a wide gap (larger than $\sim 3$ eV) between the lowest group of bands and the upper ones, it indicates that the system is an *insulator*. If the gap is smaller than $\sim 3$ eV, then the crystal is a *semi-conductor*, as the example of Silicon. On the contrary, if there is no gap, the system is a *metal* (or a *semi-metal* if $d \geq 2$ and the intersection of the bands with the Fermi level is a finite set of isolated points).

An example of such a band structure is given in Figure 1.3, for the Silicon crystal (a semi-conductor). On the $y$-axis, the energy is expressed, in electron-Volts (eV). The labels $L, \Gamma, X, K$ denote special points in $\mathbb{R}^3$, corresponding to points of high symmetry of the reciprocal lattice, that are physically relevant, forming a path in the Brillouin Zone. Note that since this path is not closed, it produces a non-periodic band structure graph, even though the energy bands themselves are periodic.

## 1.2 Wannier functions

Denote $\mathcal{U}(N)$ the group of unitary matrices of size $N \times N$, which satisfy

$$\forall U \in \mathcal{U}(N), \quad U^*U = UU^* = I,$$

where $U^*$ is the conjugate transpose of $U$. Denote $\mathcal{SU}(N)$ the group of *special unitary matrices*, the subgroup of $\mathcal{U}(N)$ for which the elements satisfy the additional condition

$$\forall U \in \mathcal{SU}(N), \quad \det(U) = 1.$$

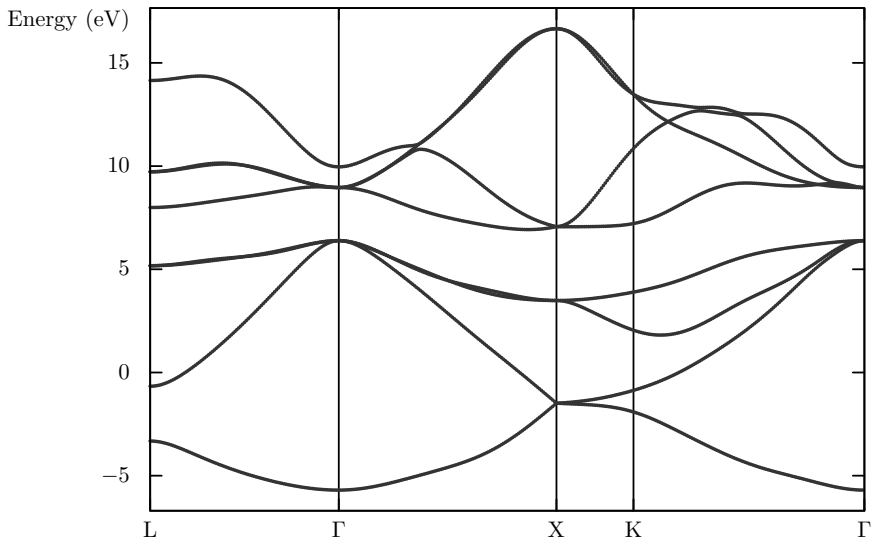


Figure 1.3: Band Structure of Silicon

### 1.2.1 Definitions: composite Wannier functions

For each band index $n \geq 1$, let us denote $\mathbf{k} \mapsto \psi_{n,\mathbf{k}}$ a Bloch eigenstate of the Hamiltonian $H$ associated with the band $\mathbf{k} \mapsto \varepsilon_n(\mathbf{k})$. It is defined up to a phase, since $\mathbf{k} \mapsto e^{i\varphi(\mathbf{k})}\psi_{n,\mathbf{k}}$ is also a Bloch eigenstate, where $\mathbf{k} \mapsto \varphi(\mathbf{k})$ is a $\mathcal{R}'$-periodic (possibly discontinuous) phase function. Moreover, if $\varepsilon_n$ is a degenerate eigenvalue, with multiplicity $m$, the associated eigenspace is $m$ dimensional, for which there is no preferential eigenbasis. Hence, the corresponding $m$ Bloch eigenstates can be rotated among themselves, using a unitary matrix at each $\mathbf{k}$ point, and still generate the same eigenspace.

The periodic part $u_{n,\mathbf{k}}$ of a Bloch eigenstate, defined by $u_{n,\mathbf{k}}(\mathbf{x}) = \mathrm{e}^{-i\mathbf{k}\cdot\mathbf{x}}\psi_{n,\mathbf{k}}(\mathbf{x})$, therefore satisfies the eigenvalue equation

$$H_{\mathbf{k}} u_{n,\mathbf{k}} = \varepsilon_n(\mathbf{k}) u_{n,\mathbf{k}}.$$

Moreover, we normalize the Bloch eigenstates according to the condition

$$\int_\Omega |\psi_{n,\mathbf{k}}(\mathbf{r})|^2 \, d\mathbf{r} = 1, \quad \forall n \geq 1, \mathbf{k} \in \mathcal{B}.$$

In practice, we are given an effective potential $V$ by a Density Functional Theory code, giving rise to a Hamiltonian operator $H = -\frac{1}{2}\Delta + V$, and a corresponding set of Bloch eigenstates $\{\psi_{n,\mathbf{k}} \mid \mathbf{k} \in \mathcal{B}, n \geq 1\}$.

**Composite Wannier functions** We now consider a set of the $N$ lowest bands

$$\sigma_N = \{\varepsilon_n(\mathbf{k}),\ \mathbf{k} \in \mathcal{B}\}_{n=1}^N,$$

and we assume that this set of bands is isolated from the others:

$$\mathrm{dist}(\sigma_N, \varepsilon_m(\mathbf{k})) > 0,\ \forall m > N, \forall \mathbf{k} \in \mathcal{B}.$$

There is no loss in generality in assuming that we consider only the lowest bands, as we took them for convenience of notation. However, taking the lowest bands also carries some physical importance, because they are associated with the ground state.

As before, there is a set of Bloch eigenstates $\left\{\psi_{n,\mathbf{k}}\right\}_{n=1}^N$, associated with the bands $\{\varepsilon_n(\mathbf{k})\}_{n=1}^N$ with $\mathbf{k} \in \mathcal{B}$. Let us remark that these Bloch eigenstates cannot be made regular with respect to

$\mathbf{k}$ in general, as eigenvalue crossings can prevent the continuity of eigenvectors [**?**]. However, the spectral projector $P_{\mathbf{k}}$ on the set of bands $\{\varepsilon_n(\mathbf{k})\}_{n=1}^N$ is not only continuous, but analytic [78]. There is a characterization of the spectral projector $P_{\mathbf{k}}$ by the Bloch eigenstates, as follows. For any $v \in L^2_{\text{per}}(\mathbb{R}^d;\mathbb{C})$, and $\langle\cdot,\cdot\rangle_{L^2_{\text{per}}}$ denoting the scalar product of $L^2_{\text{per}}(\mathbb{R}^d;\mathbb{C})$,

$$P_{\mathbf{k}} v = \sum_{n=1}^{N} \psi_{n,\mathbf{k}} \langle \psi_{n,\mathbf{k}}, v\rangle_{L^2_{\text{per}}}.$$

Since the Bloch eigenstates cannot be chosen to be regular with respect to $\mathbf{k}$ in general, one relaxes the problem to finding a set of Bloch waves $\left\{\widetilde{\psi}_{n,\mathbf{k}}\right\}_{n=1}^N$ which is an orthonormal basis of $\text{Ran}(P_{\mathbf{k}})$, called a *Bloch frame*.

We define the Wannier functions associated to the Bloch frame $\left\{\widetilde{\psi}_{n,\mathbf{k}}\right\}_{n=1}^N$ as

$$W_{n,\mathbf{R}} = \int_{\mathbf{k}\in\mathcal{B}} \mathrm{e}^{-i\mathbf{k}\cdot\mathbf{R}}\, \widetilde{\psi}_{n,\mathbf{k}}\, d\mathbf{k}.$$

Furthermore, we have the following important result. If there exists $\beta > 0$, such that the Bloch waves $\mathbf{k} \mapsto \widetilde{\psi}_{n,\mathbf{k}}$, $1 \le n \le N$ are complex analytic on a strip $\Omega_\beta$,

$$\Omega_\beta = \left\{ \mathbf{z} \in \mathbb{C}^d \,\middle|\, |\text{Im}(z_i)| < \beta,\ \forall 1 \le i \le d \right\},$$

and there exists a constant $C > 0$ such that

$$\int_{\mathcal{B}} \|\widetilde{\psi}_{n,\mathbf{k}+i\mathbf{h}}\|\, d\mathbf{k} \le C, \quad \text{for any } \mathbf{h} \text{ such that } \max_{1\le i\le d} |h_i| < \beta,$$

then the Wannier functions are exponentially localized, *i.e.* for any $0 < \alpha < \beta$, $\mathbf{x} \mapsto \mathrm{e}^{\alpha|\mathbf{x}|} W_{n,\mathbf{R}}(\mathbf{x})$ are $L^2(\mathbb{R}^d;\mathbb{C})$. It remains to compute the Bloch frame that allows for localization, when possible, which is the subject of later paragraphs. However, first, we demonstrate a particular application for which an analytic Bloch frame (hence an exponentially localized Wannier function) is useful in practice.

**Application: Wannier interpolation** Finding an analytic Bloch frame on the Brillouin Zone (or equivalently, exponentially-localized Wannier functions) is useful in practice, for example to construct accurate band diagrams with sparse sampling through Wannier interpolation (see [67] and references therein). This can be done through Fourier interpolation of the Hamiltonian operator projected on the Bloch frame.

First, we recall the general process of Fourier interpolation. Let $f$ be a smooth periodic function of $[0, 2\pi]$. Assume that we are given the values of $f$ on a set of $2M+1$ equispaced points $t_j = \frac{2\pi m}{2M+1}$, $0 \le m \le 2M$. To produce a periodic interpolation of this function, it is natural to consider approaching it by a truncated Fourier series.

$$p(x) = \sum_{m=-M}^{M} c_m \mathrm{e}^{imx}.$$

We thus have $2M+1$ values, and $2M+1$ unknowns, and it is a classical result that the associated linear system is invertible, which gives one and only one solution to this interpolation problem.

We now apply this technique to the interpolation of band structures. The naive way to construct a band diagram is to calculate the eigenvalues of the Hamiltonian at a set of sampling points, and then to interpolate between these values. However, when eigenvalues collide, this

method is not optimal, as the eigenvalues exhibit cusps at the collisions, which makes them locally non-differentiable, thus greatly reducing the precision of interpolation.

There is however a way to systematically work around this issue, (and increase the overall precision in so doing). Let us define some useful notation to that extent.

Denote $\mathbf{k} \mapsto \widetilde{u}_{n,\mathbf{k}}, 1 \leq n \leq N$, the periodic part of a Bloch frame associated with the first $N$ bands $\varepsilon_1(\mathbf{k}) \leq \cdots \leq \varepsilon_N(\mathbf{k}), \forall \mathbf{k} \in \mathcal{B}$. For each $\mathbf{k} \in \mathcal{B}$, it is a basis of the spectral subspace $\mathrm{Ran}\,(P_{\mathbf{k}})$, and in this basis, the operator $H_{\mathbf{k}}$ is reduced to the $N \times N$ matrix

$$A_{mn}(\mathbf{k}) = \langle \widetilde{u}_{m,\mathbf{k}}, H_{\mathbf{k}} \widetilde{u}_{n,\mathbf{k}} \rangle, \quad 1 \leq m, n \leq N.$$

If each $\mathbf{k} \mapsto \widetilde{u}_{n,\mathbf{k}}$ is analytic and $\mathcal{R}'$-quasi-periodic, then the matrix $\mathbf{k} \mapsto A(\mathbf{k})$ is analytic and periodic, and in particular, it does not have cusps. Thus, a Fourier interpolation of the coefficients of $\mathbf{k} \mapsto A(\mathbf{k})$ yields a more accurate band diagram than the interpolation of eigenvalues.

Figure 1.4 compares the convergence of Fourier interpolation of eigenvalues and coefficients for a $1d$ toy model, where the reduced Hamiltonian is

$$A(k) = \begin{pmatrix} 1 + \cos(2\pi k) & 0 \\ 0 & 1 - \cos(2\pi k) \end{pmatrix}, \quad \forall k \in [0, 1).$$

It follows that the eigenvalues $\varepsilon_1(k) \leq \varepsilon_2(k)$ are

$$\varepsilon_1(k) = \min\left(A_{11}(k), A_{22}(k)\right), \quad \varepsilon_2(k) = \max\left(A_{11}(k), A_{22}(k)\right), \quad \forall k \in [0, 1),$$

which both present a cusp at $\frac{1}{4}$ and $\frac{3}{4}$, where they cross each other. On the left, one can see that the interpolated eigenvalues are quite different from the exact ones, especially at the eigenvalue crossings, even for a comparatively high number of sampling points. By contrast, the right figure shows the interpolation of coefficients, where this problem is avoided. In this case, 3 sampling points are sufficient to replicate the exact eigenvalues, which is due to the particular form of the toy model.

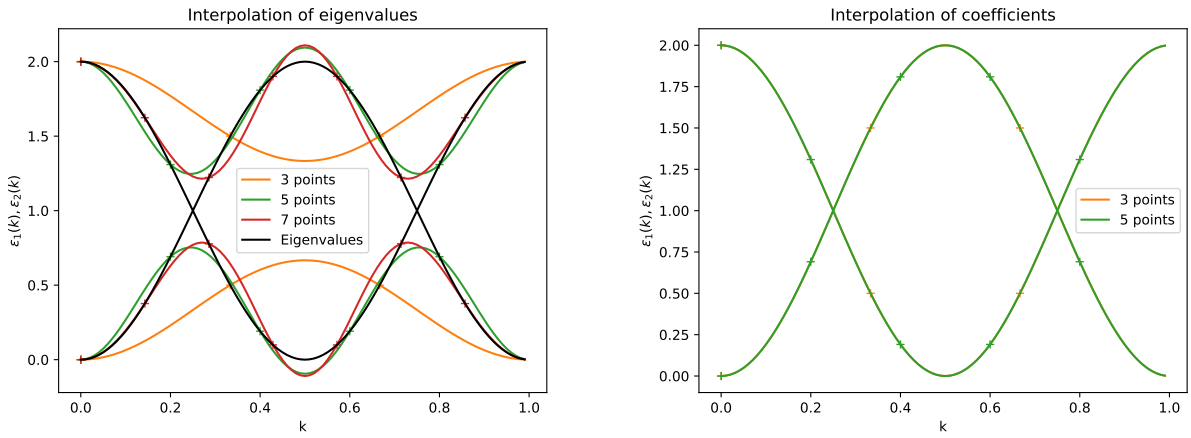


Figure 1.4: Eigenvalue and coefficient Fourier interpolation, compared for different amounts of sampling points.

**Topological obstruction to the existence of localized Wannier functions** We now discuss the matter of the optimal regularity in $\mathbf{k}$ of the Bloch frame. This is in fact a topological question, and the existence of an analytic Bloch frame is equivalent to the triviality of a topological characteristic, *i.e.* the Chern number (defined in a later paragraph in our context),

being zero [78]. It may seem surprising to need such tools, but framing the problem differently makes the connection more straightforward. Indeed, the Brillouin Zone, due to the periodic boundary conditions, has the topology of a torus, and for each point $\mathbf{k} \in \mathcal{B}$, our problem is to build an orthonormal basis of the (complex) vector space $\mathrm{Ran} P_{\mathbf{k}}$ that is as regular as possible. One can associate a topological object to this problem, called a *fiber bundle*, which allows us to characterize the existence of a regular and quasi-periodic Bloch frame on $\mathcal{B}$.

A simple example of this kind of structure is the Möbius strip, in Figure 1.5. It can be decomposed as a simple line (the fiber) relying on a circle. In this case, if we consider the real vector space on the fiber, and our problem is to find a regular normed vector that spans the fiber. As we consider a real vector space, our only choice is the orientation of the tangent vector, represented by arrows on the figure. However, because of the topology of the Möbius strip, after one turn around the circle, the vector is upside-down. It is thus impossible to have a normed continuous basis of the associated fiber bundle.

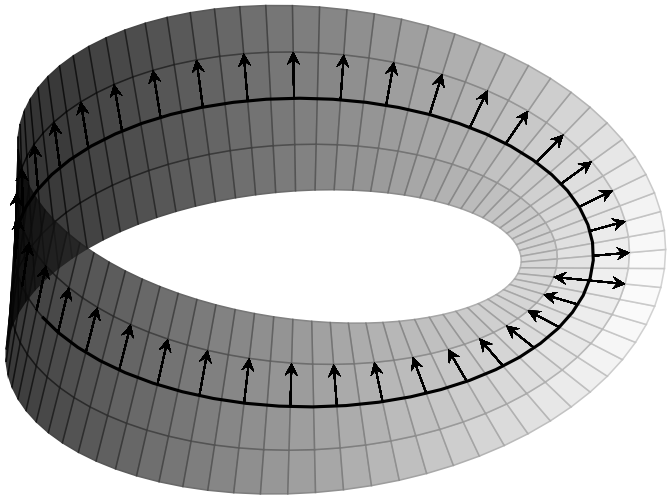

Figure 1.5: Möbius strip as a fiber bundle.

In vector bundle theory, the existence of an orthonormal basis that varies continuously with respect to $\mathbf{k}$ amounts to what is called the triviality of the bundle (see [78]). We are now equipped to discuss the *Bloch bundle*, the vector fiber bundle associated with the spectral projectors $\{P_{\mathbf{k}}\}_{\mathbf{k}\in\mathcal{B}}$.

**The Bloch bundle** Let $\{P_{\mathbf{k}}\}_{\mathbf{k}\in\mathbb{R}^d}$ be the spectral projectors of $\{H_{\mathbf{k}}\}_{\mathbf{k}\in\mathbb{R}^d}$ associated with the isolated set of bands $\sigma_N$. Define the unitary multiplication operator $\tau_{\mathbf{k}}$ for $\mathbf{k} \in \mathbb{R}^d$ given by, for $u \in L^2_{\mathrm{per}}(\mathbb{R}^d; \mathbb{C})$, for almost any $\mathbf{x} \in \mathbb{R}^d$,

$$(\tau_{\mathbf{k}} u)(\mathbf{x}) = \mathrm{e}^{i\mathbf{k}\cdot\mathbf{x}} u(\mathbf{x}).$$

This unitary operator allows to switch from the Bloch Transform picture (the $\mathbf{k} \mapsto u_{n,\mathbf{k}}$), to the Bloch waves $\mathbf{k} \mapsto \psi_{n,\mathbf{k}} = \tau_k u_{n,\mathbf{k}}$. Recall that the $\mathbf{k} \mapsto u_{n,\mathbf{k}}$ satisfy the $\mathcal{R}'$-quasi periodicity relation, which can be rewritten

$$u_{n,\mathbf{k}+\mathbf{K}} = \tau_{\mathbf{K}} u_{n,\mathbf{k}}, \quad \forall \mathbf{k} \in \mathbb{R}^d, \forall \mathbf{K} \in \mathcal{R}'.$$

One can show that the spectral projectors satisfy three conditions.

- *Analyticity:* the map $\mathbf{k} \mapsto P_{\mathbf{k}}$ is real-analytic on $\mathbb{R}^d$.
- *$\tau$-covariance:* the map $\mathbf{k} \mapsto P_{\mathbf{k}}$ satisfies:
$$P_{\mathbf{k}+\mathbf{K}} = \tau_{\mathbf{K}}^{-1} P_{\mathbf{k}} \tau_{\mathbf{K}}, \ \forall \mathbf{K} \in \mathcal{R}'.$$
- *Time-reversal symmetry:* the map $\mathbf{k} \mapsto P_{\mathbf{k}}$ satisfies
$$P_{-\mathbf{k}} = \Theta P_{\mathbf{k}} \Theta^{-1},$$
where $\Theta$ is the complex conjugation anti-unitary operator.

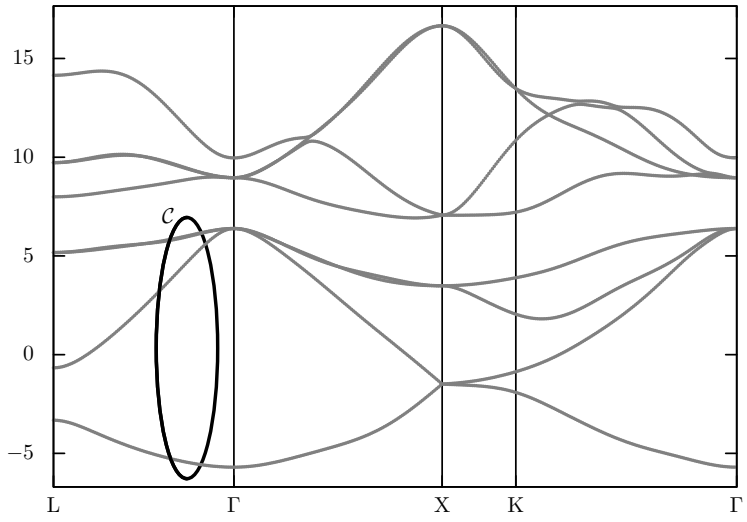


Figure 1.6: Contour enclosing the lower energy bands of Silicon

The proof of these statements can be found in [79], and is based on a characterization of the spectral projector by a Cauchy integral. Let $\mathcal{C}$ be a complex contour around the energy bands, as per Figure 1.6. Then the Riesz formula applied to the projector on the enclosed bands states that

$$P_{\mathbf{k}} = \frac{1}{2\pi i} \oint_{\mathcal{C}} (z - H_{\mathbf{k}})^{-1} \ \mathrm{d}z.$$

In the paragraphs on Wannier functions, we stated results for a Bloch frame that is complex analytic in $\mathbf{k}$. The existence of such a frame depends on the topological properties of the family of spectral projectors, a matter to which we turn next.

**The Chern number** For simplicity of presentation, we assume that $d = 2$, the only case we consider in later chapters. In that context, the Chern number associated with the spectral projectors is expressed as

$$c(P) = \frac{1}{2\pi i} \int_{\mathcal{B}} \mathrm{Tr}\left(P_{\mathbf{k}}[\partial_1 P_{\mathbf{k}}, \partial_2 P_{\mathbf{k}}]\right) \ dk_1 dk_2.$$

Informally, the Bloch bundle is the complex vector bundle associated with the $\{P_{\mathbf{k}}\}_{\mathbf{k}\in\mathcal{B}}$. For a precise definition, we refer to [78]. Furthermore, in [78] and [79], one can find a proof that the composite Wannier functions are exponentially localised if and only if the Chern number of the associated spectral projectors is zero. We rely on this characterization in what follows.

We have presented the definition of Wannier functions, given a theoretical characterization for their exponential localization through the Chern number of the associated Bloch bundle, and provided an alternative definition of the Chern number in simpler terms that hopefully give the reader more intuition on the topic. Next, we turn to the matter of how to compute Wannier functions in practice.

### 1.2.2 Numerical construction of Wannier functions

Wannier functions can be built numerically, based on *ab-initio* computations that provide a basis of Bloch waves on a grid of the Brillouin Zone. Then localising the Wannier functions is equivalent to choosing a regular gauge of these Bloch waves, a post-processing step that requires much less computational power than *ab-initio* calculations, and yet has very useful properties.

#### Marzari-Vanderbilt localization optimization

For a set of Wannier functions $\{W_{n,\mathbf{R}}\}_{n=1}^N$, we define the localization functional

$$\Omega\left(\{W_{n,\mathbf{R}}\}_{n=1}^N\right) = \sum_{n=1}^N \left( \int_{\mathbb{R}^d} \mathbf{x}^2 |W_{n,\mathbf{R}}(\mathbf{x})|^2 \, d\mathbf{x} - \left( \int_{\mathbb{R}^d} \mathbf{x} |W_{n,\mathbf{R}}(\mathbf{x})|^2 \, d\mathbf{x} \right)^2 \right).$$

It measures the quadratic spreads of the Wannier functions around their centers, and one easily checks that for any $\mathbf{R} \in \mathcal{R}$,

$$\Omega\left(\{W_{n,\mathbf{R}}\}_{n=1}^N\right) = \Omega\left(\{W_{n,\mathbf{0}}\}_{n=1}^N\right).$$

This functional is well-defined only for appropriately localized Wannier functions, which we assume in this section.

One can split the localization into two parts

$$\Omega = \Omega_I + \widetilde{\Omega},$$

where

$$\Omega_I\left(\{W_{n,\mathbf{0}}\}_{n=1}^N\right) = \sum_{n=1}^N \left( \int_{\mathbb{R}^d} \mathbf{x}^2 |W_{n,\mathbf{0}}(\mathbf{x})|^2 \, d\mathbf{x} - \sum_{\substack{\mathbf{R}\in\mathcal{R},\\ 1\le m\le N}} \left| \int_{\mathbb{R}^d} \mathbf{x} W_{m,\mathbf{R}}(\mathbf{x}) W_{n,\mathbf{0}}(\mathbf{x}) \, d\mathbf{x} \right|^2 \right).$$

and

$$\widetilde{\Omega}\left(\{W_{n,\mathbf{0}}\}_{n=1}^N\right) = \sum_{n=1}^N \sum_{(\mathbf{R},m)\neq(\mathbf{0},n)} \left| \int_{\mathbb{R}^d} \mathbf{x} W_{m,\mathbf{R}}(\mathbf{x}) W_{n,\mathbf{0}}(\mathbf{x}) \, d\mathbf{x} \right|^2.$$

$\Omega_I$ can be shown to be invariant to the choice of the Bloch frame, by rewriting its components in terms of spectral projectors. See [66] and references therein for a more in-depth presentation.

Each part of the localization functional can be alternatively written in the $\mathbf{k}$-space representation. Using the correspondence between Wannier functions and Bloch frames, one can show that

$$\int_{\mathbb{R}^d} \mathbf{x} W^*_{m,\mathbf{R}}(\mathbf{x}) W_{n,\mathbf{0}} \, d\mathbf{x} = i \frac{1}{|\mathcal{B}|} \int \mathrm{e}^{i\mathbf{k}\cdot\mathbf{R}} \langle \widetilde{u}_{m,\mathbf{k}}, \nabla_{\mathbf{k}} \widetilde{u}_{n,\mathbf{k}} \rangle \, d\mathbf{k},$$

and

$$\int_{\mathbb{R}^d} \mathbf{x}^2 W^*_{m,\mathbf{R}}(\mathbf{x}) W_{n,\mathbf{0}} \, d\mathbf{x} = -\frac{1}{|\mathcal{B}|} \int \mathrm{e}^{i\mathbf{k}\cdot\mathbf{R}} \langle \widetilde{u}_{m,\mathbf{k}}, \nabla^2_{\mathbf{k}} \widetilde{u}_{n,\mathbf{k}} \rangle \, d\mathbf{k},$$

one can rewrite $\Omega(\{W_{n,\mathbf{0}}\}_n)$ only in terms of the periodic part of the Bloch frames $\{\mathbf{k} \mapsto \widetilde{u}_{n,\mathbf{k}}\}_{n=1}^N$. This form makes it clear that the regularity of the Bloch frame is directly linked to the localization of the Wannier functions. Moreover, a finite-difference scheme yields a straightforward discrete version of the functional. The degrees of freedom being a choice of a unitary change of basis at each $\mathbf{k}$ point, one can then use a gradient descent in the space of unitary matrices to smoothen the Bloch frame, therefore producing a more localized set of Wannier functions.

In [79], it is shown that the minimizers of the localization functional $\Omega$ are maximally-localized Wannier functions (almost exponentially localized functions), and a smooth Bloch frame $\mathbf{k} \mapsto \{u_{n,\mathbf{k}}\}$. The rationale is that the algorithm should converge to these minimizers, provided we have a good initial guess that satisfies $\Omega < \infty$.

In the original paper [67], the initial guess is obtained by a projection method. Reference orbitals are given as a manual input, and result from physical considerations. They are then projected onto the eigenspace of the Hamiltonian, and renormalized. The issue with this method is that it is neither systematic, nor fully reliable: it can produce initial guesses that do not allow the procedure to converge. Hence, we turn to the problem of constructing a good initial guess, that is, a continuous and periodic Bloch frame. This problem can be formulated in terms of finding a homotopy between paths of unitary matrices.

### Building a continuous and periodic Bloch frame

To build a continuous and periodic Bloch frame, we proceed constructively, based on the approach proposed in [13].

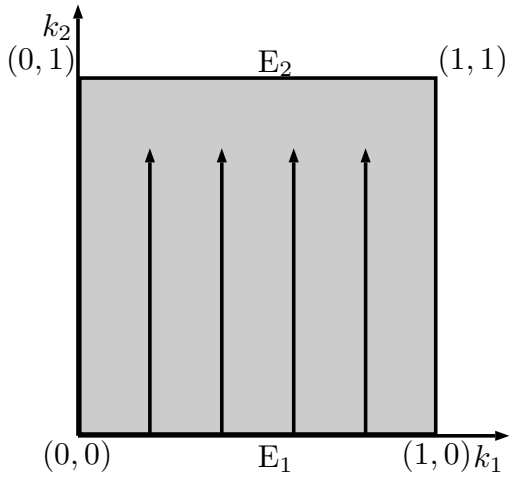


Figure 1.7: Schematic representation of the Brillouin Zone

Start by an initial (not necessarily continuous) Bloch frame $\mathbf{k} \mapsto \Psi_{\mathbf{k}} = (\psi_{1,\mathbf{k}}, \ldots, \psi_{N,\mathbf{k}})$ defined on the Brillouin Zone. From this, one can always construct a smooth Bloch frame (generating the same space) on an interval, by *parallel transport*. For some intuition, we describe the parallel transport for a discretisation of the interval $[0,1)$ with $N$ equispaced points. If $\{Q_s\}_{s\in[0,1)}$ is a smooth family of orthogonal projectors of rank 1, and if for $s = 0$, we have chosen a normalized basis vector of $\mathrm{Ran}(Q_0)$, denoted $\mathbf{v}(0)$, assuming $N$ is large enough, we have that $\|Q_{\frac{1}{N}}\mathbf{v}(0)\| > 0$, and a basis vector at $s = \frac{1}{N}$ is given by

$$\mathbf{v}\left(\frac{1}{N}\right) = \frac{Q_{\frac{1}{N}}\mathbf{v}(0)}{\|Q_{\frac{1}{N}}\mathbf{v}(0)\|}.$$

Since $Q_{\frac{1}{N}}$ is an orthogonal projector, this is the closest basis vector to $\mathbf{v}(0)$ (in the 2 norm). We then repeat this procedure until the end of the interval. It means that, at each value of $s$, we choose the basis vector that is closest to the previous basis vector, while enforcing normalization. This procedure is readily generalized to a basis of higher rank, replacing the normalization by the orthonormalization of the basis, using Löwdin orthogonalization. In the limit $N \to \infty$, we obtain a differential equation which is given in Chapter 2, where more details on this topic can be found. Hence, the only problem left to consider here is the periodicity.

- First, we consider the Bloch frame on edge 1 ($E_1$ on the figure). Construct a smooth Bloch frame on $E_1$, which we still denote $\Psi_{\mathbf{k}}$. Since the Bloch frames are a basis for the projector at $(0,0)$ and $(1,0)$, they span the same vector space, but the frames are not equal in general. Two bases of the same complex vector space being related by a unitary transformation, there exists an *obstruction matrix* $U_{\text{Obs}} \in \mathcal{U}(N)$, such that

$$\Psi_{(0,0)} = \Psi_{(1,0)} U_{\text{Obs}}^*.$$

  Because the group of unitary matrices $\mathcal{U}(N)$ is *connected* [102], there exists a continuous map $\mathcal{T} : [0,1] \to \mathcal{U}(N)$, such that $\mathcal{T}(0) = I$ and $\mathcal{T}(1) = U_{\text{Obs}}$. We can therefore modify the continuous Bloch frame to make it periodic on $E_1$, by redefining

$$\Psi_{(k_1,0)} \leftarrow \Psi_{(k_1,0)} \mathcal{T}(k_1), \quad \forall k_1 \in [0,1].$$

  One can construct such a map $\mathcal{T}$ for example using matrix powers. Since $U_{\text{Obs}}$ is unitary, it is a normal matrix $U_{\text{Obs}}^* U_{\text{Obs}} = U_{\text{Obs}} U_{\text{Obs}}^*$, and hence diagonalizable. There exists $V \in \mathcal{U}(N)$, and $\theta_1, \theta_n \in [0,1)$ such that

$$U_{\text{Obs}} = V \text{diag}\left(\mathrm{e}^{i2\pi\theta_1}, \ldots, \mathrm{e}^{i2\pi\theta_N}\right) V^*.$$

  We then define the matrix power by

$$\mathcal{T}(k_1) = U_{\text{Obs}}^{k_1} = V \text{diag}\left(\mathrm{e}^{i2\pi\theta_1 k_1}, \ldots, \mathrm{e}^{i2\pi\theta_N k_1}\right) V^*.$$

- We extend smoothly the Bloch frame on each vertical interval going from $(k_1, 0)$ to $(k_1, 1)$ for each $k_1 \in [0,1]$, represented on the figure by vertical arrows. We obtain a Bloch frame that is smooth on the Brillouin Zone, and periodic in $k_1$. As before, the Bloch frame on the edges $\mathrm{E}_1$ and $\mathrm{E}_2$ are not equal, but span the same space, and there exists a unitary obstruction matrix $U_{\text{Obs}}(k_1)$ for each $k_1 \in [0,1]$, such that

$$\Psi_{(k_1,0)} = \Psi_{(k_1,1)} U_{\text{Obs}}^*(k_1).$$

The question is therefore to know whether there exists a map $\mathcal{T}$ such that $\mathcal{T}(k_1, 0) = I$ and $\mathcal{T}(k_1, 1) = U_{\text{Obs}}(k_1)$ for each $k_1 \in [0,1]$, that is, to find a *homotopy* of $k_1 \mapsto U_{\text{Obs}}(k_1)$ to the constant map. Unfortunately, that is not always possible, and to see why, let us take the example $N = 1$, where $\mathcal{U}(1)$ is identified with the complex unit circle. For some intuition of the problem, we can rephrase the question in terms of the curves drawn by the map: $k_1 \mapsto U_{\text{Obs}}(k_1)$ parameterizes a loop on the circle, and we would like to deform it continuously to a point, without cutting the loop or letting it go through the hole of the circle. This picture hints at the impossibility of the process if the loop winds around the circle. In topological terms, the circle is not *simply connected* [102], and to know whether we can deform the loop to a point, it suffices to count the number of turns it does around the origin. This intuitive picture can be given a rigorous definition, which we turn to next.

The *winding number* $\deg(u)$ of the smooth parameterization $u : t \mapsto \mathrm{e}^{2\pi i\theta(t)}$, with $u(0) = u(1)$ and $u'(0) = u'(1)$, reads

$$\deg(u) = \frac{1}{2\pi i} \oint_{t\in[0,1]} \frac{u'(t)}{u(t)} dt.$$

It is an integer, as shown below. Since $z$ parameterizes the whole circle,

$$\mathrm{e}^{2\pi i\theta(0)} = \mathrm{e}^{2\pi i\theta(1)}, \quad \textit{i.e. } \theta(0) \equiv \theta(1) \bmod 1.$$

Moreover,

$$\deg(u) = \frac{1}{2\pi i} \oint_{t\in[0,1]} \frac{u'(t)}{u(t)} dt = \frac{1}{2\pi i} \oint_{t\in[0,1]} 2\pi i \theta'(t) dt = \theta(1) - \theta(0).$$

It follows that $\deg(u) \in \mathbb{Z}$. One can show that the winding number is a continuous map from the space of paths that can be deformed into each other to the integers. Hence, it follows that the winding number is the same for all paths that can be deformed into each other, and by contraposition, two paths with different winding numbers cannot be deformed into each other. Moreover, given a loop parameterized by $u : t \mapsto \mathrm{e}^{2\pi i \theta(t)}$ with winding number 0, one can construct such a homotopy explicitly, for example $\widetilde{u} : (t, s) \mapsto \mathrm{e}^{2\pi i s \theta(t)}$. It verifies for all $t \in [0, 1]$, $\widetilde{u}(t, 0) = 1$, $\widetilde{u}(t, 1) = u(t)$, and for each $s \in [0, 1]$, $t \mapsto \widetilde{u}(s, t)$ is continuous. Therefore, a necessary and sufficient condition for the existence of a homotopy of a loop parameterized by $u$ is that $\deg(u) = \deg(t \mapsto 1) = 0$.

Coming back to our problem for $N = 1$, this means that one can define a smooth, periodic Bloch frame if and only if the winding number of $k_1 \mapsto U_{\mathrm{Obs}}(k_1)$ is equal to 0.

We now turn to the general case $N \geq 1$, which reduces to the previous one. Indeed, one can decompose any unitary matrix $U \in \mathcal{U}(N)$ into a matrix in $\mathcal{SU}(N)$, and an element of $\mathcal{U}(1)$, its determinant. This is useful because $\mathcal{SU}(N)$ is *simply connected* [102], which means that any loop in $\mathcal{SU}(N)$ can be deformed to a point. If we have such a decomposition for the map $k_1 \mapsto U_{\mathrm{Obs}}(k_1)$, *i.e.* there exists a continuous and periodic map $k_1 \mapsto W_{\mathrm{Obs}}(k_1)$ with values in $\mathcal{SU}(N)$, such that

$$U_{\mathrm{Obs}}(k_1) = \det\left(U_{\mathrm{Obs}}(k_1)\right) W_{\mathrm{Obs}}(k_1), \quad \forall k_1 \in [0, 1].$$

Since $\mathcal{SU}(N)$ is simply connected, there exists a homotopy of $k_1 \mapsto W_{\mathrm{Obs}}(k_1)$ to the constant map, and the only problem that remains is the homotopy of the determinant, which exists if and only if its winding number is zero.

This observation suggests that the existence of a homotopy (hence, the existence of a regular Bloch frame) depends only on the winding number of the determinant of the obstruction matrix, which is confirmed by the following characterization of the Chern number. If the spectral projectors $\{P_{\mathbf{k}}\}_{\mathbf{k}\in\mathcal{B}}$ are analytic on the Brillouin Zone, the Chern number $c(P)$ of the bundle is equal to the winding number of the determinant of the obstruction loop. We have the following equalities:

$$\begin{aligned} c(P) &= \deg\left(\det\left(U_{\mathrm{Obs}}(\cdot)\right)\right) = \frac{1}{2\pi i} \oint_{\partial\mathcal{B}} \det(U_{\mathrm{Obs}}(\mathbf{k}))^{-1} \partial_{\mathbf{k}} (\det(U_{\mathrm{Obs}}(\mathbf{k}))) \, d\mathbf{k} \\ &= \frac{1}{2\pi i} \oint_{\partial\mathcal{B}} \mathrm{Tr}\left(U_{\mathrm{Obs}}(\mathbf{k})^{-1} \partial_{\mathbf{k}} U_{\mathrm{Obs}}(\mathbf{k})\right) \, d\mathbf{k}. \end{aligned}$$

The proof of this result relies on Stokes theorem, and some algebraic manipulations. To lighten this introduction, we refer the interested reader to [17] for a concise exposition.

There remains the question of how to construct such a homotopy in practice. In [13], the authors propose to use the matrix power, attempting to construct a continuous logarithm of the map $k_1 \mapsto U_{\mathrm{Obs}}(k_1)$, *i.e.* a continuous and periodic map from $[0, 1)$ to the hermitian matrices, denoted $k_1 \mapsto L(k_1)$, such that

$$U_{\mathrm{Obs}}(k_1) = \exp\left(iL(k_1)\right) \quad \forall k_1 \in [0, 1].$$

In practice, a logarithm can be constructed by diagonalizing $U_{\mathrm{Obs}}(k_1)$, and remarking that the eigenvalues are on the unit circle, hence there exists a unitary matrix $V(k_1)$, which can be chosen continuous with $k_1$ and periodic [51], and phases $\theta_1(k_1), \ldots, \theta_N(k_1)$, such that

$$U_{\mathrm{Obs}}(k_1) = V(k_1) \mathrm{diag}\left(\mathrm{e}^{i2\pi\theta_1(k_1)}, \ldots, \mathrm{e}^{i2\pi\theta_N(k_1)}\right) V^*(k_1).$$

The question is therefore whether one can find continuous and periodic phase functions $k_1 \mapsto \theta_1(k_1), \ldots, k_1 \mapsto \theta_N(k_1)$, satisfying the equation above. Unfortunately, this is not always possible, since the existence of continuous and periodic phases is determined by the winding number of each eigenvalue. However, the condition for the existence of a homotopy is only on the winding number of the determinant. There exists a simple counterexample where a homotopy exists, but no continuous logarithm can be found, which we present next.

$$U(s) = \begin{pmatrix} \mathrm{e}^{i2\pi s} & 0 \\ 0 & \mathrm{e}^{-i2\pi s} \end{pmatrix}, \quad \forall s \in [0,1].$$

The winding number of the eigenvalues is $\pm 1$, so there is no continuous and periodic logarithm, and yet, the determinant being identically 1, its winding number is trivial, hence there exists a homotopy. This counterexample is quite relevant, since it is a typical obstruction matrix path corresponding to some interesting materials called $\mathbb{Z}^2$ topological insulators, an example being the Kane-Mele model [49].

**Contribution 1**

In Chapter 2, we provide an alternative method to construct regular Bloch frames that can be proven to give an initial guess for the Marzari-Vanderbilt optimization process that is continuous, when that is possible (in the continuum limit of Brillouin Zone sampling). We give a construction of the homotopy of the obstruction that avoids the problems of the logarithm method.

Our method is based on a decomposition of the unitary matrix valued map into its columns, which corresponds to maps to the sphere. Fortunately, the sphere is simply connected, and a homotopy of a path on the sphere is readily constructed by normalizing a linear interpolation.

This method can be applied successfully to the Kane-Mele model, as shown in Figures 1.8a and 1.8b, which display selected components of the homotopy $k_1 \mapsto \mathcal{T}(k_1, k_2)$ for $k_2 = 1, \frac{2}{3}, \frac{1}{3}$.

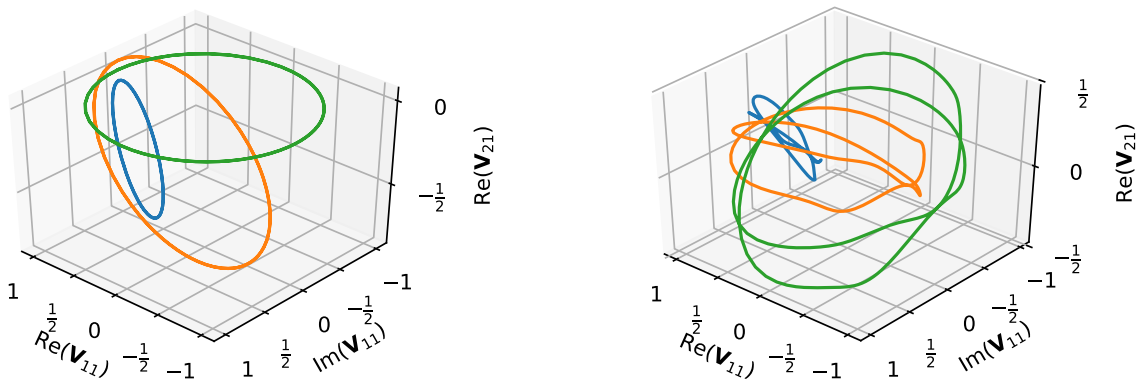


(a) $\lambda_\nu = 0, \lambda_R = 1$ (b) $\lambda_\nu = 1, \lambda_R = 1$

Figure 1.8: Contraction of the first column of the obstruction, with the initial path in green ($k_2 = 1$) being deformed to a single point (yellow at $k_2 = \frac{2}{3}$ then blue at $k_2 = \frac{1}{3}$).

### 1.2.3 Approximation of Wannier functions

As we have seen previously, Wannier functions can be used as a basis to compute tight-binding models of a perfect crystal. If the system is constituted of multiple layers of 2D perfect crystals that are weakly coupled, as is the case in Van der Waals heterostructures (see [98] and references

therein), under the physical assumption that the Wannier functions of the whole system are close to the Wannier functions of the isolated, one can parameterize an approximate tight-binding model for the whole system. This is particularly useful in the case of a non-periodic system, when the different 2D (periodic) crystals have incommensurate lattice parameters (the ratio of lattice parameters is not a rational number), or an angle that breaks the periodicity (the cosine, sine of the angle are not rational). Indeed, in that case, the standard computation methods for perfect crystals, relying on periodicity (through the Bloch transform), require to approximate the non-periodic system by a periodic one, with a large unit cell, at an increased computational cost.

### Symmetries in crystals

Each perfect crystal is invariant by a group of symmetries, that are a combination of rotations, reflections and translations, including lattice translations. These groups are called *space groups*, and there are only a finite number of them (230 space groups), although they can be represented in different ways. A general introduction to groups as they are used in physics can be found in [21].

Consider a crystal with a space group denoted $G$. Each element $g$ of the group $G$ can be represented by a pair $(R, \mathbf{a})$, where $R \in \mathcal{O}(d)$ is an orthogonal matrix, and $\mathbf{a} \in \mathbb{R}^d$ the translation vector, acting on a point $\mathbf{x} \in \mathbb{R}^d$ as

$$g\mathbf{x} = (R, \mathbf{a})\mathbf{x} = R\mathbf{x} + \mathbf{a}.$$

Given a point $\mathbf{q} \in \mathbb{R}^d$, called a *site*, the *site symmetry group* is the subgroup $G_\mathbf{q}$ of $G$ that leaves $\mathbf{q}$ invariant, that is, for each $(R, \mathbf{a}) \in G$,

$$g = (R, \mathbf{a}) \in G_\mathbf{q} \quad \text{if and only if} \quad R\mathbf{q} + \mathbf{a} = \mathbf{q}.$$

We refer the reader to [28] for an in-depth treatment of site symmetry groups.

### Symmetry-adapted Wannier functions

It is possible to choose Wannier functions that are adapted to the symmetries of the crystal. Denote $\{W_{n,\mathbf{q}}\}_{n=1}^N$ the set of Wannier functions centered at the site $\mathbf{q}$. The action of an element $g = (R, \mathbf{a}) \in G$ on a Wannier function $W$ is, for almost any $\mathbf{x} \in \mathbb{R}^d$,

$$(\widehat{g}W)(\mathbf{x}) = W(R^{-1}(\mathbf{x} - \mathbf{a})).$$

The set of Wannier functions $\{W_{n,\mathbf{q}}\}_{n=1}^N$ is said to be *symmetry-adapted* if for any $g = (R, \mathbf{a}) \in G_\mathbf{q}$, there exists a unitary matrix $U(g) \in \mathcal{U}(N)$, such that

$$\widehat{g}W_{n,\mathbf{q}} = \sum_{m=1}^{N} U_{mn}(g) W_{m,\mathbf{q}}.$$

This means that the vector space generated by the symmetry-adapted Wannier functions $\{W_{n,\mathbf{q}}\}_{n=1}^N$ centered at the site $\mathbf{q}$ is invariant under the site symmetry group $G_\mathbf{q}$. In group theory, the unitary matrices $U(g)$ are related to the so-called *irreducible representations* of the site symmetry group ([28],[21]). Furthermore, one can adapt the numerical construction introduced by Marzari and Vanderbilt to produce symmetry-adapted Wannier functions. The curious reader can refer [87] for more on this topic.

**Gaussian Type Orbitals**

*Gaussian Type Orbitals*, that is, gaussians multiplied by polynomials, are a useful set of functions for computations, for which the $L^2$ scalar product of two functions can be computed analytically. Further, one can build *symmetry adapted Gaussian Type Orbitals* by applying a symmetrization procedure (detailed later).

**Contribution 2** In Chapter 3, we present a method to approximate symmetry-adapted Wannier functions by symmetry-adapted Gaussian Type Orbitals. These approximate Wannier functions are then used to compute the reduced Hamiltonian of an aperiodic system, twisted bilayer graphene, using the lower computational cost of gaussian integrals to reduce the calculation time.

In Figure 1.9, we show the isosurface plot of a Wannier function of graphene, and its approximation with our method. The relative approximation error, measured in $H^1$ norm, is about 2.27%.

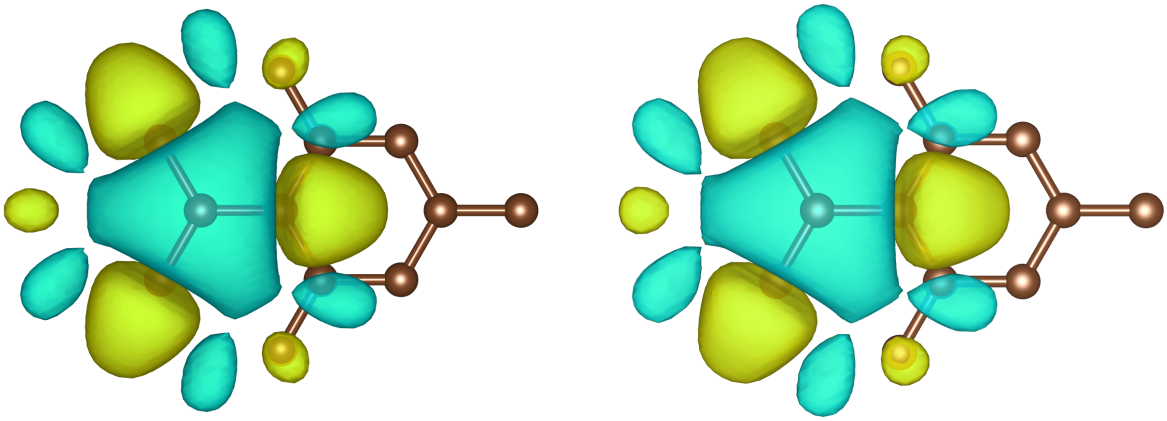

Figure 1.9: Original Wannier function (left), and best approximation with $H^1$ norm (right), isosurface at 1% of maximum value.

## 1.3 Electronic transport

Until now, we have only considered stationary electronic states. Next, we turn to electronic transport, the dynamics of electrons subjected to an external electric field.

### 1.3.1 Description of the system

In this section, we consider a system of independent spinless electrons in a perfect crystal with lattice $\mathcal{R}$, with one-body Hamiltonian

$$H = \frac{1}{2}(-i\nabla + \mathcal{A})^2 + V,$$

where $\mathcal{A} \in L^4_{\mathrm{per}}(\mathbb{R}^d;\mathbb{R}^d)$ and $V \in L^2_{\mathrm{per}}(\mathbb{R}^d;\mathbb{R})$ are $\mathcal{R}$-periodic functions, $V$ is the effective potential, describing the interaction of the electrons with the nuclei of the crystal, and $\mathcal{A}$ is the magnetic vector potential, which satisfies the Coulomb gauge choice, $\nabla \cdot \mathcal{A} = 0$ in the sense of distributions. Note that the magnetic vector potential $\mathcal{A}$, which was absent in the previous sections, is chosen to be periodic. This explicitly excludes the case of a non-zero uniform magnetic field, which is the necessary condition for the quantum Hall effect (see [53], [59]). However, our formalism allows for the Quantum Anomalous Hall effect [46].

We perform our analysis with this particular Hamiltonian, but it can easily be extended to spin-dependent continuous models, tight-binding models, or 2D materials such as graphene (for which the physical space is three-dimensional while the periodic lattice is two-dimensional).

### 1.3.2 Density matrix formalism

In the previous sections, we have described quantum pure states as unit vectors $\psi$ in $\mathcal{H}$. In the case of many independent electrons, there is an operator formulation which we will use in this section and the related chapter, with the *density matrix*.

To give a precise definition, a few prerequisites are in order. For a non-negative bounded self-adjoint operator $A$ on $\mathcal{H}$, and $\{e_n\}_{n\geq 1}$ an orthonormal Hilbert basis of $\mathcal{H}$, define the *trace* of $A$ by

$$\mathrm{Tr}(A) = \sum_{n\geq 1} \langle e_n, Ae_n \rangle,$$

whose value does not depend on the particular choice of basis. If $\mathrm{Tr}(A) < \infty$, we say that $A$ is *trace class*. If $A$ is a bounded self-adjoint operator (without sign), it is trace class if the non-negative operators $\mathbb{1}_{\mathbb{R}^+}(A)A$ and $-\mathbb{1}_{\mathbb{R}^-}(A)A$ are trace-class.

The *density matrix* $\gamma$ of a system with $N$ independent spinless electrons is a bounded self-adjoint operator on $\mathcal{H}$, which satisfies $\mathrm{Tr}(\gamma) = N$. It describes the state of the system, and for any bounded observable (bounded self-adjoint operator on $\mathcal{H}$) $A$, the expectation value of $A$ in the state $\gamma$ is given by $\mathrm{Tr}(A\gamma)$.

This definition is readily generalized to a perfect crystal, with Bravais lattice $\mathcal{R}$, and unit cell $\Omega$, at the cost of considering periodic operators, and replacing the trace by the *trace per unit volume*, denoted $\underline{\mathrm{Tr}}$. For a bounded $\mathcal{R}$-periodic operator $A$ on $\mathcal{H}$, the trace per unit volume of $A$ is defined by

$$\underline{\mathrm{Tr}}(A) = \frac{1}{|\Omega|} \mathrm{Tr}\left(\mathbb{1}_\Omega A \mathbb{1}_\Omega\right),$$

where $\mathbb{1}_\Omega$ is the characteristic function of the unit cell $\Omega$, with volume $|\Omega|$. Then, a density matrix $\gamma$ is a bounded periodic operator satisfying $\underline{\mathrm{Tr}}(\gamma) = N$, where $N$ is the number of electrons per unit cell in the crystal.

The ground state density matrix $\gamma_0$ (at zero temperature) of the system is the state with the lowest energy. This condition is satisfied when $\gamma_0 = \mathbb{1}(H \leq \varepsilon_F)$, where $\varepsilon_F$ is the Fermi level, *i.e.* when $\gamma$ is the projector onto the eigenstates of energy lower than $\varepsilon_F$.

We now turn to the dynamics of the density matrix, for which the equivalent of the Schrödinger equation is the Liouville-von Neumann equation,

$$i\partial_t \gamma = [H, \gamma], \quad \gamma(0) = \gamma_0, \tag{1.1}$$

where $H$ denotes the Hamiltonian operator. Formally, this equation is solved by

$$\gamma(t) = \exp(-itH)\gamma_0 \exp(itH), \quad \forall t \in \mathbb{R}. \tag{1.2}$$

The strong formulation (1.1) of the Liouville-von Neumann equation has some domain issues, because $H$ being an unbounded operator in general, denoting $\mathcal{D}$ its domain, it requires that $\mathrm{Ran}\gamma(t) \in \mathcal{D}$ for all $t$. Hence, in the associated chapter, we will use instead its mild formulation (1.2), since the strongly-continuous unitary group $(\exp(itH))_{t\in\mathbb{R}}$ circumvents domain issues.

### 1.3.3 Transport equation: perturbation by an electric field

If a crystal is subjected to an external electric field, one expects that the electrons (if they are "free" in some sense) while be set in motion and generate a current. How does this simple, classical picture translate to the quantum picture?

There are different types of crystals, classified by the form of their band diagram around the Fermi level, which determines the behavior of their electrons when perturbed by an electric field. As we have remarked in a previous section, a perfect crystal is called an *insulator* if its Fermi level lies within a gap between its bands, and the gap is large (more than about 3 eV). If the gap is smaller, the material is called a *semi-conductor*, which has useful properties that we do not consider in this analysis. On the other hand, if the Fermi level crosses the bands, and the intersection is not degenerate (forming a surface), then the crystal is a *metal*. If, on the other hand, the intersection is degenerate, *e.g.* constituted by a set of isolated points, then the material is a *semi-metal*. An example of this is graphene, a $2D$ crystal with a honeycomb lattice of carbon atoms, where the bands present a conical singularity(a *Dirac cone*) at the Fermi level, crossing at so-called *Dirac points* (see Figure 1.10).

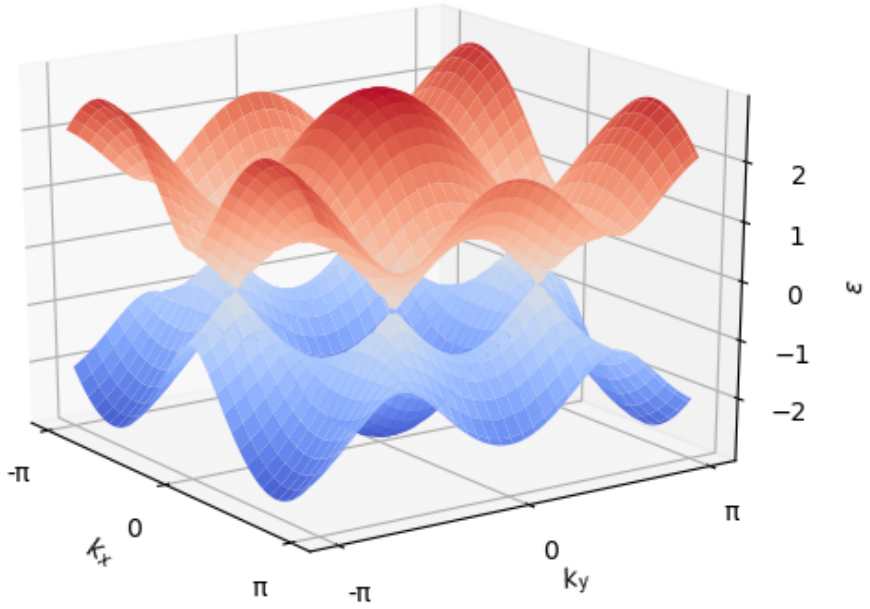


Figure 1.10: A simple model of Graphene, with conical singularities at the Dirac points.

A uniform electric field $E = \epsilon e_\beta$, where $e_\beta$ is the vector giving the direction of the field, and $\epsilon$ a parameter defining its strength, can modify the Hamiltonian of the system in two equivalent ways: an electrostatic potential, and a time-dependent vector potential. This is a result of Maxwell's equations, which give the electric field produced by a scalar potential $V_E$ and a time-dependent vector potential $\mathcal{A}_E$ as

$$E = -\nabla V_E - \partial_t \mathcal{A}_E.$$

Hence, for the gauge choice $V_E = \epsilon x_\beta, \mathcal{A}_E = 0$ one can obtain the Hamiltonian of the system,

$$H^\epsilon_\beta = \frac{1}{2}(-i\nabla + \mathcal{A})^2 + V - \epsilon x_\beta.$$

We study the evolution of the density matrix for a system starting in the ground state $\gamma_0 = \mathbb{1}(H \leq \varepsilon_F)$ (the equilibrium without an electric field), and for $t > 0$, the dynamics given by the Hamiltonian $H^\epsilon_\beta$,

$$\gamma^\epsilon_\beta(t) = \exp\left(-iH^\epsilon_\beta t\right) \gamma_0 \exp\left(iH^\epsilon_\beta t\right), \quad \forall t \geq 0.$$

Using the choice of gauge $V_E = 0$ and $\mathcal{A}_E = -\epsilon e_\beta t$, we obtain the alternative, but equivalent Hamiltonian

$$\widetilde{H}^\epsilon_\beta(t) = \frac{1}{2}(-i\nabla + \mathcal{A} - \epsilon e_\beta t)^2 + V.$$

The equivalence is understood introducing the change of electromagnetic gauge operator $G_q$, for some $q \in \mathbb{R}^d$, a unitary multiplication operator on $L^2(\mathbb{R}^d)$, defined by

$$\forall u \in L^2(\mathbb{R}^d), \quad (G_q u)(x) = e^{iq\cdot x} u(x), \quad \text{for a.a. } x \in \mathbb{R}^d.$$

Then, one can show that, for any $t \in \mathbb{R}$,

$$\widetilde{H}^\epsilon_\beta(t) = G_{\epsilon t e_\beta} H^\epsilon_\beta G^*_{\epsilon t e_\beta}.$$

Because $\widetilde{H}^\epsilon_\beta(t)$ does not break periodicity, in the proofs, we will use both Hamiltonians, and the associated density matrices.

To measure the electrical current, we introduce the *current operator* $J_\alpha$ in the direction $e_\alpha$ (and in the gauge $\mathcal{A}_E = 0$), defined by

$$J_\alpha = -(-i\nabla + \mathcal{A}) \cdot e_\alpha.$$

This operator contains the momentum of the electrons $\widehat{p} = (-i\nabla + \mathcal{A})$, multiplied by the charge of the electron, $q = -1$ in atomic units. The system at time $t$ is described by the density matrix $\gamma^\epsilon_\beta(t)$, hence the electrical current per unit volume is given by

$$j^\epsilon_{\alpha,\beta}(t) = \underline{\mathrm{Tr}}(J_\alpha \gamma^\epsilon_\beta(t)).$$

We will consider only the motion of electrons in the limit of "weak" external electric fields, that is, $\epsilon \ll 1$, and compute a first order expansion of the current, relying on two established approaches: adiabatic theory and linear response. Adiabatic theory characterizes the evolution of a system driven by a time-dependent Hamiltonian, such as $\widetilde{H}^\epsilon_\beta(t)$ that is slowly varying in time. Linear response theory studies the first order perturbation of a system in which a small additional term has been implemented in the Hamiltonian, as in $H^\epsilon_\beta$. We define the time-averaged conductivity

$$\sigma_{\alpha,\beta} = \lim_{t\to\infty} \frac{1}{t} \int_0^t \lim_{\epsilon\to 0} \frac{j^\epsilon_{\alpha,\beta}(t')}{\epsilon} dt',$$

which is the linear response coefficient (when it is finite) of the current in the limit $\epsilon \to 0$. Since there is no dissipation in our model, the linear response to the stepwise introduction of a perturbation can be oscillatory, and averaging in time might be necessary.

**Contribution 3:** In Chapter 4, we develop a unified framework to compute transport properties of electrons in various materials, based on the tools described in this introduction. In particular, we show that:

- For insulators, the time-averaged conductivity $\sigma_{\alpha,\beta}$ has a finite value, which is zero in longitudinal directions, and, for 2D materials, is proportional to the Chern number in the transverse direction (quantum anomalous Hall effect).
- For metals, when $t \ll \epsilon^{-1}$, the electrons are in the ballistic regime, and the current increases linearly: $j^\epsilon_{\alpha,\beta}(t) \approx D_{\alpha,\beta}\epsilon t$. Under some additional assumptions on the Bloch bands, the current displays Bloch oscillations of order 1 when $\epsilon^{-1} \ll t \ll \epsilon^{-1}\log(\varepsilon^{-\zeta})$ for some small enough $\zeta > 0$.
- For time-reversible 2D semimetals such as graphene, the time-averaged conductivity $\sigma_{\alpha,\beta}$ defined in (4.7) has a finite value equal to $\frac{1}{16} e_\alpha \cdot e_\beta$ times the number of Dirac points in the Brillouin zone.

A numerical application for the Haldane model [46] in the linear response regime ($\epsilon = 10^{-6}$, $t \ll \frac{1}{\epsilon}$) is presented in Figure 1.11. We also investigate the Bloch oscillations regime $\epsilon \ll 1$, $\frac{1}{\varepsilon} \ll t$ in Figure 1.12.

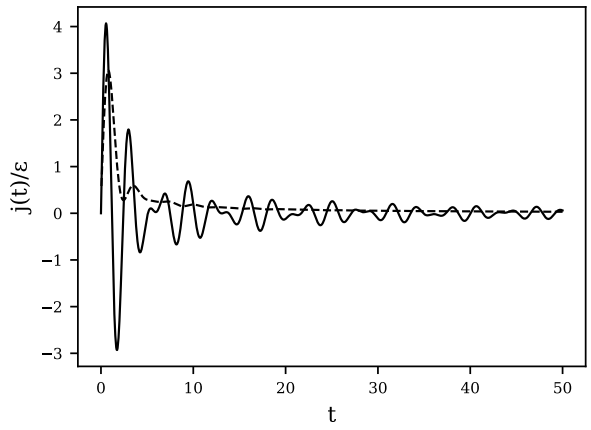


(a) Normal insulator phase, longitudinal current.

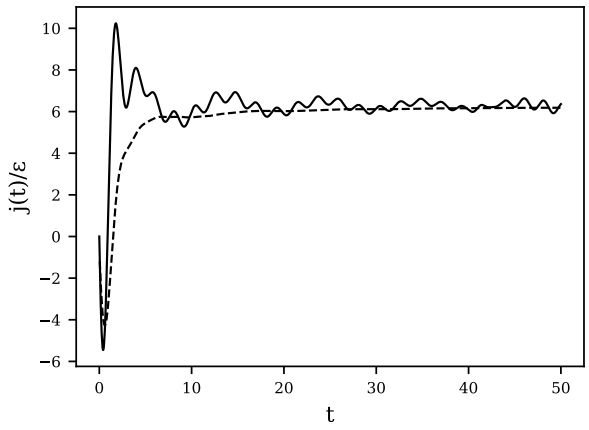


(b) Chern insulator phase, transverse current.

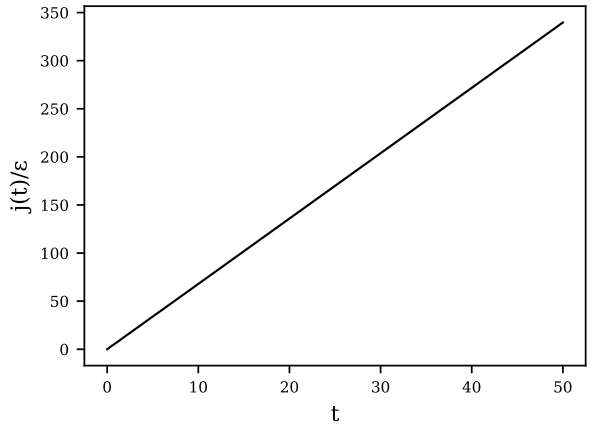


(c) Metallic phase.

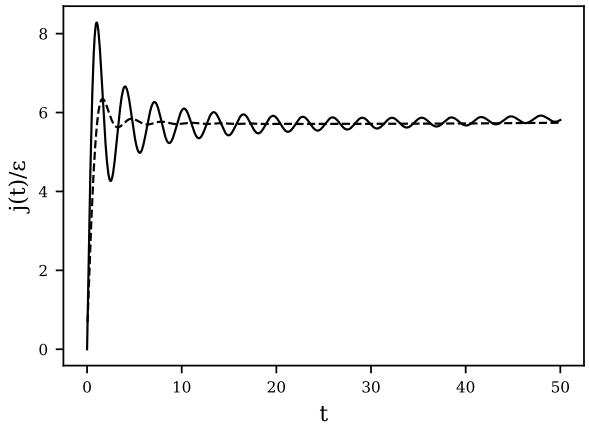


(d) Graphene phase.

Figure 1.11: Instantaneous conductivity $\frac{j^{\varepsilon}_{\alpha,\beta}(t)}{\varepsilon}$ (solid line) and running average $\frac{1}{t}\int_0^t \frac{j^{\varepsilon}_{\alpha,\beta}(t')}{\epsilon}dt'$ (dotted line) for several phases, in the linear response regime ($\epsilon = 10^{-4}$, $t \ll \frac{1}{\epsilon}$).

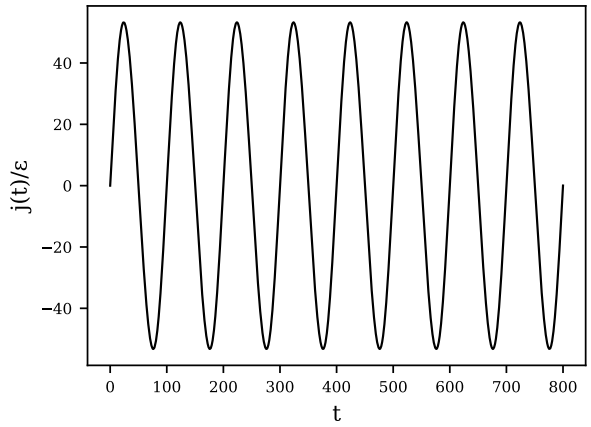


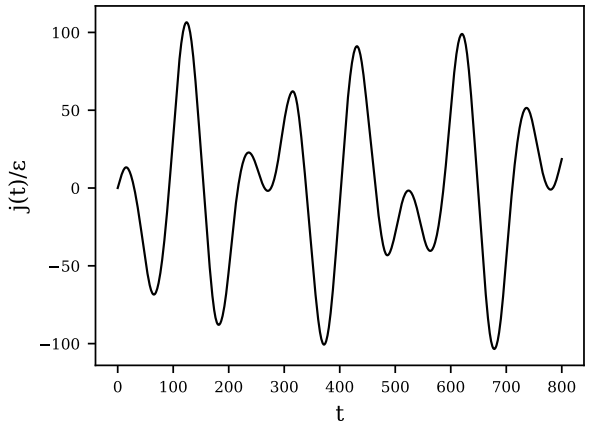


Figure 1.12: Instantaneous conductivity $\frac{j^{\epsilon}_{\alpha,\beta}(t)}{\epsilon}$ in the Bloch oscillations regime ($\epsilon = 10^{-2}$, $\frac{1}{\varepsilon} \ll t$).

# Chapter 2

# Numerical construction of Wannier functions through homotopy

This work was done in collaboration with David Gontier and Antoine Levitt.

**Abstract**

We provide a mathematically proven, simple and efficient algorithm to build localised Wannier functions, with the only requirement that the system has vanishing Chern numbers. Our algorithm is able to build localised Wannier for topological insulators such as the Kane-Mele model. It is based on an explicit and constructive proof of homotopies for the unitary group. We provide numerical tests validating the methods for several systems, including the Kane-Mele model.

## 2.1 Introduction

The occupied states of a periodic model of independent electrons are described by Bloch waves, which are (delocalised) modulated plane waves. Wannier functions are localised combinations of Bloch waves that span the occupied space. Due to the gauge freedom for the Bloch waves, Wannier functions are non-unique, and their localisation properties depend strongly on the choice of gauge. A specific gauge choice ensuring localisation was made in [67]. These maximally-localised Wannier functions (MLWF) are useful as a conceptual tool, to interpret bonding and polarisation in crystals [52], as well as a numerical tool, to construct effective tight-binding models [67] and compute exact exchange terms [106]. Methods to construct these MLWFs enable their routine use as a post-processing of density functional theory computations in solids. We refer to [66] for a review on applications.

The existence of localised Wannier functions for insulators is not guaranteed. Through the Bloch transform, it is equivalent to the following problem: given a smooth family of rank-$N$ projectors $P(k)$ defined on the $d$-dimensional torus $\mathbb{T}^d$, can we find a smooth Bloch frame representing the range of $P(k)$, *i.e.* a set of $N$ orthogonal smooth functions $u(k) := (u_1(k), \dots, u_N(k))$ on $\mathbb{T}^d$ such that $\mathrm{Ran} P(k) = \mathrm{Span} u(k)$ for all $k \in \mathbb{T}^d$. If it is indeed possible, then the inverse Bloch transform of $u(\cdot, x)$ yields localised Wannier functions.

In dimensions $d \geq 2$, such problems involve a competition between local smoothness and global periodicity. This is because the space $\mathrm{Ran} P(k)$ might twist with $k$, analogous to the twisting of the tangent space of a Möbius strip. Accordingly, there might be topological obstructions to finding such a Bloch frame. These obstructions are characterised by Chern numbers (one number in $d = 2$, three numbers in $d = 3$). In dimension 2 and 3, it is possible to construct

localised Wannier functions if and only if the Chern numbers vanish [10, 78]. In systems with time-reversal symmetry, one has the additional property that

$$\text{(TRS)} \qquad P(-k) = \theta P(k)\theta^{-1}, \text{ where } \theta \text{ is an anti-unitary operator.}$$

This implies that all Chern numbers vanish, and it is therefore possible to construct Wannier functions for such systems. By constrast, Chern insulators (a simple model of which is the Haldane model [**?**]), characterised by a broken time-reversal symmetry and non-trivial Chern invariants, can not support localised Wannier functions.

A further distinction appears depending on the type of time-reversal symmetry: bosonic (BTRS, occuring for instance in electrons whose spin degrees of freedom are neglected) or fermionic (FTRS, when spin-orbit coupling is present). Mathematically, these different types are characterised by $\theta^2 = 1$ (BTRS) or $\theta^2 = -1$ (FTRS). In the FTRS case, but not in the BTRS case, a further topological obstruction appears when trying to find Wannier functions respecting the natural symmetry of the problem [36]. In $d = 2$, there are two classes of systems: those for which one can find localised symmetric Wannier functions and those for which this is not possible. This is reflected by the $\mathbb{Z}_2$-valued Fu-Kane-Mele invariant [37]. Physically, this appears as symmetry-protected edge states.

In the common case of BTRS (when spin-orbit coupling is ignored and electrons pairs can be considered as spinless particles), several algorithms exist to compute localised Wannier functions. The most popular one was introduced by Marzari and Vanderbilt [67]. This optimises the locality of Wannier functions, starting from an initial guess. This algorithm is able to yield exponentially localised Wannier functions [80], but depends strongly on the choice of the initial guess. Recent advances, based on the use of matrix logarithms [13], selected columns of the density matrix (SCDM [22, 23]) or an extended set of projections [74], provide ways to automatically construct initial projections, without any specific physical input.

However, in the topologically non-trivial FTRS case, such as the Kane-Mele model of topological insulators, substantial difficulties appear. Since no symmetric Bloch frame can exist, algorithms that do not explicitly break this symmetry fail. This means that the initial guess for the method of [67] has to break this symmetry manually, which often proves challenging in practice. In the method of [13], this manifests as a crossing of eigenvalues, making the logarithm ill-defined (see Appendix of [13]). In the SCDM method, this appears as a loss of rank, unless a system-specific choice of columns is imposed [63].

The goal of this paper is to provide an automatic method that constructs localised Wannier functions even in the FTRS case. Our method is based on a standard reduction of the problem of finding Wannier functions to that of finding homotopies in the unitary group $\mathrm{U}(N)$. This problem was solved using matrix logarithms in [13], and using a multi-step logarithm based on a perturbation argument in [18, 19]. In this paper, we instead use a iterative method where the columns of the unitaries are contracted one by one. This method, which is natural and robust, implements an idea hinted at, but not detailed, in [35, p.81]. Unlike the similar method of [18, 19], it does not exploit the eigenstructure, which proves unstable in practice.

We emphasise that methods to construct Wannier functions specifically for the case of $\mathbb{Z}_2$ insulators were proposed in [89], [90], [105] and [75]. These methods however require model-specific information, while our method is completely automatic.

The paper is organised as follows. We present in Section 2.2 the definition of Wannier functions, and the equivalence between localised Wannier functions and smooth Bloch frames. Then, we recall in Section 2.3 the standard reduction from the problem of finding smooth Bloch frames to that of finding homotopies of unitary matrices. We explain in Section 2.4 the difficulties of this problem and our solution, which we illustrate numerically in Section 2.5.

## 2.2 From Wannier functions to Bloch frames

### 2.2.1 The Schrödinger equation in crystals

The goal of Wannier functions is to represent the subspace of occupied orbitals of a $d$-dimensional periodic Hamiltonian $H$ with localised functions. More specifically, we consider a $d$-dimensional periodic crystal described by a lattice $\mathcal{R} \sim (2\pi\mathbb{Z})^d$. We denote by $\mathcal{A} \sim \mathbb{R}^d/(2\pi\mathbb{Z})^d$ its unit cell, by $\mathcal{R}^* \sim \mathbb{Z}^d$ its reciprocal lattice, and by $\mathcal{B} \sim \mathbb{R}^d/\mathbb{Z}^d$ the reciprocal unit cell, also called the Brillouin zone. The behaviour of independent electrons (or electrons in mean-field approaches such as Kohn-Sham density functional theory) is described by the linear Schrödinger operator $H$, given by

$$H = -\frac{1}{2}\Delta + V, \quad \text{acting on} \quad L^2(\mathbb{R}^d, \mathbb{C}),$$

where $V$ is a (sufficiently well-behaved) $\mathcal{R}$-periodic potential modelling the external (mean-field) potential. Here, we dropped the spin variable for simplicity, as it plays no role in the argument.

As $H$ commutes with $\mathcal{R}$-translations, it follows from Bloch-Floquet theory [86] that $H$ is described with its fibers $H(k)$, which, in our case, are operators acting on $\mathcal{R}$-periodic functions, and given by

$$H(k) = \frac{1}{2}(-i\nabla + k)^2 + V \quad \text{acting on} \quad L^2(\mathcal{A}, \mathbb{C}).$$

For all $k \in \mathcal{B}$ and $K \in \mathcal{R}'$, the operators $H(k)$ and $H(k+K)$ are unitarily equivalent:

$$H(k+K) = \tau_K H(k) \tau_K^* \quad \text{with} \quad \tau_K(u)(x) := e^{-iK\cdot x} u(x). \tag{2.1}$$

The operators $H_k$ have a compact resolvent, with eigenvalues $\varepsilon_{1,k} \leq \varepsilon_{2,k} \leq \cdots$ going to infinity. The functions $k \mapsto \varepsilon_{n,k}$ are continuous and $\mathcal{R}'$-periodic. We assume in the sequel that there is a gap $g > 0$ such that

$$\forall k \in \mathcal{B}, \quad \varepsilon_{N+1,k} - \varepsilon_{N,k} \geq g$$

where $N \in \mathbb{N}^*$ is the number of electrons per unit cell. In this case, the operators $H(k)$ have a spectral gap, and we can define the projector $P(k) := \mathbb{1}(H(k) \leq \varepsilon_{N,k} + g/2)$. This projector is of rank $N$, it is smooth with respect to $k$ and satisfies the quasi-periodic conditions

$$P(k+K) = \tau_K P(k) \tau_K^*.$$

The projector on the occupied states $P$ is the operator acting on $L^2(\mathbb{C}^d, \mathbb{C})$, whose Bloch fibers are $P(k)$.

### 2.2.2 Bloch frames and localisation of Wannier functions

We say that $u(k) := (u_1(k), \cdots, u_N(k)) \in (L^2(\mathcal{A}, \mathbb{C}))^N$ is a Bloch frame for $P(k)$ if, for all $k \in \mathbb{R}^d$, $u(k)$ is an orthonormal family spanning the range of $P(k)$, and if $u(k+K) = \tau_K u(k)$ for all $K \in \mathcal{R}^*$. The Wannier functions are then defined for $1 \leq n \leq N$ and $R \in \mathcal{R}$ as

$$w_{n,R}(x) := \frac{1}{|\mathcal{B}|} \int_{\mathcal{B}} e^{ik\cdot(x-R)} u_n(k,x) \mathrm{d}k. \tag{2.2}$$

We have $w_{n,R}(x) = w_{n,0}(x-R)$. Moreover, as the family $\{u_n(k)\}_{1\leq n\leq N}$ is an orthonormal basis of $\mathrm{Ran} P(k)$, the family $\{w_{n,R}\}_{1\leq n\leq N, R\in\mathcal{R}}$ is orthonormal in $L^2(\mathbb{R}^d, \mathbb{C})$, and spans the range of $P$. Finally, if furthermore the map $k \mapsto u_n(k)$ is smooth, then the functions $w_{n,R}$ are localised, as can be seen by integrating by part (2.2).

We deduce that the existence of localised Wannier functions is equivalent to the existence of a smooth frame $u$ for $P$. In other words, we have reduced the problem of constructing localised Wannier functions to that of the following problem: *given a smooth map of rank-$N$ projectors $k \in \mathbb{R}^d \mapsto P(k)$ satisfying $P(k+K) = \tau_K P(k) \tau_K^*$ for $K \in \mathcal{R}^*$, can we find a smooth frame $u(k)$ for $P(k)$ which satisfies $u(k+K) = \tau_K u(k)$?*

### 2.2.3 Symmetries and topology

The existence of smooth Bloch frames (and therefore, of localised Wannier functions) in dimension $d \geq 2$ is not automatic, and depends on the topological properties of the Bloch bundle [10]. In dimension 2 and 3, the existence of localised Wannier functions is equivalent to the vanishing of topological invariants known as Chern numbers (one number in dimension $d = 2$, and three numbers in dimension $d = 3$).

In the important case where the map $k \mapsto P(k)$ satisfies the extra time-reversal symmetry (TRS), that is

$$P(-k) = \theta P(k) \theta^{-1}, \quad \text{with} \quad \theta \text{ antiunitary}, \tag{2.3}$$

then these Chern numbers always vanish, and a smooth frame, together with its corresponding localised Wannier functions, always exists in dimension $d < 3$ [76, 78].

In the context of Schrödinger operators, condition (2.3) is satisfied with $\theta u := \overline{u}$ the complex conjugation operator. This operator is of bosonic type, squaring to 1. If we start instead of $H = -\frac{1}{2}\Delta + V$ with a Hamiltonian including spin-orbit coupling, we obtain a TRS of fermionic type, with an operator $\theta$ squaring to $-1$. In the case of FTRS, it is not always possible to build localised Wannier functions that additionally respect a natural symmetry condition [36], causing many natural algorithms to fail.

*Remark* 2.2.1. The existence of a smooth and quasi-periodic Bloch frame is a topological property. A consequence of the topological nature of the problem for our purposes is that, provided sufficient regularity on $k \mapsto H(k)$, if a continuous and quasi-periodic Bloch frame exists, then it can be lifted to a smooth and quasi-periodic one. Hence, in what follows, we will restrict ourselves to constructing continuous frames, as this can be regularised later, theoretically by the arguments in [35] and numerically by using the Marzari-Vanderbilt procedure [66].

## 2.3 From Bloch frames to homotopies

### 2.3.1 Parallel transport

An important notion that we use throughout the proof is *parallel transport*. We recall in this section the main properties of parallel transport, and explain how to solve it numerically.

Consider a smooth family of orthogonal projectors $[0,1] \ni t \mapsto P(t)$, where $P(t)$ is a rank-$N$ projector acting on some Hilbert space $\mathcal{H}$. Let $u(0) = (u_1(0), \ldots, u_m(0)) \in \mathcal{H}^m$ be any set of $m$ vectors in $\mathrm{Ran} P(0)$, with $m \leq N$. Then the solution to the ordinary differential equation

$$u'(t) = [P'(t), P(t)]\, u(t), \quad \text{with} \quad u(t=0) = u(0) \tag{2.4}$$

satisfies

$$(u^* u)'(t) = (u^*)'(t) u(t) + u^*(t) u'(t) = u^* \left( - [P'(t), P(t)] + [P'(t), P(t)] \right) u = 0$$

and

$$\begin{aligned} (u^* P u)'(t) &= u^*(t) \left( - [P'(t), P(t)]\, P(t) + P'(t) + P(t)\, [P'(t), P(t)] \right) u(t) \\ &= u^*(t) \left( -P'(t)P + P(t)P'(t)P(t) + P'(t) + P(t)P'(t)P(t) - P(t)P'(t) \right) u(t) \\ &= 0, \end{aligned}$$

where we used the fact that $P^2(t) = P(t)$, which first leads to $P(t)P'(t) + P'(t)P(t) = P'(t)$, then to $P(t)P'(t)P(t) = 0$. It follows that $u(t)$ is an orthonormal set of vectors in $\mathrm{Ran}P(t)$ for all $t \in [0,1]$. In particular, one can simplify (2.4) with

$$u'(t) = P'(t)P(t)u(t) - P(t)P'(t)u(t) = P'(t)u(t) - P(t)P'(t)P(t)u(t) = P'(t)u(t),$$

where we used the fact that $P(t)u(t) = u(t)$, and again the equality $P(t)P'(t)P(t) = 0$. This gives the following orthogonality-preserving discretisation scheme. We assume that we are given $P(t_i)$ for $0 = t_0 \leq t_1 \leq \cdots \leq t_I = 1$, and $u(0)$ an orthonormal family in the range of $P(0)$. Then we set

$$\begin{cases} \widetilde{u}_{t_{i+1}} & = P(t_{i+1})u_{t_i}, \\ u_{t_{i+1}} & = \widetilde{u}_{t_{i+1}} \left[\widetilde{u}^*_{t_{i+1}} \widetilde{u}_{t_{i+1}}\right]^{-1/2}. \end{cases} \tag{2.5}$$

This is a convergent discretisation of (2.4), in the sense that when the spacing $\sup_i t_{i+1} - t_i$ converges to zero, $u_{t_i}$ converges to $u(t_i)$.

### 2.3.2 Obstruction matrices and homotopy

In this section, we explain how to reduce the problem of constructing a smooth Bloch frame in $d$ dimensions to that of finding a $(d-1)$-homotopy of unitary matrices in $U(N)$. This is a standard construction that was used in several articles (for instance, [13, 90] and references therein). We proceed by induction on the dimension $d = 1, 2, 3$.

#### Construction for $d = 1$

In dimension $d = 1$, we are given a smooth family of projectors $P(k_1)$ with $k_1 \in [0,1]$, which satisfies the quasi-periodic condition $P(1) = \tau_1 P(0) \tau_1^*$. We choose an arbitrary orthonormal basis $\widetilde{u}(0)$ of $\mathrm{Ran}P(0)$. We then use parallel transport (2.4) to construct a smooth frame $\widetilde{u}(k_1)$ for $P(k_1)$, for all $k_1 \in [0,1]$. The problem is that $\widetilde{u}(1)$ is not equal to $\tau_1 \widetilde{u}(0)$ *a priori*. Still, they both form an orthonormal basis of $\mathrm{Ran}P(1) = \mathrm{Ran}P(0)$, and therefore are related by a unitary matrix $V_{\mathrm{obs}} \in \mathrm{U}(N)$, called the obstruction matrix:

$$\widetilde{u}(1) = (\tau_1 \widetilde{u}(0)) V_{\mathrm{obs}}$$

Since $V_{\mathrm{obs}} \in U(N)$, there is a anti-hermitian matrix $L$ such that $V_{\mathrm{obs}} = \exp(L)$. We then set

$$u(k_1) := \widetilde{u}(k_1) \exp(-k_1 L).$$

By construction, $k_1 \mapsto u(k_1)$ is smooth on $[0,1]$, and satisfies $u(1) = \tau_1 u(0)$ as wanted. The continuous map $k_1 \mapsto u(k_1)$ can be smoothed out following Remark 2.2.1. This gives the desired Bloch frame for $d = 1$.

#### Construction for $d = 2$

The construction in two dimensions relies on the previous one-dimensional construction. We assume that we are given a smooth family $[0,1]^2 \ni (k_1, k_2) \to P(k_1, k_2)$ of operators satisfying $P(k + K) = \tau_K P(k) \tau_K^*$ for all $K \in \mathcal{R}^*$.

First, we use the previous $d = 1$ construction on the segment $k_2 = 0$, and get a smooth and quasi-periodic frame $\widetilde{u}(k_1, 0)$ for the family of projectors $[0,1] \ni k_1 \to P(k_1, 0)$. Now for every $k_1 \in [0,1]$, we parallel transport the frame $u(k_1, 0)$ along the second direction, to produce a frame $\widetilde{u}(k_1, k_2)$ on $[0,1]^2$. The frame is continuous, and satisfies $\widetilde{u}(1, k_2) = \tau_{(1,0)} \widetilde{u}(0, k_2)$ for all

$k_2 \in [0,1]$. However, there may be a mismatch on the $k_2$-boundary: for all $k_1 \in [0,1]$, there is $V_{\text{obs}}(k_1)$ so that

$$\widetilde{u}(k_1,1) = (\tau_{(0,1)}\widetilde{u}(k_1,0))V_{\text{obs}}(k_1)$$

In addition, since $\widetilde{u}(1,0) = \tau_{(1,0)}\widetilde{u}(0,0)$ and $= \widetilde{u}(1,1) = \tau_{(1,0)}\widetilde{u}(0,1)$, we have $V_{\text{obs}}(0) = V_{\text{obs}}(1)$. The map $k \mapsto V_{\text{obs}}(k)$ is periodic, continuous and piecewise smooth on $\mathbb{R}$, and can be seen as a loop $\mathbb{T}^1 \to \mathrm{U}(N)$. We recall the following well-known fact.

**Proposition 2.3.1.** *Let $\mathbb{T}^1 \ni k \mapsto V(k) \in \mathrm{U}(N)$ be a continuous and piecewise smooth loop in $\mathrm{U}(N)$. The two following assertions are equivalent:*

1. *The winding number $W(\det V)$ of the determinant of $V$ vanishes, where*

$$W(\det V) := \frac{1}{2\pi}\int_0^1 \frac{1}{\det(V(k))}\det(V(k))'\mathrm{d}k = \frac{1}{2\pi}\int_0^1 \mathrm{Tr}(V^*(k)V'(k))\mathrm{d}k. \tag{2.6}$$

2. *There is a homotopy from $V(\cdot)$ to $\mathbb{I}_N$, that is a piecewise smooth map $\mathbb{T}^1 \times [0,1] \ni (k,t) \mapsto V(k,t) \in \mathrm{U}(N)$ which satisfies*

$$\forall k \in \mathbb{T}^1, \quad V(k,0) = V(k) \quad \textit{and} \quad V(k,1) = \mathbb{I}_N.$$

In the next section, we give a constructive proof of this fact, in the sense that if the winding number vanishes, we construct algorithmically the homotopy $V$. In our case, it can be further shown (see [35]) that $W(\det V_{\text{obs}})$ equals the Chern number of $P(k_1,k_2)$. According to this proposition, and assuming that $W(\det V_{\text{obs}}) = 0$, there is a homotopy $V_{\text{obs}}(k_1,t)$ from $V_{\text{obs}}$ to $\mathbb{I}_N$. We finally set

$$u(k_1,k_2) := \widetilde{u}(k_1,k_2)V_{\text{obs}}(k_1,k_2).$$

By construction, this Bloch frame is continuous and satisfies the quasi-periodic boundary condition. It can be smoothed out following Remark 2.2.1.

### Construction for $d = 3$

The extension to the third dimension is identical. First, use the $d = 2$ procedure on the face $k_3 = 0$, *i.e.* on $\{(k_1,k_2,0)\ ,\ (k_1,k_2) \in [0,1]^2\}$, to obtain a Bloch frame $\widetilde{u}(k_1,k_2,0)$ on this face. According to the previous section, this is possible if and only if the winding number of the obstruction on this face vanishes. Then, we parallel transport this frame along the third dimension and get $\widetilde{u}(k_1,k_2,k_3)$. We obtain another obstruction matrix $V_{\text{obs}}(k_1,k_2) \in \mathrm{U}(N)$, such that

$$\forall k_1,k_2 \in [0,1]^2, \quad \widetilde{u}(k_1,k_2,1) = (\tau_{(0,0,1)}\widetilde{u}(k_1,k_2,0))V_{\text{obs}}(k_1,k_2).$$

As before, we have $V_{\text{obs}}(0,k_2) = V_{\text{obs}}(1,k_2)$ and $V_{\text{obs}}(k_1,0) = V_{\text{obs}}(k_1,1)$, and so $V_{\text{obs}}$ can be seen as a map from $\mathbb{T}^2$ to $\mathrm{U}(N)$. In the sequel, we prove the following classical result, which is the 2-dimensional counterpart of Proposition 2.3.1

**Proposition 2.3.2.** *Let $\mathbb{T}^2 \ni (k_1,k_2) \mapsto V(k_1,k_2) \in \mathrm{U}(N)$ be a continuous and piecewise smooth surface in $\mathrm{U}(N)$. The two following assertions are equivalent:*

1. *The winding numbers $W(\det V(\cdot,0))$ and $W(\det V(0,\cdot))$ both vanish;*

2. *There is a 2-homotopy from $V$ to $\mathbb{I}_N$, that is a smooth map $\mathbb{T}^2 \times [0,1] \ni (k_1,k_2,t) \mapsto V(k_1,k_2,t) \in \mathrm{U}(N)$ which satisfies*

$$\forall k_1,k_2 \in \mathbb{T}^2, \quad V(k_1,k_2,0) = V(k_1,k_2) \quad \textit{and} \quad V(k_1,k_2,1) = \mathbb{I}_N.$$

If the assertions are satisfied for our map $V_{\text{obs}}(k_1, k_2)$, there is a 2-homotopy $V_{\text{obs}}(k_1, k_2, t)$ that contracts $V_{\text{obs}}$ to $\mathbb{I}_N$, and we set

$$u(k_1, k_2, k_3) := \widetilde{u}(k_1, k_2, k_3) V_{\text{obs}}(k_1, k_2, k_3)$$

to obtain the final Bloch frame.

As in the $d = 2$ case, the three winding numbers appearing in the construction correspond to the three Chern numbers.

*Remark* 2.3.3. This construction process extends trivially to dimensions $d > 3$, but the analogue of Propositions 2.3.1 and 2.3.2 are no longer true, and an additional obstruction (the second Chern class) appears.

It remains to explain our constructive proof of Propositions 2.3.1 and 2.3.2. This is the topic of the next section.

## 2.4 Constructive homotopies in the unitary group

In this section, we describe a simple and efficient algorithm to construct 1-homotopies and 2-homotopies in $\mathrm{U}(N)$. We first examine how the logarithm algorithm in [13] fails for simple systems such as the Kane-Mele model. We then explain our algorithm in the context of 1-homotopies, and then extend our result for 2-homotopies.

### 2.4.1 Logarithm algorithm

Let $\mathbb{T}^1 \ni k \mapsto V(k) \in \mathrm{U}(N)$ be a smooth loop. A very natural approach, that was used in [13], is to find a global logarithm for $V(k)$, that is a smooth loop $L(k)$ of anti-hermitian matrices such that

$$V(k) = \exp\left(L(k)\right), \quad \forall k \in [0, 1].$$

If such a logarithm exists, then a homotopy from $V(k)$ to $\mathbb{I}_N$ is given by

$$\forall k \in \mathbb{T}^1, \forall t \in [0, 1], \quad V(k, t) = \exp\left((1 - t)L(k)\right).$$

The authors of [13] then proposed to work with the eigenvalues of $U(k)$, to find a continuous phase for each on. However, even if the winding number $W(\det V)$ vanishes, this approach can fail, as shown by this simple example

*Example* 2.4.1. Consider the analytic and periodic matrix path

$$V(k) = \begin{pmatrix} \exp(2i\pi k) & 0 \\ 0 & \exp(-2i\pi k) \end{pmatrix}$$

Here, it is impossible to find a logarithm of the path that is continuous and periodic on $[0, 1]$, since each eigenvalue has a winding number, hence receives a phase increment of $\pm 2\pi$ respectively when going from 0 to 1.

The case of eigenvalues having a winding number appears in practice for systems with fermionic time-reversal symmetry such as the Kane-Mele model in its QSH phase (see Section 2.5.1). In Figure 2.1, we display the eigenvalues of the obstruction matrix for a representative set of parameters. Here, the determinant is identically 1. Hence, we know that a homotopy does exist, but the logarithm method fails to construct it.

A similar method, proposed in [19], is to introduce a small perturbation in order to avoid eigenvalue crossings, which makes each winding number trivial, and look for a family of logarithms satisfying

$$V(k) = \mathrm{e}^{L_1(k)} \mathrm{e}^{L_2(k)} \dots \mathrm{e}^{L_N(k)},$$

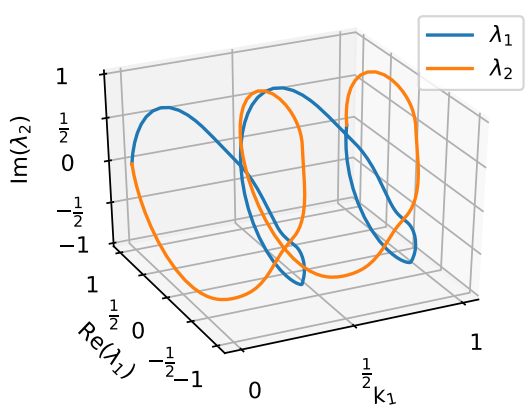


(a) Eigenvalues winding in opposite directions

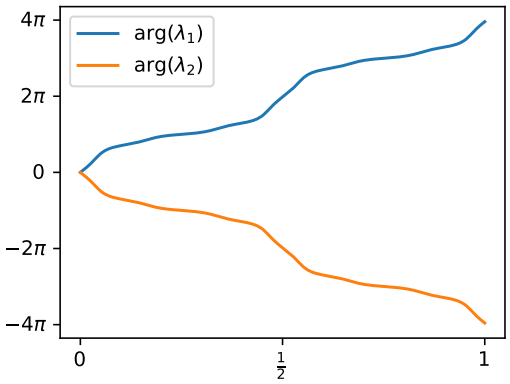


(b) Phase of the eigenvalues, corrected for continuity

Figure 2.1: Eigenvalues of the obstruction for the Kane-Mele model

where $L_i(s)$, $i \in 1 \dots N$ are anti-Hermitian. However, small perturbations of eigenvalues can introduce large changes in the eigenvectors, and hence produce a continuous but irregular path, which makes this method algorithmically difficult to implement.

### 2.4.2 Column interpolation method

From the counter-example given in Example 2.4.1, we see that constructing a homotopy of unitary matrices based from their eigenvalues may fail, as these can wind. In our method, instead of contracting eigenvalues, we rather contract the columns of $V(k)$ one by one. Algebraically, this corresponds to exploiting the fibration

$$\mathrm{U}(N-1) \to \mathrm{U}(N) \to \mathbb{S}^{2N-1},$$

which was suggested (but not explored further) in [35, p.81].

let $\mathbb{T}^1 \ni k \mapsto V(k) \in \mathrm{U}(N)$ be a smooth map. We write $V(k) = (v_1(k), \dots, v_N(k))$ where $v_n(k) \in \mathbb{S}^{2N-1}$ is the $n$-th column of $V(k)$. Our strategy is to first contract the columns $v_n(k)$ iteratively to a fixed column $\underline{v_n}$, ensuring that they stay orthonormal, and then homotopise $\underline{V} = (\underline{v_1}, \dots, \underline{v_N})$ to the identity.

Let us assume that at step $1 \leq n \leq N$, we have found how to contract the first $n-1$ columns to some fixed vectors: we have constructed $n-1$ smooth maps of orthonormal vectors $v_1(k,t), \dots, v_{n-1}(k,t)$ such that $v_j(k, t=0) = v_j(k)$ and $v_j(k, t=1) = \underline{v_j}$. We denote by

$$P_{n-1}(k,t) := \mathbb{I}_N - \sum_{j=1}^{n-1} |v_j(k,t)\rangle\langle v_j(k,t)|,$$

the projection on the orthogonal of this family, of rank $N-n+1$. By hypothesis, at $t=1$, the projectors $P_{n-1}(k, t=1)$ are equal to a constant projector $\underline{P_{n-1}}$.

We now contract the $n$-th column $v_n(k,t)$ to a fixed column $\underline{v_n} \in \mathrm{Ran}\underline{P_{n-1}}$ while satisfying $v_n(k,t) \in \mathrm{Ran}P_{n-1}(k,t)$ for all $k, t \in \mathbb{T}^1 \cup [0,1]$. This ensures that the constructed map for the $n$-th column is orthogonal to the previously constructed ones. First, for all fixed $k \in \mathbb{T}^1$, we parallel transport the orthogonal family $(v_n(k), \cdots, v_N(k))$ with respect to $P_{n-1}(k,\cdot)$, and obtain a smooth family of orthonormal frames $(\widetilde{v_n}(k,t), \cdots, \widetilde{v_N}(k,t))$ for $k, t \in \mathbb{T}^1 \times [0,1]$. At this point, $\widetilde{v_n}(k, t=1)$ forms a non-trivial loop in $\mathrm{Ran}\underline{P_{n-1}}$. We now contract this to a single vector $\underline{v_n}$, distinguishing two cases, depending on whether $\widetilde{v_n}(k, t=1)$ can or cannot cover the whole of the unit sphere in $\mathrm{Ran}\underline{P_{n-1}}$.

**Case $n < N$.** When $n < N$, the unit sphere in $\mathrm{Ran}\underline{P_{n-1}}$ is a manifold of real dimension $2(N-n)+1 \geq 3$. The family $\{\widetilde{v_n}(k, t=1)\}_{k\in\mathbb{T}^1}$ describes a piecewise smooth loop on that manifold, and from Sard's lemma it follows that there exists a vector $\underline{v_n} \in \mathbb{S}^{2N-1} \cap \mathrm{Ran}\underline{P_{n-1}}$ such that $-\underline{v_n}$ does not belong to the loop $\{\widetilde{v_n}(k, t=1)\}_{k\in\mathbb{T}^1}$ (see Remark 2.4.2).

For all $k \in \mathbb{T}^1$, the family $(\widetilde{v_n}(k,1), \cdots, \widetilde{v_N}(k,1))$ is a basis of $\underline{P_{n-1}}$, so there exist (smooth) coefficients $c(k) := (c_n(k), \ldots, c_N(k)) \in \mathbb{C}^{N-n+1}$ with $|c(k)| = 1$ such that

$$\forall k \in \mathbb{T}^1, \quad \underline{v_n} = \sum_{j=n}^{N} c_j(k)\widetilde{v_j}(k,1).$$

The map $\mathbb{T}^1 \ni k \mapsto c(k)$ is a loop on the sphere $\mathbb{S}^{2(N-n)+1}$. In addition, since $-\underline{v_n}$ never touches the loop $\{\widetilde{v_n}(k, t=1)\}_{k\in\mathbb{T}^1}$, $c(k)$ never touches the vector $-e_1 := (-1, 0, \cdots, 0)$. We can therefore contract the loop $c(k)$ to $e_1$ on $\mathbb{S}^{2(N-n)+1}$ with the explicit contraction

$$c(k,t) := \frac{tc(k) + (1-t)e_1}{\|tc(k) + (1-t)e_1\|}, \tag{2.7}$$

which is a well-defined smooth map from $\mathbb{T}^1 \times [0,1]$ to $\mathbb{S}^{2(N-n)+1}$. This contraction of coefficients directly translates into a contraction of $v_n(k)$ to $\underline{v_n}$ by setting

$$v_n(k,t) := \sum_{j=n}^{N} c_j(k,t)\widetilde{v_j}(k,t).$$

By construction, $v_n(k,t)$ is a normalised vector which is orthogonal to $(v_1(k,t), \ldots, v_{n-1}(k,t))$ for all $k, t \in \mathbb{T}^1 \times [0,1]$. This concludes the construction in this case.

*Remark* 2.4.2. In theory, almost every $v_n$ gives rise to a continuous gauge, since the forbidden set $\{-\widetilde{v_n}(k,1)\}_{k\in\mathbb{T}^1}$ is of zero measure in $v_n \in \mathbb{S}^{2N-1} \cap \mathrm{Ran}P_{n-1}$. In practice however, it is important to choose it such that $\|\widetilde{v_n}(k,1) + v_n\|$ is not too small. Therefore, we draw several random or well-chosen points $p_j \in \mathbb{S}^{2N-1}$, which we project on $\underline{P_{n-1}}$ and normalise. We then pick

$$\underline{v_n} := \arg\max_j \min_{k\in\mathbb{T}^1} \|\widetilde{v_n}(k,1) + p_j\|.$$

This ensures that the denominator in (2.7) is not too close to zero.

**Case $n = N$.** For the last vector, *i.e.* when $n = N$, the previous construction can fail because $\widetilde{v_N}(k, t=1)$ can cover the whole of the unit sphere in $\mathrm{Ran}\underline{P_{n-1}}$. We therefore follow a different route. For all $k \in \mathbb{T}^1$, the vector $\widetilde{v_N}(k, t=1)$ always lies in the same one-dimensional subspace. In particular, there is a piecewise smooth phase $\phi : [0,1] \to \mathbb{R}$ so that

$$\forall k \in [0,1], \quad \widetilde{v_N}(k) = \underline{v_N} e^{i\phi(k)} \quad \text{with} \quad \underline{v_N} := \widetilde{v_N}(0) \quad \text{(for instance)}.$$

By periodicity, one must have $\phi(1) = \phi(0) + 2\pi m$ with $m \in \mathbb{Z}$. This gives

$$m = \frac{1}{2\pi}(\phi(1) - \phi(0)) = \frac{1}{2\pi}\int_0^1 \phi'(k)\mathrm{d}k = \frac{1}{2\pi i}\int_0^1 \left\langle \widetilde{v_N}(k), \frac{\mathrm{d}}{\mathrm{d}k}\widetilde{v_N}(k) \right\rangle \mathrm{d}k.$$

We set $\widetilde{V}(k,t) := (v_1(k,t), \ldots v_{N-1}(k,t), \widetilde{v_N}(k,t)) \in \mathrm{U}(N)$. This is a smooth deformation between $V(k)$ at $t=0$ and $\widetilde{V}(k,1) = (\underline{v_1}, \ldots \underline{v_{N-1}}, \widetilde{v_N}(k,1))$ at $t=1$. Also, we have

$$\left\langle \widetilde{v_N}(k), \frac{\mathrm{d}}{\mathrm{d}k}\widetilde{v_N}(k) \right\rangle = \mathrm{Tr}\left( \widetilde{V}(k,1)^* \frac{\mathrm{d}}{\mathrm{d}k}\widetilde{V}(k,1) \right) \mathrm{d}k.$$

This leads to

$$m = \frac{1}{2\pi i}\int_0^1 \mathrm{Tr}\left(\widetilde{V}(k,1)^* \frac{\mathrm{d}}{\mathrm{d}k}\widetilde{V}(k,1)\right)\mathrm{d}k = W\left(\det \widetilde{V}(\cdot,1)\right) = W(\det V(\cdot)), \tag{2.8}$$

where we recall that $W(\cdot)$ was defined in (2.6), and where we used the fact that the winding number is not affected by a smooth deformation: $W\left(\widetilde{V}(\cdot,t)\right)$ does not depend on $t$. We conclude that can contract the vector $\widetilde{v_N}$ to $\underline{v_N}$ if and only if $m = 0$, or equivalently if $W(\det V) = 0$. In this case, an explicit contraction is given by

$$v_N(k,t) = \widetilde{v_N}(k,t)e^{-it\phi(k)}.$$

**Last step.** At this point, we have algorithmically constructed a smooth map $\mathbb{T}^1 \times [0,1] \ni (k,t) \mapsto V(k,t) \in \mathrm{U}(N)$ such that $V(k,t=0) = V(k)$ and $V(k,t=1) = \underline{V} := (\underline{v_1}, \cdots, \underline{v_N})$. To get a contraction to the identity matrix $\mathbb{I}_N$, we write $\underline{V} = \exp(\underline{L})$, where $\underline{L}$ is anti-hermitian, and we take as our final homotopy

$$(k,t) \mapsto V(k,t)e^{-t\underline{L}}.$$

This concludes our constructive proof for Proposition 2.3.1.

*Remark* 2.4.3. In our algorithm, we have tried to make the homotopy as smooth as possible. This means that we avoid composing homotopies sequentially, which is inefficient numerically, and that we wish that the method reduces to the logarithm method in the case where $V(k)$ is constant (where we know that the logarithm gives the geodesic in $\mathrm{U}(N)$ and therefore the most efficient path). If that is not a concern, then a simpler version of the algorithm can be given. After the first column is homotopised to a column $\underline{v_1}$, this vector can further be deformed to $e_1$, and therefore we can assume that $\underline{v_1} = e_1$. This implies that the homotopy $\widetilde{V}(k,t) := (v_1(k,t), \widetilde{v_2}(k,t), \ldots, \widetilde{v_N}(k,t)))$ satisfies $V(k,0) = V(k)$ and

$$\widetilde{V}(k,1) = \begin{pmatrix} 1 & \widetilde{v_{1,2}}(k,1) & \cdots & \widetilde{v_{1,N}}(k,1) \\ 0 & \widetilde{v_{2,2}}(k,1) & \cdots & \widetilde{v_{2,N}}(k,1) \\ \vdots & \vdots & \cdots & \vdots \\ 0 & \widetilde{v_{2,N}}(k,1) & \cdots & \widetilde{v_{N,N}}(k,1) \end{pmatrix} =: \begin{pmatrix} 1 & 0 \\ 0 & V_1(k) \end{pmatrix},$$

where we used the fact that $\widetilde{V}(k,1)$ is unitary, so that $\widetilde{v_{1,2}}(k,1) = \cdots = \widetilde{v_{1,N}}(k,1) = 0$. We have reduced the homotopy problem in $\mathrm{U}(N)$ to the homotopy problem in $\mathrm{U}(N-1)$, and therefore solve the problem by induction on $N$, using the case $n = N$ above to treat the base step.

*Remark* 2.4.4 (Parallelisability of the sphere). In the case $N = 2$, we can use the identification of $\mathrm{SU}(2)$ with $\mathbb{S}^3$ given by

$$\begin{pmatrix} a & -b^* \\ b & a^* \end{pmatrix} \mapsto \begin{pmatrix} a \\ b \end{pmatrix}$$

to simplify the algorithm, as done in [35]. More generally, if given a vector $x \in \{z \in \mathbb{C}^N, |z| = 1\}$ we had a systematic way to build an orthogonal basis of the (complex-)orthogonal $x^\perp$ in a way that is smooth with respect to $x$, we could exploit that in our algorithm. This is easily achieved in dimension 2 by the mapping $(a,b) \mapsto (-b^*, a^*)$. However, this is impossible when $N = 3$ (because this would imply the parallelisability of the 5-dimensional sphere, which is false). We therefore have to follow a different route, using parallel transport to build this basis incrementally.

#### Extension for 2-homotopies

We now consider the case of 2-homotopies, and we want to contract a map $\mathbb{T}^2 \ni (k_1, k_2) \mapsto V(k_1, k_2) \in \mathrm{U}(N)$. Following the same iterations as in the previous section, we see that at step $n < N$, the $n$-th column $\widetilde{v}(k_1, k_2, t = 1)$ defines a 2-dimensional sub-manifold on $\mathbb{S}^{2N-1} \cap \mathrm{Ran}\underline{P_{n-1}}$ of dimension $2(N-n)+1 \geq 3$, and we can find $\underline{v_n}$ so that $\underline{v_n}$ does not belong to this sub-manifold. We then follow the same steps.

For the last step $n = N$, there is a smooth phase function $\mathbb{T}^2 \ni (k_1, k_2) \mapsto \phi(k_1, k_2)$ such that

$$\forall k_1, k_2 \in [0,1]^2, \quad \widetilde{v_N}(k_1, k_2, 1) = \underline{v_N} \exp(i\phi(k_1, k_2)) \quad \text{with} \quad \underline{v_N} := \widetilde{v_N}(0, 0, 1) \quad \text{for instance.}$$

By periodicity and continuity, there is $m_1, m_2 \in \mathbb{Z}$ such that $\phi(k_1 + 1, k_2) = \phi(k_1, k_2) + 2\pi m_1$ and $\phi(k_1, k_2 + 1) = \phi(k_1, k_2) + 2\pi m_2$. As in (2.8), we find

$$\forall k_2 \in \mathbb{T}^1, \quad m_1 = W(\det V(\cdot, k_2)) \quad \text{and} \quad \forall k_2 \in \mathbb{T}^1, \quad m_2 = W(\det V(k_1, \cdot)).$$

If both number vanish, then a contraction is given by $v_n(k_1, k_2, t) := \widetilde{v_n}(k_1, k_2, t) \exp(-it\phi(k_1, k_2))$. The constructive proof of Proposition 2.3.2 follows.

*Remark* 2.4.5. This proof fails for 3-homotopies. The reason is that with $N = 2$, the first vector of $\mathbb{T}^3 \ni (k_1, k_2, t_3) \mapsto V(k_1, k_2, t_3) \in \mathrm{U}(2)$ is now a 3-dimensional sub-manifold in $\mathbb{S}^3$, hence can wrap the whole sphere $\mathbb{S}^3$. It can be contracted to a point only if the second Chern class vanishes.

## 2.5 Numerical results

In this section, we apply the constructive method outlined above to the case of the Kane-Mele model ($d = 2$), and silicon ($d = 3$). We discretise the Brillouin zone with equispaced points (the Monkhorst-Pack grid). At each discrete point $k$, we diagonalise $H(k)$ and obtain the eigenvectors $(u_{n,k})_{1 \leq n \leq N}$ corresponding to the $N$ lowest eigenvalues of $H(k)$. We then seek a unitary matrix $U_{m,n}(k)$ that makes $u'_n(k) = \sum_{1 \leq m \leq N} u_{mk} U_{mn}(k)$ as smooth as possible. The quantities needed by our algorithm are the overlaps $\langle u_{mk}, u_{n,k+b} \rangle$ between neighbouring points $k$ and $k + b$, similar to other methods such as Wannier90 [82]. More information on this methodology can be found in [13].

### 2.5.1 The Kane-Mele model

The Kane-Mele model, first proposed in [49], is a toy model of a $\mathbb{Z}^2$ topological insulator. It is a tight-binding model on a 2D hexagonal lattice, with four degrees of freedom per site (two orbitals and two spins), two of which are occupied ($H(k)$ is a $4 \times 4$ matrix, and $N = 2$).

#### Description of the model

The Bloch representation of this model can be written as follows.

$$H_k = \sum_{a=1}^{5} d_a(k) \Gamma^a + \sum_{\substack{a,b=1 \\ a<b}}^{5} d_{ab}(k) \Gamma^{ab}, \tag{2.9}$$

where $\Gamma^{ab} := \frac{1}{2i}[\Gamma^a, \Gamma^b]$, and $\Gamma^a$ are the Dirac matrices $(\sigma^x \otimes \mathbb{I}_N, \sigma^z \otimes \mathbb{I}_N, \sigma^y \otimes s^x, \sigma^y \otimes s^y, \sigma^y \otimes s^z)$, $\sigma^j$ and $s^j$ being the Pauli matrices of sublattice and spin respectively.

The functions $d_a(k)$ and $d_{ab}(k)$ in (2.9) are chosen as in [49]. In particular, $d_a$ is even and $d_{ab}$ odd, and the model satisfies a fermionic time-reversal symmetry. The model has 4 free parameters: $t$, $\lambda_{S0}$, $\lambda_\nu$ and $\lambda_R$. Here, we fix the parameters $t = 1, \lambda_{SO} = 1$, and only vary $\lambda_\nu$ and $\lambda_R < 2\sqrt{3}$. For every value of $\lambda_R < 2\sqrt{3}$, the system undergoes a phase transition as $\lambda_\nu$ is varied:

- For $\lambda_\nu > 3\sqrt{3}$, the material is in a regular insulating phase.
- For $\lambda_\nu = 3\sqrt{3}$, the material is in a transitional metallic phase: the gap closes, which means that the material is conducting.
- For $\lambda_\nu < 3\sqrt{3}$, the material is in the Quantum Spin Hall (QSH) phase.

**Numerical construction of Wannier functions for the Kane-Mele model**

In order to construct localised Wannier functions for the Kane-Mele model, one needs to provide a Bloch frame that is regular enough on the Brillouin zone. In the QSH phase, no continuous and symmetric frame exists, but since the Chern number is trivial for any time-reversal symmetric Bloch bundle, there exists a non-symmetric continuous frame. Moreover, in this case, the eigenvalues of the obstruction have a non-trivial winding number, so the logarithm method of [13] cannot provide a homotopy of the obstruction.

In this section, we use the algorithm described above to construct a continuous initial guess of the Bloch frame, which can then be refined to a more regular one by a smoothing method, thus providing a well-localised Wannier function. The Brillouin zone was discretised with a $200 \times 200$ grid. In the topologically trivial case, both methods produce a reasonable output (Figures 2.2a and 2.2b).

In order to measure localisation, we follow [67], and measure the spread of the Wannier functions $\Omega$. We also measure the quantity $\|\nabla_k u_k\|$, estimated using finite differences. Localised Wannier functions correspond to smooth gauge, and singularities in this quantity is therefore a sign of delocalisation.

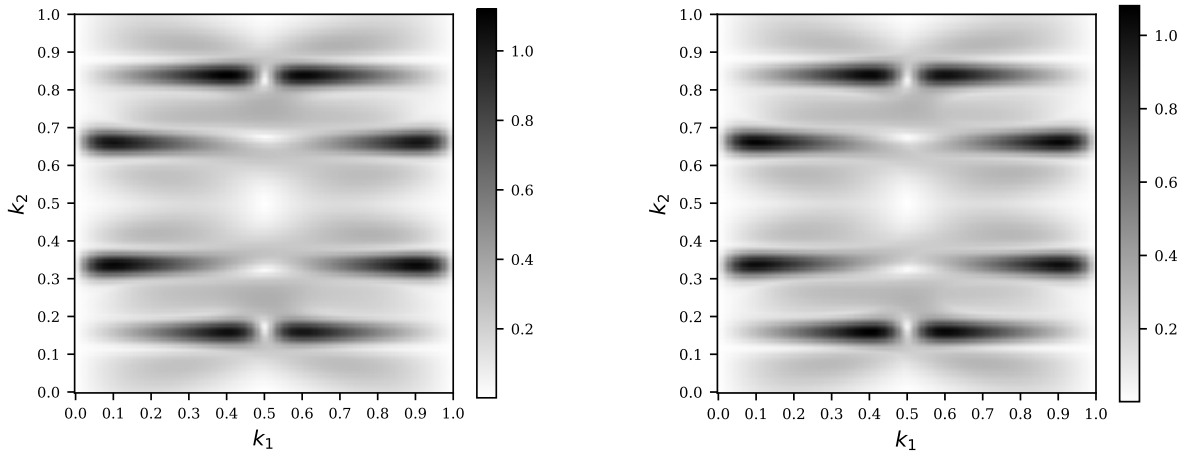


(a) Logarithm interpolation

(b) Column interpolation

Figure 2.2: Local regularity $\|\nabla_k u\|$, $\lambda_\nu = 6$ and $\lambda_R = 1$ (regular insulating phase).

In Figure 2.3a, the log interpolation method fails at constructing a continuous map in the topologically non-trivial QSH phase, as the measure of regularity $\|\nabla_k u\|$ exhibits lines of discontinuity, with very high maximal values. In contrast, in Figure 2.3b, the column interpolation produces a smoother output, which also yields a lower maximal value of the regularity $\|\nabla_k u\|$.

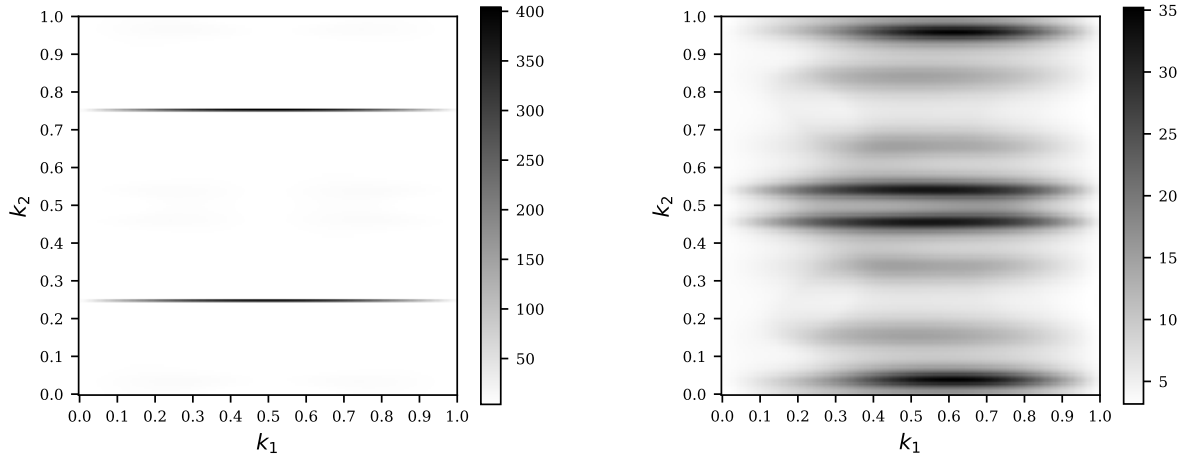


(a) Logarithm interpolation (b) Column interpolation

Figure 2.3: Local regularity $\|\nabla_k u\|$, $\lambda_\nu = 0$ and $\lambda_R = 1$ (QSH phase).

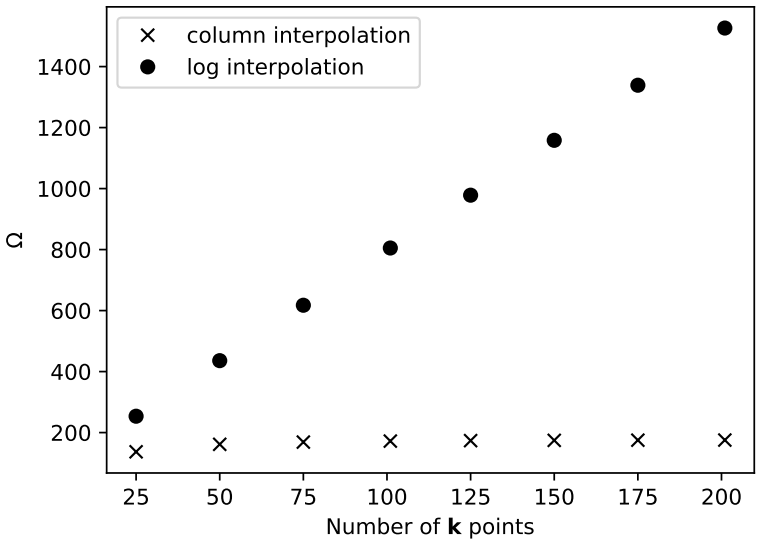


Figure 2.4: Convergence of $\Omega$ obtained by both methods, in the QSH phase ($\lambda_\nu = 0, \lambda_R = 1$)

The (dis)continuity of the resulting Bloch frame after each method is further demonstrated by the convergence with respect to $k$ point discretisation, displayed in Figure 2.4. In the log interpolation method, the discrete Bloch frames converge to a discontinuous one, as we see from the divergence of the norm of the gradient (estimated with finite differences). In contrast, the column interpolation produces a frame that has a smooth limit.

Figures 2.5a and 2.5b display selected components of $k_1 \mapsto V_{\text{obs}}(k_1, k_2)$ for $k_2 = 1, \frac{2}{3}, \frac{1}{3}$. In Figure 2.5a, we see how the obstruction path is contracted into the null path by our algorithm, in the QSH phase, with no Rashba term. In this case, the system decomposes into two independent copies of the Haldane model, one for each spin, which implies that the obstruction matrix is diagonal. This explains that the obstruction (the largest path in the plot) is horizontal, since $V_{21} = 0$. Notice also that the diagonality of the obstruction, as well as time reversal symmetry, implying that $k \mapsto \text{Re}V_{21}(k)$ is odd (which is verified up to rounding errors in the horizontal path), is broken by the method, as expected.

In Figure 2.5b, for a Rashba term $\lambda_R = 1$, the obstruction (the largest path, in green)

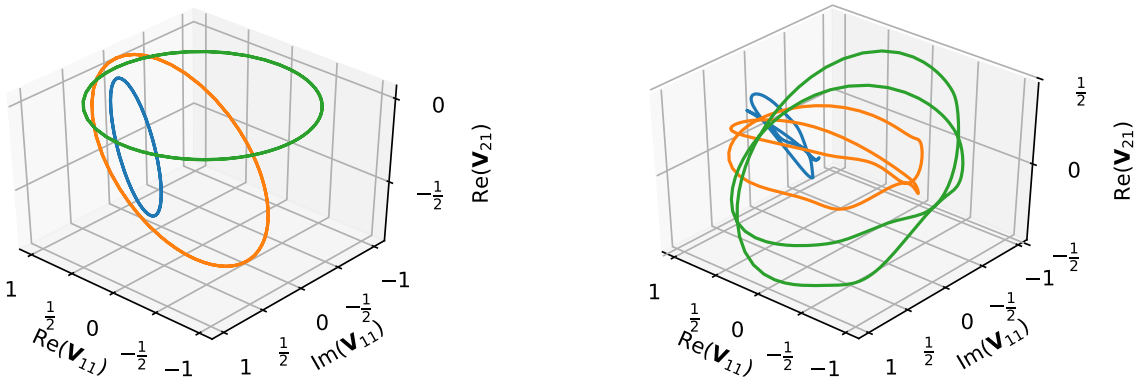


(a) $\lambda_\nu = 0, \lambda_R = 1$ (b) $\lambda_\nu = 1, \lambda_R = 1$

Figure 2.5: Contraction of the first column of the obstruction, with the initial path in green ($k_2 = 1$) being deformed to a single point (yellow at $k_2 = \frac{2}{3}$ then blue at $k_2 = \frac{1}{3}$).

is no longer diagonal (it has non-zero off-diagonal elements), but it still satisfies time-reversal symmetry, since $k \mapsto \mathrm{Re}V_{21}(k)$ is odd. The method breaks time-reversal symmetry to construct the continuous interpolation to the trivial path.

### 2.5.2 Numerical results for Silicon

Using Quantum Espresso, [41], the Bloch waves of Silicon for various discretisations of the Brillouin zone were provided to the homotopy constructing methods, in order to compare the numerical results of our column interpolation algorithm with the ones provided by the logarithm method of [13].

Table 2.1: Value of the Marzari-Vanderbilt localisation functional $\Omega$ (in Bohr$^2$) for frames on various discretisations of the Brillouin zone

| Discretisation of the BZ | $5 \times 5 \times 5$ | $10 \times 10 \times 10$ | $15 \times 15 \times 15$ | $20 \times 20 \times 20$ |
|---|---|---|---|---|
| After logarithm method | 25.72 | 29.70 | 30.62 | 30.94 |
| After column interpolation | 40.88 | 35.31 | 53.68 | 46.80 |
| After MV optimisation (log initial guess) | 19.30 | 22.06 | 22.71 | 22.95 |
| After MV optimisation (col initial guess) | 19.30 | 22.06 | 22.71 | 22.95 |

In Table 2.1, we can see that the value of the localisation functional $\Omega$ is better for the logarithm method than for ours, but, after optimisation of the Marzari-Vanderbilt procedure [66], both methods agree.

In Figure 2.6, we display some Wannier functions computed by both methods, before optimisation. The representation was done through Wannier90 [82] and VESTA [69]. The localisation of both is not optimal, which is expected, but the Wannier functions are still localised, and physically relevant.

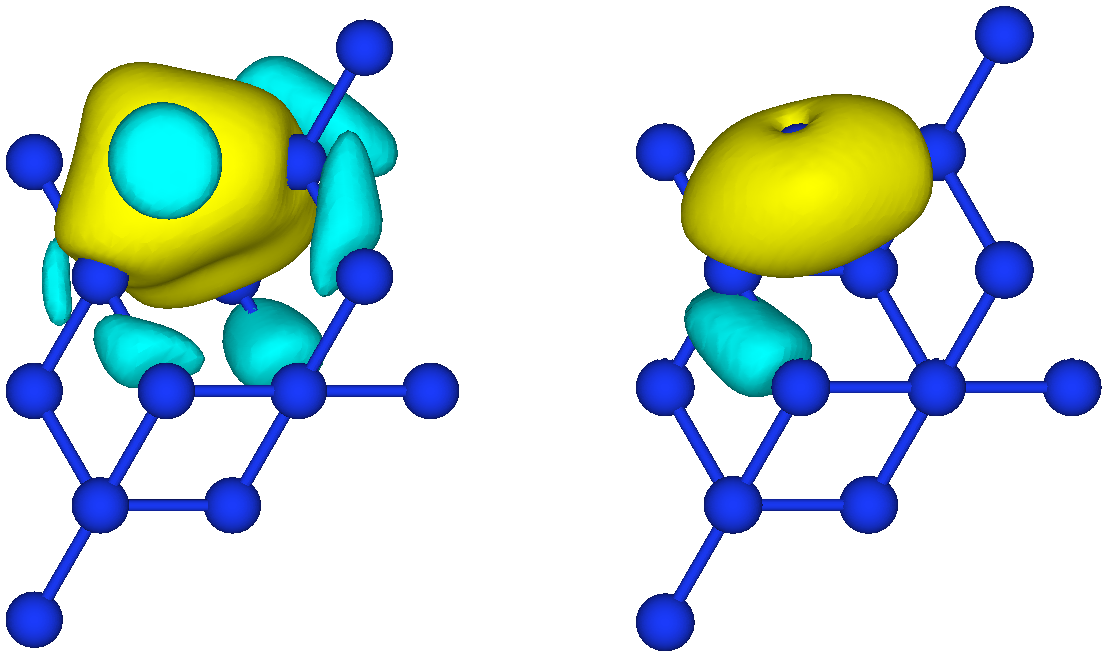

(a) Logarithm method

(b) Column interpolation method

Figure 2.6: One of the four Wannier functions of silicon, isosurface plot at 20% of maximal value.

# Conclusion

We presented a new method to construct localised Wannier functions. It is proven to work even in the case of topological insulators which causes most published algorithms to fail. In the "easy" cases, it works similarly to the method of [13]. As that method, it only localises Wannier functions across unit cells, and does not attempt to localise the functions inside the unit cell. This is problematic in the case of large unit cells, which is the case of many real topological insulators. The efficient numerical construction of Wannier functions in these cases remains therefore an open problem.

# Chapter 3

# Symmetry-adapted approximation of Wannier functions by Gaussian-type orbitals

## 3.1 Introduction

In this chapter, we introduce an approximation method for Wannier functions that is adapted to the computing of tight-binding Hamiltonians in non-periodic van der Waals heterostructures, that is, layers of 2D materials stacked on top of each other, bound together by the comparatively weak van der Waals forces [39]. 2D materials are perfect two-dimensional crystals, an example of which is graphene, constituted by carbon atoms arranged in a honeycomb lattice (see Figure 3.1).

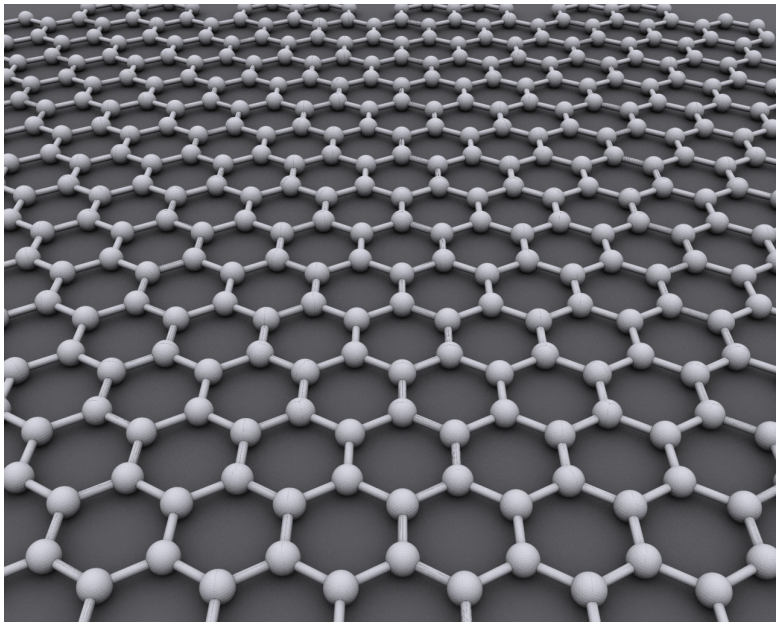

Figure 3.1: Graphene [2]

Notice that, in our setting, 2D materials are periodic. However, stacking layers with different primitive lattice vectors can break the periodicity of the whole system. This happens when the layers are *incommensurate*, *i.e.* when the lattice vectors of one layer cannot be expressed as a linear combination of the lattice vectors of the other layers with rational coefficients. This setting is challenging for the usual computational tools of solid-state physics, which rely on the periodicity of crystals through the use of the Bloch Transform, that cannot be applied

here. However, van der Waals heterostructures are built from periodic 2d materials that are comparatively well-separated, since the distance between nuclei in the same layer is smaller than the distance between nuclei in different layers, and hence the interactions between electrons on separated layers is weak. This is the premise of [98], where the authors see the weak interactions between layers as a perturbation, and compute an approximate ground state by applying perturbation theory to the ground states of the isolated layers. In this context, a first-order approximation is to consider the Wannier functions computed on each layer independently as a basis on which to construct a tight-binding approximation of the first-order perturbed (non-periodic) Hamiltonian. In this chapter, building on the approach proposed in [6], we construct an approximation scheme for Wannier functions that allows for an efficient computation of tight-binding matrix coefficients, even in the non-periodic case.

## 3.2 Wannier functions and their symmetries

### 3.2.1 Wannier functions in solid-state physics

Introduced by Gregory Wannier in [101], Wannier functions are a set of localized electronic orbitals, whose translates span the eigenspaces associated to an energy window. They are a useful tool to visualize the electron states in a crystal, and also to parameterize tight-binding approximations to the continuum Hamiltonian.

Consider a crystal with Bravais lattice $\mathcal{R}$, and reciprocal lattice $\mathcal{R}'$. In the independent electron approximation, using atomic units, the Hamiltonian for an electron reduces to $H = -\frac{1}{2}\Delta + V$, where $V$ is an $\mathcal{R}$-periodic potential, that is assumed to be $L^2_{\text{per}}(\mathbb{R}^d;\mathbb{R})$. The Bloch transform decomposes the Hamiltonian into its fibers $H_{\mathbf{k}}$, for $\mathbf{k} \in \mathcal{B}$, the Brillouin Zone:

$$H_{\mathbf{k}} = \frac{1}{2}(-i\nabla + \mathbf{k})^2 + V,$$

each $H_{\mathbf{k}}$ being an unbounded operator on $L^2_{\text{per}}(\mathbb{R}^d;\mathbb{C})$, with domain $H^2_{\text{per}}(\mathbb{R}^d;\mathbb{C})$. This operator has compact resolvent for each $\mathbf{k}$, hence its spectrum is a non-decreasing sequence of discrete eigenvalues $\{\varepsilon_{n,\mathbf{k}}\}_{n\in\mathbb{N}^*}$ (counted with their multiplicities) going to $+\infty$, which can be chosen continuous with respect to $\mathbf{k}$. The associated eigenvectors, denoted $\mathbf{x} \mapsto u_{n,\mathbf{k}}(\mathbf{x})$, are $\mathcal{R}$-periodic functions.

Wannier functions are then defined as the inverse Bloch transform of a family of functions $\{v_{n,\mathbf{k}}\}_{n\in\mathcal{I},\mathbf{k}\in\mathcal{B}}$, which, for each $\mathbf{k}$, are another basis of the span of the $\{u_{n,\mathbf{k}}\}_{n\in\mathcal{I}}$. The gauge freedom in the choice of the $\{v_{n,\mathbf{k}}\}_{n\in\mathcal{I},\mathbf{k}\in\mathcal{B}}$ is not relevant to study the eigenspace, but its regularity in $\mathbf{k}$ determines the localization of the Wannier functions [71].

### 3.2.2 Symmetry-adapted Wannier functions

It is possible to choose Wannier functions that are adapted to the symmetries of the crystal. There is a group $G$ of symmetry operations that preserves the lattice structure of the crystal, called the *space group* of the crystal. This group includes translations by integer linear combinations of the primitive vectors, rotations around specific points, reflections with respect to planes, and composite operations. It is a subgroup of the Euclidean group of isometries, and as such, any element $g \in G$ can be identified with a pair $(R|\mathbf{a})$, where $R$ is an orthogonal matrix, and $\mathbf{a}$ is a translation vector, which acts on a point $\mathbf{x} \in \mathbb{R}^d$ as $(R|\mathbf{a})\mathbf{x} = R\mathbf{x} + \mathbf{a}$. Since it includes lattice translations, the space group is at least countably infinite.

A $m$-dimensional (unitary) *representation* $D$ of $G$ is a group homomorphism $D : G \to \mathbb{R}^{m\times m}$ from the abstract group $G$ to the group of orthogonal matrices. A representation is said to be *reducible* if there is an invertible matrix $P$, such that for all $g \in G$, $PD(g)P^{-1} =$

$d^{(1)}(g) \oplus \cdots \oplus d^{(k)}(g)$ is block-diagonal, with $k > 1$ blocks of non-trivial size, with a block decomposition that is independent of the element $g$. Then, the group morphisms $d^{(\beta)}, \beta = 1 \dots k$ are called *subrepresentations* of $D$, and if they are not reducible, they are called *irreducible representations* of $G$. For an in-depth treatment of these concepts, we refer to [21].

A more manageable group that we will use to define the symmetry-adapted Wannier functions around a certain *site* $\mathbf{q} \in \mathbb{R}^d$, is the subgroup of the space group that preserves the site $\mathbf{q}$, called the *site-symmetry* group [28]. Explicitly, it is defined by

$$G_q = \{g = (R|\mathbf{a}) \in G \mid g\mathbf{q} = R\mathbf{q} + \mathbf{a} = \mathbf{q}\}.$$

Then, we can try to construct a set of symmetry-adapted Wannier functions that span a subspace that is stable under the action of $G_q$. In group-theoretic language, the symmetry-adapted Wannier functions are chosen to be a basis for an irreducible representation of the site symmetry group [87]. The symmetry-adapted (with respect to $G_q$) Wannier functions, centered at the point $q$ will be denoted $W_i^{(\beta)}$, where $\beta$ labels the irreducible representations, and $i = 1, \dots, n_\beta$ labels the basis functions of the irreducible representation $d^{(\beta)}$. As a consequence, any element $g_q$ of the site symmetry group will act on the symmetry-adapted Wannier functions as

$$(\hat{g}_q W_i)^{(\beta)}(\mathbf{r}) = W_i^{(\beta)}(g_q^{-1}\mathbf{r}) = \sum_{i'=1}^{n_\beta} d_{i'i}^{(\beta)}(g_q) W_{i'}^{(\beta)}(\mathbf{r}),$$

where $d^\beta(g_q)$ is the irreducible matrix representation labeled by $\beta$ of the element $g_q \in G_q$.

## 3.3 Symmetry-adapted Gaussian Type Orbitals

Recall that we aim to approximate Wannier functions in a basis that allows for efficient integral computations, and that is adapted to the physical symmetries of the system. To that end, we construct an approximation of a Wannier function as a sum of gaussians centered at high symmetry points (atomic sites, bond centers...) multiplied by polynomials, called a *Gaussian Type Orbital*,

$$W(\mathbf{r} = (x, y, z)) = \sum_{\mathbf{c} \in \mathcal{C}} \sum_{\mathbf{n_c} \in \mathcal{P}} \lambda_{\mathbf{c},\mathbf{n_c}} (x - c_1)^{n_{c,1}} (y - c_2)^{n_{c,2}} (z - c_3)^{n_{c,3}} \exp\left(-\frac{(\mathbf{r} - \mathbf{c})^2}{2\sigma_{\mathbf{c},\mathbf{n_c}}^2}\right),$$

where $\mathcal{C}$ denotes the set of centers, and for each $\mathbf{c} = (c_1, c_2, c_3)$, the set

$$\mathcal{P}_\mathbf{c} = \left\{\mathbf{n_c} = (n_{\mathbf{c},1}, n_{\mathbf{c},2}, n_{\mathbf{c},3}) \in \mathbb{N}^3\right\}$$

are the powers of the polynomials centered at $\mathbf{c}$. These will be fixed before the optimization of the approximation error. The degrees of freedom are the gaussian widths $\sigma_{\mathbf{c},\mathbf{n_c}}$ and the coefficients $\lambda_{\mathbf{c},\mathbf{n_c}}$.

In graphene, in the usual conditions, the electronic conduction is dominated by the contribution of the $\pi$-orbitals, giving rise to two half-filled bands. The corresponding two mother symmetry-adapted Wannier functions are centered at the two carbon atoms in the unit cell, and are images of one another by a mirror symmetry. The full set of symmetry-adapted Wannier functions for these two bands are lattice translates of these mother Wannier functions. The group containing the site symmetries of the carbon atoms in graphene is denoted $D_{3h}$ in the standard crystallographic tables.

From the point of view of group theory, each mother Wannier function is a basis for the one dimensional irreducible representation $A_2''$ of the site symmetry group $D_{3h}$, with the character table given in Table 3.1.

| $D_3h$ | $E$ | $2C_3(z)$ | $3C_2'$ | $\sigma_h(xy)$ | $2S_3$ | $3\sigma_v$ |
|---|---|---|---|---|---|---|
| $A_2''$ | $+1$ | $+1$ | $-1$ | $-1$ | $-1$ | $+1$ |

Table 3.1: Character table of the $A_2''$ representation of the site symmetry group $D_{3h}$

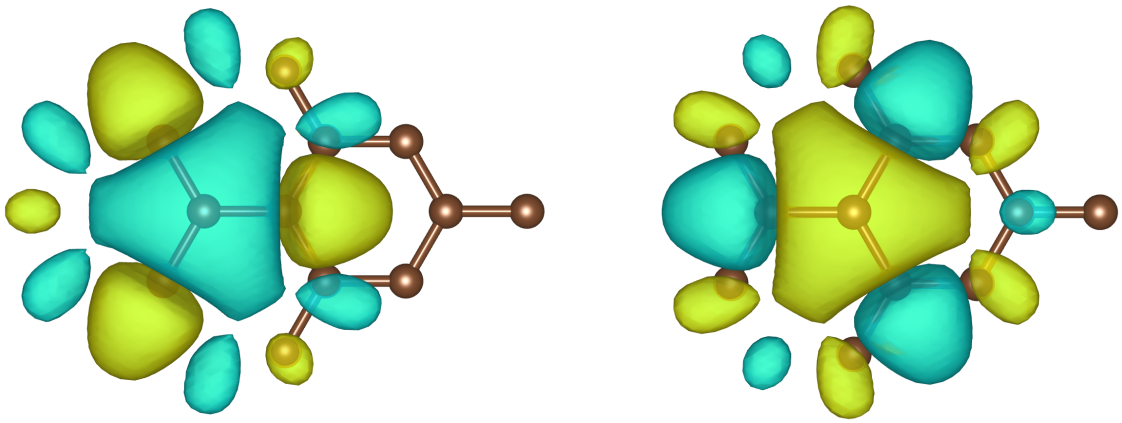

Figure 3.2: Symmetry-adapted mother Wannier functions of graphene, centered on site $A$ (left) and $B$ (right), isosurface at 1% of maximum value.

The two mother Wannier functions are plotted in Figure 3.2.

In this case, the mother Wannier functions centered at the origin is even under in-plane $\frac{2\pi}{3}$ rotations, even under $y \mapsto -y$ reflection, and odd under $z \mapsto -z$ reflection, where we have chosen the $(Ox)$ axis the horizontal axis in the picture, the $(Oy)$ axis pointing up, and $(Oz)$ point out of plane, chosen so that $(Oxyz)$ is direct.

The Gaussian Type Orbitals do not satisfy these symmetries in general, but we can define a symmetrization procedure which makes them so:

$$\widetilde{W}(\mathbf{r}) = \frac{1}{|D_{3h}|} \sum_{g \in D_{3h}} \chi(g) W(g^{-1}\mathbf{r}),$$

where $\chi(g) = \pm 1$ is the character of the group element $g$ for the representation $A_2''$ of the site symmetry group $D_{3h}$ (see Table 3.1), and $\widetilde{W}$ is called a *symmetry-adapted Gaussian Type Orbital*. If $\chi(g) = 1$, then $\widetilde{W}(\mathbf{r})$ is even under transformation by $g$, that is, $\widetilde{W}(\mathbf{r}) = \widetilde{W}(g^{-1}\mathbf{r})$, and otherwise, if $\chi(g) = -1$, it is odd, $\widetilde{W}(\mathbf{r}) = -\widetilde{W}(g^{-1}\mathbf{r})$, for any $g \in D_{3h}$. Notice that some monomials terms are deleted by symmetry, for example, the odd $z \mapsto -z$ symmetry removes terms with even $z$ power $n_{\mathbf{c},3}$.

We obtain that the symmetry-adapted Gaussian Type-Orbital centered at 0 is rewritten:

$$\widetilde{W}(\mathbf{r} = (x, y, z)) = \frac{1}{|D_{3h}|} \sum_{g \in D_{3h}} \sum_{\mathbf{c} \in \mathcal{C}} \sum_{\mathbf{n_c} \in \mathcal{P}} \chi(g) \lambda_{\mathbf{c},\mathbf{n_c}} \left( \prod_{i=1}^{3} \left( \left(g^{-1}\mathbf{r}\right)_i - c_i \right)^{n_{c,i}} \right) \exp\left( -\frac{(\mathbf{r} - g\mathbf{c})^2}{2\sigma^2_{\mathbf{c},\mathbf{n_c}}} \right),$$

This symmetrized function can be recast as a Gaussian Type-Orbital of the same degree with an expanded list of centers,

$$\mathcal{C}' = \{ g\mathbf{c} \mid g \in D_{3h}, \mathbf{c} \in \mathcal{C} \}.$$

and modified coefficients $\{\lambda'_{\mathbf{c},\mathbf{n_c}}\}_{\mathbf{c} \in \mathcal{C}'}$, calculated with the Newton multinomial formula.

## 3.4 Approximation scheme

We have defined the functional form of the approximation we propose, but it is not obvious how to choose all the parameters to best approximate a given Wannier function. In fact, varying the centers, the gaussian widths, and the polynomials at the same time yields such a high computational cost that the problem becomes intractable in practice. Rather than the greedy approach proposed in [6], we use a fixed set of centers, and optimize all the other parameters at the same time.

### 3.4.1 Input data and pre-processing

Let $W^0$ denote the discretized Wannier function we aim to approximate. In practice, we obtain it from Quantum Espresso [40] and Wannier90 [82], in the XSF format, which contains the point-wise values of the function on a supercell regular grid, with discretization volume element $\mathcal{V}$. In what follows, we denote by $\widetilde{W}_{\lambda,\sigma}$ the symmetry-adapted gaussian type orbital with coefficients $\lambda = \{\lambda_{\mathbf{c},\mathbf{n_c}}\}_{\mathbf{c}\in\mathcal{C}}$ and widths $\{\sigma_{\mathbf{c},\mathbf{n_c}}\}_{\mathbf{c}\in\mathcal{C}}$.

$W^0$ is taken to be a multi-dimensional array with multi-indices in $\mathcal{I}$, and we measure the approximation error by $\left\|\widetilde{W}_{\lambda,\sigma} - W^0\right\|^2$, where $\|.\|$ denotes either the $L^2$ discrete norm given by

$$\|A\|^2 = \mathcal{V} \sum_{\mathbf{n}=(n_1,n_2,n_3)\in\mathcal{I}} A_{\mathbf{n}}^2,$$

or the $H^1$ norm

$$\|A\|^2 = \mathcal{V} \sum_{\mathbf{n}=(n_1,n_2,n_3)\in\mathcal{I}} \left(A_{\mathbf{n}}^2 + |(\nabla A)_{\mathbf{n}}|^2\right),$$

where $\nabla A$ is the multi-dimensional array containing the gradient of $A$ at each grid point. The gradient is either calculated by symmetric finite-difference, or by computing a Fast Fourier Transform (FFT) of the data, then multiplying by the wavevector, and computing the inverse Fast Fourier Transform. The number of grid points being too large to work with, we reduce it by cropping to a coarser grid, where we can also subsample by taking every second grid point. In order to fit the symmetry-adapted gaussian type orbital $\widetilde{W}$ to the original Wannier function $W^0$, we split the optimization in two steps: coefficient optimization and gaussian width optimization.

### 3.4.2 Coefficients optimization

For a fixed set of gaussian widths $\{\sigma_{\mathbf{c},\mathbf{n_c}}\}_{\mathbf{c}\in\mathcal{C}}$, the coefficients $\{\lambda_{\mathbf{c},\mathbf{n_c}}\}_{\mathbf{c}\in\mathcal{C}}$ are found by minimizing the objective function

$$\mathrm{obj}\left(\{\sigma_{\mathbf{c},\mathbf{n_c}}\}_{\mathbf{c}\in\mathcal{C}}, \{\lambda_{\mathbf{c},\mathbf{n_c}}\}_{\mathbf{c}\in\mathcal{C}}\right) = \left\|\widetilde{W}_{\lambda,\sigma} - W^0\right\|^2.$$

Reshaping the multi-dimensional array $W^0$ into a column vector, and accordingly each monomial gaussian term in $\widetilde{W}_{\lambda,\sigma}$, we obtain the following equivalent formulation

$$\mathrm{obj}\left(\{\sigma_{\mathbf{c},\mathbf{n_c}}\}_{\mathbf{c}\in\mathcal{C}}, \{\lambda_{\mathbf{c},\mathbf{n_c}}\}_{\mathbf{c}\in\mathcal{C}}\right) = \left\|M_\sigma \lambda - \mathrm{vect}\left(W^0\right)\right\|^2,$$

where $M_\sigma$ is the rectangular matrix of the monomials, where each column contains the values of one monomial on the whole reshaped grid, $\lambda$ the vector containing the coefficients, and $\mathrm{vect}(W^0)$ the vectorized (reshaped) original Wannier function on the grid. This is a linear least squares problem, which is not well-posed in general. Indeed, the matrix $M_\sigma$ is in practice tall

and skinny, and undetermined (if some monomials are deleted by symmetry), and so $M_\sigma$ might not have full rank. This kind of problem can fortunately be solved efficiently numerically by first performing a pivoted QR factorization of the matrix $M_\sigma$, and then using the \ subroutine of Julia.

If $M_\sigma$ does not have full numerical rank, pivoted QR finds a decomposition with a non-singular (numerically well-conditioned) triangular matrix $R$, and \ solves the associated linear system.

If the norm chosen is the $H^1$ norm, one solves the extended linear system obtained by appending to $M_\sigma$ and $\mathrm{vect}(W^0)$ their gradients.

### 3.4.3 Gaussian widths optimization

The objective function is defined as follows: for a given set of widths $\{\sigma_{\mathbf{c},\mathbf{n_c}}\}_{\mathbf{c}\in\mathcal{C}}$, optimize the coefficients $\lambda$, and return the approximation error.

$$\mathrm{obj}_0(\{\sigma_{\mathbf{c},\mathbf{n_c}}\}_{\mathbf{c}\in\mathcal{C}}) = \inf_{\{\lambda_{\mathbf{c},\mathbf{n_c}}\}_{\mathbf{c}\in\mathcal{C}}} \left\| \widetilde{W}_{\lambda,\sigma} - W^0 \right\|^2 = \inf_{\{\lambda_{\mathbf{c},\mathbf{n_c}}\}_{\mathbf{c}\in\mathcal{C}}} \left\| M_\sigma \lambda - \mathrm{vect}\left(W^0\right) \right\|^2 .$$

For simplicity, we use a non-differentiable optimization method, the Nelder-Mead algorithm, from the **Optim.jl** Julia package. We are aware that better methods exist, but this algorithm was sufficient for our purposes.

### 3.4.4 Numerical results

We test the procedure on one of the Wannier functions of graphene. The centers of the Gaussian polynomials are chosen at four atoms (inequivalent by symmetry), with the following coordinates, where $a = 1.42$ Å denotes the lattice constant,

$$c^{(0)} = \begin{pmatrix} 0 \\ 0 \\ 0 \end{pmatrix} \quad c^{(1)} = \begin{pmatrix} a \\ 0 \\ 0 \end{pmatrix} \quad c^{(2)} = \begin{pmatrix} \frac{3}{2}a \\ \frac{\sqrt{3}}{2}a \\ 0 \end{pmatrix}, \quad c^{(3)} = \begin{pmatrix} \frac{5}{2}a \\ \frac{\sqrt{3}}{2}a \\ 0 \end{pmatrix}.$$

The powers are all the symmetry-allowed multi-indices with angular momentum less than 6. For more degrees of freedom, we set two Gaussian Type Orbitals per atom (with different gaussian widths).

In Figure 3.3, we show the isosurface plot of the Wannier functions (original and approximation with $L^2$ norm).

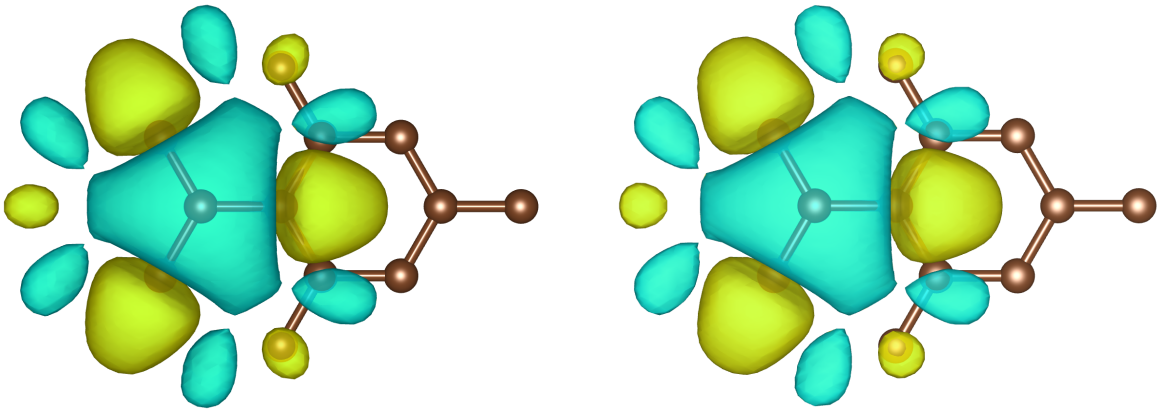

Figure 3.3: Original Wannier function (left), and best approximation with $L^2$ norm (right), isosurface at 1% of maximum value.

This approximation has a relative $L^2$ error of 1.20% on the cropped grid, and 1.66% on the full grid, and a $H^1$ error of 1.40% on the cropped grid, and 2.28% on the full grid.

In Figure 3.4, we show the isosurface plot of the Wannier functions (original and approximation with $H^1$ norm).

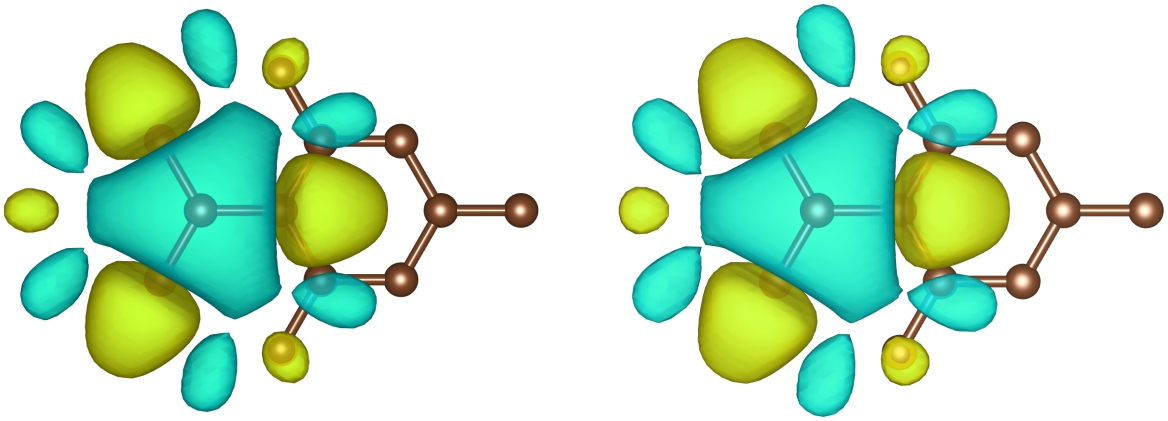

Figure 3.4: Original Wannier function (left), and best approximation with $H^1$ norm (right), isosurface at 1% of maximum value.

This approximation has a relative $L^2$ error of 1.22% on the cropped grid, and 1.68% on the full grid, and a $H^1$ error of 1.38% on the cropped grid, and 2.27% on the full grid. Since the results of the optimization using $H^1$ or $L^2$ norm differ by only 0.02% (or less), we conclude that the norm used to define the objective function has little impact in our case. However, to ensure the control of the error on the kinetic energy, we will choose the $H^1$ norm for the rest of our study.

## 3.5 Matrix elements calculations

### 3.5.1 Computation of integrals

Given two Wannier functions $W_0, W_1$, their overlap integral is defined as

$$\int_{\mathbb{R}^3} W_0(\mathbf{r}) W_1(\mathbf{r}) \, \mathrm{d}\mathbf{r},$$

and their kinetic integral is

$$\int_{\mathbb{R}^3} (\nabla W_0 \cdot \nabla W_1)(\mathbf{r}) \, \mathrm{d}\mathbf{r}.$$

In the physics literature, these terms are called matrix elements, as they are constituents of the tight-binding "matrix".

For Wannier functions on (possibly different) grids, these integrals require to interpolate one of the Wannier functions on the grid of the other one, and then to compute the discretized integrals.

Using Gaussian-Type orbitals, all this can be done analytically, using the Gaussian moment integration formula

$$\int_{\mathbb{R}} x^n \exp\left(-\alpha x^2\right) = \frac{\Gamma\left(\frac{n+1}{2}\right)}{2\alpha^{\frac{n+1}{2}}},$$

where $\Gamma$ is the Gamma function. Gaussians are widely used in Quantum chemistry for this reason, and there exists a variety of integral computation packages for Gaussian Type orbitals.

In practice, we chose to interface the gaussian approximation of the Wannier functions with the libcint [92] library through PySCF [93].

### 3.5.2 Numerical results

We compute the overlap and kinetic integrals between the Wannier function of graphene and its translated image (in the paragraph "pure translations"), and the Wannier and its translated-rotated image ("Translations and rotations" paragraph), for different values of shifts. The results are compared for the $H^1$ compressed Wannier function, with analytic gaussian integration, and the original Wannier function, with linear interpolation, grid integration, and gradient computation through Fourier transform, or finite difference.

#### Pure translations

In Figures 3.5 and 3.6, we display the value of the overlap integrals between a Wannier function and its translates by a vector $(0, 0, z_{shift})$, and in Figures 3.7, and 3.8 the value of the kinetic integrals. The curves are indistinguishable in the first three, and the difference is rather small in Figure 3.8, hence, the impact of the approximation on the integrals is negligible.

In Figures 3.9 and 3.10, the Wannier functions are shifted by a vector $(x_{shift}, 0, 3.4)$Å, where we have chosen a $z$ shift of 3.4Å because it corresponds roughly to the interlayer distance in bilayer graphene. There, the approximation error is more visible, but still comparatively small.

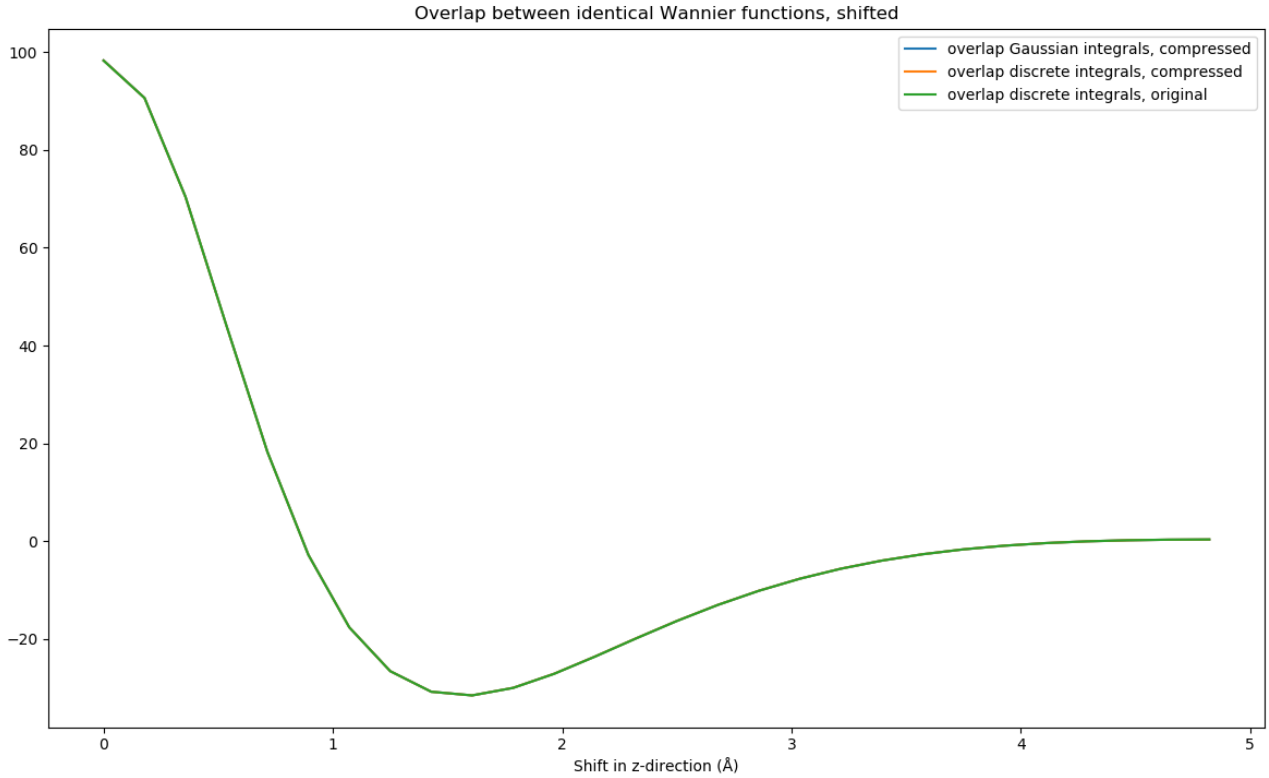


Figure 3.5: Overlaps, shift $(0, 0, z_{shift})$

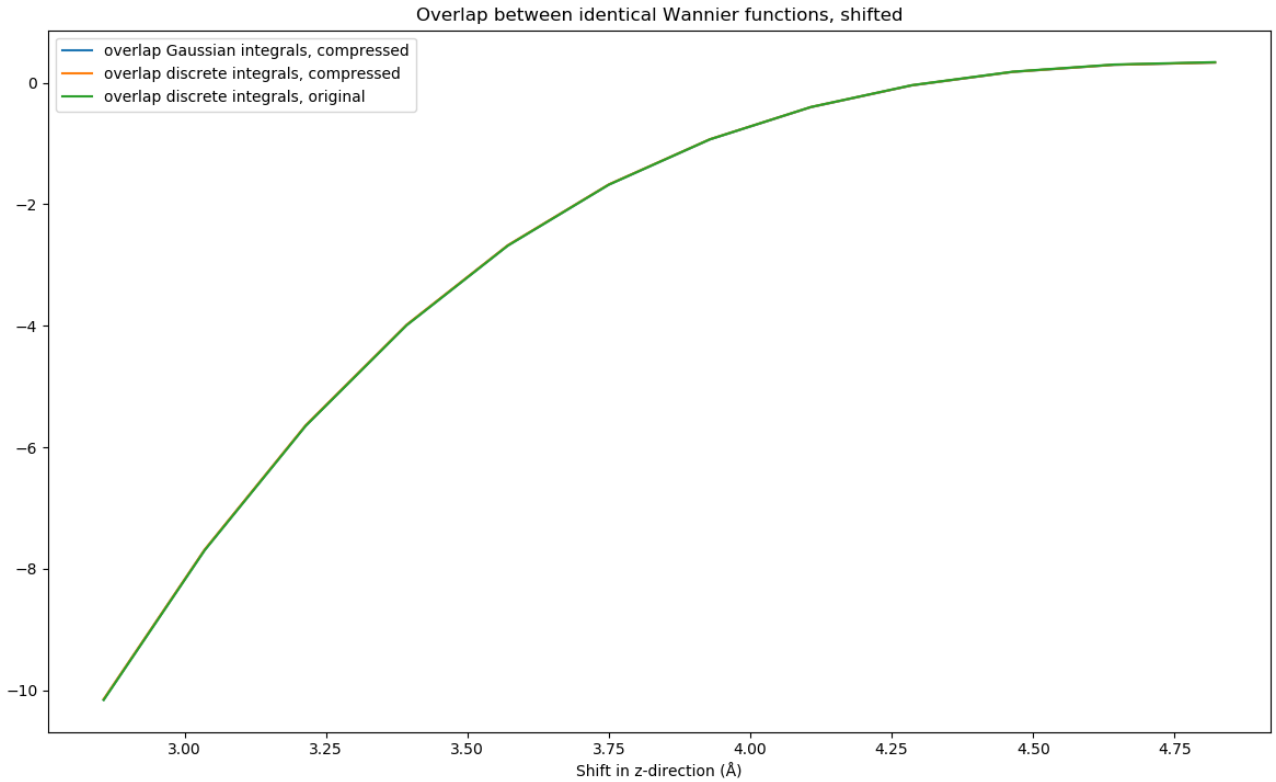


Figure 3.6: Overlaps, zoomed, shift $(0, 0, z_{shift})$

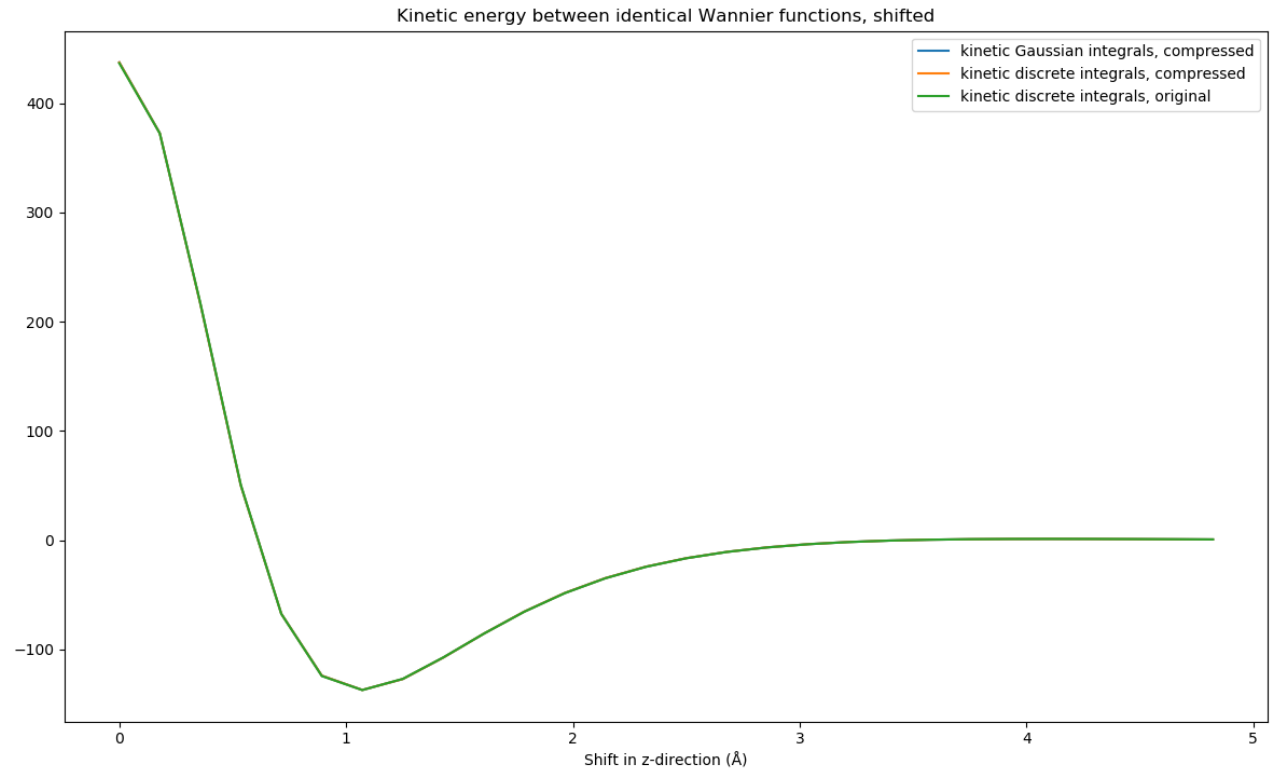


Figure 3.7: Kinetic energy, gradient by Fourier transform, shift $(0, 0, z_{shift})$

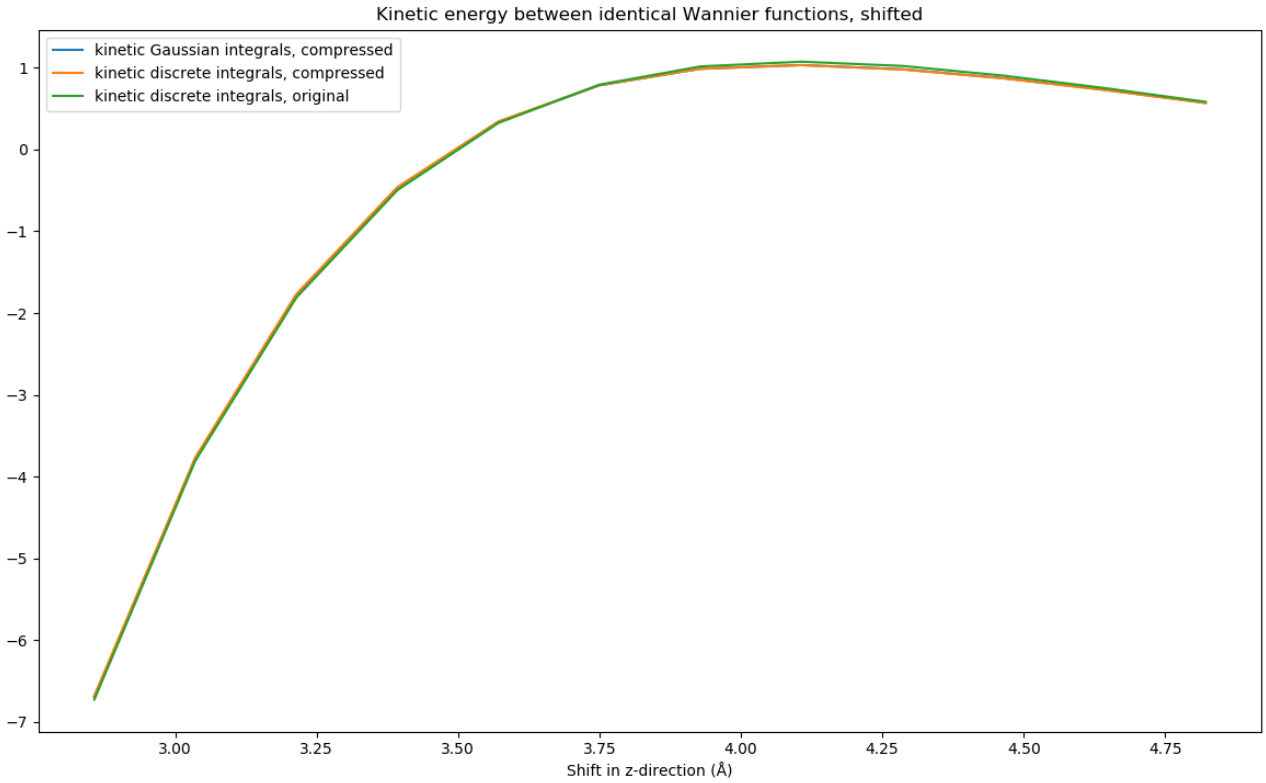


Figure 3.8: Kinetic energy, gradient by Fourier transform, zoomed, shift $(0, 0, z_{shift})$

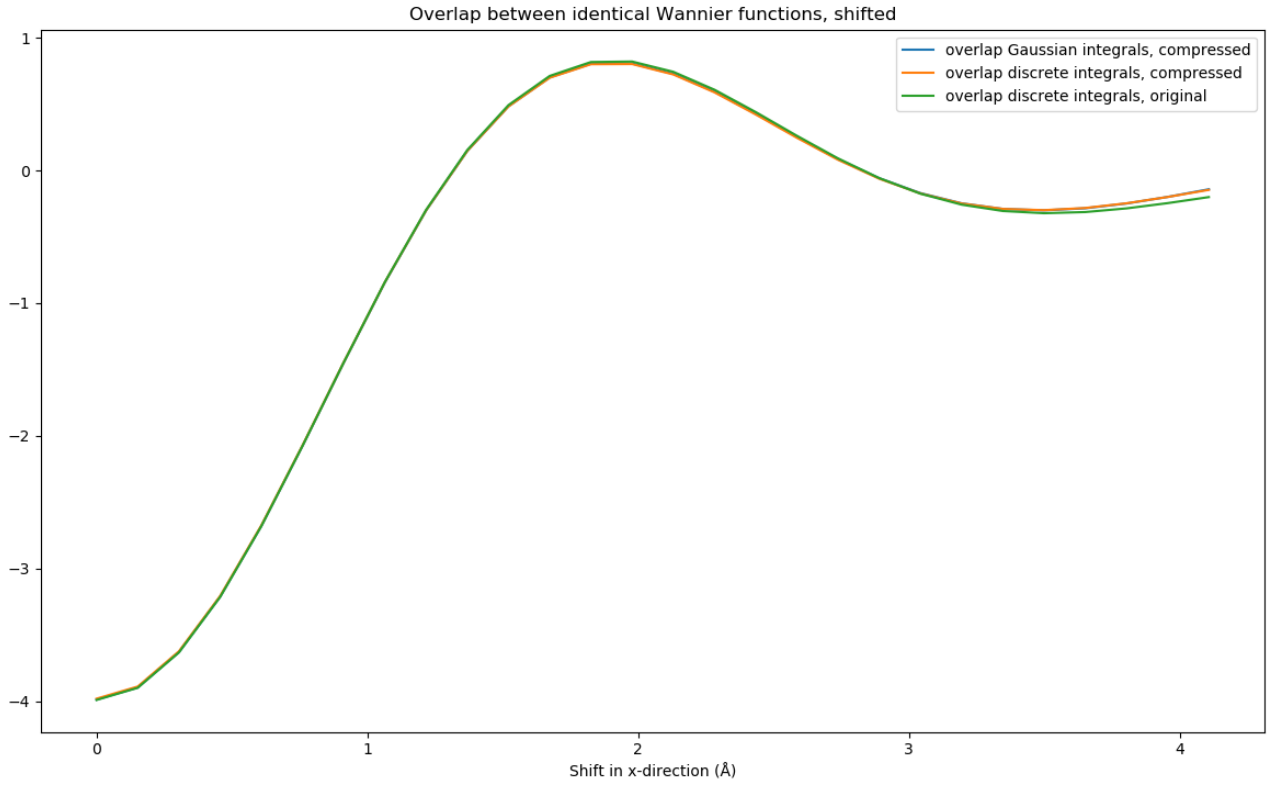


Figure 3.9: Overlaps, shift $(x_{shift}, 0, 3.4)$Å

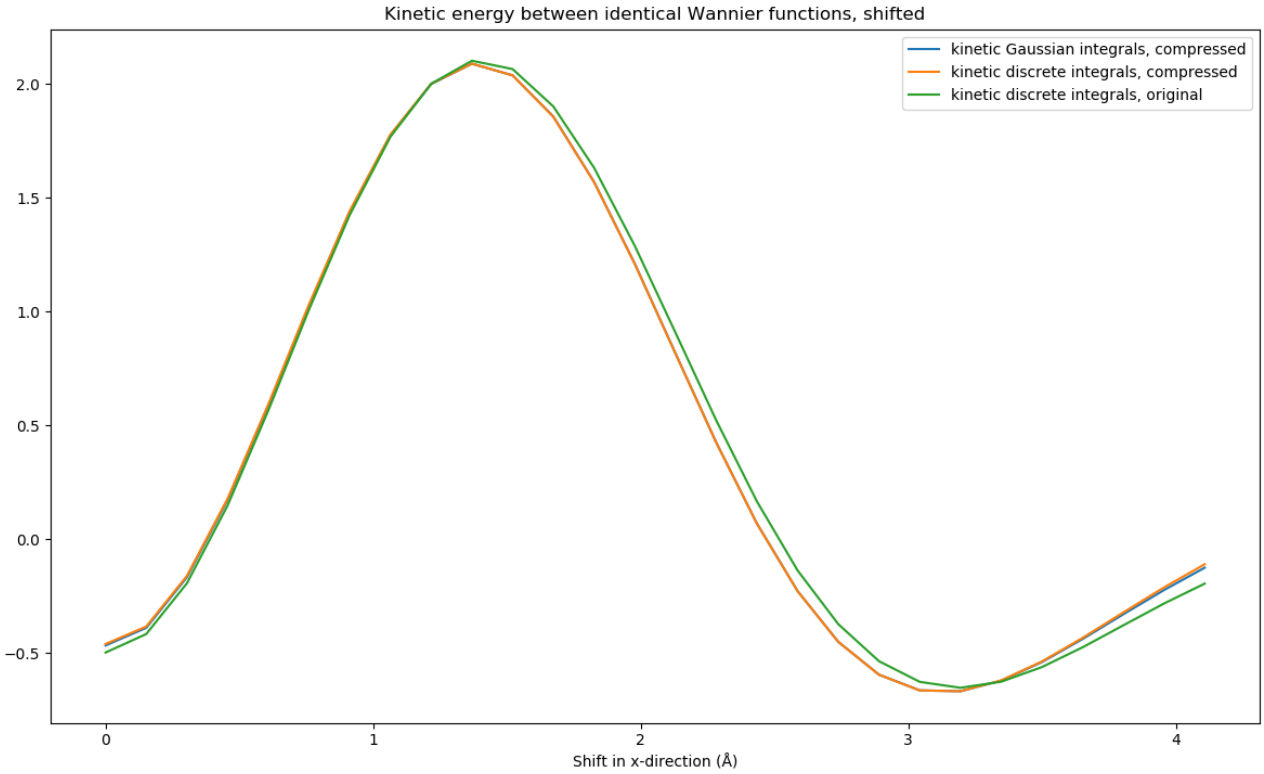


Figure 3.10: Kinetic energy, gradient by Fourier transform, shift $(x_{shift}, 0, 3.4)$Å

### Translations and rotations

In this paragraph, we display the overlaps and kinetic energies between the original and the shifted, rotated Wannier function. To compute the values of the rotated Wannier function on the grid, we use a linear interpolation, both on the values of the function and on the gradients.

Denote $\overline{W}_0$ the array containing the discrete Wannier function on the grid. For $1 \leq i \leq N_1, 1 \leq j \leq N_2, 1 \leq k \leq N_3$, the value of the function $W_0$ at the grid point

$$(\text{grid}[1,i,j,k], \text{grid}[2,i,j,k], \text{grid}[3,i,j,k])$$

is denoted $\overline{W}_0[i,j,k]$. Denote $\Delta x, \Delta y, \Delta z$ and $\Delta x_R, \Delta y_R, \Delta z_R$ the vectors defined by

$$\Delta x = \begin{pmatrix} \text{grid}[1,2,1,1] \\ \text{grid}[2,2,1,1] \\ \text{grid}[3,2,1,1] \end{pmatrix} - \begin{pmatrix} \text{grid}[1,1,1,1] \\ \text{grid}[2,1,1,1] \\ \text{grid}[3,1,1,1] \end{pmatrix},$$
$$\Delta y = \begin{pmatrix} \text{grid}[1,1,2,1] \\ \text{grid}[2,1,2,1] \\ \text{grid}[3,1,2,1] \end{pmatrix} - \begin{pmatrix} \text{grid}[1,1,1,1] \\ \text{grid}[2,1,1,1] \\ \text{grid}[3,1,1,1] \end{pmatrix},$$
$$\Delta z = \begin{pmatrix} \text{grid}[1,1,1,2] \\ \text{grid}[2,1,1,2] \\ \text{grid}[3,1,1,2] \end{pmatrix} - \begin{pmatrix} \text{grid}[1,1,1,1] \\ \text{grid}[2,1,1,1] \\ \text{grid}[3,1,1,1] \end{pmatrix}.$$

Let $\mathbf{r} \mapsto W_0(\mathbf{r})$ denote the linear interpolation of the Wannier function, its $Q_1$ interpolation

according to the finite-element terminology, defined by

$$\begin{aligned}W_0(\mathbf{r}) =&(1-u)(1-v)(1-w)\overline{W}_0[i_1,j_1,k_1] + u(1-v)(1-w)\overline{W}_0[i_1+1,j_1,k_1]\\ &+(1-u)v(1-w)\overline{W}_0[i_1,j_1+1,k_1] + uv(1-w)\overline{W}_0[i_1+1,j_1+1,k_1]\\ &+(1-u)(1-v)w\overline{W}_0[i_1,j_1,k_1+1] + u(1-v)w\overline{W}_0[i_1+1,j_1,k_1+1]\\ &+(1-u)vw\overline{W}_0[i_1,j_1+1,k_1+1] + uvw\overline{W}_0[i_1+1,j_1+1,k_1+1],\end{aligned}$$

where $(i_1,j_1,k_1)$ are the indices of the grid point such that $\mathbf{r}$ is in the parallelepiped defined by the vertex $(\text{grid}[1,i_1,j_1,k_1],\text{grid}[2,i_1,j_1,k_1],\text{grid}[3,i_1,j_1,k_1])$ and the vectors $\Delta x,\Delta y,\Delta z$, and $1\leq u,v,w<1$ are the rescaled coordinates of $\mathbf{r}$ in the parallelepiped cell, satisfying

$$\mathbf{r} = \begin{pmatrix}\text{grid}[1,i_1,j_1,k_1]\\ \text{grid}[2,i_1,j_1,k_1]\\ \text{grid}[3,i_1,j_1,k_1]\end{pmatrix} + u\Delta x + v\Delta y + w\Delta z.$$

Let $R\in\mathcal{SO}(3)$ denote the rotation matrix which we apply to one of the Wannier functions, and $\text{grid}_R$ the rotated grid, defined by

$$\begin{pmatrix}\text{grid}_R[1,i,j,k]\\ \text{grid}_R[2,i,j,k]\\ \text{grid}_R[3,i,j,k]\end{pmatrix} = R^{-1}\begin{pmatrix}\text{grid}[1,i,j,k]\\ \text{grid}[2,i,j,k]\\ \text{grid}[3,i,j,k]\end{pmatrix}.$$

As previously, $\Delta x_R,\Delta y_R,\Delta z_R$ are the grid vectors of $\text{grid}_R$. Let $W_R$ be the rotated Wannier function, defined by

$$W_R(\mathbf{r}) = W_0(R^{-1}\mathbf{r}) \quad \forall\mathbf{r}.$$

We define the array $\overline{W}_R$ of the rotated Wannier function on the grid as follows.

$$\begin{aligned}\overline{W}_R[i,j,k] &= W_R\left((\text{grid}[1,i,j,k],\text{grid}[2,i,j,k],\text{grid}[3,i,j,k])\right)\\ &= W_0\left(R^{-1}(\text{grid}[1,i,j,k],\text{grid}[2,i,j,k],\text{grid}[3,i,j,k])\right)\\ &= W_0\left((\text{grid}_R[1,i,j,k],\text{grid}_R[2,i,j,k],\text{grid}_R[3,i,j,k])\right).\end{aligned}$$

We denote the array containing the gradient of $W_0$ by $\nabla\overline{W}_0$, and its value at the grid point with indices $(i,j,k)$ is $\left(\nabla\overline{W}_0[1,i,j,k],\nabla\overline{W}_0[2,i,j,k],\nabla\overline{W}_0[3,i,j,k]\right)$. As previously, we denote $\nabla W_0$ the linear interpolation of the gradient array. Similarly, we denote $\nabla\overline{W}_R$ the array containing the gradient of the rotated Wannier function, and $\nabla W_R$ the function given by the linear interpolation. Let us remark that

$$\nabla W_R(\mathbf{r}) = R^{-1}\nabla W_0(R^{-1}\mathbf{r}),$$

which means that we can obtain the gradient of $W_R$ by a rotation of the gradient of $W_0$. This is how we proceed in practice, by first computing the gradient of $\overline{W}_0$ through its Fast Fourier Transfom, and then rotating. Indeed, the Wannier function comes from a planewave calculation, where the planewave basis is adapted to the grid on which we work, hence, computing the gradient in Fourier gives a very accurate result for the original discretized Wannier function $W_0$. However, the rotated Wannier function does not necessarily retain this accurate planewave representation, and we thus found it more accurate to compute the gradient by Fast Fourier Transform before applying the rotation, rather than computing directly the gradient of the rotated function.

As written before, a Gaussian-Type orbital transforms under the action of a rotation $R$ as

$$\begin{aligned}W(R^{-1}\mathbf{r}) &= \sum_{c\in\mathcal{C}}\sum_{n_c\in\mathcal{P}}\lambda_{c,n_c}\left(\left(R^{-1}\mathbf{r}\right)_1 - c_1\right)^{n_{c,1}}\left(\left(R^{-1}\mathbf{r}\right)_2 - c_2\right)^{n_{c,2}}\left(\left(R^{-1}\mathbf{r}\right)_3 - c_3\right)^{n_{c,3}}\exp\left(-\frac{(R^{-1}\mathbf{r}-c)^2}{2\sigma_{c,n_c}^2}\right)\\ &= \sum_{c\in\mathcal{C}}\sum_{n_c\in\mathcal{P}}\lambda_{c,n_c}\left(R^{-1}\left(\mathbf{r}-Rc\right)\right)_1^{n_{c,1}}\left(R^{-1}\left(\mathbf{r}-Rc\right)\right)_2^{n_{c,2}}\left(R^{-1}\left(\mathbf{r}-Rc\right)\right)_3^{n_{c,3}}\exp\left(-\frac{(\mathbf{r}-Rc)^2}{2\sigma_{c,n_c}^2}\right),\end{aligned}$$

which can be recast as another Gaussian-Type orbital with the rotated centers, and coefficients calculated by a Newton multinomial formula.

Isosurface plots of linearly interpolated Wannier functions are presented in Figures 3.11 and 3.12, and of the analytically rotated compressed Wannier function in Figures 3.13 and 3.14.

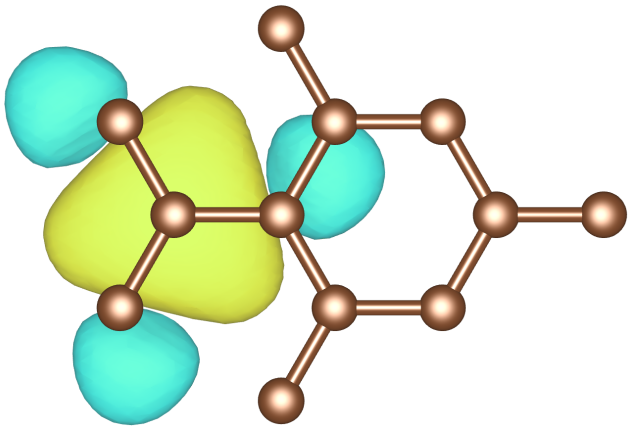

Figure 3.11: Wannier function, rotation by $\theta = 15$ degrees, linear interpolation

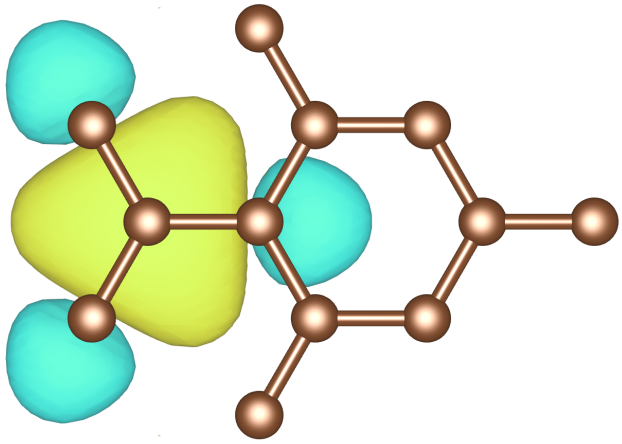

Figure 3.12: Wannier function, rotation by $\theta = 120$ degrees, linear interpolation

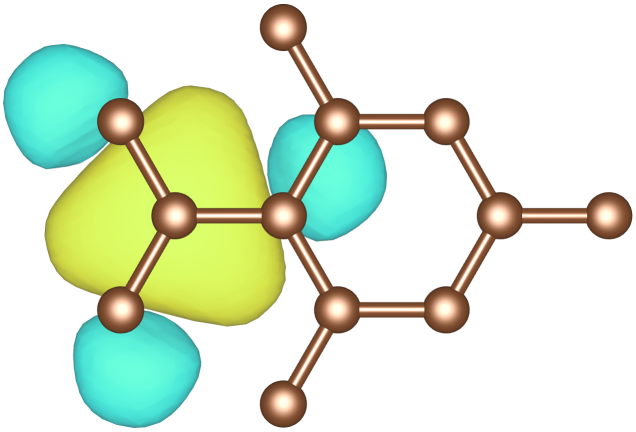

Figure 3.13: Compressed Wannier function, rotation by $\theta = 15$ degrees

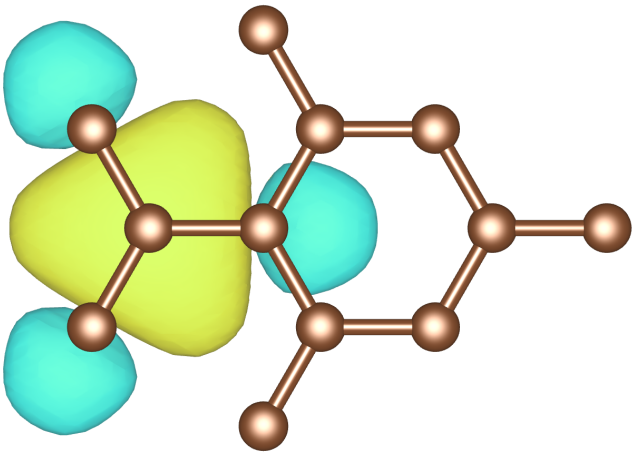

Figure 3.14: Compressed Wannier function, rotation by $\theta = 120$ degrees

In Figures 3.15 and 3.16, an in-plane rotation of an angle of $\theta = 1.09$ degrees is introduced between the two Wannier functions, corresponding to the case of two layers of graphene stacked onto each other, with the "magic-angle" between them [15]. This setting is particularly interesting because the electronic band structure exhibits an almost flat band near the Fermi level, leading to unconventional superconductivity [14].

In Figures 3.17 and 3.18, the angle chosen is $\theta = 55$ degrees, chosen because it does not correspond to a particular symmetry of the Wannier function, and it is an angle for which the Wannier and its rotated image are quite different. One can see on these graphs that the approximation error has the most impact on the overlap and kinetic energy at a shift $(x_{shift}, 0, 3.4)$Å for $x_{shift} \simeq 5$Å.

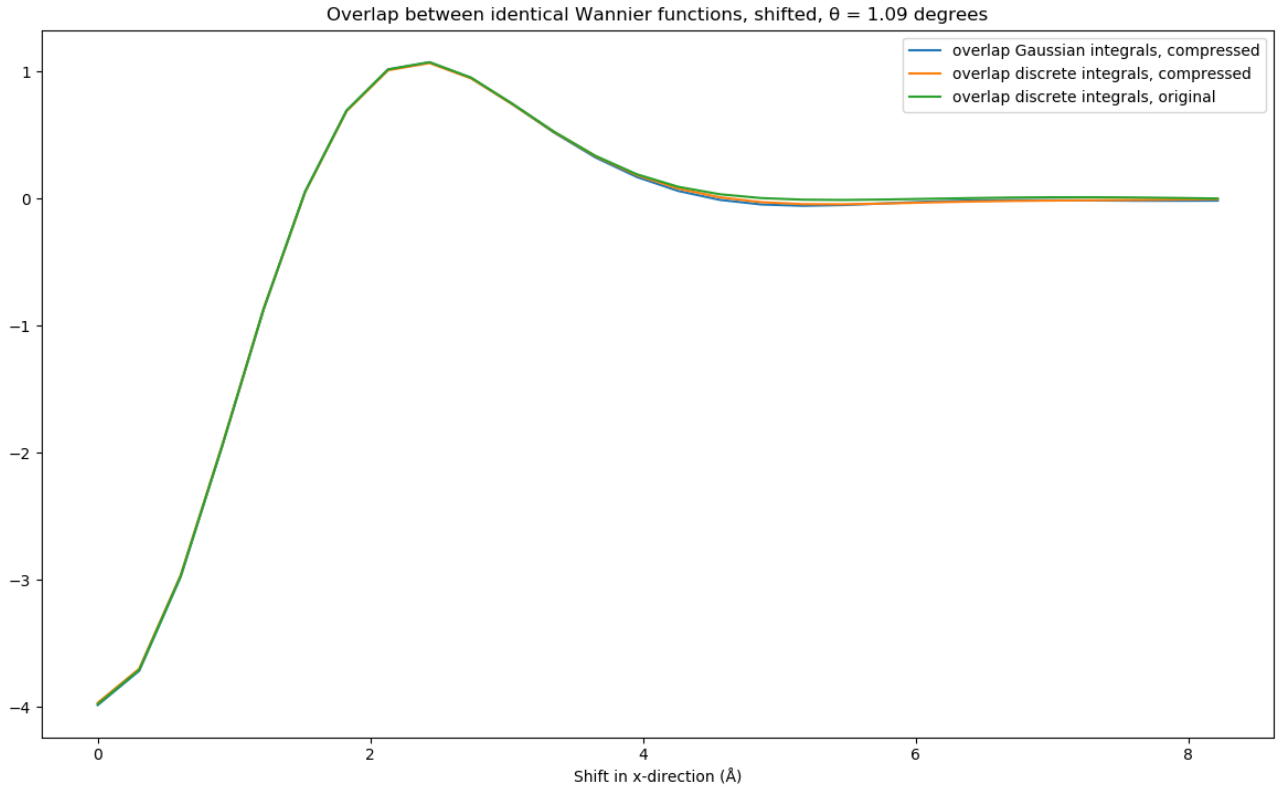


Figure 3.15: Overlaps, shift $(x_{shift}, 0, 3.4)$Å, $\theta = 1.09$ degrees

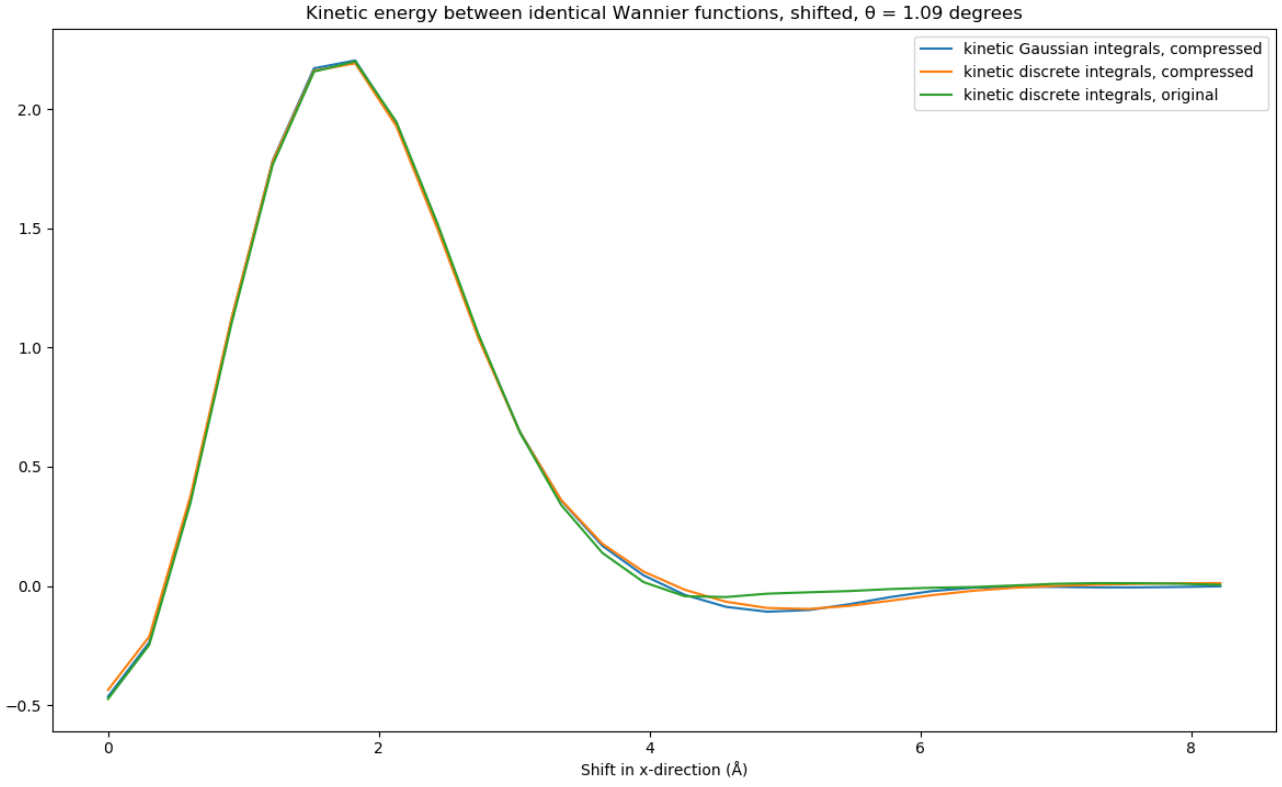


Figure 3.16: Kinetic energy, gradient by Fourier transform, shift $(x_{shift}, 0, 3.4)$Å, $\theta = 1.09$ degrees

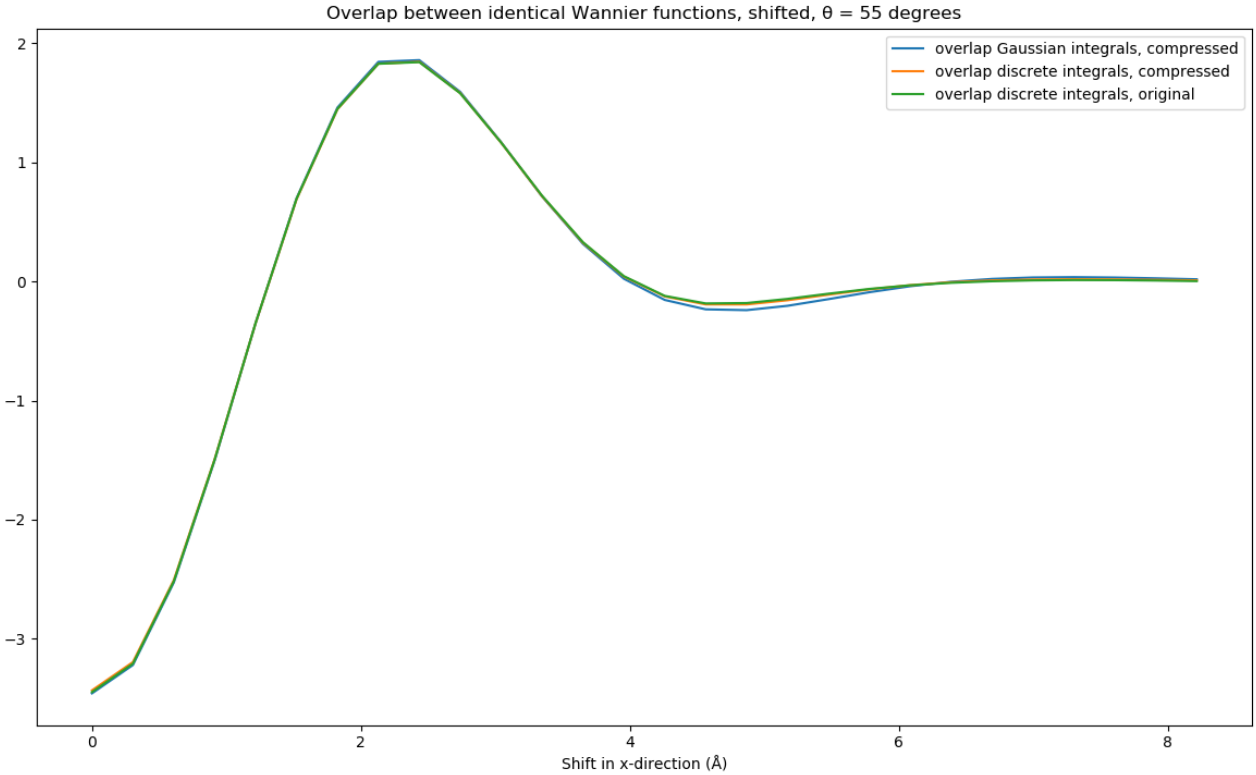


Figure 3.17: Overlaps, shift $(x_{shift}, 0, 3.4)$Å, $\theta = 55$ degrees

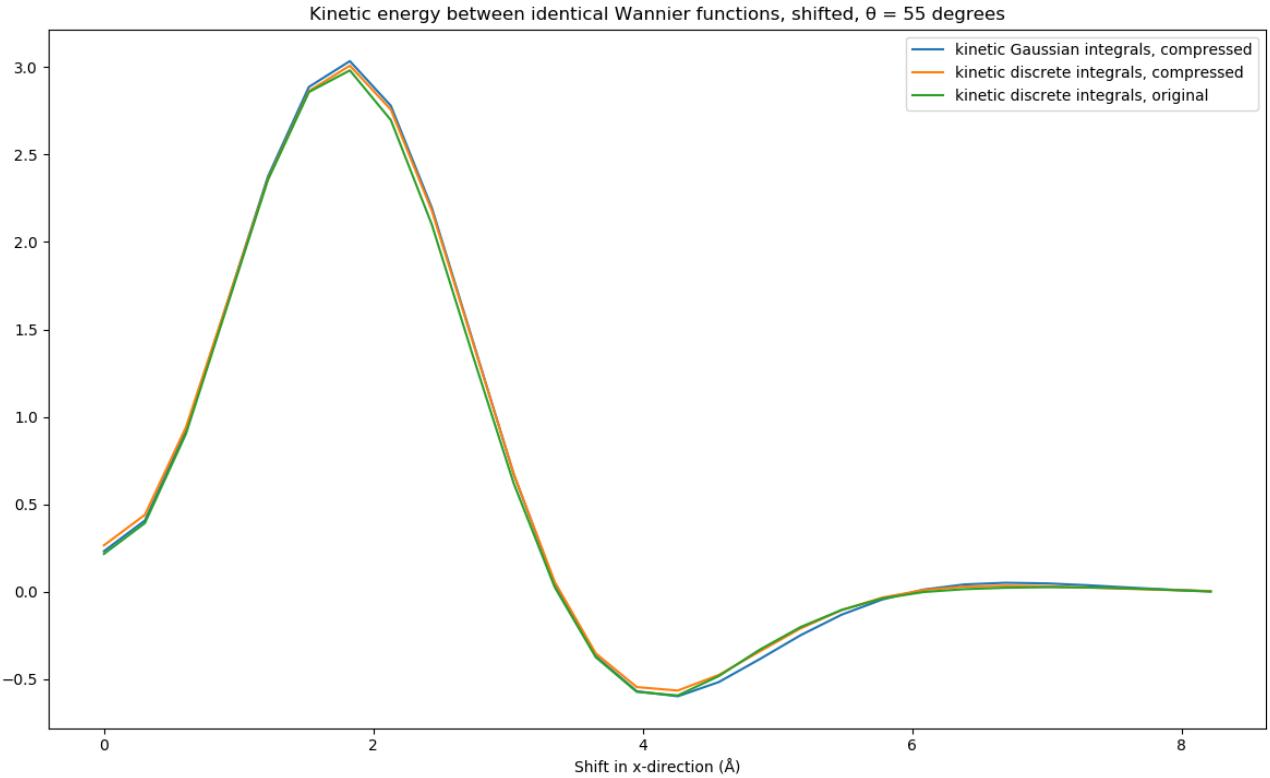


Figure 3.18: Kinetic energy, gradient by Fourier transform, shift $(x_{shift}, 0, 3.4)$Å, $\theta = 55$ degrees

In Figures 3.19 to 3.26, we display the overlap and kinetic integrals for a fixed translation vector, with respect to the rotation angle (restricted to the range $[0, 60]$ degrees by symmetry). In these plots, the errors become comparatively more significant, although we should temper this observation by reminding ourselves that we are looking at approximation errors in the tails of the function.

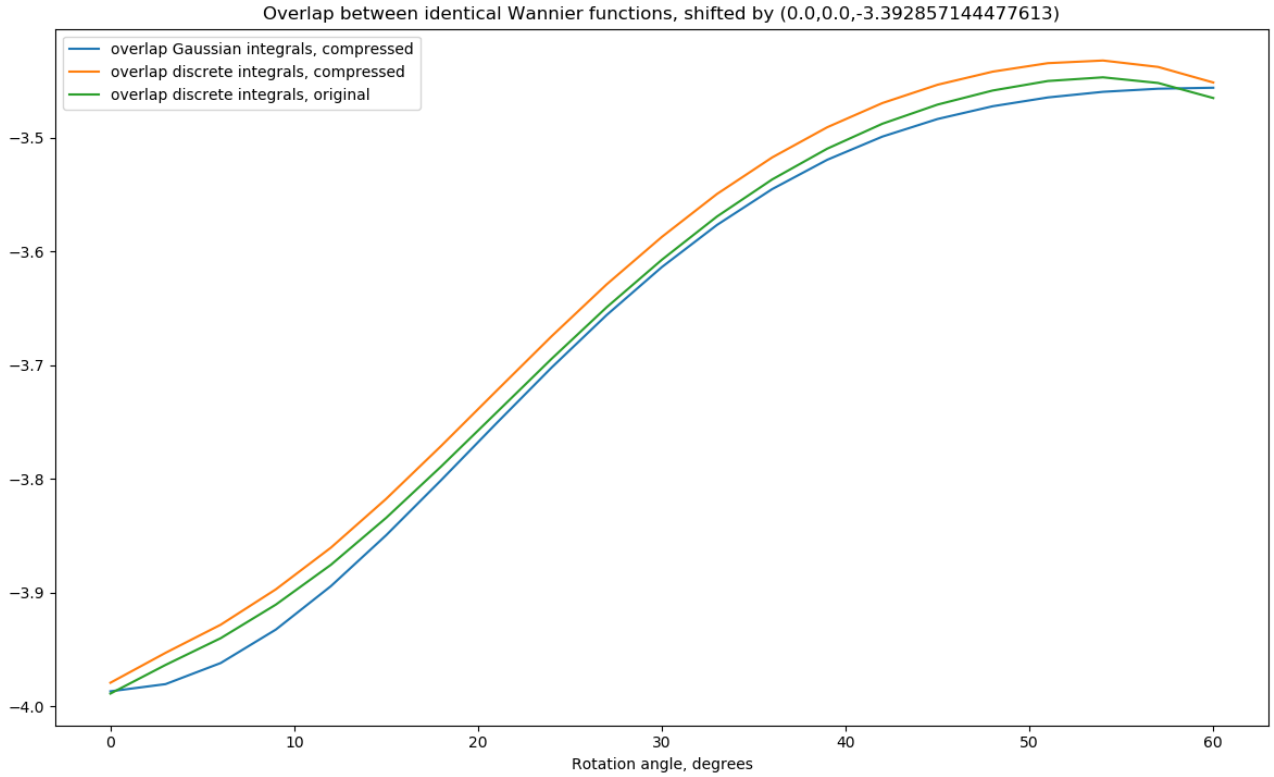


Figure 3.19: Overlaps, Wannier functions shifted by $(0, 0, 3.4)$Å, with respect to the rotation angle

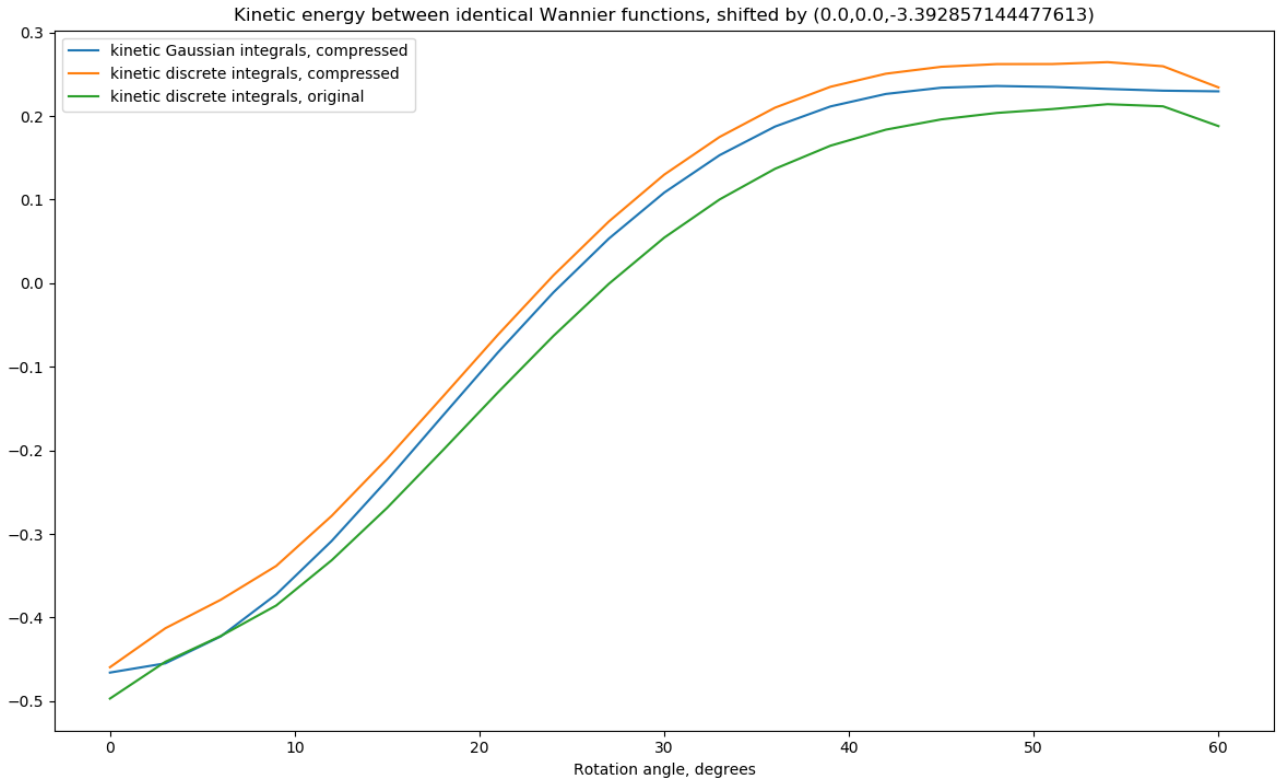


Figure 3.20: Kinetic energy, Wannier functions shifted by $(0, 0, 3.4)$Å, with respect to the rotation angle

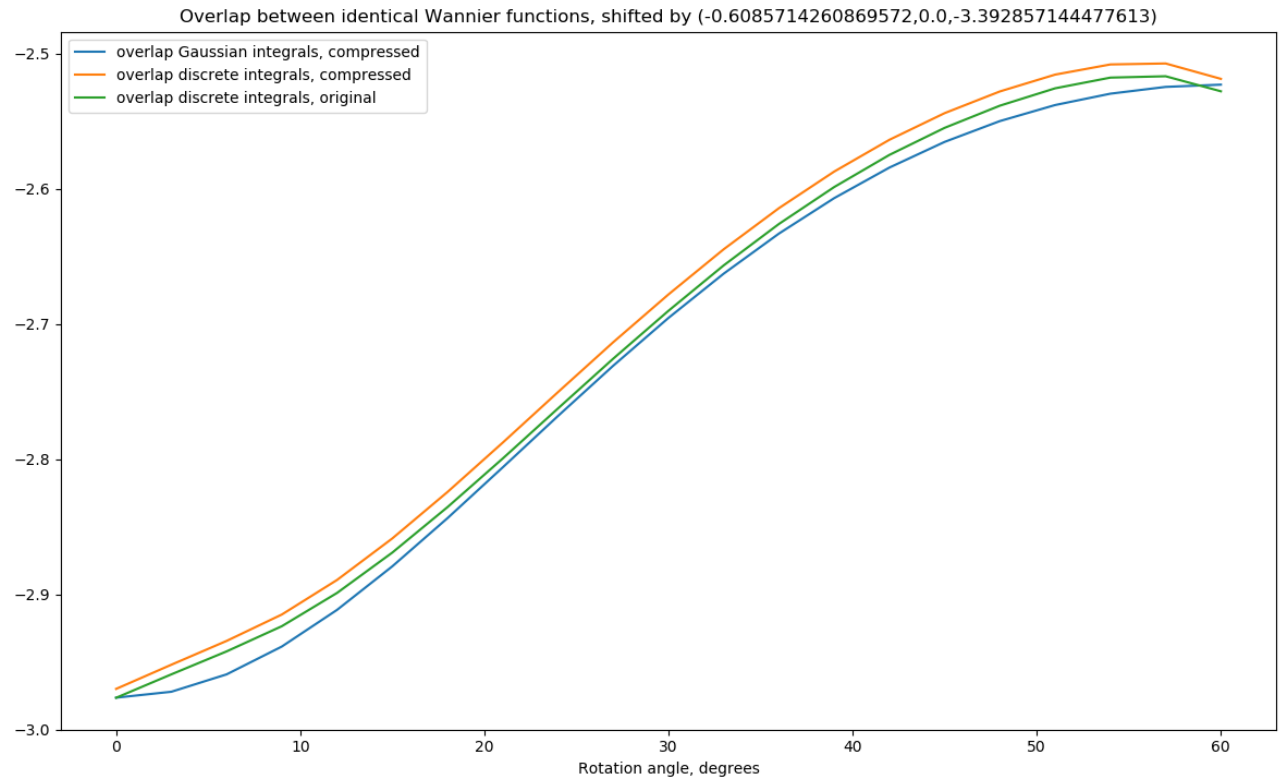


Figure 3.21: Overlaps, Wannier functions shifted by $(0.61, 0, 3.4)$Å, with respect to the rotation angle

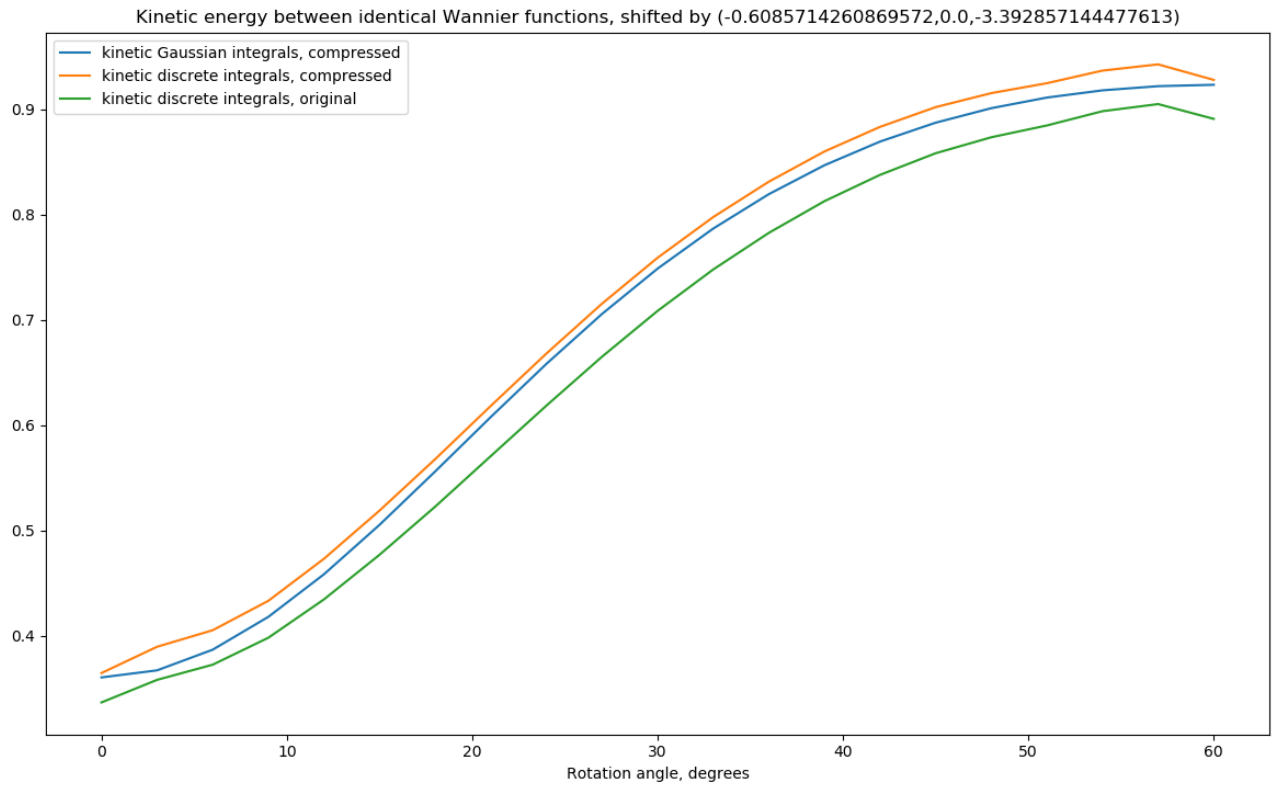


Figure 3.22: Kinetic energy, Wannier functions shifted by $(0.61, 0, 3.4)$Å, with respect to the rotation angle

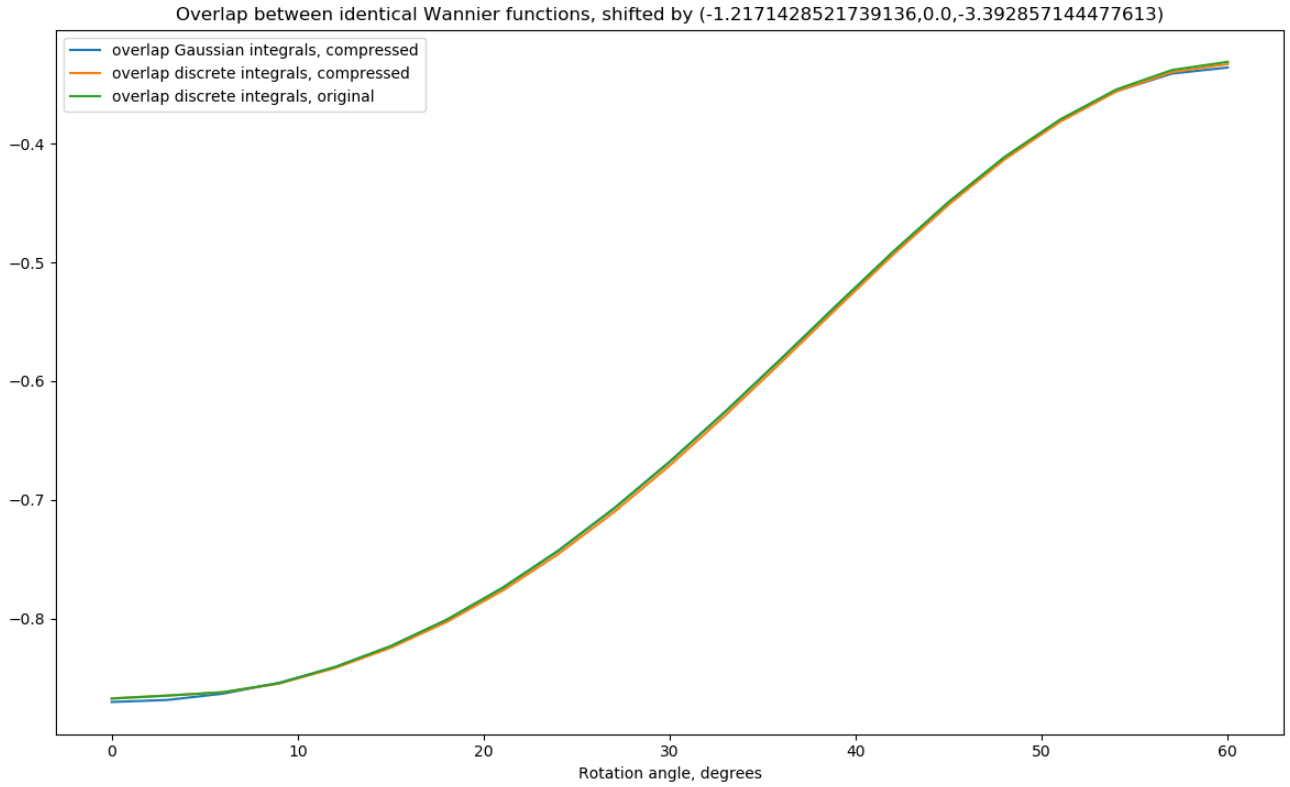


Figure 3.23: Overlaps, Wannier functions shifted by $(1.2, 0, 3.4)$Å, with respect to the rotation angle

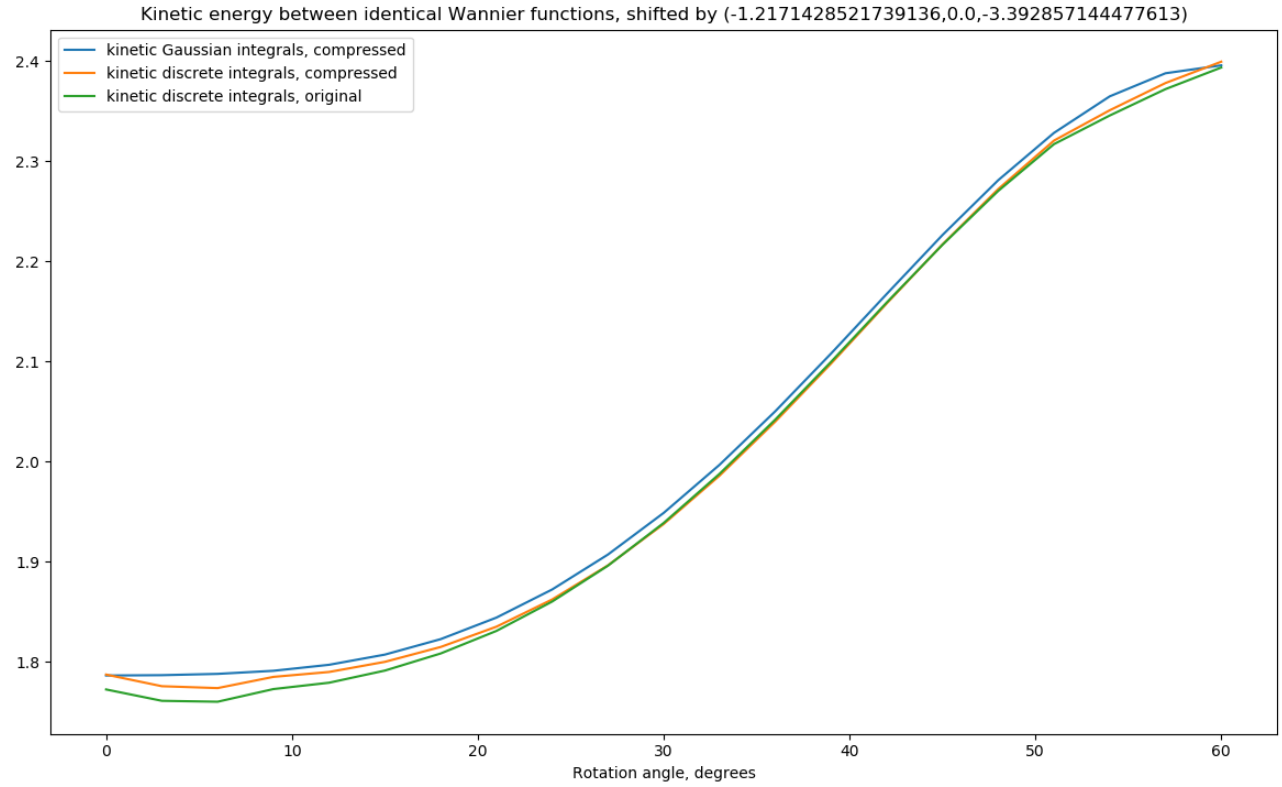


Figure 3.24: Kinetic energy, Wannier functions shifted by $(1.2, 0, 3.4)$Å, with respect to the rotation angle

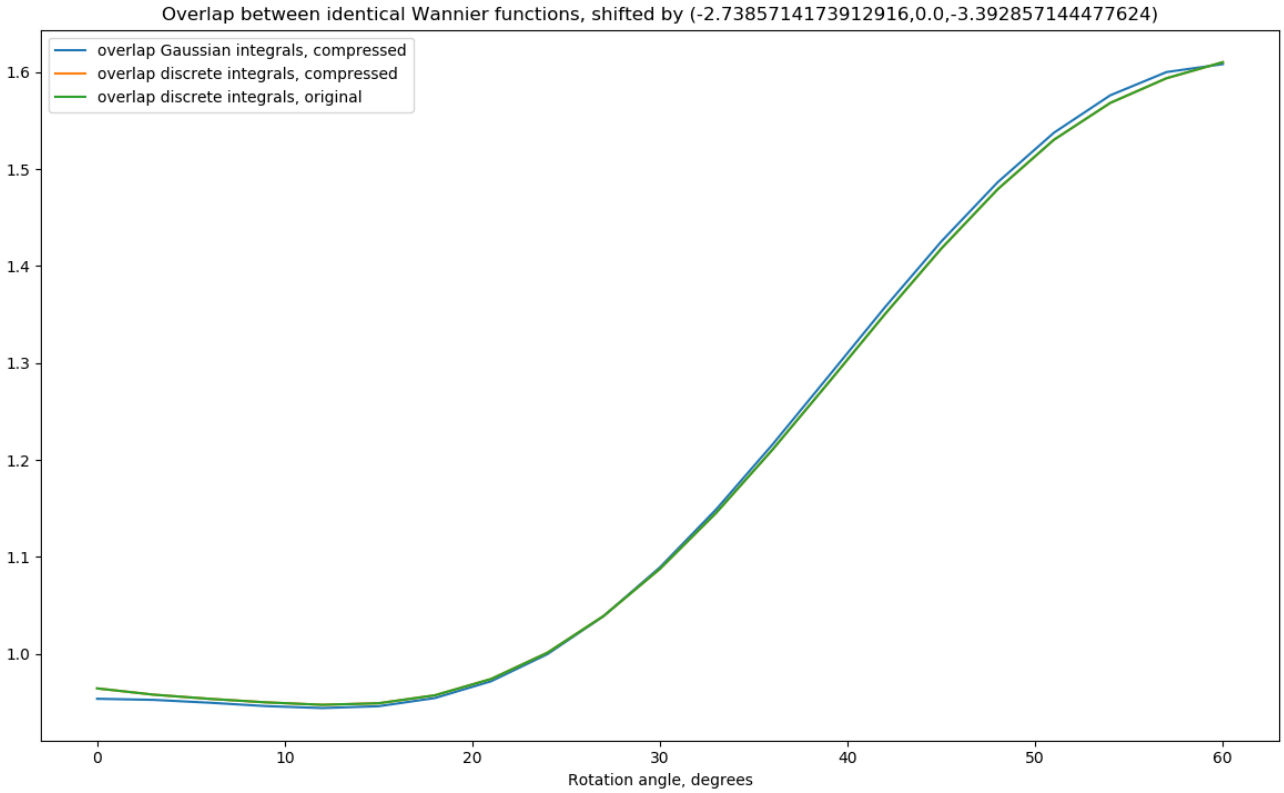


Figure 3.25: Overlaps, Wannier functions shifted by $(2.7, 0, 3.4)$Å, with respect to the rotation angle

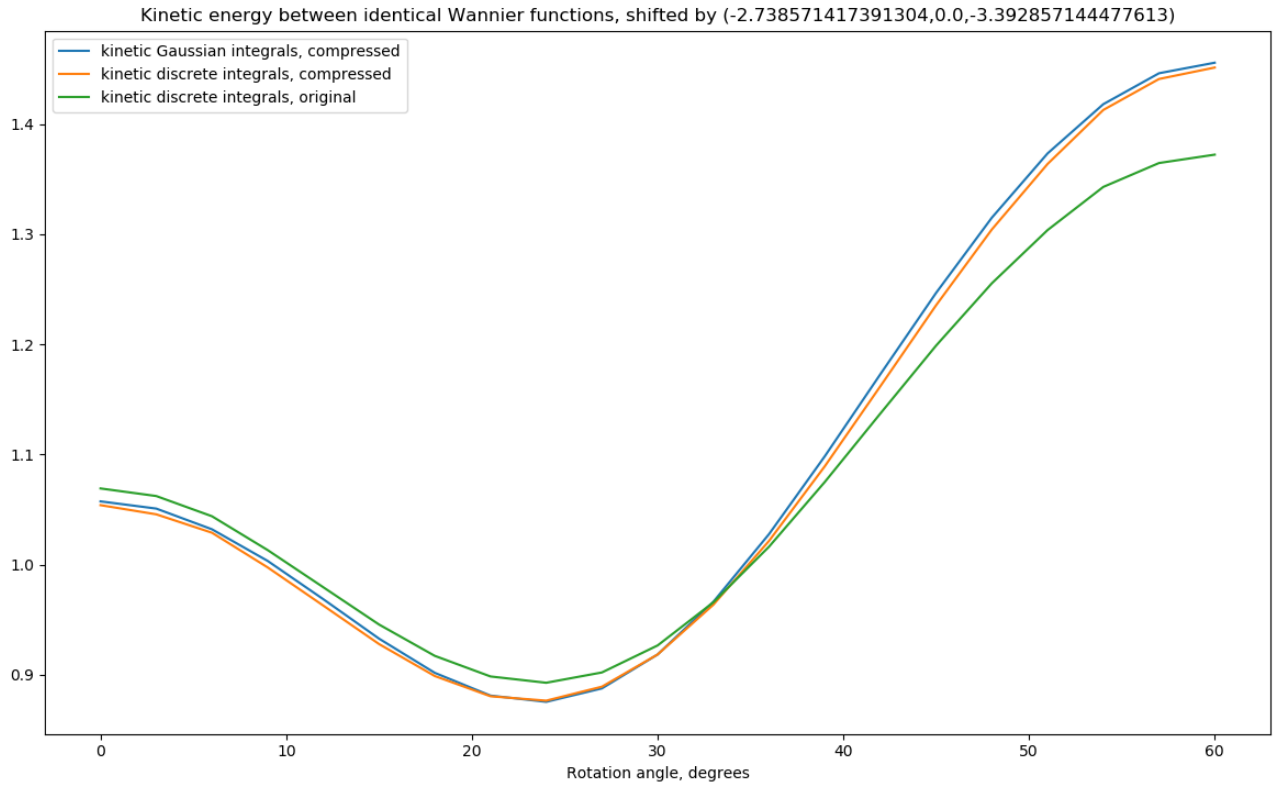


Figure 3.26: Kinetic energy, Wannier functions shifted by $(2.7, 0, 3.4)$Å, with respect to the rotation angle

## 3.6 Conclusion and perspectives

We have proposed an approach to approximate symmetry-adapted Wannier functions by symmetrized Gaussian-Type Orbitals, and provided proof of principle overlap and kinetic energy computations by analytic gaussian integration for various configurations, which is a faster computation method. The matrix element values obtained for the symmetrized Gaussian-Type Orbitals show a relatively good agreement to the values obtained through discrete integration for the original Wannier function.

To provide more conclusive evidence on whether this method can be used to accurately approximate the matrix elements of non-periodic systems, one would need to include the effective potential obtained from DFT computations. However, this approach is a promising method to approximate tight-binding models for non-periodic systems.

# Chapter 4

# Coherent electronic transport in periodic crystals

This work was done in collaboration with Éric Cancès, Clotilde Fermanian Kammerer, and Antoine Levitt.

## 4.1 Introduction

We consider a $d$-dimensional perfect crystal ($d = 1$, 2 or 3) with periodic lattice $\mathcal{R}$ and assume that its electronic structure can be described by an effective linear Hamiltonian $H$ acting on some Hilbert space $\mathcal{H}$. In physical terms, we place ourselves within the Born-Oppenheimer approximation, and consider that the electrons are independent. Moreover, we focus here on the case of spinless continuous models, for which $\mathcal{H} = L^2(\mathbb{R}^d; \mathbb{C})$ and

$$H = \frac{1}{2}(-i\nabla + \mathcal{A})^2 + V, \tag{4.1}$$

where $\mathcal{A} \in L^4_{\mathrm{per}}(\mathbb{R}^d; \mathbb{R}^d)$ and $V \in L^2_{\mathrm{per}}(\mathbb{R}^d; \mathbb{R})$ are $\mathcal{R}$-periodic functions, $V$ is the scalar potential encoding the electrostatic interaction of the electrons with the atoms of the crystal, and $\mathcal{A}$ is the magnetic vector potential, which allows to account for magnetic spin effects without including spin explicitly in our description. We adopt the Coulomb gauge choice, $\nabla \cdot \mathcal{A} = 0$ in the sense of distributions. This operator is self-adjoint on $L^2(\mathbb{R}^d; \mathbb{C})$, with domain $H^2(\mathbb{R}^d; \mathbb{C})$ (a proof is given in section 4.9.1 for the sake of completeness). At zero temperature, the ground-state density matrix is given by

$$\gamma(0) = \mathbb{1}(H \leq \mu_{\mathrm{F}}), \tag{4.2}$$

where $\mu_{\mathrm{F}} \in \mathbb{R}$ is the Fermi level, chosen to have a prescribed number of electrons per unit cell.

Depending on the position of $\mu_{\mathrm{F}}$ in the spectrum $\sigma(H)$ of $H$, this can model different types of physical systems. If $\mu_{\mathrm{F}} \notin \sigma(H)$, the system is an insulator. If $\mu_{\mathrm{F}}$ is an interior point of $\sigma(H)$, the system is a metal, or a semi-metal, depending on the density of states of $H$ at $\mu_{\mathrm{F}}$. We refer to Section 4.2.3 for the precise hypotheses we use in each case.

The vector potential $\mathcal{A}$ is chosen to be periodic, which excludes the case of a uniform external magnetic field. Our analysis therefore does not cover the quantum Hall effect, but is relevant to the quantum anomalous Hall effect [46], and to emergent flat bands [94]. We perform our analysis with this particular Hamiltonian, but it can easily be extended to spin-dependent continuous models, tight-binding models, or 2D materials such as graphene (for which the physical space is three-dimensional while the periodic lattice is two-dimensional).

The purpose of this article is to analyze mathematically the behavior of the electrical current appearing in the crystal when a uniform external electric field is turned on instantaneously at the initial time $t = 0$. In the case of a uniform stationary electric field of magnitude $\varepsilon > 0$ along a (not necessarily normalized) vector $e_\beta \in \mathbb{R}^d$, the Hamiltonian of the system at time $t > 0$ is

$$H_\beta^\varepsilon = H + \varepsilon x_\beta, \tag{4.3}$$

where $x_\beta = x \cdot e_\beta$. This operator is self-adjoint on $L^2(\mathbb{R}^d; \mathbb{C})$ (see Proposition 4.2.1 below), and therefore gives rise to a unitary group $(\mathrm{e}^{-itH_\beta^\varepsilon})_{t\in\mathbb{R}}$ on $L^2(\mathbb{R}^d; \mathbb{C})$. The electronic state of the system at time $t \geq 0$ then is

$$\gamma_\beta^\varepsilon(t) = \mathrm{e}^{-itH_\beta^\varepsilon} \gamma(0) \mathrm{e}^{itH_\beta^\varepsilon}. \tag{4.4}$$

The electrical current in the $e_\alpha$-direction at time $t \geq 0$ is defined as

$$j_{\alpha,\beta}^\varepsilon(t) = \underline{\mathrm{Tr}}(J_\alpha \gamma_\beta^\varepsilon(t)), \tag{4.5}$$

where $\underline{\mathrm{Tr}}$ is the trace per unit volume (which will be precisely defined in Section 4.2.1) and $J_\alpha$ the current operator along the vector $e_\alpha \in \mathbb{R}^d$ (not necessarily normalized nor orthogonal to $e_\beta$), defined as

$$J_\alpha = -(-i\nabla + \mathcal{A}) \cdot e_\alpha. \tag{4.6}$$

*Remark* 4.1.1 (on units and sign convention). If a spinless particle with mass $m$ and charge $q$ is subjected to a electromagnetic field generated by a vector potential $\mathcal{A}$ and a scalar potential $-\varepsilon x_\beta$ generated by a uniform electric field $\varepsilon e_\beta$, its Hamiltonian in atomic units is $H = \frac{1}{2m}(-i\nabla - q\mathcal{A})^2 - q\varepsilon x_\beta$ and the charge current operator is $J = q(-i\nabla - q\mathcal{A})$. In our definitions (4.1), (4.3) and (4.6), we have set $m = 1$ and $q = -1$ (atomic units) which are the physical values for the electron: this corresponds to applying a force in the direction $-e_\beta$ to the electrons, and measuring their velocity in the direction $-e_\alpha$.

In the limit of weak external fields ($\varepsilon \ll 1$), the qualitative properties of the function $t \mapsto j_{\alpha,\beta}^\varepsilon(t)$ heavily depends on the physical nature of the material (insulator, metal, semimetal), as well as on the regime (short, intermediate or long times). Our main results, stated in Theorems 4.2.7, 4.2.8 and 4.2.10, show that the behavior is as follows (see Figure 4.3 in Section 4.3)

- For insulators, the time-averaged conductivity

$$\sigma_{\alpha,\beta} = \lim_{t\to\infty} \frac{1}{t} \int_0^t \lim_{\varepsilon\to 0} \frac{j_{\alpha,\beta}^\varepsilon(t')}{\varepsilon}\, dt' \tag{4.7}$$

  has a finite value, which is zero in longitudinal directions, and, for 2D materials, is proportional to the Chern number in the transverse direction (quantum anomalous Hall effect).

- For metals, when $t \ll \varepsilon^{-1}$, the electrons are in the ballistic regime, and the current increases linearly: $j_{\alpha,\beta}^\varepsilon(t) \approx D_{\alpha,\beta}\varepsilon t$. Under some additional assumptions on the Bloch bands, the current displays Bloch oscillations of order 1 when $\varepsilon^{-1} \ll t \ll \varepsilon^{-1}\log(\varepsilon^{-\zeta})$ for some small enough $\zeta > 0$.

- For time-reversible 2D semimetals such as graphene, the time-averaged conductivity $\sigma_{\alpha,\beta}$ defined in (4.7) has a finite value equal to $\frac{1}{16} e_\alpha \cdot e_\beta$ times the number of Dirac points in the Brillouin zone.

Although our formalism is different, our results for insulators and metals are consistent with those obtained using the semiclassical equations of motion

$$\begin{cases} \dot{x} &= \nabla \lambda_{n,k}, \\ \dot{k} &= -\nabla V(x) + \dot{x} \times (\nabla \times A)(x), \end{cases}$$

and their higher-order refinements in the case when the $n^{\text{th}}$ band is isolated, where the $\lambda_{n,k}$'s are the Bloch eigenvalues of $H$ (see Section 4.2.1). We refer to [81] for a mathematical analysis of the insulating case.

Note that our results use an averaging in time, and we are unable to conclude anything about what would be the naive definition of the conductivity

$$\lim_{t\to\infty} \lim_{\varepsilon\to 0} \frac{j^{\varepsilon}_{\alpha,\beta}(t)}{\varepsilon}. \tag{4.8}$$

A form of averaging of time fluctuations is always necessary to infer zero-frequency behavior from step responses in non-dissipative systems, even in the linear case. The easiest way to see this is by the very simple model for the relationship between an input $I(t)$ and an output $O(t)$:

$$i\dot{O}(t) = \omega O(t) + I(t). \tag{4.9}$$

This simplified model describes a forced oscillator with eigenfrequency $\omega$, and arises from the linear response of the time-dependent Schrödinger equation of a two-level system. For a constant input $I_0$, there is a steady state solution $O_0 = \widehat{R}_0 I_0$, where $\widehat{R}_0 = -\frac{1}{\omega}$ is the zero-frequency transfer function of the system. However, since this system is oscillatory, this steady state may never be reached: if $I$ is brutally switched on at time 0 with $I(t) = O(t) = 0$, if $t \leq 0$, $I(t) = I_0$ if $t > 0$, then $O(t) = O_0(1 - \mathrm{e}^{-i\omega t}) = \widehat{R}_0 I_0(1 - \mathrm{e}^{-i\omega t})$ and we cannot define $\widehat{R}_0$ as the limit of $O(t)/I_0$ when $t$ goes to infinity. However, by averaging we obtain

$$\lim_{t\to\infty} \frac{1}{t} \int_0^t \frac{O(t')}{I_0}\, dt' = \widehat{R}_0.$$

Another common way of retrieving the value of $\widehat{R}_0$ is by an adiabatic switching of the electric field $I(t) = I_0 \mathrm{e}^{\eta t}$ for $t \leq 0$, $I(t) = I_0$ for $t > 0$ [9, 25]. Another possibility is to represent the relationship between $O$ and $I$ by a convolution with a causal response function $R(t)$: $O(t) = (R * I)(t)$, and define the zero-frequency transfer function as $\lim_{\eta\to 0^+} \widehat{R}(i\eta)$, as is often done implicitly in the physics literature. Yet another, more physical, possibility is to use a model with dissipation (in this case $i\dot{O}_\eta(t) + i\eta O_\eta(t) = \omega O_\eta(t) + I(t)$), compute the zero-frequency transfer function as the long-time limit of $O_\eta(t)/I_0$, and then let the dissipation $\eta$ tend to zero. A particular variant of this scheme is known as the relaxation time approximation [7] (the relaxation time being proportional to $1/\eta$). For simple systems, all these methods are equivalent.

Note that the problems in the toy model (4.9) are related to the presence of a *resonance* at $\omega$ in the model, i.e. a pole in the Fourier transform of the response function. For our perfect crystal model however, the oscillatory components of the response are integrated over the Brillouin zone of the periodic crystal, which induces an averaging. Therefore, these procedures might not be necessary. Indeed, we observe numerically in simple tight-binding models that the naive limit in (4.8) seems to be well-defined (see Section 4.3). Identifying precise conditions on the band structure so that this holds will be the subject of future work.

In the metallic case, the conductivity is either infinity or zero, depending on the definition adopted. Indeed, our results imply that

$$\lim_{t\to\infty} \frac{1}{t} \int_0^t \lim_{\varepsilon\to 0} \frac{j^{\varepsilon}_{\alpha,\alpha}(t')}{\varepsilon}\, dt' = +\infty$$

is infinite, because $j^{\varepsilon}_{\alpha,\alpha}(t) \approx D_{\alpha\alpha}\varepsilon t$ in the regime $t \ll \varepsilon^{-1}$. On the other hand, in tight-binding models, a simple argument [7, Proposition 4] shows that

$$\lim_{\varepsilon\to 0} \frac{1}{\varepsilon} \lim_{t\to\infty} \frac{1}{t} \int_0^t j^{\varepsilon}_{\alpha,\alpha}(t')\, dt' = 0.$$

These two limits correspond to different regimes. In the first one, the electrons undergo ballistic transport, being uniformly accelerated by the electric field. In the second one, the electrons undergo Bloch oscillations, a phenomenon whereby particles in a periodic potential accelerated by a constant force oscillate rather than propagate, as first noticed by Zener [109].

Of course, our model is extremely simple. We assume that the electrons are at zero temperature and we ignore electron-electron interactions, the reaction of the lattice (electron-phonon interactions), and electron scattering by impurities in the crystal. These collision events play a relatively minor role in insulators, with the quantum Hall effect in particular being very robust to perturbations [7]. However, they impact significantly the properties of metals. In fact, in the linear response regime ($\varepsilon \ll 1$, $t \ll \varepsilon^{-1}$), the current increases linearly, representing ballistic transport (see Theorem 4.2.8). This increase in the velocity of the electrons physically results in an increased collision rate, which acts as dissipation and eventually limits the current. This results in the finite conductivity observed experimentally in macroscopic physics (Ohm's law). The mathematical understanding of this effect in the mathematical framework considered here is left to future work.

The question of quantum transport in solids has attracted significant attention in the mathematical community, with one of the main drivers being the explanation of Anderson localization on the one hand, and the quantum Hall effect and its relation to topological properties on the other hand [96, 72, 34, 78]. Other topics of interest include the properties of graphene (see for instance [42]), and mesoscopic transport in the Landauer-Buttiker formalism. Comparatively few works have looked specifically at transport in metals. To the best of our knowledge, the present work is the first to present mathematically rigorous results on insulators, metals and semi-metals in a unified framework.

Our method of proof is based on the standard gauge change $\widetilde{\psi}(x,t) = \mathrm{e}^{i\varepsilon t x_\beta}\psi(x,t)$ that transforms the constant in time but non-spatially-periodic Hamiltonian $H^{\varepsilon}_{\beta} = H + \varepsilon x_\beta$ into the time-dependent Hamiltonian $\widetilde{H}^{\varepsilon}_{\beta}(t) = \frac{1}{2}(-i\nabla + \mathcal{A} - \varepsilon e_\beta t)^2 + V$. This Hamiltonian is spatially periodic, and the study of its dynamics can be reduced via Bloch-Floquet theory to that of its fibers $\widetilde{H}^{\varepsilon}_{\beta,k}(t) = \frac{1}{2}(-i\nabla + k + \mathcal{A} - \varepsilon e_\beta t)^2 + V$ acting on periodic functions (Section 4.4), for all values of the pseudo-momentum $k \in \mathbb{R}^d$. Fiber by fiber, this time-dependent Hamiltonian can then be treated using the tools of time-dependent perturbation theory (Section 4.5). Since time is scaled by $\varepsilon$, the Hamiltonian can be seen as either a small perturbation of the rest Hamiltonian $H$ for small times (in which case we can use linear response to expand $j^{\varepsilon}_{\alpha,\beta}(t)$ to first order in $\varepsilon$ for a fixed $t$, Proposition 4.5.7), or as a slow perturbation (in which case the adiabatic theorem allows us to access larger time scales $t \approx \frac{1}{\varepsilon}$, Proposition 4.5.3). For insulators and metals in the short-time regime, both tools are applicable and yield the same result. For metals in the Bloch oscillations regime, only the adiabatic theorem is applicable, and for semimetals, only linear response is applicable due to the gap closing at the Dirac points.

We describe our results in Section 4.2: we define the current in Proposition 4.2.1, and study its properties for insulators, metals and semi-metals in Theorems 4.2.7, 4.2.8 and 4.2.10. We illustrate numerically the different behaviors we obtain in each of the three settings in Section 4.3. We devote Section 4.4 to preliminaries about the regularity and Bloch decomposition of the current. Section 4.5 states and proves results in adiabatic and linear response perturbation theory. Sections 4.6, 4.7 and 4.8 are devoted to the proof of our results in the case of insulators, metals and semi-metals. Finally, two short sections are devoted to technical issues.

## 4.2 Main results: electrical current in periodic materials

### 4.2.1 Notation

In this chapter we fix $\mathcal{A} \in L^4_{\rm per}(\mathbb{R}^d;\mathbb{R}^d)$, $V \in L^2_{\rm per}(\mathbb{R}^d;\mathbb{R})$ (see below for the definition of these spaces), $\mu_{\rm F} \in \mathbb{R}$, and $\mathcal{R}$ is the lattice of the $d$-dimensional crystal.

Let $(e_\alpha)_{\alpha=1,\dots,d}$ denote a (non-necessarily orthonormal) basis of the momentum space $\mathbb{R}^d$, and set $x_\alpha = x \cdot e_\alpha, \mathcal{A}_\alpha = \mathcal{A} \cdot e_\alpha$ for $\alpha = 1, \dots, d$.

We denote by $\mathcal{R}^*$ the *dual lattice* of the periodic lattice $\mathcal{R}$, by $\Omega$ an arbitrary unit cell in the physical space, and by $\mathcal{B}$ an arbitrary unit cell in the reciprocal space (which we will call by abuse of language the *Brillouin zone*). In the special case of a cubic crystal of lattice parameter $a > 0$, we have $\mathcal{R} = a\mathbb{Z}^d$, $\mathcal{R}^* = \frac{2\pi}{a}\mathbb{Z}^d$, and we can take $\Omega = [0,a)^d$, $\mathcal{B} = [-\frac{\pi}{a}, \frac{\pi}{a})^d$.

The *$\mathcal{R}$-periodic Lebesgue and Sobolev spaces* are denoted by

$$L^p_{\rm per} := \left\{ u \in L^p_{\rm loc}(\mathbb{R}^d;\mathbb{C}) \mid u \ \mathcal{R}\text{-periodic} \right\},$$
$$H^s_{\rm per} := \left\{ u \in H^s_{\rm loc}(\mathbb{R}^d;\mathbb{C}) \mid u \ \mathcal{R}\text{-periodic} \right\}.$$

The space of bounded linear operators on a Hilbert space $\mathcal{H}$ is denoted by $\mathcal{L}(\mathcal{H})$, and the Schatten class of bounded operators $A \in \mathcal{L}(\mathcal{H})$ such that $\mathrm{Tr}(|A|^p) < \infty$ by $\mathfrak{S}_p(\mathcal{H})$.

For $R \in \mathcal{R}$, we denote by $\tau_R$ the translation operator formally defined by $\tau_R \phi = \phi(\cdot - R)$. Depending on the context, $\tau_R$ will be seen as a unitary operator on $L^2(\mathbb{R}^d;\mathbb{C})$, or as a linear operator on some $\mathcal{R}$-translation invariant subspace of $\mathcal{D}'(\mathbb{R}^d;\mathbb{C})$.

A bounded operator on $L^2(\mathbb{R}^d;\mathbb{C})$ is called $\mathcal{R}$-periodic if it commutes with $\tau_R$ for all $R \in \mathcal{R}$. An unbounded self-adjoint operator on $L^2(\mathbb{R}^d;\mathbb{C})$ is called $\mathcal{R}$-periodic if its resolvent is $\mathcal{R}$-periodic.

A bounded $\mathcal{R}$-periodic operator $A \in \mathcal{L}(L^2(\mathbb{R}^d;\mathbb{C}))$ is called locally trace-class if $\chi A \chi \in \mathfrak{S}_1(L^2(\mathbb{R}^d;\mathbb{C}))$ for any compactly supported function $\chi \in L^\infty(\mathbb{R}^d;\mathbb{C})$. For $p \geq 1$, we denote by $\mathfrak{S}_{p,\rm per}$ the space of $\mathcal{R}$-periodic operators $A \in \mathcal{L}(L^2(\mathbb{R}^d;\mathbb{C}))$ such that $|A|^p$ is locally trace class. Any operator $A \in \mathfrak{S}_{1,\rm per}$ has a density $\rho_A \in L^1_{\rm per}$ characterized by

$$\forall \chi \in C^\infty_{\rm c}(\mathbb{R}^d;\mathbb{C}), \quad \mathrm{Tr}(A\chi) = \int_{\mathbb{R}^d} \rho_A \chi.$$

The trace per unit volume of an operator $A \in \mathfrak{S}_{1,\rm per}$ is defined as

$$\underline{\mathrm{Tr}}(A) = \frac{1}{|\Omega|} \mathrm{Tr}_{L^2(\mathbb{R}^d;\mathbb{C})}(\mathbb{1}_\Omega A \mathbb{1}_\Omega) = \fint_\Omega \rho_A,$$

where $\mathbb{1}_\Omega$ is the characteristic function of the unit cell $\Omega$, and $\fint_\Omega$ is a shorthand notation for $\frac{1}{|\Omega|}\int_\Omega$. This formula is independent of the choice of the unit cell $\Omega$.

Since we are dealing here with periodic materials, we will use the Bloch transform (also called Bloch-Floquet transform) [86]. For $K \in \mathcal{R}^*$, let $T_K$ be the unitary multiplication operator on $L^2_{\rm per}$ defined by

$$\forall v \in L^2_{\rm per}, \quad (T_K v)(x) = \mathrm{e}^{-iK\cdot x} v(x) \quad \text{for a.a. } x \in \mathbb{R}^d,$$

and

$$L^2_{\rm qp}(L^2_{\rm per})$$
$$:= \left\{ \mathbb{R}^d \ni k \mapsto u_k \in L^2_{\rm per} \mid \int_{\mathcal{B}} \|u_k\|^2_{L^2_{\rm per}}\, dk < \infty,\ u_{k+K} = T_K u_k \text{ for all } K \in \mathcal{R}^* \text{ and a.a. } k \in \mathbb{R}^d \right\},$$

the Hilbert space of $\mathcal{R}^*$-quasi-periodic $L^2_{\rm per}$-valued functions on $\mathbb{R}^d$ endowed with the inner product

$$\langle u, v\rangle_{L^2_{\rm qp}(L^2_{\rm per})} = \fint_{\mathcal{B}} \langle u_k, v_k\rangle_{L^2_{\rm per}}\, dk.$$

Here and below, the subscript qp refers to the quasi-periodicity property. The Bloch transform then is the unitary map from $L^2(\mathbb{R}^d;\mathbb{C})$ to $L^2_{\rm qp}(L^2_{\rm per})$ defined for $u \in C^\infty_{\rm c}(\mathbb{R}^d;\mathbb{C})$ by

$$\forall k \in \mathbb{R}^d, \quad \forall x \in \mathbb{R}^d, \quad u_k(x) = \sum_{R\in\mathcal{R}} u(x+R)\, {\rm e}^{-ik\cdot(x+R)}. \tag{4.10}$$

Its inverse is given by

$$u(x) = \fint_{\mathcal{B}} {\rm e}^{ik\cdot x} u_k(x)\, dk, \quad \text{for a.a. } x \in \mathbb{R}^d. \tag{4.11}$$

Any $\mathcal{R}$-periodic operator $A \in \mathcal{L}(L^2(\mathbb{R}^d;\mathbb{C}))$ is decomposed by the Bloch transform in the sense that there exists a function $k \mapsto A_k$ in $L^\infty_{\rm qp}(\mathcal{L}(L^2_{\rm per}))$ such that for any $u \in L^2(\mathbb{R}^d;\mathbb{C})$ and almost all $k \in \mathbb{R}^d$, $(Au)_k = A_k u_k$.

$$A_{k+K} = T_K A_k T_K^*, \qquad \text{for all } K \in \mathcal{R}^* \text{ and a.a. } k \in \mathbb{R}^d. \tag{4.12}$$

The $A_k$'s are called the fibers of the operator $A$. If $A \in \mathfrak{S}_{1,\rm per}$, then the function $k \mapsto A_k$ is in $L^1_{\rm qp}(\mathfrak{S}_1(L^2_{\rm per}))$, the function $k \mapsto {\rm Tr}(A_k)$ is in $L^1_{\rm per}$, and we have

$$\underline{\rm Tr}(A) = (2\pi)^{-d} \int_{\mathcal{B}} {\rm Tr}(A_k)\, dk,$$

where we used $|\Omega|.|\mathcal{B}| = (2\pi)^d$. The Bloch decomposition theorem can be extended to unbounded $\mathcal{R}$-periodic self-adjoint operators using the resolvent [86].

In the case of the periodic Hamiltonian operator $H$ given by (4.1), we have

$$H_k = \frac{1}{2}(-i\nabla + k + \mathcal{A})^2 + V. \tag{4.13}$$

For each $k \in \mathbb{R}^d$, $H_k$ is a bounded below self-adjoint operator on $L^2_{\rm per}$ with domain $H^2_{\rm per}$ and compact resolvent. Let $(\lambda_{n,k})_{n\in\mathbb{N}^*}$ be the non-decreasing sequence of eigenvalues of $H_k$ counting multiplicities

$$\lambda_{1,k} \le \lambda_{2,k} \le \lambda_{3,k} \le \cdots, \quad \lim_{n\to\infty} \lambda_{n,k} = +\infty,$$

where we use the convention $\lambda_{0,k} = -\infty$. We denote by $(u_{n,k})_{n\in\mathbb{N}^*} \in (H^2_{\rm per})^{\mathbb{N}^*}$ an $L^2_{\rm per}$-orthonormal basis of associated eigenfunctions:

$$H_k u_{n,k} = \lambda_{n,k} u_{n,k}, \quad \langle u_{m,k}, u_{n,k}\rangle_{L^2_{\rm per}} = \delta_{m,n}.$$

For $N \in \mathbb{N}^*$ and $k \in \mathbb{R}^d$, we will denote by

$$P_{N,k} = \mathbb{1}(H_k \le \lambda_{N,k}). \tag{4.14}$$

Whenever $\lambda_{N,k} < \lambda_{N+1,k}$, $P_{N,k}$ is the spectral projector on the eigenspace associated with the lowest $N$ eigenvalues of $H_k$ (counting multiplicities):

$$P_{N,k} = \sum_{n=1}^{N} |u_{n,k}\rangle\langle u_{n,k}|. \tag{4.15}$$

Since $H_k$ is quasi-periodic, so is $P_{N,k}$, and the eigenvalues $\lambda_{n,k}$ are $\mathcal{R}^*$-periodic functions of $k$. By a classical min-max argument (proved in section 4.9.2 for the sake of completeness), there exists $\underline{C_1}, \overline{C_1} \in \mathbb{R}$, and $\underline{C_2}, \overline{C_2} > 0$ such that

$$\underline{C_1} + \underline{C_2} n^{2/d} \leq \lambda_{n,k} \leq \overline{C_1} + \overline{C_2} n^{2/d}. \tag{4.16}$$

Denoting $N_k$ the number of eigenvalues below the Fermi level $\mu_{\mathrm{F}}$ at $k$

$$N_k = \left| \left\{ \lambda_{n,k} \leq \mu_{\mathrm{F}}, n \in \mathbb{N}^* \right\} \right|, \tag{4.17}$$

we see that $N_k$ is bounded uniformly in $k$.

Let us now consider the ground-state density matrix $\gamma(0) = \mathbb{1}(H \leq \mu_{\mathrm{F}})$ defined in (4.2). Its Bloch fibers are

$$\gamma_k(0) = \mathbb{1}(H_k \leq \mu_{\mathrm{F}}) = P_{N_k,k}. \tag{4.18}$$

The *current operator* $J_\alpha = -(-i\nabla + \mathcal{A}) \cdot e_\alpha$ defined in (4.6) is also $\mathcal{R}$-periodic, with fibers

$$J_{\alpha,k} = -(-i\nabla + k + \mathcal{A}) \cdot e_\alpha = -\nabla_k H_k \cdot e_\alpha =: -\partial_\alpha H_k.$$

Note that the notation $\partial_\alpha$ denotes a derivative along the (not necessarily normalized) vector $e_\alpha$.

Lastly, for each $q \in \mathbb{R}^d$, we denote that $G_q$ the unitary multiplication operator on $L^2(\mathbb{R}^d; \mathbb{C})$ defined by

$$\forall u \in L^2(\mathbb{R}^d; \mathbb{C}), \quad (G_q u)(x) = \mathrm{e}^{iq \cdot x} u(x) \quad \text{for a.a. } x \in \mathbb{R}^d. \tag{4.19}$$

The operator $G_q$ is not $\mathcal{R}$-periodic, except when $q \in \mathcal{R}^*$ (in which case $G_q$ is fibered, with $G_{q,k} = T_{-q}$ for all $k$). However, for any $\mathcal{R}$-periodic operator $A \in \mathcal{L}(L^2(\mathbb{R}^d; \mathbb{C}))$ and any $q \in \mathbb{R}^d$, the operator $G_q A G_q^*$ is $\mathcal{R}$-periodic, and its Bloch decomposition is given by

$$(G_q A G_q^*)_k = A_{k-q}, \quad \text{for a.a. } k \in \mathbb{R}^d. \tag{4.20}$$

Indeed, for $\varphi \in L^2(\mathbb{R}^d; \mathbb{C})$, with Bloch transform $(u_k)_{k \in \mathcal{B}}$, and for almost any $x$,

$$(G_q A G_q^*)\varphi(x) = G_q A \fint_{\mathcal{B}} \mathrm{e}^{i(k-q)\cdot x} u_k dk = \fint_{\mathcal{B}} \mathrm{e}^{ik \cdot x} A_{k-q} u_k dk.$$

### 4.2.2 Definition of the current

For $\varepsilon > 0$, the operator

$$H_\beta^\varepsilon = H + \varepsilon x_\beta = \frac{1}{2}(-i\nabla + \mathcal{A})^2 + V + \varepsilon x \cdot e_\beta$$

already introduced in (4.3) is not $\mathcal{R}$-periodic, and we would naively expect that the density matrix

$$\gamma_\beta^\varepsilon(t) = \mathrm{e}^{-itH_\beta^\varepsilon} \gamma(0) \mathrm{e}^{itH_\beta^\varepsilon}$$

at time $t > 0$ (already introduced in (4.4)) is not either. Yet, this operator is in fact $\mathcal{R}$-periodic. Physically, this is due to the fact that although the potential $V_{\mathrm{el}}(x) := \varepsilon x \cdot e_\beta$ is not periodic, the field $\mathcal{E} = -\nabla V_{\mathrm{el}} = -\varepsilon e_\beta$ to which the electrons are subjected is constant, hence periodic. The proof of this result relies on the standard gauge transform

$$\widetilde{\psi}(x,t) = \left( (G_{\varepsilon t e_\beta} \psi(\cdot, t)) \right)(x) = \mathrm{e}^{i\varepsilon t x_\beta} \psi(x,t), \tag{4.21}$$

where the operator $G_q$ has been defined in (4.19), and the introduction of the gauge-transformed operators

$$\widetilde{\mathcal{U}}^{\varepsilon}_{\beta}(t,t') := G_{\varepsilon t e_\beta} \mathrm{e}^{-i(t-t')H^{\varepsilon}_{\beta}} G^{*}_{\varepsilon t' e_\beta},$$

and

$$\widetilde{\gamma}^{\varepsilon}_{\beta}(t) := G_{\varepsilon t e_\beta} \gamma^{\varepsilon}_{\beta}(t) G^{*}_{\varepsilon t e_\beta} = \widetilde{\mathcal{U}}^{\varepsilon}_{\beta}(t) \gamma(0) \widetilde{\mathcal{U}}^{\varepsilon}_{\beta}(t)^{*}, \tag{4.22}$$

where $\mathcal{U}^{\varepsilon}_{\beta}(t)$ is a short-hand notation for

$$\widetilde{\mathcal{U}}^{\varepsilon}_{\beta}(t) := \widetilde{\mathcal{U}}^{\varepsilon}_{\beta}(t,0) = G_{\varepsilon t e_\beta} \mathrm{e}^{-itH^{\varepsilon}_{\beta}}.$$

Through the change of gauge (4.21), the dynamics induced by the time-independent but non-periodic Hamiltonian $H^{\varepsilon}_{\beta}$ is equivalent to the dynamics induced by the time-dependent periodic Hamiltonian

$$\widetilde{H}^{\varepsilon}_{\beta}(t) = G_{\varepsilon t e_\beta} H^{\varepsilon}_{\beta} G^{*}_{\varepsilon t e_\beta} = \frac{1}{2}(-i\nabla + \mathcal{A} - \varepsilon e_\beta t)^2 + V. \tag{4.23}$$

Physically, this is a manifestation of the gauge invariance of the Schrödinger equation, where an electric field $\varepsilon e_\beta$ can be realized either through a scalar potential $V_{\mathrm{el}} = -\varepsilon x_\beta$, or through a vector potential $\mathcal{A}_{\mathrm{el}} = -\varepsilon e_\beta t$, the second being more convenient to deal with because it does not break the $\mathcal{R}$-translation invariance. The Bloch fibers of $\widetilde{H}^{\varepsilon}_{\beta}(t)$ are

$$\widetilde{H}^{\varepsilon}_{\beta,k}(t) = \frac{1}{2}(-i\nabla + k + \mathcal{A} - \varepsilon e_\beta t)^2 + V = H_{k-\varepsilon e_\beta t}. \tag{4.24}$$

We sum up these arguments in the proposition below, together with elements that we shall use for defining the current. The reader can refer to the articles [9, 60] where part of the results of that Proposition are proved.

**Proposition 4.2.1.** *Let $\mathcal{A} \in L^4_{\mathrm{per}}(\mathbb{R}^d;\mathbb{R}^d)$ such that $\nabla \cdot \mathcal{A} = 0$, and $V \in L^2_{\mathrm{per}}(\mathbb{R}^d;\mathbb{R})$.*

1. *For all $\varepsilon \in \mathbb{R}$, the operator $H^{\varepsilon}_{\beta}$ defined in (4.3) is essentially self-adjoint on $C^{\infty}_{\mathrm{c}}(\mathbb{R}^d;\mathbb{C})$, and therefore admits a unitary propagator $(\mathrm{e}^{-itH^{\beta}_{\varepsilon}})_{t\in\mathbb{R}}$ in $L^2(\mathbb{R}^d;\mathbb{C})$.*

2. *For all $t \in \mathbb{R}$, and $\varepsilon \in \mathbb{R}$, the operator $\widetilde{H}^{\varepsilon}_{\beta}(t)$ defined in (4.23) is self-adjoint on $L^2(\mathbb{R}^d)$ with domain $H^2(\mathbb{R}^d;\mathbb{C})$, and $\mathcal{R}$-periodic. There exists a strongly continuous unitary propagator $(\widetilde{\mathcal{U}}^{\varepsilon}_{\beta}(t,t'))_{(t,t')\in\mathbb{R}\times\mathbb{R}}$ on $L^2(\mathbb{R}^d;\mathbb{C})$, so that $\widetilde{\mathcal{U}}^{\varepsilon}_{\beta}(t,t')$ is $\mathcal{R}$-periodic for all $t,t' \in \mathbb{R}$, with fibers $\widetilde{\mathcal{U}}^{\varepsilon}_{\beta,k}(t,t')$ solving*

$$i\partial_t \widetilde{\mathcal{U}}^{\varepsilon}_{\beta,k}(t,t') = \widetilde{H}^{\varepsilon}_{\beta,k}(t) \widetilde{\mathcal{U}}^{\varepsilon}_{\beta,k}(t,t'), \quad \widetilde{\mathcal{U}}^{\varepsilon}_{\beta,k}(t',t') = \mathrm{Id}_{L^2_{\mathrm{per}}}. \tag{4.25}$$

3. *For all $t \geq 0$, and $\varepsilon \in \mathbb{R}$, $J_\alpha \gamma^{\varepsilon}_{\beta}(t) \in \mathfrak{S}_{1,\mathrm{per}}$. The current $j^{\varepsilon}_{\alpha,\beta}(t) = \underline{\mathrm{Tr}}(J_\alpha \gamma^{\varepsilon}_{\beta}(t))$ is well-defined and*

$$j^{\varepsilon}_{\alpha,\beta}(t) = -(2\pi)^{-d} \int_{\mathcal{B}} \mathrm{Tr}\Big(\partial_\alpha \widetilde{H}^{\varepsilon}_{\beta,k}(t) \widetilde{\gamma}^{\varepsilon}_{\beta,k}(t)\Big)\, dk \tag{4.26}$$

$$= -(2\pi)^{-d} \int_{\mathcal{B}} \mathrm{Tr}\Big(\partial_\alpha H_{k-\varepsilon e_\beta t} \widetilde{\mathcal{U}}^{\varepsilon}_{\beta,k}(t) \gamma_k(0) \widetilde{\mathcal{U}}^{\varepsilon}_{\beta,k}(t)^{*}\Big)\, dk \tag{4.27}$$

The results of Proposition 4.2.1 are not new (some are classical) but are nevertheless proved in Section 4.4 for the sake of completeness. The situation can be summed up in the commutative diagrams of Figure 4.1.

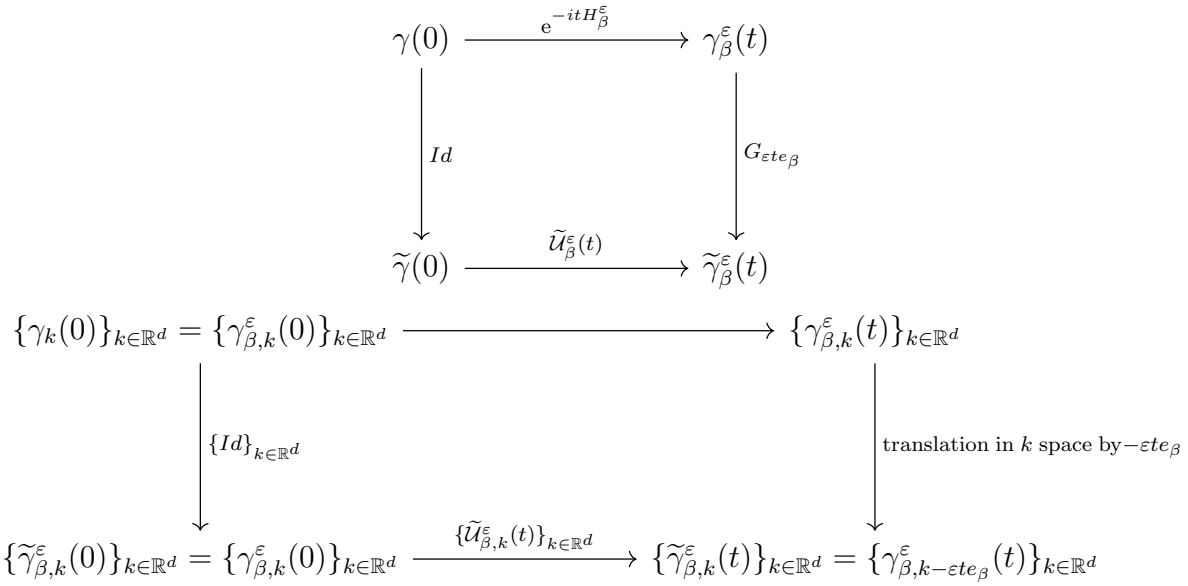


Figure 4.1: Commutative diagrams of the relationships between density matrices $\gamma^\varepsilon_\beta$ and $\widetilde{\gamma}^\varepsilon_\beta$ (top) and the fibers $\gamma^\varepsilon_{\beta,k}$ of $\gamma^\varepsilon_\beta$ which decompose both $\gamma^\varepsilon_\beta$ and $\widetilde{\gamma}^\varepsilon_\beta$ (bottom). In the top diagram, $A \xrightarrow{U} B$ means that $B = UAU^*$. In the bottom diagram $\{A_k\}_{k\in\mathbb{R}^d} \overset{\{U_k\}_{k\in\mathbb{R}^d}}{\to} \{B_k\}_{k\in\mathbb{R}^d}$ means that $A$ et $B$ are $\mathcal{R}$-periodic and that their fibers are related by $B_k = U_k A_k U_k^*$.

*Remark* 4.2.2. This proposition reduces the study of $j^\varepsilon_{\alpha,\beta}(t)$ to that of the dynamics of the time-dependent Hamiltonian $H_{k-\varepsilon e_\beta t}$. In particular, although we have focused on the specific Hamiltonian $H$ given by (4.1), all computations beyond the proof of this proposition will be based on the use of the three formulae: for all $k \in \mathbb{R}^d, t \in \mathbb{R}_+$,

$$\gamma_k(0) = \mathbb{1}(H_k \le \mu_{\mathrm{F}}), \tag{4.28}$$

$$i\partial_t \widetilde{\mathcal{U}}^\varepsilon_{\beta,k}(t) = H_{k-\varepsilon e_\beta t}\widetilde{\mathcal{U}}^\varepsilon_{\beta,k}(t), \quad \widetilde{\mathcal{U}}^\varepsilon_{\beta,k}(0) = \mathrm{Id}, \tag{4.29}$$

$$j^\varepsilon_{\alpha,\beta}(t) = -(2\pi)^{-d}\int_{\mathcal{B}} \mathrm{Tr}\Big(\partial_\alpha H_{k-\varepsilon e_\beta t}\widetilde{\mathcal{U}}^\varepsilon_{\beta,k}(t)\gamma_k(0)\widetilde{\mathcal{U}}^\varepsilon_{\beta,k}(t)^*\Big)\,dk, \tag{4.30}$$

where the fiber $\mathcal{H}_{\mathrm{f}}$ is equal to $L^2_{\mathrm{per}}$ in our setting. Our results in the following sections can therefore be extended to other Hamiltonians where $(H_k)_{k\in\mathbb{R}^d}$ is a family of bounded below self-adjoint operators on a Hilbert space $\mathcal{H}_{\mathrm{f}}$ with compact resolvent satisfying the quasi-periodicity conditions

$$H_{k+K} = T_K H_k T_K^*, \quad \forall K \in \mathcal{R}^*,\ k \in \mathbb{R}^d,$$

where $(T_K)_{K\in\mathcal{R}^*}$ is a unitary representation of the group $\mathcal{R}^*$ on $\mathcal{H}_{\mathrm{f}}$ (see (4.12)), and the boundedness conditions in Section 4.5. This includes in particular spin-dependent continuous models, tight-binding lattice models (for which $\mathcal{H}_{\mathrm{f}} = \mathbb{C}^M$), and 2D materials.

### 4.2.3 Insulators, non-degenerate metals, semimetals

As we said before, the position of the Fermi level in the band diagram $(\lambda_{n,k})_{n\in\mathbb{N}^*,\,k\in\mathcal{B}}$ is key to determining the electronic properties of the medium. We define the Fermi surface sheets

$$\mathcal{S}_n = \{k \in \mathcal{B} \mid \lambda_{n,k} = \mu_{\mathrm{F}}\}, \quad n \in \mathbb{N}^*$$

and the Fermi surface

$$\mathcal{S} = \bigcup_{n\in\mathbb{N}^*} \mathcal{S}_n = \{k \in \mathcal{B} \mid \exists n \in \mathbb{N}^* \text{ s.t. } \lambda_{n,k} = \mu_{\mathrm{F}}\}. \tag{4.31}$$

We will be interested here in three types of systems that we now describe in three mutually exclusive assumptions.

**Assumption 4.2.3** (insulator)**.** *The Fermi surface $\mathcal{S}$ is empty, and there exists $N_{\rm ins} \in \mathbb{N}^*$ such that $N_k = N_{\rm ins}$ for all $k \in \mathcal{B}$, i.e.*

$$\forall k \in \mathcal{B}, \quad \lambda_{N_{\rm ins},k} < \mu_{\rm F} < \lambda_{N_{\rm ins}+1,k},$$

*or equivalently $\mu_{\rm F} \notin \sigma(H)$.*

In the case of insulators, we have for all $k \in \mathbb{R}^d$

$$\gamma_k(0) = P_{N_{\rm ins},k},$$

and $\gamma_k(0)$ is a real-analytic $\mathcal{R}^*$-quasi-periodic function.

**Assumption 4.2.4** (non-degenerate metal)**.** *The Fermi surface $\mathcal{S}$ is non-empty and the following conditions are satisfied: for all $n \in \mathbb{N}^*$,*

- *$\mathcal{S}_n \cap \mathcal{S}_{n+1} = \emptyset$ (no crossing at the Fermi level);*
- *for all $k \in \mathcal{S}_n$, $\nabla \lambda_{n,k} \neq 0$ (no flat bands at the Fermi level).*

Note that this assumption was used in [12]. It ensures a smooth density of states at the Fermi level. In this case, the Fermi surface consists of a finite union of disjoint smooth closed surfaces $\mathcal{S}_n$. Letting

$$\mathcal{B}_n = \{k \in \mathcal{B} \mid \lambda_{n,k} < \mu_{\rm F} < \lambda_{n+1,k}\},$$

we obtain a partitioning

$$\mathcal{B} = \mathcal{S} \bigcup \left( \bigcup_{n \in \mathbb{N}^*} \mathcal{B}_n \right).$$

Both $N_k$ and the fibers $\gamma_k(0) = P_{N_k,k}$ of the density matrix $\gamma(0)$ are smooth on each $\mathcal{B}_n$, and have discontinuities on the sheets $\mathcal{S}_n$.

**Assumption 4.2.5** (semimetal)**.** *The dimension $d$ is equal to 2, there is $N_{\rm sm}$ such that $\lambda_{N_{\rm sm},k} \leq \mu_F$ for all $k \in \mathcal{B}$, and the Fermi surface $\mathcal{S}$ consists of a finite number of isolated points $(k_i)_{i \in \mathcal{I}}$ ("Dirac points"). All these points are conical crossings: for all $i \in \mathcal{I}$,*

$$\lambda_{N_{\rm sm}-1,k_i} < \lambda_{N_{\rm sm},k_i} = \mu_{\rm F} = \lambda_{N_{\rm sm}+1,k_i} < \lambda_{N_{\rm sm}+2,k_i}, \tag{4.32}$$

$$\lambda_{N_{\rm sm},k} = \mu_{\rm F} - v_{F,i}|k - k_i| + O(|k - k_i|^2), \tag{4.33}$$

$$\lambda_{N_{\rm sm}+1,k} = \mu_{\rm F} + v_{F,i}|k - k_i| + O(|k - k_i|^2), \tag{4.34}$$

*for some $v_{F,i} \in \mathbb{R}$. Furthermore, in this case we assume that $\mathcal{A} = 0$, so that the system has the time-reversal symmetry $H_{-k} = \overline{H_k}$.*

Note that we assumed in Assumption 4.2.5 that $\mathcal{A} = 0$ to ensure time-reversal symmetry. We require more regularity on $V$ than in the previous theorems to be able to prove a Dyson expansion for the propagator (see Proposition 4.5.7). For the sake of clarity, we consider a model of 2D semimetals set in $\mathbb{R}^2$, but our arguments can be adapted to the more physical case of a model set in $\mathbb{R}^3$ (see also Remark 4.2.2).

Assumption 4.2.5 is generic in the case of potentials possessing the symmetry of honeycomb lattices, such as graphene [29]. In this case, there are two non-equivalent Dirac points in the Brillouin zone ($|\mathcal{I}| = 2$), usually denoted by $K$ and $K'$, and we have $K' = -K$ and $v_{F,1} = v_{F,2}$. The constant $v_F = v_{F,1} = v_{F,2}$ is known as the Fermi velocity. More generally, Dirac points generate specific dynamical behaviors that have been studied in [30, 33] in the context of the Dirac operator. Such phenomena also appear in molecular dynamics (see [43, 32, 31]).

In the semimetal case, $N_k = N_{\mathrm{sm}}$ for almost every $k \in \mathbb{R}^3$, and $\gamma_k(0)$ is singular at each $k_i \in \mathcal{S}$.

We conclude this section by a result valid in the three cases under investigation.

**Proposition 4.2.6.** *Under Assumption 4.2.3 (insulator), 4.2.4 (non-degenerate metal), or 4.2.5 (semimetal), the current $j^{\varepsilon}_{\alpha,\beta}(t) = \underline{\mathrm{Tr}}(J_\alpha \gamma^{\varepsilon}_\beta(t))$ satisfies*

$$j^0_{\alpha,\beta}(t) = 0, \quad \forall t \geq 0 \quad \textit{(no current in the absence of external field)},$$
$$j^{\varepsilon}_{\alpha,\beta}(0) = 0, \quad \forall \varepsilon \geq 0 \quad \textit{(continuity of the current at } t = 0\textit{)}.$$

We prove this result in Section 4.4.

### 4.2.4 Main results: the current

In the following results, we use the notation $O(f(\varepsilon, t))$ to denote a quantity bounded by $Cf(\varepsilon, t)$ where $C$ is a constant that might depend on the material through $V$, $\mathcal{A}$ and $\mu_F$, but not on $t$ and $\varepsilon$.

**Theorem 4.2.7** (insulators)**.** *Assume the system is an insulator (Assumption 4.2.3). Then there exists $\eta > 0$ such that for all $\varepsilon, t \in \mathbb{R}_+$,*

$$\frac{1}{t}\int_0^t \frac{j^{\varepsilon}_{\alpha,\beta}(t')}{\varepsilon} dt' = -i(2\pi)^{-d} \int_{\mathcal{B}} \mathrm{Tr}\left(\gamma_k(0)[\partial_\alpha \gamma_k(0), \partial_\beta \gamma_k(0)]\right) dk + O\left(\left(\frac{1}{t} + \varepsilon(1+t)\right) \mathrm{e}^{\eta\varepsilon t}\right).$$

Note that this implies in particular that

$$\sigma_{\alpha,\beta} = \lim_{t\to\infty} \frac{1}{t}\int_0^t \lim_{\varepsilon\to 0} \frac{j^{\varepsilon}_{\alpha,\beta}(t')}{\varepsilon} dt' = e_\alpha^T \sigma^\perp e_\beta,$$

where $\sigma^\perp$ is a real antisymmetric matrix with components

$$\sigma^\perp_{ij} := (2\pi)^{-d} \int_{\mathcal{B}} -i\,\mathrm{Tr}\left(\gamma_k(0)\left[\frac{\partial \gamma_k}{\partial k_i}(0), \frac{\partial \gamma_k}{\partial k_j}(0)\right]\right) dk. \tag{4.35}$$

The integrand in (4.35) is related to the well-known Berry curvature associated to the first $N_{\mathrm{ins}}$ bands, that is to the 2-form

$$\sum_{1\leq i<j\leq d} \Omega_{ij}(k)\, dk_i \wedge dk_j \quad \text{where} \quad \Omega_{ij} := -i\,\mathrm{Tr}\left(\gamma_k(0)\left[\frac{\partial \gamma_k}{\partial k_i}(0), \frac{\partial \gamma_k}{\partial k_j}(0)\right]\right).$$

For $d = 2$, we have

$$\sigma^\perp_{12} = (2\pi)^{-1} \mathrm{Ch}_1(\gamma_\bullet(0)),$$

where $\mathrm{Ch}_1(\gamma_\bullet(0)) \in \mathbb{Z}$ is the first Chern number of the fiber bundle defined by the quasi-periodic function $k \mapsto \gamma_k(0)$ [97, 88]. This relationship between the transverse bulk transport properties and the Chern number, characteristic of the integer quantum Hall effect, is known as the TKNN formula.

If $\mathcal{A} = 0$, then the system has the time-reversal symmetry $H_{-k} = \overline{H_k}$. The Berry curvature is then odd [78], and the transverse conductivity matrix $\sigma^\perp$ equal to zero.

**Theorem 4.2.8** (conductivity in non-degenerate metals)**.** *Assume the system is a non-degenerate metal (Assumption 4.2.4).*

1. *Let $\theta > 0$. For all $\varepsilon > 0$ small enough and $0 \leq t \leq \frac{1}{\varepsilon}\varepsilon^{\theta}$, we have*

$$j^{\varepsilon}_{\alpha,\beta}(t) = D_{\alpha,\beta}\varepsilon t + O(\varepsilon + \varepsilon^2 t^2) \tag{4.36}$$

*where*

$$D_{\alpha,\beta} := (2\pi)^{-d} \sum_{n\in\mathbb{N}^*} \int_{\mathcal{S}_n} \partial_\alpha \lambda_{n,k} \, (ds \cdot e_\beta) \tag{4.37}$$

2. *If furthermore there exists $N_{\mathrm{met}} \in \mathbb{N}^*$ such that $\lambda_{N_{\mathrm{met}}-1,k} < \mu_{\mathrm{F}} < \lambda_{N_{\mathrm{met}}+1,k}$ for all $k \in \mathcal{B}$ and there are uniform gaps between $\lambda_{N_{\mathrm{met}}-1,k}$ and $\lambda_{N_{\mathrm{met}},k}$ on the one hand, and $\lambda_{N_{\mathrm{met}},k}$ and $\lambda_{N_{\mathrm{met}}+1,k}$ on the other hand, then there exists $\eta > 0$ such that, for all $\varepsilon, t \in \mathbb{R}_+$,*

$$j^{\varepsilon}_{\alpha,\beta}(t) = -(2\pi)^{-d} \int_{\mathcal{B}} \mathbb{1}(\lambda_{N_{\mathrm{met}},k} \leq \mu_{\mathrm{F}}) \partial_\alpha \lambda_{N_{\mathrm{met}},k+\varepsilon e_\beta t} dk + O((\varepsilon + \varepsilon^2 t)\mathrm{e}^{\eta\varepsilon t}). \tag{4.38}$$

Note that under the assumptions of the case 2 above, the lowest $N-1$ bands are completely filled, the $N^{\mathrm{th}}$ band is partially filled, and the other bands are empty. Still in the setup of case 2, it follows from (4.36) and (4.38) that four different regimes can be observed for $\varepsilon \ll 1$

1. For very short times $t \ll 1$, quantum fluctuations of order $O(\varepsilon)$ dominate the current:

$$j^{\varepsilon}_{\alpha,\beta}(t) = O(\varepsilon);$$

2. For $1 \ll t \ll \frac{1}{\varepsilon}$, the electrons undergo ballistic transport:

$$j^{\varepsilon}_{\alpha,\beta}(t) \approx D_{\alpha,\beta}\varepsilon t,$$

where $D_{\alpha,\beta}$ is defined in (4.37);

3. For $\frac{1}{\varepsilon} \ll t \ll \frac{1}{\varepsilon}\log\left(\varepsilon^{-\zeta}\right)$ with $\zeta \in (0, \eta^{-1})$, we observe Bloch oscillations

$$j^{\varepsilon}_{\alpha,\beta}(t) \approx -(2\pi)^{-d} \int_{\mathcal{B}} \mathbb{1}(\lambda_{N_{\mathrm{met}},k} \leq \mu_{\mathrm{F}}) \partial_\alpha \lambda_{N_{\mathrm{met}},k+\varepsilon e_\beta t} \, dk.$$

In particular, when $e_\beta$ is commensurate with the reciprocal lattice $\mathcal{R}^*$, the current is well approximated in this regime by a periodic function of time with zero mean;

4. for times $t \gg \frac{1}{\varepsilon}\log\left(\varepsilon^{-\zeta}\right)$, our estimates do not allow us to conclude. The proofs show that the factor $\mathrm{e}^{\eta\varepsilon t}$ is due to the unboundedness of the operator $H$ defined in (4.1). For tight-binding models, this factor $\mathrm{e}^{\eta\varepsilon t}$ is not present, and we would observe Bloch oscillations up to times $t \ll \frac{1}{\varepsilon^2}$. The behavior for larger times is open.

Note that some periodic metallic systems have a more complex crossing structure than that assumed in the second case of Theorem 4.2.8. This is the case in particular for the free electron gas ($V = 0$, $\mathcal{A} = 0$, seen as a periodic system with an arbitrary periodic lattice), which does not display Bloch oscillations.

*Remark* 4.2.9. The coherent electronic transport model considered here neglects all sources of dissipation (phonons, impurities, electron-electron interactions). In the Drude approximation, these phenomena give rise to an effective timescale $\tau$ such that $1 \ll \tau \ll 1/\varepsilon$ (larger than the coherence timescale of the electrons, but smaller than the Bloch oscillations timescale), yielding a finite DC conductivity $\sigma_{\alpha,\beta} \sim D_{\alpha,\beta}\tau$. In usual metals at room temperature, dissipation is dominated by phonon scattering, and the relaxation time $\tau$ is of the order of tens of femtoseconds [38]. By contrast, the timescale of Bloch oscillations in most experiments is much larger. Only in structures such as semiconductor superlattices or cold atoms have Bloch oscillations been observed experimentally [61].

**Theorem 4.2.10** (conductivity in semi-metals)**.** *Assume that the system is a semimetal (Assumption 4.2.5). Assume furthermore that $V \in H^1_{\mathrm{per}}$. Then,*

$$\sigma_{\alpha,\beta} = \lim_{t\to\infty} \frac{1}{t} \int_0^t \lim_{\varepsilon\to 0} \frac{j^{\varepsilon}_{\alpha,\beta}(t')}{\varepsilon} dt' = \frac{|\mathcal{I}|}{16}\, e_\alpha \cdot e_\beta.$$

Semimetals are intermediate between insulators and metals, possessing a finite longitudinal conductivity in the linear response regime. This is due to the peculiar properties of the Dirac points. Note that the value of the conductivity is universal, not depending on the characteristics of the Hamiltonian but only on the number of conical crossings. More precisely, the conductivity tensor is isotropic and each conical intersection contributes as $\frac{1}{16}$ to the total conductivity. Note that this result is consistent with formula (1.17a) in [24].

## 4.3 Numerics

Before turning to the proofs, we illustrate our results with numerical simulations. As mentioned in Remark 4.2.2, our results also apply to tight-binding models, and only depend on the form of $H_k$. We test on a very simple model of $H_k$, adapted from the Haldane model [46] (itself based on a tight-binding model of graphene), that can support many phases depending on the values of its parameters.

The graphene lattice $\mathcal{R}$ is spanned by the vectors

$$a_1 = \left(\frac{\sqrt{3}}{2}, \frac{1}{2}\right), \quad a_2 = \left(\frac{\sqrt{3}}{2}, -\frac{1}{2}\right),$$

and $\mathcal{R}^*$ by the vectors

$$b_1 = 2\pi\left(\frac{1}{\sqrt{3}}, 1\right), \quad b_2 = 2\pi\left(\frac{1}{\sqrt{3}}, -1\right).$$

There are two sublattices, denoted $A$ and $B$, with the same lattice vectors $a_1, a_2$, and for a site in sublattice $B$, the three nearest neighbors are in sublattice $A$, with translation vectors given by

$$\delta_1 = \left(\frac{1}{\sqrt{3}}, 0\right), \quad \delta_2 = \left(-\frac{1}{2\sqrt{3}}, \frac{1}{2}\right), \quad \delta_3 = \left(-\frac{1}{2\sqrt{3}}, -\frac{1}{2}\right).$$

In a tight-binding model, one considers that the electronic orbitals of low enough energy are well-localized around atoms, so that electrons can only hop between adjacent atoms. In mathematical terms, the tight-binding approximation is the decomposition of the Hamiltonian on a reduced set of adequately chosen orthonormal localized functions, with low energy. These functions correspond sometimes to approximate eigenfunctions (orthonormalized eigenfunctions of

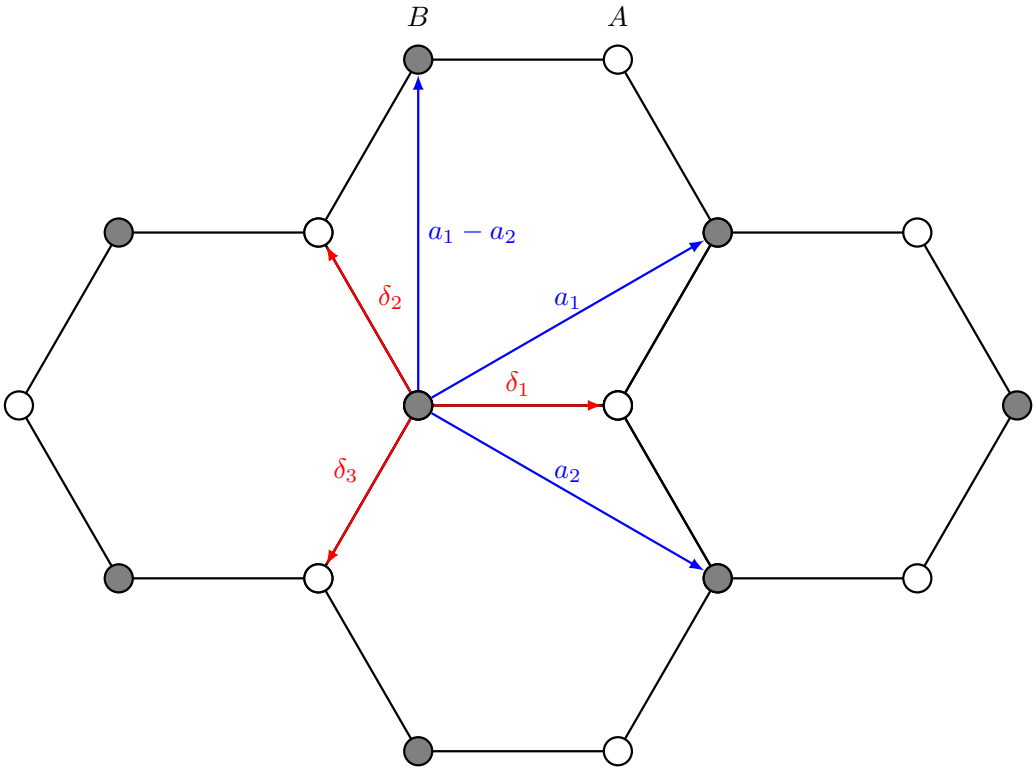


Figure 4.2: Honeycomb lattice of graphene, with sublattices $A$ and $B$, and hopping vectors

a single atom in vacuum, the $s, p, d, f...$ orbitals), or to Wannier functions, which constitute an orthonormal basis of the low-energy eigenspaces.

Denoting such approximate functions by $\{W_{n,R}\}_{R\in\mathcal{R},n\leq N}$, where $W_{n,R}$ is localized around the lattice site $R$, we impose further that these functions are adapted to the symmetries of the crystal: any space group operation mapping $R$ to $R'$ should map the set $\{W_{n,R}\}_{n\leq N}$ onto $\{W_{n,R'}\}_{n\leq N}$.

Then, the elements of the tight-binding Hamiltonian (also called hopping integrals) in real space are given by

$$\forall R, R' \in \mathcal{R}, \forall n, n' \in \mathbb{N}, \quad t_{R,R',n,n'} = \langle W_{n,R}| \, H \, |W_{n',R'}\rangle \, .$$

For some $n$, for some $R, R' \in \mathcal{R}$, there exists a $n'$, and a space group operation $g_{R,R',n,n'}$ that maps $W_{n,R}$ to $W_{n',R'}$. Hence the tight-binding Hamiltonian can be rewritten as the formal sum

$$H^{\mathrm{TB}} = \sum_{R,R',n,n'} t_{R,R',n,n'} g_{R,R',n,n'}.$$

Hence, the tight-binding Hamiltonian is decomposed into the action of space group symmetries on some set of functions, together with multiplication by a scalar. This is the mathematical definition of hopping, and the physical picture is that the particle is in a state $n$ at site $R$, and it can jump to a neighboring state $n'$ at site $R'$, with the probability amplitude $t_{R,R',n,n'}$. In practice, one truncates this sum by considering only hopping between close enough sites (nearest neighbors, next nearest neighbors...), for which $|R - R'|$ is small enough.

By Bloch decomposition, it is sufficient to study the effect of hopping on Bloch waves $\Psi_k(x) = \mathrm{e}^{-ik\cdot x}u_k(x)$. Since a translation $\tau_R$ by a lattice vector $R$ does not change the periodic part of the Bloch wave,

$$\left(\tau_R \Psi_k\right)(x) = \mathrm{e}^{ik\cdot R}\mathrm{e}^{-ik\cdot x}u_k(x) = \mathrm{e}^{ik\cdot R}\Psi_k(x),$$

it follows that a translation $\tau_R$ in real space is represented in reciprocal space by the unitary operator of multiplication by $\mathrm{e}^{ik\cdot R}$. The tight-binding Hamiltonian in reciprocal space is then a $N \times N$ matrix valued map, with elements

$$(H_k^{TB})_{n,n'} = \sum_{|R|\leq R_{\mathrm{cut}}} \mathrm{e}^{ik\cdot R} t_{0,R,n,n'}.$$

In the case of a honeycomb lattice considered here, the unit cell contains two atoms, one of each sublattice. We consider only one state per site, which corresponds physically to the $\pi$ orbital. In this case, $R$ labels where each unit cell is centered, and $n = 1, 2$ labels which sublattice the state corresponds to, with $n = 1$ corresponding to sublattice $A$ and $n = 2$ to sublattice $B$. We introduce two different on-site energies on each sublattice: $g$ on sublattice $A$, and $-g$ on sublattice $B$. This corresponds to diagonal terms without hopping, $(H_k)_{11} = g$ and $(H_k)_{22} = -g$.

Next, we consider first and second nearest neighbor hopping with amplitudes $t_{11}, t_{12}, t_{21}, t_{22}$.

Let us first consider nearest neighbor hopping, from the origin, taken to be on sublattice $B$. Since the closest sites are on the sublattice $A$, the hopping corresponds to the off-diagonal terms of $H_k$. Hence,

$$(H_k)_{21} = t_{21} \sum_{i=1}^{3} \mathrm{e}^{ik\cdot\delta_i}, \qquad (H_k)_{12} = \overline{t_{21}} \sum_{i=1}^{3} \mathrm{e}^{-ik\cdot\delta_i}.$$

In what follows, we will take $t_{21} = t_{12} = 1$. The second neighbor hopping terms, on the other hand, stay on the same sublattice, hence correspond to the diagonal of $H_k$.

$$(H_k)_{22} = -g + t_{22}\mathrm{e}^{ik\cdot a_1} + t_{22}\mathrm{e}^{ik\cdot a_2} + t_{22}\mathrm{e}^{ik\cdot(a_1-a_2)} + c.c.$$

Now, suppose we take a purely imaginary hopping $t_{22} = it_2$, with $t_2 \in \mathbb{R}$. This corresponds to introducing a magnetic potential $x \mapsto \mathcal{A}(x)$ for the sublattice $B$, and using Peierls substitution, this magnetic potential acts as multiplication of the hopping integral by a phase $\mathrm{e}^{-i\int_R^{R'} \mathcal{A}(x)\cdot dx}$. However, to preserve the periodicity of the Hamiltonian, we choose to impose that the total magnetic flux through the unit cell is zero. This is possible if we introduce an opposite flux through the unit cell of sublattice $A$, which means that $t_{11} = \overline{t_{22}} = -it_2$. Hence, it follows that

$$\begin{aligned}
(H_k)_{11} &= g - it_2\left(\mathrm{e}^{ik\cdot a_1} + \mathrm{e}^{ik\cdot a_2} + \mathrm{e}^{ik\cdot(a_1-a_2)} - \mathrm{e}^{-ik\cdot a_1} - \mathrm{e}^{-ik\cdot a_2} - \mathrm{e}^{-ik\cdot(a_1-a_2)}\right), \\
(H_k)_{22} &= -g + it_2\left(\mathrm{e}^{ik\cdot a_1} + \mathrm{e}^{ik\cdot a_2} + \mathrm{e}^{ik\cdot(a_1-a_2)} - \mathrm{e}^{-ik\cdot a_1} - \mathrm{e}^{-ik\cdot a_2} - \mathrm{e}^{-ik\cdot(a_1-a_2)}\right).
\end{aligned}$$

For short, we then denote

$$H_k = \begin{pmatrix} m(k) & \overline{f(k)} \\ f(k) & -m(k) \end{pmatrix},$$

with

$$\begin{aligned}
m(k) &= g + 2t_2\Big(\sin(k\cdot a_1) + \sin(k\cdot a_2) + \sin(k\cdot(a_1-a_2))\Big), \\
f(k) &= \sum_{i=1}^{3} \mathrm{e}^{ik\cdot\delta_i},
\end{aligned}$$

The eigenvalues of $H_k$ are $\lambda_\pm = \pm\sqrt{m(k)^2 + |f(k)|^2}$. With $g = 0$, $t_2 = 0$, this is the standard model of graphene: no on-site energy or magnetic flux breaking the symmetry between the two lattices, and one can show that this results in two bands touching at level 0 at two inequivalent points in the Brillouin zone, where $f(k)$ vanishes. The parameter $g \neq 0$ opens a gap between

the bands of size $2g$. The parameter $t_2$ can turn the system into a Chern topological insulator (in particular, with $g = 1, t_2 = -1$, the system is a Chern insulator with Chern number $+1$). Therefore, varying the parameters $g$, $t_2$ and $\mu_{\mathrm{F}}$, we can obtain a normal insulator, a Chern insulator, a semimetal or a metal.

For a given set of parameters, we compute the current by using formulae (4.28)-(4.30). We sample the Brillouin zone using a uniform grid with $N_{\mathrm{grid}} = 300$ points per direction, and solve the ordinary differential equation

$$i\frac{du}{dt}(t) = H_{k-\varepsilon e_\beta t}u(t), \quad u(0) = u_{n,k},$$

for various $n$ and $k$ using the `DifferentialEquations.jl` Julia package [83] with the default Tsitouras method of order 5.

Our parameter values are collected in Table 4.1.

| Panel | $g$ | $\mu_{\mathrm{F}}$ | $t_2$ | Phase |
|---|---|---|---|---|
| (a) | 1 | 0 | 0 | Normal insulator |
| (b) | 1 | 0 | $-1$ | Chern insulator |
| (c) | 1 | $-2$ | 0 | Metal |
| (d) | 0 | 0 | 0 | Semimetal |

Table 4.1: Parameter values for the experiments in Figure 4.3

Our results are presented in the linear response regime ($\varepsilon = 10^{-6}$, $t \ll \frac{1}{\varepsilon}$) in Figure 4.3.

These results are consistent with our theoretical results, including the limit values of the conductivity in cases (b) and (d), where we obtain $4\pi/\sqrt{3} \approx 7.26$ and $|b_1|^2/8 = 2\pi^2/3 \approx 6.58$ respectively. However, there is an additional phenomenon worth of note: in the case of insulators and graphene, the linear response instantaneous conductivity $j_{\alpha,\beta}(t) = \lim_{\varepsilon\to 0} \frac{j^\varepsilon_{\alpha,\beta}(t)}{\varepsilon}$ seems to possess a finite limit as $t \to +\infty$. This is not captured by our results, where we used an averaging process to suppress the oscillations. Note that for a finite $N_{\mathrm{grid}}$, the linear response oscillates with frequencies $\lambda_{n',k} - \lambda_{n,k}$ for $\lambda_{n,k} < \mu_{\mathrm{F}} < \lambda_{n',k}$, and $k$ in the discrete Brillouin zone. Only in the limit $N_{\mathrm{grid}} \to \infty$ do these resonances merge together to yield a finite limit for the current. This is linked to the absence of resonances (parallel bands) in our model. A deeper investigation of this effect would be interesting future work.

We also investigate the Bloch oscillations regime $\varepsilon \ll 1$, $\frac{1}{\varepsilon} \ll t$ in Figure 4.4, where we use the same parameters as in case (c) above. The result is consistent with our theoretical result: periodic or quasi-periodic oscillations, depending on whether $e_\beta$ is commensurate with the reciprocal lattice or not.

## 4.4 Bloch decomposition of $\gamma^\varepsilon_\beta(t)$ and regularity of the current

In this section, we prove Propositions 4.2.1 and 4.2.6. We point out that, formally, $\gamma^\varepsilon_\beta(t)$ satisfies the equation

$$i\partial_t\gamma^\varepsilon_\beta = [H, \gamma^\varepsilon_\beta] + \varepsilon[x_\beta, \gamma^\varepsilon_\beta].$$

The operator $[x_\beta, \gamma^\varepsilon_\beta]$ can easily be seen to be $\mathcal{R}$-periodic, with fibers $i\partial_\beta\gamma^\varepsilon_{\beta,k}$ (where $\partial_\beta = e_\beta\cdot\nabla_k$), and therefore, $\gamma^\varepsilon_\beta(t)$ is $\mathcal{R}$-periodic and its fibers $\gamma^\varepsilon_{\beta,k}(t)$ satisfy the equation

$$i\partial_t\gamma^\varepsilon_{\beta,k} - i\varepsilon\partial_\beta\gamma^\varepsilon_{\beta,k} = [H_k, \gamma^\varepsilon_{\beta,k}] = L_{H_k}\gamma^\varepsilon_{\beta,k},$$

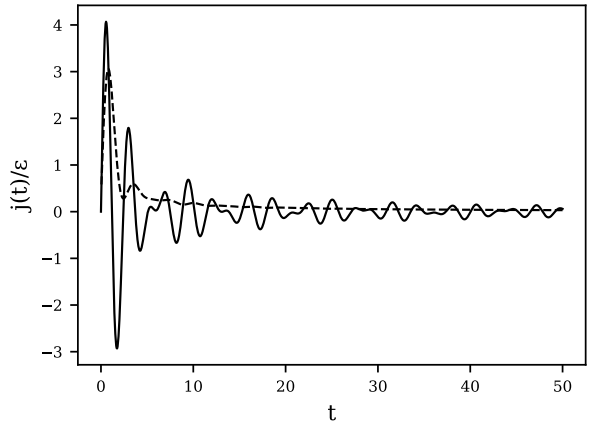


(a) Normal insulator phase, longitudinal current.

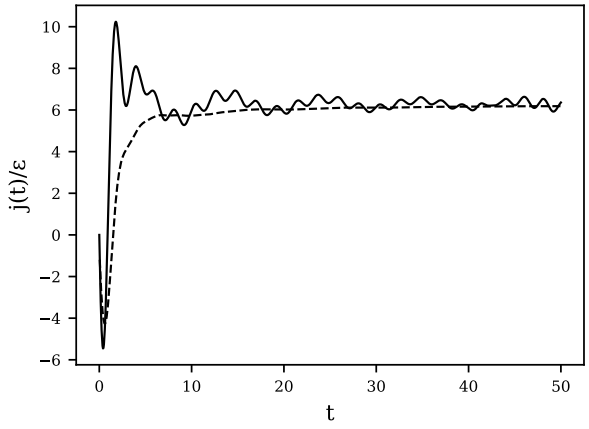


(b) Chern insulator phase, transverse current.

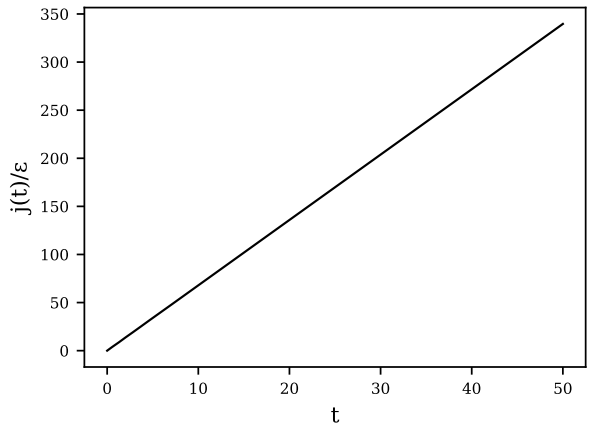


(c) Metallic phase.

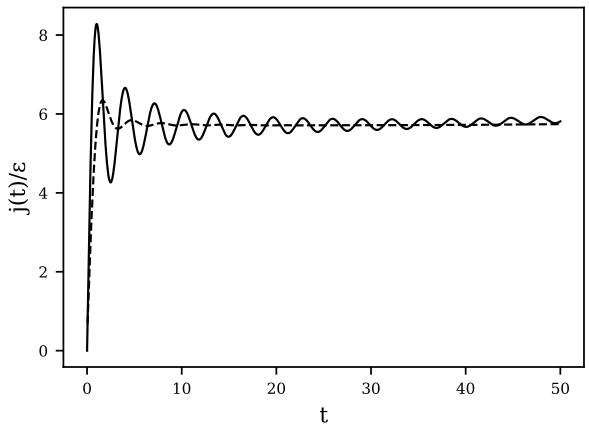


(d) Graphene phase.

Figure 4.3: Instantaneous conductivity $\frac{j^{\varepsilon}_{\alpha,\beta}(t)}{\varepsilon}$ (solid line) and running average $\frac{1}{t}\int_0^t \frac{j^{\varepsilon}_{\alpha,\beta}(t')}{\varepsilon}dt'$ (dotted line) for several phases, in the linear response regime ($\varepsilon = 10^{-4}$, $t \ll \frac{1}{\varepsilon}$). In all cases $e_\beta = b_1$, and $e_\alpha = e_\beta$, except in panel (b) where $e_\alpha = b_2$.

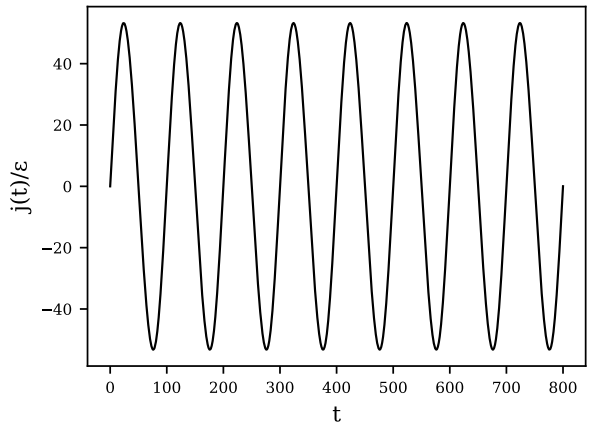


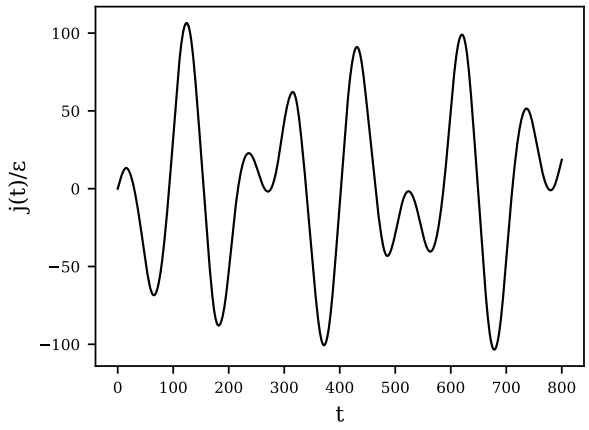


Figure 4.4: Instantaneous conductivity $\frac{j^{\varepsilon}_{\alpha,\beta}(t)}{\varepsilon}$ in the Bloch oscillations regime ($\varepsilon = 10^{-2}$, $\frac{1}{\varepsilon} \ll t$). We take $e_\alpha = b_1$. The left figure is with $e_\beta = b_1 + b_2$, the right one with $e_\beta = b_1 + \frac{1+\sqrt{5}}{2}b_2$.

where $L_{H_k} := [H_k, \cdot]$ is the Liouvillian associated with the operator $H_k$ (see Section 4.5.1). The left-hand side of this equation is a linear advection equation, which suggests the use of the

method of characteristics: setting

$$\widetilde{\gamma}^{\varepsilon}_{\beta,k}(t) = \gamma^{\varepsilon}_{\beta,k-\varepsilon e_\beta t}(t), \tag{4.39}$$

we obtain

$$i\partial_t \widetilde{\gamma}^{\varepsilon}_{\beta,k}(t) = [H_{k-\varepsilon e_\beta t}, \widetilde{\gamma}^{\varepsilon}_{\beta,k}(t)] = L_{H_{k-\varepsilon e_\beta t}} \widetilde{\gamma}^{\varepsilon}_{\beta,k}(t),$$

which is equivalent to (4.29). The use of the gauge transform operator $G_{\varepsilon t e_\beta}$, equivalent to the change of variable (4.39), makes these remarks rigorous.

### 4.4.1 Proof of Proposition 4.2.1

As outlined above, the results in Proposition 4.2.1 are well-known; they can in fact be extended to the more general setting of ergodic magnetic Schrödinger operators (see [9]). We provide here an elementary proof specific to the periodic case, and take this opportunity to introduce notations and tools which will be useful in the sequel.

**Proof of the first assertion.** The essential self-adjointness of $H^{\varepsilon}_{\beta}$ follows from an extension of the Faris-Lavine theorem [85, Theorem X.38]. Let $\mathcal{C} = C^{\infty}_{\mathrm{c}}(\mathbb{R}^d;\mathbb{C})$ be the set of infinitely differentiable, compactly supported functions.

**Lemma 4.4.1** (Faris-Lavine theorem with periodic vector potentials)**.** *Let $V$ and $W$ be real-valued measurable functions on $\mathbb{R}^d$, $W \in L^2_{\mathrm{loc}}(\mathbb{R}^d;\mathbb{R})$ and $\mathcal{A} \in L^4_{\mathrm{per}}(\mathbb{R}^d;\mathbb{R}^d)$ such that $\nabla \cdot \mathcal{A} = 0$ in the sense of distributions. Suppose that*

1. *there exists $c, f \in \mathbb{R}_+$ such that $W(x) \geq -c|x|^2 - f$, for a.a. $x \in \mathbb{R}^d$;*
2. *$\frac{1}{2}(-i\nabla + \mathcal{A})^2 + V + W + 2c|x|^2$ is essentially self-adjoint on $\mathcal{C}$;*
3. *for some $a < 1$, $\frac{a}{2}(-i\nabla + \mathcal{A})^2 + V$ is bounded below on $\mathcal{C}$.*

*Then $\frac{1}{2}(-i\nabla + \mathcal{A})^2 + V + W$ is essentially self-adjoint on $\mathcal{C}$.*

The proof of the above lemma is postponed until section 4.10.1.

We apply Lemma 4.4.1 with $V \in L^2_{\mathrm{per}}(\mathbb{R}^d;\mathbb{R}), W = \varepsilon x_\beta$. The operator $\frac{1}{2}(-i\nabla + \mathcal{A})^2 + V + \varepsilon x_\beta + 2|x|^2$ is essentially self-adjoint on the core $\mathcal{C}$ in view of [60, Theorem 3] (note that $\varepsilon x \cdot e_\beta \geq -|x|^2 - \frac{\varepsilon^2 |e_\beta|^2}{4}$). Moreover, since $V$ is $L^2_{\mathrm{per}}(\mathbb{R}^d;\mathbb{R})$, it is infinitesimally $-\Delta$-bounded, and hence, there exists $0 < a < 1$, such that $\frac{a}{2}(-i\nabla + \mathcal{A})^2 + V$ is bounded below. This can be seen directly, or as a consequence of [60, Theorem 3]. Then, Lemma 4.4.1 gives that $H^{\varepsilon}_{\beta}$ is essentially self-adjoint on $\mathcal{C}$ and therefore admits a unique self-adjoint extension on $L^2(\mathbb{R}^d;\mathbb{C})$. Hence, the propagator of the associated Schrödinger equation is well-defined, and explicitly given by $(\mathrm{e}^{-itH^{\varepsilon}_{\beta}})_{t\in\mathbb{R}}$.

**Proof of the second assertion.** The self-adjointness of the time-dependent Hamiltonian

$$\widetilde{H}^{\varepsilon}_{\beta}(t) = \frac{1}{2}(-i\nabla + \mathcal{A} - \varepsilon e_\beta t)^2 + V,$$

is a consequence of Lemma 4.4.1, by replacing $\mathcal{A}$ with $(\mathcal{A} - \varepsilon e_\beta t)$. To show the well-posedness of the dynamics, since $\widetilde{H}^{\varepsilon}_{\beta}(t)$ is $\mathcal{R}$-periodic, it suffices to study its fibers. Hence we consider the dynamics of a Schrödinger equation with Hamiltonian

$$\widetilde{H}^{\varepsilon}_{\beta,k}(t) = \frac{1}{2}(-i\nabla + \mathcal{A} + k - \varepsilon e_\beta t)^2 + V$$

and we use the following lemma on the dynamics generated by time-dependent perturbations of the free-particle Hamiltonian on $L^2_{\mathrm{per}}$.

**Lemma 4.4.2.** *Let $H_0 := -\frac{1}{2}\Delta$ be the free-particle Hamiltonian on $L^2_{\mathrm{per}}$, and a map*

$$[0,T] \ni t \mapsto H_1(t)$$

*taking its values in the set of $H_0$-bounded self-adjoint operators on $L^2_{\mathrm{per}}$ with relative bound lower than 1, that is: there exist $0 < a < 1$ and $b > 0$ such that*

$$\forall t \in [0,T], \quad \forall \phi \in H^2_{\mathrm{per}}, \quad \|H_1(t)\phi\|_{L^2_{\mathrm{per}}} \leq a\|H_0\phi\|_{L^2_{\mathrm{per}}} + b\|\phi\|_{L^2_{\mathrm{per}}}. \tag{4.40}$$

*Then, for all $t \in [0,T]$, the operator defined by $H(t) = H_0 + H_1(t)$ is self-adjoint on $L^2_{\mathrm{per}}$ with domain $H^2_{\mathrm{per}}$, and there exists a unique unitary propagator $(\mathcal{U}(t))_{t\in[0,T]}$ on $L^2_{\mathrm{per}}$ such that for $t \in [0,T]$, and $\phi_0 \in H^2_{\mathrm{per}}$, $\phi : t \mapsto \mathcal{U}(t)\phi_0$ is in $C^1(\mathbb{R}; H^2_{\mathrm{per}})$, and solves the time-dependent Schrödinger equation*

$$i\partial_t\phi(t) = H(t)\phi(t), \qquad \phi(0) = \phi_0.$$

The proof of the above lemma is postponed to section 4.10.2.

For $t \in [0,T], k \in \mathbb{R}^d$, we have $\widetilde{H}^{\varepsilon}_{\beta,k}(t) = H_0 + H_1(t)$, with

$$H_1(t) = \frac{1}{2}\Big[(-i\nabla)\cdot(\mathcal{A} + k - \varepsilon e_\beta t) + (\mathcal{A} + k - \varepsilon e_\beta t)\cdot(-i\nabla) + (\mathcal{A} + k - \varepsilon e_\beta t)^2\Big] + V.$$

Using the Sobolev embeddings $H^2_{\mathrm{per}} \subset L^\infty_{\mathrm{per}}$, $H^1_{\mathrm{per}} \subset L^6_{\mathrm{per}}$, the Coulomb gauge choice $\nabla\cdot\mathcal{A} = 0$ and the fact that $\mathcal{A} \in L^4_{\mathrm{per}}(\mathbb{R}^d;\mathbb{R}^d)$ and $V \in L^2_{\mathrm{per}}(\mathbb{R}^d;\mathbb{R})$, it is standard that $H_1$ satisfies the conditions of Lemma 4.4.2, and the result follows.

**Proof of the third assertion.** We first compute the fibers of the $\mathcal{R}$-periodic operator $\gamma^{\varepsilon}_{\beta}(t)$. Using (4.20), we have

$$\begin{aligned}
\gamma^{\varepsilon}_{\beta,k}(t) &= \Big(G^*_{\varepsilon t e_\beta}\widetilde{\mathcal{U}}^{\varepsilon}_{\beta}(t)\gamma(0)\widetilde{\mathcal{U}}^{\varepsilon}_{\beta}(t)^* G_{\varepsilon t e_\beta}\Big)_k && (4.41)\\
&= \Big(\widetilde{\mathcal{U}}^{\varepsilon}_{\beta}(t)\gamma(0)\widetilde{\mathcal{U}}^{\varepsilon}_{\beta}(t)^*\Big)_{k+\varepsilon t e_\beta}\\
&= \widetilde{\mathcal{U}}^{\varepsilon}_{\beta,k+\varepsilon t e_\beta}(t)\gamma_{k+\varepsilon t e_\beta}(0)\widetilde{\mathcal{U}}^{\varepsilon}_{\beta,k+\varepsilon t e_\beta}(t)^* && (4.42)\\
&= \sum_{n=1}^{N_{k+\varepsilon t e_\beta}} |\widetilde{\mathcal{U}}^{\varepsilon}_{\beta,k+\varepsilon t e_\beta}(t)u_{n,k+\varepsilon t e_\beta}\rangle\langle\widetilde{\mathcal{U}}^{\varepsilon}_{\beta,k+\varepsilon t e_\beta}(t)u_{n,k+\varepsilon t e_\beta}|.
\end{aligned}$$

Since the $u_{n,k}$ are in $H^2_{\mathrm{per}}$, we deduce that

$$(J_\alpha\gamma^{\varepsilon}_{\beta}(t))_k = -(-i\nabla + k + \mathcal{A})\cdot e_\alpha\gamma^{\varepsilon}_{\beta,k}(t) = -\partial_\alpha H_k\gamma^{\varepsilon}_{\beta,k}(t)$$

is finite-rank (hence trace-class) uniformly in $k \in \mathcal{B}$ and therefore that the current $j^{\varepsilon}_{\alpha,\beta}(t) = \underline{\mathrm{Tr}}\left(J_\alpha\gamma^{\varepsilon}_{\beta}(t)\right)$ is well-defined.

As the function $k \mapsto \mathrm{Tr}\big(\partial_\alpha H_k\gamma^{\varepsilon}_{\beta,k}(t)\big)$ is $\mathcal{R}^*$-periodic, we also have

$$j^{\varepsilon}_{\alpha,\beta}(t) = -(2\pi)^{-d}\int_{\mathcal{B}}\mathrm{Tr}\big(\partial_\alpha H_k\gamma^{\varepsilon}_{\beta,k}(t)\big)\,dk = -(2\pi)^{-d}\int_{\mathcal{B}}\mathrm{Tr}\Big(\partial_\alpha H_{k-\varepsilon e_\beta t}\gamma^{\varepsilon}_{\beta,k-\varepsilon e_\beta t}(t)\Big)\,dk.$$

## 4.4.2 Proof of Proposition 4.2.6

We have

$$j^0_{\alpha,\beta}(t) = j^{\varepsilon}_{\alpha,\beta}(0) = \underline{\mathrm{Tr}}(J_\alpha\gamma(0)) = -(2\pi)^{-d}\int_{\mathcal{B}}\mathrm{Tr}(\partial_\alpha H_k\gamma_k(0))\,dk$$

and, when $k \in \mathcal{B}_N$ for some $N \in \mathbb{N}^*$, we have $\mathrm{Tr}(\partial_\alpha H_k\gamma_k(0)) = \partial_\alpha\sum_{n=1}^{N}\lambda_{n,k}$ by the Hellmann-Feynman theorem.

1. Under Assumption 4.2.3 (insulators), $\mathcal{B}_{N_{\rm ins}} = \mathcal{B}$ and $k \mapsto \sum_{n=1}^{N_{\rm ins}} \lambda_{n,k}$ is smooth and $\mathcal{R}^*$-periodic so that $j^0_{\alpha,\beta}(t) = j^\varepsilon_{\alpha,\beta}(0) = 0$ by Stokes theorem.

2. Under Assumption 4.2.4 (non-degenerate metals), the Fermi surface $\mathcal{S}$ is a negligible subset of $\mathcal{B}$, each non-empty $\mathcal{B}_N$ has a smooth boundary, and we have

$$\begin{aligned}\underline{\mathrm{Tr}}(J_\alpha \gamma(0)) &= -(2\pi)^{-d} \sum_{N\in\mathbb{N}^*} \int_{\mathcal{B}_N} \partial_\alpha \sum_{n=1}^{N} \lambda_{n,k} dk \\ &= -(2\pi)^{-d} \sum_{N\in\mathbb{N}^*} \left( \int_{\mathcal{S}_N} - \int_{\mathcal{S}_{N-1}} \right) \left( \sum_{n=1}^{N} \lambda_{n,k} \right) (ds \cdot e_\alpha) \\ &= -(2\pi)^{-d} \sum_{N\in\mathbb{N}^*} \int_{\mathcal{S}_N} \lambda_{N,k} (ds \cdot e_\alpha) = -\frac{\mu_{\rm F}}{(2\pi)^d} \sum_{N\in\mathbb{N}^*} e_\alpha \cdot \left( \int_{\mathcal{S}_N} ds \right) = 0. \quad (4.43)\end{aligned}$$

3. Under Assumption 4.2.5 (semi-metals), the Fermi surface $\mathcal{S}$ reduces to a finite number of points and $k \mapsto \sum_{n=1}^{N_{\rm sm}} \lambda_{n,k}$ is globally Lipschitz and $\mathcal{R}^*$-periodic on $\mathbb{R}^d$, and smooth on $\mathcal{B}_{N_{\rm sm}} = \mathcal{B} \setminus \mathcal{S}$, which leads to $j^0_{\alpha,\beta}(t) = j^\varepsilon_{\alpha,\beta}(0) = 0$.

## 4.5 Perturbation theory for time-dependent Hamiltonians

In this section we consider the dynamics generated by a Hamiltonian $H(s) = H(\varepsilon t)$, and in particular its action on eigenspaces of $H(0)$. We begin with some elementary properties of the Liouvillian in Section 4.5.1, then use it to study subspace perturbation theory in Section 4.5.2. We establish an adiabatic theorem in Section 4.5.3, and use it to study the time-dependent Hamiltonian $H_{k-\varepsilon e_\beta t}$ in Section 4.5.4. Finally, we prove a result in linear response with a remainder independent of the gap in Section 4.5.5.

### 4.5.1 The Liouvillian and its partial inverse

In order to formulate and interpret our results, it is convenient to make use of the Liouvillian formalism. Recall that if $h$ is a bounded self-adjoint operator on a Hilbert space $\mathcal{H}_{\rm f}$, the Liouvillian $L_h$ associated with $h$ is the bounded linear operator on $\mathcal{L}(\mathcal{H}_{\rm f})$ (such a mathematical object is sometimes called a superoperator in the physics literature) defined by

$$\forall A \in \mathcal{L}(\mathcal{H}_{\rm f}), \quad L_h A = [h, A]. \quad (4.44)$$

Note that if $A$ is self-adjoint, then $L_h A$ is anti-self-adjoint ($iL_hA = i[h,A]$ is self-adjoint). The restriction of $L_h$ to the space $\mathfrak{S}_2(\mathcal{H}_{\rm f})$ of Hilbert-Schmidt operators on $\mathcal{H}_{\rm f}$ is self-adjoint: for all $A, B \in \mathfrak{S}_2(\mathcal{H}_{\rm f})$, the products of $h$ with $A$ and $B$ are still $\mathfrak{S}_2(\mathcal{H}_{\rm f})$, and, by cyclicity of the trace,

$$(L_h A, B)_{\mathfrak{S}_2} = \mathrm{Tr}\left([h,A]^* B\right) = \mathrm{Tr}\left((A^* h - h A^*) B\right) = \mathrm{Tr}\left(A^*(hB - Bh)\right) = (A, L_h B)_{\mathfrak{S}_2}. \quad (4.45)$$

The operator $L_h$ is to density matrices what the Hamiltonian $h$ is to pure states: it is the infinitesimal generator of the norm-continuous unitary group $(\mathfrak{U}_h(t))_{t\in\mathbb{R}}$ on $\mathcal{L}(\mathcal{H}_{\rm f})$ defined by

$$\forall A \in \mathcal{L}(\mathcal{H}_{\rm f}), \quad \mathfrak{U}_h(t) A = e^{-ith} A e^{ith}. \quad (4.46)$$

In the case when $h$ is an unbounded self-adjoint operator, (4.44) does not make sense for all $A \in \mathcal{L}(\mathcal{H}_{\rm f})$, but it is still possible to define the Liouvillian $L_h$ as the infinitesimal generator

of the strongly-continuous unitary group $(\mathfrak{U}_h(t))_{t\in\mathbb{R}}$ on $\mathcal{L}(\mathcal{H}_\mathrm{f})$ defined by (4.46). It is then an unbounded operator on $\mathcal{L}(\mathcal{H}_\mathrm{f})$, self-adjoint on $\mathfrak{S}_2(\mathcal{H}_\mathrm{f})$.

If $\mathcal{H}_f$ is of finite-dimension $N_f$, the action of $L_h$ is easily understood in an orthonormal eigenbasis $(e_n)_{1\le n\le N_f}$ of $h$ with associated eigenvalues $\lambda_1 \le \cdots \le \lambda_{N_f}$. Then,

$$L_h|e_n\rangle\langle e_m| = (\lambda_n - \lambda_m)|e_n\rangle\langle e_m|.$$

The operator $L_h$ is not invertible (for instance, $L_h|e_n\rangle\langle e_n| = 0$). However, it is invertible when restricted to the subspace of block off-diagonal matrices, i.e. matrices $A$ such that $A_{nn'} = A_{mm'} = 0$ for $n, n' \le N < m, m'$ for a given $N$ such that $\lambda_{N+1} > \lambda_N$. Its partial inverse $L^+_{h,N}$ is given by

$$L^+_{h,N}\left(\sum_{1\le n\le N,\, N<m\le N_f} A_{mn}\,|e_m\rangle\,\langle e_n| + A_{nm}\,|e_n\rangle\,\langle e_m|\right) = \left(\sum_{1\le n\le N,\, N<m\le N_f} \frac{A_{mn}\,|e_m\rangle\,\langle e_n| - A_{nm}\,|e_n\rangle\,\langle e_m|}{\lambda_m - \lambda_n}\right) \quad (4.47)$$

and $L^+_{h,N}$ is bounded in operator norm by $\frac{1}{\lambda_{N+1}-\lambda_N}$.

More generally, if $h$ is an unbounded self-adjoint operator, let $I$ be a closed bounded interval of $\mathbb{R}$, and assume that

$$g := \min\left(1, \mathrm{dist}\left(I, \sigma(h) \setminus (\sigma(h)\cap I)\right)\right) > 0.$$

The associated spectral projector is

$$P_{I,h} := \mathbb{1}_I(h) = \frac{1}{2\pi i}\oint_{\mathcal{C}} (z-h)^{-1}\,dz, \quad (4.48)$$

where $\mathcal{C}$ is a Cauchy contour in the complex plane such that $\sigma(h)\cap I$ is inside $\mathcal{C}$ and $\sigma(h)\setminus(\sigma(h)\cap I)$ is outside $\mathcal{C}$. Generalizing the terminology of the finite-dimensional case, we call off-diagonal operators (with respect to the splitting of $\mathcal{H}_f$ induced by $P_{I,h}$) the elements of the closed subspace

$$\mathcal{L}^{\mathrm{OD}}_{h,I} := \{A \in \mathcal{L}(\mathcal{H}_\mathrm{f}) \mid P_{h,I}AP_{h,I} = (1-P_{h,I})A(1-P_{h,I}) = 0\}$$

of $\mathcal{L}(\mathcal{H}_\mathrm{f})$. This defines a $\mathfrak{S}_2$-orthogonal splitting of operators into their diagonal and off-diagonal parts. It is easily seen that $\mathcal{L}^{\mathrm{OD}}_{h,I}$ is $L_h$-stable, and that $L_h$ is invertible on $\mathcal{L}^{\mathrm{OD}}_{h,I}$ with a bounded inverse. We denote its partial inverse by $L^+_{h,I}$, extended to all of $\mathcal{L}(\mathcal{H}_f)$ by imposing that it vanishes on diagonal operators. $L^+_{h,I}$ has an explicit contour integral representation:

$$L^+_{h,I}A = \frac{1}{2\pi i}\oint_{\mathcal{C}} (z-h)^{-1}[P_{h,I},A](z-h)^{-1}\,dz, \quad \forall A \in \mathcal{L}(\mathcal{H}_\mathrm{f}), \quad (4.49)$$

where $\mathcal{C}$ is a contour as above. We check this by computing $L^+_{h,I}L_{h,I}A$ with the contour integral for some $A \in \mathcal{L}(\mathcal{H}_\mathrm{f})$. Since $P_{h,I}$ is a spectral projector of $h$, we have $P_{h,I}h = hP_{h,I}$, from which it follows that $[P_{h,I},[h,A]] = [h,[P_{h,I},A]]$, and using $h = h - z + z$, we finally obtain $[P_{h,I},[h,A]] = [[P_{h,I},A], z-h]$. Hence,

$$\begin{aligned} L^+_{h,I}L_{h,I}A =& \frac{1}{2\pi i}\oint_{\mathcal{C}} (z-h)^{-1}[P_{h,I},A](z-h)(z-h)^{-1}\,dz \\ &- \frac{1}{2\pi i}\oint_{\mathcal{C}} (z-h)^{-1}(z-h)[P_{h,I},A](z-h)^{-1}\,dz, \\ =& P_{h,I}[P_{h,I},A] - [P_{h,I},A]P_{h,I} = (1-P_{h,I})AP_{h,I} + P_{h,I}A(1-P_{h,I}). \end{aligned}$$

Since $h$ and $(z-h)^{-1}$ commute, we obtain $L_{h,I}L_{h,I}^{+}A = L_{h,I}^{+}L_{h,I}A$. We then have

$$L_{h,I}L_{h,I}^{+}A = L_{h,I}^{+}L_{h,I}A = P_{h,I}A(1-P_{h,I}) + (1-P_{h,I})AP_{h,I}$$

for all $A \in \mathcal{L}(\mathcal{H}_f)$. From (4.49), we see that, when $P_{h,I}$ is of finite rank $\mathcal{N}$, $L_{h,I}^{+}A$ is of rank of most $2\mathcal{N}$.

### 4.5.2 Subspace perturbation theory

The Liouvillian is a powerful tool to write concisely the results of subspace perturbation theory, which studies the time dependence of a gapped subspace of a time-dependent Hamiltonian. We consider $T > 0$ and $(H(s))_{s\in[0,T)}$ a family of self-adjoint operators on a Hilbert space $\mathcal{H}_{\mathrm{f}}$ sharing the same domain $D \subset \mathcal{H}_f$ and satisfying the following assumptions:

**H1** $H(s) \geq 1$ for all $s \in [0,T)$;

**H2** for each $\phi \in D$, the map $s \mapsto H(s)\phi$ is in $C^n([0,T),\mathcal{H}_{\mathrm{f}})$ for some $n \geq 1$. For all $1 \leq l \leq n$, the operator $H^{(l)}(s)$ is self-adjoint on $\mathcal{H}_{\mathrm{f}}$ for all $s \in [0,T)$, and

$$\alpha_l := \sup_{s\in[0,T)} \|H^{(l)}(s)H(s)^{-1}\|_{\mathcal{L}(\mathcal{H}_{\mathrm{f}})} < \infty; \tag{4.50}$$

**H3** there exist $M \in \mathbb{R}_+$ and bounded continuous functions $a_\pm : [0,T] \to \mathbb{R}$ with $0 \leq a_- \leq a_+ \leq M$ defining bounded closed intervals $I(s) = [a_-(s), a_+(s)] \subset \mathbb{R}$ such that, for all $s \in [0,T)$,

$$g(s) := \min\left(1, \mathrm{dist}(I(s), \sigma(H(s)) \setminus (\sigma(H(s)) \cap I(s)))\right) > 0,$$
$$P(s) := \mathbb{1}_{I(s)}(H(s)) \text{ has a finite (constant) rank } \mathcal{N} \in \mathbb{N}^*,$$

Under these assumptions, we set

$$L^{+}(s) := L^{+}_{H(s),I(s)}.$$

**Proposition 4.5.1.** *Assume* **H1**, **H2** *and* **H3**. *Then,* $P \in C^n([0,T),\mathcal{L}(\mathcal{H}_{\mathrm{f}}))$, $L^{+} \in C^n([0,T),\mathcal{L}(\mathcal{L}(\mathcal{H}_{\mathrm{f}})))$, *and*

$$\dot{P}(s) = L(s)^{+}[P(s), \dot{H}(s)]. \tag{4.51}$$

*Furthermore, there exist constants* $C_1, \cdots, C_n \in \mathbb{R}_+$ *depending only on* $\alpha_1, \cdots, \alpha_n$ *and* $M$ *such that the following bounds hold for all* $0 \leq l \leq n$, $s \in [0,T)$ *and* $A \in \mathcal{L}(\mathcal{H}_{\mathrm{f}})$*:*

$$\|H(s)P(s)\| \leq M, \tag{4.52}$$
$$\|H(s)P^{(l)}(s)\| \leq \frac{C_l}{g(s)^{l+1}}, \tag{4.53}$$
$$\|H(s)(L^{+})^{(l)}(s)A\| \leq \frac{C_l}{g(s)^{l+3}}\|A\|. \tag{4.54}$$

*In addition,* $P^{(l)}(s)$ *has rank at most* $(l+1)\mathcal{N}$, *and* $(L^{+})^{(l)}(s)A$ *has rank at most* $c_l\mathcal{N}$ *where* $c_l$ *is a constant that only depends on* $l$ *(in particular,* $c_0 = 2$ *and* $c_1 = 10$*).*

*Remark* 4.5.2. The powers of the gap in the bounds (4.53) and (4.54) are too pessimistic, as could be shown by a more detailed analysis. For instance, in the case $l = 0$, $L^{+}(s)$ can be seen from the arguments at the beginning of this section to be bounded by a constant times $\frac{1}{g(s)}$. Similarly, the operator $\dot{P}$ is bounded by a constant times $\frac{1}{g(s)}$, using (4.51). Nevertheless, the above bounds are more straightforward to establish and will suffice for our purposes.

*Proof.* Differentiating $L_{H(s)}P(s) = 0$, we get

$$L_{H(s)}\dot{P}(s) = [P(s), \dot{H}(s)].$$

Since both $[P(s), \dot{H}(s)]$ and $\dot{P}(s)$ are off-diagonal operators (the first by direct calculation, the second by differentiating the relationship $P(s)^2 = P(s)$), we deduce (4.51). By the functional calculus, $\|H(s)P(s)\| = \|H(s)\mathbb{1}_{I(s)}(H(s))\| \leq a_+(s) \leq M$, whence (4.52).

In the following we take for $\mathcal{C}(s)$ the rectangular contour centered at the center of $I(s)$, of length $|I(s)| + g(s)$ and height $g(s)$, so that

$$|\mathcal{C}(s)| \leq 2M + 4 \quad \text{and for all } z \in \mathcal{C}(s), \quad \left\| \frac{1}{z - H(s)} \right\| \leq \frac{2}{g(s)}. \tag{4.55}$$

We use the integral representation (4.48):

$$P(s) = \frac{1}{2\pi i} \oint_{\mathcal{C}(s)} \frac{1}{z - H(s)}\, dz. \tag{4.56}$$

Using for all $z \in \mathcal{C}(s)$ the bound

$$\left\| \frac{H(s)}{z - H(s)} \right\| = \sup_{\lambda \in \sigma(H(s))} \left| \frac{\lambda}{z - \lambda} \right| \leq 1 + \sup_{\lambda \in \sigma(H(s))} \left| \frac{z}{z - \lambda} \right| \leq 1 + \frac{2(M + g(s))}{g(s)} \leq \frac{2M + 3}{g(s)} \tag{4.57}$$

establishes (4.53) for $l = 0$.

Since $\sigma\left(H(s)\right)$ varies continuously, the contour $\mathcal{C}(s)$ in (4.56) above can be kept fixed equal to $\mathcal{C}(s_0)$ for $s$ in a neighborhood of any $s_0 \in [0, T)$. Using

$$\frac{d}{ds} \frac{1}{z - H(s)} = \frac{1}{z - H(s)} \dot{H}(s) \frac{1}{z - H(s)} \tag{4.58}$$

it follows that $P \in C^1([0, T), \mathcal{L}(\mathcal{H}_{\mathrm{f}}))$ and

$$\dot{P}(s) = \frac{1}{2\pi i} \oint_{\mathcal{C}(s)} \frac{1}{z - H(s)} \dot{H}(s) \frac{1}{z - H(s)}\, dz.$$

Using the bounds (4.50), (4.55) and (4.57), it follows that

$$\|H(s)\dot{P}(s)\| \leq \frac{(2M + 3)(2M + 4)\alpha_1}{\pi g(s)^2}$$

which proves (4.53) for $l = 1$. The general case for $l > 1$ follows from repeated application of the chain rule to (4.56) and (4.58), and the bounds (4.50), (4.55) and (4.57).

The differentiability and bounds on the inverse Liouvillian are treated using the same arguments on the representation

$$L^+(s)A = \frac{1}{2\pi i} \oint_{\mathcal{C}(s)} \frac{1}{z - H(s)} [P(s), A] \frac{1}{z - H(s)}\, dz.$$

Let $(u_n^0)_{n=1,\ldots,\mathcal{N}}$ be an orthonormal basis of $P(0)$. Then the solutions to the parallel transport equation $\dot{u}_n(s) = \dot{P}(s)u_n(s)$ with $u_n(0) = u_n^0$ are easily checked to be a $C^n$ orthogonal basis of $\mathrm{Ran}P(s)$. It follows that one has

$$P^{(l)}(s) = \sum_{n=1}^{\mathcal{N}} \sum_{m=0}^{l} \binom{l}{m} |u_n^{(m)}(s)\rangle\langle u_n^{(l-m)}(s)|.$$

Therefore, $P^{(l)}(s)$ is of rank at most $(l + 1)\mathcal{N}$. From the integral representation of $L^+(s)$ (see (4.49)), it follows that, for any bounded operator $A$, $L^+(s)A$ is of rank at most $2\mathcal{N}$. Its derivatives are sums of terms which all contain as a factor $P(s)$ or one of its derivative, and the result follows with $c_l = 2 \sum_{k_1 + k_2 + k_3 = l,\, k_j \in \mathbb{N}} (k_2 + 1)$. □

### 4.5.3 Adiabatic theory

The following proposition is an adaptation in our context of the classical adiabatic theorem that the Schrödinger evolution with a slowly evolving Hamiltonian $H(\varepsilon t)$ approximately preserves gapped eigenspaces [95]. We explicitly compute the corrections to first order in $\varepsilon$.

**Proposition 4.5.3.** *Assume the same hypotheses as in Proposition 4.5.1. Let $(U^\varepsilon(t,t'))_{0\leq t'\leq t<\varepsilon^{-1}T}$ be the propagator associated with the family of time-scaled Hamiltonians $(H(\varepsilon t))_{t\in[0,\varepsilon^{-1}T)}$, i.e.*

$$i\frac{\partial U^\varepsilon}{\partial t}(t,t') = H(\varepsilon t)U^\varepsilon(t,t'), \quad t\in[t',\varepsilon^{-1}T) \qquad U^\varepsilon(t',t') = \mathrm{Id}, \tag{4.59}$$

*and $U^\varepsilon(t) = U^\varepsilon(t,0)$. For all $\varepsilon \geq 0$ and $t\in[0,\varepsilon^{-1}T)$, it holds*

$$U^\varepsilon(t)P(0)U^\varepsilon(t)^* = P(\varepsilon t) + i\varepsilon L^+(\varepsilon t)\dot P(\varepsilon t) - i\varepsilon U^\varepsilon(t)\left(L^+(0)\dot P(0)\right)U^\varepsilon(t)^* + R^\varepsilon(t), \tag{4.60}$$

*with*

$$R^\varepsilon(t) = -i\varepsilon^2\int_0^t U^\varepsilon(t,t')\,\frac{d}{ds}\left(L(s)^{-1}\dot P(s)\right)\Big|_{s=\varepsilon t'} U^\varepsilon(t,t')^*\,dt'. \tag{4.61}$$

*In addition, we have the following estimates:*

$$\forall 0\leq t'\leq t<\varepsilon^{-1}T, \quad \left\|H(\varepsilon t)U^\varepsilon(t,t')H(\varepsilon t')^{-1}\right\|_{\mathcal{L}(\mathcal{H}_\mathrm{f})} \leq e^{\alpha_1\varepsilon(t-t')}, \tag{4.62}$$

$$\left\|H(\varepsilon t)^{1/2}U^\varepsilon(t,t')H(\varepsilon t')^{-1/2}\right\|_{\mathcal{L}(\mathcal{H}_\mathrm{f})} \leq e^{\alpha_1\varepsilon(t-t')/2}. \tag{4.63}$$

*Proof.* The existence and uniqueness of the strongly-continuous unitary propagator $(U^\varepsilon(t,t'))$ satisfying (4.59) can be obtained using (4.50) for $l=1$, and Theorem X.70 and the arguments in the proof of Theorem X.71 in [85]. We pass to the interaction picture defined by $H(\varepsilon t)$ and compute the evolution of a $C^1$ time-dependent Hilbert-Schmidt observable $A^\varepsilon(t)$ in that picture:

$$\frac{d}{dt}\left(U^\varepsilon(t)^*A^\varepsilon(t)U^\varepsilon(t)\right) = U^\varepsilon(t)^*\left(\dot A^\varepsilon(t) + i[H(\varepsilon t), A^\varepsilon(t)]\right)U^\varepsilon(t). \tag{4.64}$$

We first apply (4.64) to $A^\varepsilon(t) = P(\varepsilon t)$ and obtain

$$\frac{d}{dt}\left(U^\varepsilon(t)^*P(\varepsilon t)U^\varepsilon(t)\right) = \varepsilon\, U^\varepsilon(t)^*\dot P(\varepsilon t)U^\varepsilon(t). \tag{4.65}$$

Estimating this to be of size $\varepsilon$ is not enough because we look at long time scales. What allows us to proceed further is that this quantity is oscillating on a timescale of order $O(1)$. Indeed, applying (4.64) to $A^\varepsilon(t) = L^+(\varepsilon t)\dot P(\varepsilon t)$, for which $[H(\varepsilon t), A^\varepsilon(t)] = \dot P(\varepsilon t)$, we obtain

$$U^\varepsilon(t)^*\dot P(\varepsilon t)U^\varepsilon(t) = -i\frac{d}{dt}\left(U^\varepsilon(t)^*(L^+(\varepsilon t)\dot P(\varepsilon t))U^\varepsilon(t)\right) + iU^\varepsilon(t)^*\frac{d}{dt}\left(L^+(\varepsilon t)\dot P(\varepsilon t)\right)U^\varepsilon(t).$$

Integrating (4.65) over $[0,t]$ and using the above equality leads to

$$\begin{aligned} U^\varepsilon(t)^*P(\varepsilon t)U^\varepsilon(t) &= P(0) + \varepsilon\int_0^t U^\varepsilon(t')^*\dot P(\varepsilon t')U^\varepsilon(t')\,dt' \\ &= P(0) - i\varepsilon U^\varepsilon(t)^*\left(L^+(\varepsilon t)\dot P(\varepsilon t)\right)U^\varepsilon(t) + i\varepsilon L^+(0)\dot P(0) + r^\varepsilon(t) \end{aligned}$$

with

$$r^\varepsilon(t) = i\varepsilon\int_0^t U^\varepsilon(t')^*\frac{d}{dt'}\left(L^+(\varepsilon t')\dot P(\varepsilon t')\right)U^\varepsilon(t')\,dt' = i\varepsilon^2\int_0^t U^\varepsilon(t')^*\,\frac{d}{ds}\left(L^+(s)\dot P(s)\right)\Big|_{s=\varepsilon t'} U^\varepsilon(t')\,dt'.$$

This implies

$$U^\varepsilon(t)P(0)U^\varepsilon(t)^* = P(\varepsilon t) + i\varepsilon L^+(\varepsilon t)\dot{P}(\varepsilon t) - i\varepsilon U^\varepsilon(t)\left(L^+(0)\dot{P}(0)\right)U^\varepsilon(t)^* + R^\varepsilon(t), \tag{4.66}$$

with

$$R^\varepsilon(t) = -i\varepsilon^2 \int_0^t U^\varepsilon(t,t')\,\frac{d}{ds}\left(L^+(s)\dot{P}(s)\right)\Big|_{s=\varepsilon t'} U^\varepsilon(t,t')^*\,dt',$$

which establishes (4.60).

Let us now prove (4.62). Let $\psi \in D$. For all $t \in [t', \varepsilon^{-1}T)$, we set $\psi_\varepsilon(t) = U^\varepsilon(t,t')\psi$ and $\phi_\varepsilon(t) = H(\varepsilon t)\psi_\varepsilon(t)$. We have

$$i\frac{d\phi_\varepsilon}{dt}(t) = i\frac{d}{dt}\left(H(\varepsilon t)\psi_\varepsilon(t)\right) = H(\varepsilon t)\phi_\varepsilon(t) + i\varepsilon\dot{H}(\varepsilon t)H(\varepsilon t)^{-1}\phi_\varepsilon(t),$$

from which we obtain

$$\phi_\varepsilon(t) = U^\varepsilon(t,t')H(\varepsilon t')\psi + i\varepsilon\int_{t'}^t \dot{H}(\varepsilon t'')H(\varepsilon t'')^{-1}\phi_\varepsilon(t'')\,dt'',$$

and finally

$$\|\phi_\varepsilon(t)\|_{\mathcal{H}_\mathrm{f}} \leq \|H(\varepsilon t')\psi\|_{\mathcal{H}_\mathrm{f}} + \alpha_1\varepsilon\int_{t'}^t \|\phi_\varepsilon(t'')\|_{\mathcal{H}_\mathrm{f}}\,dt''.$$

By the Grönwall lemma,

$$\|H(\varepsilon t)U^\varepsilon(t,t')\psi\|_{\mathcal{H}_\mathrm{f}} = \|\phi_\varepsilon(t)\|_{\mathcal{H}_\mathrm{f}} \leq \|H(\varepsilon t')\psi\|_{\mathcal{H}_\mathrm{f}} e^{\alpha_1\varepsilon(t-t')}.$$

Applying this inequality to $\psi = H(\varepsilon t')^{-1}\phi$ for all $\phi \in \mathcal{H}_\mathrm{f}$ gives (4.62). We obtain (4.63) by interpolation (see e.g. [85, Section IX.4, Proposition 9]). □

The third term

$$-U^\varepsilon(t)\left(iL^+(0)\dot{P}(0)\right)U^\varepsilon(t)^*$$

of the right-hand side of (4.60) is oscillatory, and can be written as the derivative controllingof a bounded function up to higher order terms. Its time-average therefore becomes negligible in the considered regimes. Let us introduce the space

$$\mathcal{L}^{\mathrm{OD}}(s) := \{A \in \mathcal{L}(\mathcal{H}_\mathrm{f}) \mid P(s)AP(s) = (1-P(s))A(1-P(s)) = 0\}$$

of bounded off-diagonal operators relatively to the decomposition $\mathcal{H}_\mathrm{f} = \mathrm{Ran}(P(s)) \oplus \mathrm{Ker}(P(s))$.

**Lemma 4.5.4.** *Under the assumptions of Propositions 4.5.1 and 4.5.3, we have for any self-adjoint operator $A \in \mathcal{L}^{\mathrm{OD}}(0)$,*

$$U^\varepsilon(t)AU^\varepsilon(t)^* = \frac{d}{dt}\left(iL^+(\varepsilon t)\left(U^\varepsilon(t)AU^\varepsilon(t)^*\right)\right) + R_A^\varepsilon(t), \tag{4.67}$$

*where*

$$R_A^\varepsilon(t) = 2U^\varepsilon(t)r^\varepsilon(t)Ar^\varepsilon(t)U^\varepsilon(t)^* - \left(U^\varepsilon(t)(1-2P(0))Ar^\varepsilon(t)U^\varepsilon(t)^* + \mathrm{h.c.}\right) + \varepsilon i\frac{dL^+}{ds}(\varepsilon t)\left(U^\varepsilon(t)AU^\varepsilon(t)^*\right)$$

*and*

$$r^\varepsilon(t) = -i\varepsilon U^\varepsilon(t)^*\left(L^+(\varepsilon t)\dot{P}(\varepsilon t)\right)U^\varepsilon(t) + i\varepsilon L^+(0)\dot{P}(0) + U^\varepsilon(t)^*R^\varepsilon(t)U^\varepsilon(t).$$

*Proof.* We have

$$\frac{d}{dt}\left(iL^+(\varepsilon t)\left(U^\varepsilon(t)AU^\varepsilon(t)^*\right)\right) = \varepsilon i\frac{dL^+}{ds}(\varepsilon t)\left(U^\varepsilon(t)AU^\varepsilon(t)^*\right) + L^+(\varepsilon t)L(\varepsilon t)\left(U^\varepsilon(t)AU^\varepsilon(t)^*\right)$$
$$= \varepsilon i\frac{dL^+}{ds}(\varepsilon t)U^\varepsilon(t)AU^\varepsilon(t)^* + P(\varepsilon t)U^\varepsilon(t)AU^\varepsilon(t)^*(1-P(\varepsilon t)) + \text{h.c.},$$

and we deduce from (4.60) that $P(\varepsilon t)U^\varepsilon(t) = U^\varepsilon(t)\left(P(0)+r^\varepsilon(t)\right)$. We therefore have

$$\begin{aligned} P(\varepsilon t)U^\varepsilon(t)AU^\varepsilon(t)^*(1-P(\varepsilon t)) + \text{h.c.} =& U^\varepsilon(t)\left(P(0)+r^\varepsilon(t)\right)A(1-P(0)-r^\varepsilon(t))U^\varepsilon(t)^* + \text{h.c.} \\ =& U^\varepsilon(t)AU^\varepsilon(t)^* + \left(U^\varepsilon(t)\left(1-2P(0)\right)Ar^\varepsilon(t)U^\varepsilon(t)^* + \text{h.c.}\right) \\ &+ 2U^\varepsilon(t)r^\varepsilon(t)Ar^\varepsilon(t)U^\varepsilon(t)^*, \end{aligned}$$

where we have used that $A = P(0)A(1-P(0)) + (1-P(0))AP(0)$. □

### 4.5.4 Application to coherent transport in Bloch representation

Let $H$ be the periodic magnetic Hamiltonian defined in (4.1), $J$ the current operator whose components are defined in (4.6), $\mu_{\rm F}$ the Fermi level,

$$\mu := 1 + \min\sigma(H) \quad \text{and} \quad \eta = \max_{|e|\le|e_\alpha|,|e_\beta|} \|(J\cdot e)(H+\mu)^{-1}\|_{\mathcal{L}(L^2(\mathbb{R}^d;\mathbb{C}))} < \infty.$$

Let $k\in\mathbb{R}^d$. Assume that $\lambda_{N_k+1,k} - \lambda_{N_k,k} > 0$ and set

$$s_k = \inf\{s>0 \,|\, g_k(s)=0\} \quad \text{where} \quad g_k(s) := \min(1, \lambda_{N_k+1,k-se_\beta} - \lambda_{N_k,k-se_\beta}).$$

We consider the family of Hamiltonians

$$H(s) := H_{k-e_\beta s} + \mu. \tag{4.68}$$

We have

$$\dot H(s) = -\partial_\beta H_{k-se_\beta} = -((-i\nabla + k + \mathcal{A} - se_\beta)\cdot\varepsilon_\beta) = J_{\beta,k-se_\beta}, \tag{4.69}$$
$$\ddot H(s) = |e_\beta|^2 \mathrm{Id}_{L^2_{\rm per}}, \tag{4.70}$$

and so hypotheses H1-H3 of Proposition 4.5.1 are satisfied with $\mathcal{H}_{\rm f} = L^2_{\rm per}$, $D = H^2_{\rm per}$, $T = s_k$, $n$ arbitrarily large, $\alpha_1 \le \eta$, $\alpha_2 = |e_\beta|^2$, $\alpha_l = 0$ for $l\ge 3$, $a_-(s) = \min\sigma(H)+\mu$, $a_+(s) = \lambda_{N_k,k-se_\beta}+\mu$, $M = \max_{k'\in\mathcal{B}}\lambda_{N_{k'}+1,k'}+\mu$, $g(s) = g_k(s)$, and $\mathcal{N} = N_k$.

**Corollary 4.5.5.** *Let $k\in\mathbb{R}^d$ such that $\lambda_{N_k+1,k} - \lambda_{N_k,k} > 0$. Then, for all $\varepsilon>0$ and $t\in[0,\varepsilon^{-1}s_k)$, the operator $\partial_\alpha H_{k-\varepsilon e_\beta t}\gamma^\varepsilon_{\beta,k-\varepsilon e_\beta t}(t)$ is in $\mathfrak{S}_{1,\rm per}$, and we have*

$$\begin{aligned} \mathrm{Tr}(\partial_\alpha H_{k-\varepsilon e_\beta t}\widetilde{\mathcal{U}}^\varepsilon_{\beta,k}(t)\gamma_k(0)\widetilde{\mathcal{U}}^\varepsilon_{\beta,k}(t)^*) =& \partial_\alpha\left(\mathrm{Tr}\left(H_{k-\varepsilon e_\beta t}P_{N_k,k-\varepsilon e_\beta t}\right)\right) \\ &+ i\varepsilon\,\mathrm{Tr}\Big(\partial_\alpha H_{k-\varepsilon e_\beta t}L^+_{N_k,k-\varepsilon e_\beta t}\partial_\beta P_{N_k,k-\varepsilon e_\beta t}\Big) \\ &- i\varepsilon\,\mathrm{Tr}\Big(\partial_\alpha H_{k-\varepsilon e_\beta t}\widetilde{\mathcal{U}}^\varepsilon_{\beta,k}(t)\; L^+_{N_k,k}\partial_\beta P_{N_k,k}\,\widetilde{\mathcal{U}}^\varepsilon_{\beta,k}(t)^*\Big) \\ &+ \mathfrak{R}^\varepsilon_k(t), \end{aligned} \tag{4.71}$$

*where each term of the right-hand side is a well-defined real number and $L^+_{N,k}$ is a shorthand notation for the inverse Liouvillian $L^+_{H_k,[\lambda_{1,k},\lambda_{N,k}]}$. In addition, we have the following bounds*

$$|\mathrm{Tr}(\partial_\alpha H_{k-\varepsilon e_\beta t}\widetilde{\mathcal{U}}^\varepsilon_{\beta,k}(t)\gamma_k(0)\widetilde{\mathcal{U}}^\varepsilon_{\beta,k}(t)^*)| \leq Ce^{\eta\varepsilon t}, \tag{4.72}$$

$$|\partial_\alpha \left(\mathrm{Tr}\big(H_{k-\varepsilon e_\beta t}P_{N_k,k-\varepsilon e_\beta t}\big)\right)| \leq C,$$

$$|\varepsilon\,\mathrm{Tr}\Big(\partial_\alpha H_{k-\varepsilon e_\beta t}L^+_{N_k,k-\varepsilon e_\beta t}\partial_\beta P_{N_k,k-\varepsilon e_\beta t}\Big)| \leq C\frac{\varepsilon}{g_k(\varepsilon t)^4},$$

$$|\varepsilon\,\mathrm{Tr}\Big(\partial_\alpha H_{k-\varepsilon e_\beta t}\widetilde{\mathcal{U}}^\varepsilon_{\beta,k}(t)\ L^+_{N_k,k}\partial_\beta P_{N_k,k}\widetilde{\mathcal{U}}^\varepsilon_{\beta,k}(t)^*\Big)| \leq C\frac{\varepsilon e^{\eta\varepsilon t}}{g_k(0)^4}, \tag{4.73}$$

$$|\mathfrak{R}^\varepsilon_k(t)| \leq \frac{C\varepsilon^2 te^{\eta\varepsilon t}}{\min_{s\in[0,\varepsilon t]}\,g_k(s)^6}, \tag{4.74}$$

*for a constant $C\in\mathbb{R}_+$ independent of $k$, $\varepsilon$ and $t$.*

*Proof.* Applying the second assertion in Proposition 4.5.3, we get

$$\begin{aligned}\widetilde{\mathcal{U}}^\varepsilon_{\beta,k}(t)\gamma_k(0)\widetilde{\mathcal{U}}^\varepsilon_{\beta,k}(t)^* =& P_{N_k,k-\varepsilon e_\beta t} + i\varepsilon L^+_{N_k,k-\varepsilon e_\beta t}\partial_\beta P_{N_k,k-\varepsilon e_\beta t}\\ &- i\varepsilon\widetilde{\mathcal{U}}^\varepsilon_{\beta,k}(t)\ \left(L^+_{N_k,k}\partial_\beta P_{N_k,k}\right)\widetilde{\mathcal{U}}^\varepsilon_{\beta,k}(t)^* + R^\varepsilon_k(t),\end{aligned} \tag{4.75}$$

Each term $A$ in (4.75) being a finite-rank self-adjoint operator, it holds

$$\|\partial_\alpha H_{k-\varepsilon e_\beta t}A\|_{\mathfrak{S}_1} \leq \mathrm{Rank}(A)\|\partial_\alpha H_{k-\varepsilon e_\beta t}A\| \leq \eta\mathrm{Rank}(A)\|(H_{k-\varepsilon e_\beta t}+\mu)A\|,$$

and again by Proposition 4.5.3 we get

$$\begin{aligned}\mathrm{Tr}(\partial_\alpha H_{k-\varepsilon e_\beta t}\widetilde{\mathcal{U}}^\varepsilon_{\beta,k}(t)\gamma_k(0)\widetilde{\mathcal{U}}^\varepsilon_{\beta,k}(t)^*) = \mathrm{Tr}\big(\partial_\alpha H_{k-\varepsilon e_\beta t}P_{N_k,k-\varepsilon e_\beta t}\big)+i\varepsilon\,\mathrm{Tr}\Big(\partial_\alpha H_{k-\varepsilon e_\beta t}L^+_{N_k,k-\varepsilon e_\beta t}\partial_\beta P_{N_k,k-\varepsilon e_\beta t}\Big)\\ -i\varepsilon\,\mathrm{Tr}\Big(\partial_\alpha H_{k-\varepsilon e_\beta t}\widetilde{\mathcal{U}}^\varepsilon_{\beta,k}(t)\ \left(L^+_{N_k,k}\partial_\beta P_{N_k,k}\right)\widetilde{\mathcal{U}}^\varepsilon_{\beta,k}(t)^*\Big) + \mathrm{Tr}\left(\partial_\alpha H_{k-\varepsilon e_\beta t}R^\varepsilon_k(t)\right)\end{aligned}$$

with

$$R^\varepsilon_k(t) = i\varepsilon^2\int_0^t \widetilde{\mathcal{U}}^\varepsilon_{\beta,k}(t,t')\partial_{k_\beta}\left(L^+_{N_k,k-\varepsilon e_\beta t'}\partial_{k_\beta}P_{N_k,k-\varepsilon e_\beta t'}\right)\widetilde{\mathcal{U}}^\varepsilon_{\beta,k}(t,t')^*\,dt'. \tag{4.76}$$

It results from the Hellmann-Feynman formula that

$$\mathrm{Tr}\big(\partial_\alpha H_{k-\varepsilon e_\beta t}P_{N,k-\varepsilon e_\beta t}\big) = \partial_\alpha\left(\mathrm{Tr}\big(H_{k-\varepsilon e_\beta t}P_{N,k-\varepsilon e_\beta t}\big)\right).$$

Finally, using Propositions 4.5.1 and 4.5.3, we obtain the bounds (4.72)-(4.74). In particular,

$$\begin{aligned}|\mathfrak{R}^\varepsilon_k(t)| &= \left|\mathrm{Tr}\left(\partial_\alpha H_{k-\varepsilon e_\beta t}R^\varepsilon_k(t)\right)\right|\\ &\leq 4N_k\varepsilon^2\eta t\sup_{t'\in[0,t)}\left(e^{\eta\varepsilon(t-t')}\left\|H_{k-\varepsilon e_\beta t'}\partial_{k_\beta}\left(L^+_{N_k,k-\varepsilon e_\beta t'}\partial_{k_\beta}P_{N_k,k-\varepsilon e_\beta t'}\right)\right\|\right)\\ &\leq C\frac{\eta\varepsilon^2 te^{\eta\varepsilon t}}{\inf_{s\in[0,\varepsilon t)}\,g_k(s)^6},\end{aligned}$$

where $C\in\mathbb{R}_+$ is independent of $k$, $\varepsilon$ and $t$. □

*Remark* 4.5.6. The decomposition (4.71) will be key to computing the current in insulators, non-degenerate metals and semimetals. The first three terms in the right-hand side of (4.71) have different physical meanings. The first term is the adiabatic term: electrons simply are transported adiabatically across the Brillouin zone. This term will be responsible for the ballistic transport of electrons in metals. The second is the first-order static response, and will be the cause of the Hall conductivity in insulators. The third is oscillatory, and is related to the AC response of solids (not treated here). This decomposition only makes sense for a non-zero gap; in particular, it cannot be used to compute the contribution to the current for $k$ points close to Dirac points for semimetals.

### 4.5.5 Linear response

We now aim at obtaining an expansion of the current to first order in $\varepsilon$ for a given $t$, based on a Dyson expansion instead of the adiabatic theorem. In contrast to the previous result, this gives a remainder that does not depend on a gap, and will therefore be useful for the study of semimetals near Dirac points.

**Proposition 4.5.7.** *Let $H$ be the periodic magnetic Hamiltonian defined in (4.1). Under the additional assumptions that $V \in H^1_{\rm per}$ and $\mathcal{A} \in (H^2_{\rm per})^d$, there exists a constant $C \in \mathbb{R}_+$ such that for all $k \in \mathbb{R}^d$ such that $\lambda_{N_k+1,k} - \lambda_{N_k,k} > 0$, we have for all $\varepsilon, t \in \mathbb{R}_+$,*

$$\begin{aligned}\mathrm{Tr}\left(\partial_\alpha H_{k-\varepsilon e_\beta t}\widetilde{\mathcal{U}}^\varepsilon_{\beta,k}(t)\,\gamma_k(0)\,\widetilde{\mathcal{U}}^\varepsilon_{\beta,k}(t)^*\right) =&\partial_\alpha \mathrm{Tr}\left(H_k\gamma_k(0)\right) - \varepsilon t\partial_\alpha\partial_\beta\left(\mathrm{Tr}(H_k\gamma_k(0))\right)\\ &+ i\varepsilon\,\mathrm{Tr}\big(\partial_\alpha H_k(e^{-itL_k}-1)L_k^+\partial_\beta\gamma_k(0)\big) + \rho^\varepsilon_k(t), \qquad (4.77)\end{aligned}$$

*with, when $\varepsilon t \le 1$,*

$$|\rho^\varepsilon_k(t)| \le C\varepsilon^2 t^3(1+t^3). \qquad (4.78)$$

*Proof.* Let $k$ be such that $\lambda_{N_k+1,k} - \lambda_{N_k,k} > 0$. Since $k' \mapsto \mathrm{Tr}\left(H_{k'}\gamma_{k'}(0)\right)$ is real-analytic in a neighborhood of $k$, we have by Hellmann-Feynman theorem

$$\partial_\alpha \mathrm{Tr}\left(H_k\gamma_k(0)\right) = \mathrm{Tr}\left(\partial_\alpha H_k\gamma_k(0)\right) \quad \text{and} \quad \partial_\alpha\partial_\beta \mathrm{Tr}\left(H_k\gamma_k(0)\right) = \mathrm{Tr}\left(\partial_\alpha\partial_\beta H_k\gamma_k(0)\right) + \mathrm{Tr}\left(\partial_\alpha H_k\partial_\beta\gamma_k(0)\right).$$

We also have $\partial_\alpha H_{k-\varepsilon e_\beta t} = \partial_\alpha H_k - \varepsilon t e_\alpha \cdot e_\beta$. It follows that

$$\begin{aligned}\rho^\varepsilon_k(t) =&\mathrm{Tr}\left(\partial_\alpha H_k\widetilde{\mathcal{U}}^\varepsilon_{\beta,k}(t)\,\gamma_k(0)\,\widetilde{\mathcal{U}}^\varepsilon_{\beta,k}(t)^*\right) - \mathrm{Tr}\left(\partial_\alpha H_k\gamma_k(0)\right) + \varepsilon t\mathrm{Tr}\left(\partial_\alpha H_k\partial_\beta\gamma_k(0)\right)\\ &- i\varepsilon\,\mathrm{Tr}\big(\partial_\alpha H_k(e^{-itL_k}-1)L_k^+\partial_\beta\gamma_k(0)\big).\end{aligned}$$

We now expand the first term in the right hand side of this equation. We set $\mu := 1 + \min\sigma(H)$,

$$H(s) := H_{k-se_\beta} + \mu, \quad A = \partial_\alpha H_k, \quad I_0 = [0, \frac{1}{2}(\lambda_{N_k,k} + \lambda_{N_k+1,k}) + \mu], \quad P(s) = \mathbb{1}_{I_0}(H(s)).$$

It holds

$$H(s) = h_0 + sh_1 + \frac{s^2|e_\beta|^2}{2}$$

with $h_0 = H_k + \mu$ and $h_1 = J_{\beta,k} = -\partial_\beta H_k$. The operators $h_0$, $h_1$ and $A$ are self-adjoint on $L^2_{\rm per}$ and we have $h_0 \ge 1$ and $h_1 h_0^{-1/2}$ and $Ah_0^{-1/2}$ bounded. Besides, $P(s) = \gamma_{k-se_\beta}(0)$, so that $\dot P(0) = -\partial_\beta\gamma_k(0)$. Let $(U^\varepsilon(t,t'))_{t,t'\in\mathbb{R}}$ be the propagator associated with the family $(H(\varepsilon t))_{t\in\mathbb{R}}$ and $U^\varepsilon(t) := U^\varepsilon(t,0)$. We have $U^\varepsilon(t,t') = e^{-i\mu(t-t')}\mathcal{U}^\varepsilon_k(t,t')$ and $U^\varepsilon(t) = e^{-i\mu t}\mathcal{U}^\varepsilon_k(t)$. With these notations, we have

$$\rho^\varepsilon_k(t) = \mathrm{Tr}\left(AU^\varepsilon(t)\,P(0)U^\varepsilon(t)^*\right) - \mathrm{Tr}\left(AP(0)\right) - \varepsilon t\mathrm{Tr}\left(A\dot P(0)\right) + i\varepsilon\,\mathrm{Tr}\Big(A(e^{-itL_0}-1)L_0^+\dot P(0)\Big),$$

where $L_0 = L_{h_0,I_0}$ and $L_0^+ = L^+_{h_0,I_0}$, and we focus on expanding the operator $U^\varepsilon(t)\,P(0)U^\varepsilon(t)^*$ close to $t = 0$.

**Lemma 4.5.8.** *We have*

$$U^\varepsilon(t)\,P(0)U^\varepsilon(t)^* = P(0) + \varepsilon\left(t\dot P(0) - i\left(e^{-itL_0}-1\right)\left(L_0^+\dot P(0)\right)\right) + \Pi^\varepsilon_2(t) \qquad (4.79)$$

*with $\rho^\varepsilon_k(t) = \mathrm{Tr}\left(A\Pi^\varepsilon_2(t)\right)$. Moreover, we have the bound (4.78)*

$$|\rho^\varepsilon_k(t)| \le C\varepsilon^2 t^3(1+t^3).$$

Lemma 4.5.8 closes the proof of Proposition 4.5.7. □

*Proof of Lemma 4.5.8.* We deduce from the Dyson expansion that

$$U^\varepsilon(t) = U^0(t) + V^\varepsilon(t) + W^\varepsilon(t),$$

where $U^0(t) = e^{-ith_0}$ and

$$V^\varepsilon(t) = -i\varepsilon \int_0^t U^0(t-t')t'h_1U^0(t')\,dt',$$
$$W^\varepsilon(t) = \varepsilon^2 \left( -i\frac{t^3}{6}U^0(t) + \int_0^t \left( \int_0^{t'} U^\varepsilon(t,t')t'(h_1+\varepsilon t'/2)U^0(t'-t'')t''(h_1+\varepsilon t''/2)U^0(t'')\,dt'' \right) dt' \right).$$

This induces $U^\varepsilon(t)\,P(0)U^\varepsilon(t)^* = P(0) + \Pi_1^\varepsilon(t) + \Pi_2^\varepsilon(t)$ where

$$\Pi_1^\varepsilon(t) = V^\varepsilon(t)P(0)U^0(t)^* + \text{h.c.} = -i\varepsilon \int_0^t t'U^0(t-t')[h_1, P(0)]U^0(t-t')^*\,dt',$$
$$\Pi_2^\varepsilon(t) = V^\varepsilon(t)P(0)V^\varepsilon(t)^* + \big(W^\varepsilon(t)P(0)(U^0(t)+V^\varepsilon(t))^* + \text{h.c.}\big) + W^\varepsilon(t)P(0)W^\varepsilon(t)^*.$$

We first analyze $\Pi_1^\varepsilon(t)$ by computing

$$\begin{aligned} U^0(t-t')[h_1, P(0)]U^0(t-t')^* &= -e^{-i(t-t')L_0}L_0\dot{P}(0) \\ &= i\frac{d}{dt'}e^{-i(t-t')L_0}\dot{P}(0) \\ &= \frac{d^2}{dt'^2}e^{-i(t-t')L_0}L_0^+\dot{P}(0), \end{aligned}$$

where we have used $\dot{P}(0) = L_0^+[P_0, h_1]$ and $\dot{P}(0) = L_0^+L_0$. Using integration by parts, we obtain

$$\Pi_1^\varepsilon(t) = \varepsilon\left(t\dot{P}(0) - i\left(e^{-itL_0} - 1\right)(L_0^+\dot{P}(0))\right)$$

and (4.79) follows.

We now work on the bound (4.78). For that purpose, we introduce the following quantities, which are independent of $k, \varepsilon$ and $t$:

$$\begin{aligned} \nu_0 &= \max_{|e|\le|e_\alpha|,|e_\beta|} \|(J\cdot e)(H+\mu)^{-1/2}\|_{\mathcal{L}(L^2(\mathbb{R}^d;\mathbb{C}))}, \\ \nu_1 &= \max_{|e|\le|e_\alpha|,|e_\beta|} \|(H+\mu)^{1/2}(J\cdot e)(H+\mu)^{-1}\|_{\mathcal{L}(L^2(\mathbb{R}^d;\mathbb{C}))}, \\ \nu_2 &= \max_{|e|\le|e_\alpha|,|e_\beta|} \|(H+\mu)(J\cdot e)(H+\mu)^{-2}\|_{\mathcal{L}(L^2(\mathbb{R}^d;\mathbb{C}))}, \\ \lambda &= \max_{k\in\mathbb{R}^d,|k-k'|\le|e_\beta|} \|(H_k+\mu)^{1/2}(H_{k'}+\mu)^{-1/2}\|_{\mathcal{L}(L^2_{\text{per}})}. \end{aligned}$$

Note that the assumptions $\mathcal{A} \in (L^4_{\text{per}})^d$, $\nabla\cdot\mathcal{A} = 0$, and $V \in L^2_{\text{per}}$ are sufficient to ensure that the quantities $\nu_0$, $\nu_1$ and $\lambda$ are finite. Besides, since $\|h_0h_1h_0^{-2}\| \le \|(H+\mu)J_\beta(H+\mu)^{-2}\|$ and

$$(H+\mu)J_\beta(H+\mu)^{-2} = J_\beta(H+\mu)^{-1} - 2i\sum_{\alpha=1}^d(\partial_\alpha\mathcal{A}_\beta - \partial_\beta\mathcal{A}_\alpha)J_\alpha(H+\mu)^{-2} - (\Delta\mathcal{A}_\beta)(H+\mu)^{-2} + i\partial_\beta V(H+\mu)^{-2},$$

we deduce from the assumptions $\mathcal{A} \in (H^2_{\text{per}})^d$ and $V \in H^1_{\text{per}}$ that $\|(H+\mu)J_\beta(H+\mu)^{-2}\| < \infty$, hence that $\nu_2 < \infty$.

We now aim at controlling $\rho_k(t)$ thanks to $\nu_0$, $\nu_1$, $\nu_2$ and $\lambda$. Using the relations $P(0) = P(0)^2$ and $P(0) = h_0^{-m} h_0^m P(0)$ with

$$\|h_0^m P(0)\| \leq (\mu_{\rm F} + \mu)^m, \quad \|h_0^{-1}\| \leq \|h_0^{-1/2}\| \leq 1 \quad \text{and} \quad \mathrm{Rank}(P(0)) = N_k \leq \overline{N} := \max_{k'} N_{k'},$$

we deduce

$$\begin{aligned}
|\rho_k^\varepsilon(t)| &\leq \overline{N}\Big( (\mu_{\rm F}+\mu)^2 \|AV^\varepsilon(t)h_0^{-1}\| \, \|V^\varepsilon(t)h_0^{-1}\| + 2(\mu_{\rm F}+\mu)^3 \|AW^\varepsilon(t)h_0^{-2}\| \, (\|h_0^{-1}\| + \|V^\varepsilon(t)h_0^{-1}\|) \\
&\qquad + (\mu_{\rm F}+\mu)^3 \|AW^\varepsilon(t)h_0^{-2}\| \|W^\varepsilon(t)h_0^{-1}\| \Big) \\
&\leq \overline{N}\nu_0 \Big( (\mu_{\rm F}+\mu)^2 \|h_0^{1/2} V^\varepsilon(t) h_0^{-1}\|^2 + (\mu_{\rm F}+\mu)^3 \|h_0^{1/2} W^\varepsilon(t) h_0^{-2}\| \, \big(2 + 2\|V^\varepsilon(t)h_0^{-1}\| \\
&\qquad + \|W^\varepsilon(t)h_0^{-1}\|\big) \Big).
\end{aligned}$$

Next, we get

$$\begin{aligned}
\|V^\varepsilon(t)h_0^{-1}\| &\leq \frac{\varepsilon t^2}{2}\|h_1 h_0^{-1}\| \leq \frac{\varepsilon t^2}{2}\nu_0, \quad \|h_0^{1/2}V^\varepsilon(t)h_0^{-1}\| \leq \frac{\varepsilon t^2}{2}\nu_1, \\
\|W^\varepsilon(t)h_0^{-1}\| &\leq \varepsilon^2 t^3 \left( \frac{1}{6} + \nu_0\nu_1 \frac{t}{8} + (\varepsilon t) t \left( \frac{\nu_0}{30} + \frac{\nu_1}{20} \right) + (\varepsilon t)^2 t \frac{1}{72} \right), \\
\|h_0^{1/2} W^\varepsilon(t) h_0^{-2}\| &\leq \varepsilon^2 t^3 \lambda e^{\eta\varepsilon t/2} \left( \frac{1}{6} + \nu_1\nu_2 \frac{t}{8} + (\varepsilon t) t \left( \frac{\nu_1}{30} + \frac{\nu_2}{20} \right) + (\varepsilon t)^2 t \frac{1}{72} \right).
\end{aligned}$$

It follows that there exists a constant $C$ depending only on $V$, $\mathcal{A}$ and $\mu_{\rm F}$, such that

$$|\rho_k^\varepsilon(t)| \leq C\varepsilon^2 t^3 \left( t + e^{\eta\varepsilon t/2} \left( 1 + t(1 + (\varepsilon t)^2) + (\varepsilon t) t^2 (1 + (\varepsilon t)^3) + (\varepsilon t)^4 t^3 (1 + (\varepsilon t)^2) \right) \right),$$

which leads to (4.78) when $\varepsilon t \leq 1$. □

## 4.6 Insulators

In this section and the following ones, we use the notation $O(f(\varepsilon, t, t', \delta))$ to denote a term that is bounded in absolute value by $Cf(\varepsilon, t, t', \delta)$, where $C$ is a constant that can depend on the system under consideration (through $\mathcal{A}$, $V$, $\mu_{\rm F}$, $e_\alpha$ and $e_\beta$), but not on the parameters $\varepsilon, t, t', \delta$. We also denote $\gamma_k^0$ for $\gamma_k(0)$.

We now prove Theorem 4.2.7. For insulators, $N_k = N_{\rm ins}$ for all $k$, and $\lambda_{N_k+1,k} - \lambda_{N_k,k}$, hence $g_k(s)$, is uniformly bounded away from zero. We use the notation $L_k^+$ for $L_{N_{\rm ins},k}^+$. We apply Corollary 4.5.5 and obtain by integrating over the Brillouin zone

$$\begin{aligned}
j_{\alpha,\beta}^\varepsilon(t) =& -(2\pi)^{-d} \int_{\mathcal{B}} \partial_\alpha \left( \mathrm{Tr}\Big( H_{k-\varepsilon e_\beta t} \gamma^0_{k-\varepsilon e_\beta t} \Big) \right) dk - i\varepsilon (2\pi)^{-d} \int_{\mathcal{B}} \mathrm{Tr}\Big( \partial_\alpha H_{k-\varepsilon e_\beta t} L^+_{k-e_\beta t} \partial_\beta \gamma^0_{k-\varepsilon e_\beta t} \Big) dk \\
&+ i\varepsilon (2\pi)^{-d} \int_{\mathcal{B}} \mathrm{Tr}\Big( \partial_\alpha H_{k-\varepsilon e_\beta t} \, \widetilde{\mathcal{U}}^\varepsilon_{\beta,k}(t) \, (L_k^+ \partial_\beta \gamma_k^0) \, \widetilde{\mathcal{U}}^\varepsilon_{\beta,k}(t)^* \Big) dk + O\left( \varepsilon^2 t e^{\eta\varepsilon t} \right).
\end{aligned}$$

As mentioned in Remark 4.5.6, these three terms are adiabatic, static and oscillatory respectively.

- The first term of the right-hand side vanishes for all $t$, as the integral of the derivative of the smooth periodic function $k \mapsto \mathrm{Tr}(H_k \gamma_k^0)$ on a unit cell.

- The second term is dealt with using the relation

$$L_k^+((\partial_\alpha H_k)^{\mathrm{OD}}) = [\gamma_k^0\ ,\ \partial_\alpha \gamma_k^0],$$

where $(\partial_\alpha H_k)^{\mathrm{OD}} = \gamma_k^0(\partial_\alpha H_k)(1-\gamma_k^0) + (1-\gamma_k^0)(\partial_\alpha H_k)\gamma_k^0$. By periodicity, we have

$$\int_{\mathcal{B}} \mathrm{Tr}\left(\partial_\alpha H_{k-\varepsilon e_\beta t} L^+_{k-\varepsilon e_\beta t} \partial_\beta \gamma^0_{k-\varepsilon e_\beta t}\right) dk = \int_{\mathcal{B}} \mathrm{Tr}\left(\partial_\alpha H_k L_k^+ \partial_\beta \gamma_k^0\right) dk,$$

and we observe that

$$\begin{aligned}\mathrm{Tr}\left(\partial_\alpha H_k L_k^+ \partial_\beta \gamma_k^0\right) &= \mathrm{Tr}\left((\partial_\alpha H_k)^{\mathrm{OD}} L_k^+ \partial_\beta \gamma_k^0\right) \\ &= \mathrm{Tr}\left(L_k^+((\partial_\alpha H_k)^{\mathrm{OD}})\partial_\beta \gamma_k^0\right) = \mathrm{Tr}\left([\gamma_k^0, \partial_\alpha \gamma_k^0]\partial_\beta \gamma_k^0\right), \end{aligned} \tag{4.80}$$

so that

$$\int_{\mathcal{B}} \mathrm{Tr}\left(\partial_\alpha H_{k-\varepsilon e_\beta t} L^+_{k-\varepsilon e_\beta t} \partial_\beta \gamma^0_{k-\varepsilon e_\beta t}\right) dk = \int_{\mathcal{B}} \mathrm{Tr}\left(\gamma_k^0[\partial_\alpha \gamma_k^0, \partial_\beta \gamma_k^0]\right) dk.$$

- We now focus on the time-average of the oscillating term

$$\omega^\varepsilon(t) := \frac{1}{t}\int_0^t dt' \int_{\mathcal{B}} \mathrm{Tr}\Big(\partial_\alpha H_{k-\varepsilon e_\beta t'}\, \widetilde{\mathcal{U}}^\varepsilon_{\beta,k}(t')\ (iL_k^+\partial_\beta\gamma_k^0)\, \widetilde{\mathcal{U}}^\varepsilon_{\beta,k}(t')^*\Big)\, dk.$$

In order to bound this term, we apply Lemma 4.5.4 to $A = iL_k^+\partial_\beta\gamma_k^0$, which is a self-adjoint off-diagonal operator for the decomposition $L^2_{\mathrm{per}} = \mathrm{Ran}(\gamma_k^0)\oplus\mathrm{Ker}(\gamma_k^0)$. We thus get

$$\widetilde{\mathcal{U}}^\varepsilon_{\beta,k}(t)\left(iL_k^+\partial_\beta\gamma_k^0\right)\widetilde{\mathcal{U}}^\varepsilon_{\beta,k}(t)^* = \frac{d}{dt}\left(iL^+_{k-\varepsilon e_\beta t}\Big(\widetilde{\mathcal{U}}^\varepsilon_{\beta,k}(t)(iL_k^+\partial_\beta\gamma_k^0)\widetilde{\mathcal{U}}^\varepsilon_{\beta,k}(t)^*\Big)\right) + \widetilde{R}^\varepsilon_k(t),$$

where

$$\begin{aligned}\widetilde{R}^\varepsilon_k(t) = {}& 2\widetilde{\mathcal{U}}^\varepsilon_{\beta,k}(t) r^\varepsilon_k(t)(iL_k^+\partial_\beta\gamma_k^0) r^\varepsilon_k(t)\widetilde{\mathcal{U}}^\varepsilon_{\beta,k}(t)^* - \Big(\widetilde{\mathcal{U}}^\varepsilon_{\beta,k}(t)(1-2\gamma_k^0)(iL_k^+\partial_\beta\gamma_k^0) r^\varepsilon_k(t)\widetilde{\mathcal{U}}^\varepsilon_{\beta,k}(t)^* + \mathrm{h.c.}\Big) \\ & - \varepsilon i\partial_\beta L^+_{k-\varepsilon t e_\beta}\widetilde{\mathcal{U}}^\varepsilon_{\beta,k}(t)(iL_k^+\partial_\beta\gamma_k^0)\widetilde{\mathcal{U}}^\varepsilon_{\beta,k}(t))^*\end{aligned}$$

and

$$r^\varepsilon_k(t) = i\varepsilon\widetilde{\mathcal{U}}^\varepsilon_{\beta,k}(t)^*\left(L^+_{k-\varepsilon t e_\beta}\partial_\beta\gamma^0_{k-\varepsilon t e_\beta}\right)\widetilde{\mathcal{U}}^\varepsilon_{\beta,k}(t) - i\varepsilon L_k^+\partial_\beta\gamma_k^0 + \widetilde{\mathcal{U}}^\varepsilon_{\beta,k}(t)^* R^\varepsilon_k(t)\widetilde{\mathcal{U}}^\varepsilon_{\beta,k}(t),$$

where $R^\varepsilon_k(t)$ is defined in (4.76). Therefore,

$$\begin{aligned}&\mathrm{Tr}\Big(\partial_\alpha H_{k-\varepsilon e_\beta t}\widetilde{\mathcal{U}}^\varepsilon_{\beta,k}(t)\ (iL_k^+\partial_\beta\gamma_k^0)\,\widetilde{\mathcal{U}}^\varepsilon_{\beta,k}(t)^*\Big) \\ &\quad = \mathrm{Tr}\left(\partial_\alpha H_{k-\varepsilon e_\beta t}\frac{d}{dt}\left(\widetilde{\mathcal{U}}^\varepsilon_{\beta,k}(t)\ (iL_k^+\partial_\beta\gamma_k^0)\,\widetilde{\mathcal{U}}^\varepsilon_{\beta,k}(t)^*\right)\right) + \mathrm{Tr}\left(\partial_\alpha H_{k-\varepsilon e_\beta t}\widetilde{R}^\varepsilon_k(t)\right) \\ &\quad = \frac{d}{dt}\,\mathrm{Tr}\left(\partial_\alpha H_{k-\varepsilon e_\beta t}\left(\widetilde{\mathcal{U}}^\varepsilon_{\beta,k}(t)\ (iL_k^+\partial_\beta\gamma_k^0)\,\widetilde{\mathcal{U}}^\varepsilon_{\beta,k}(t)^*\right)\right) + \mathrm{Tr}\left(\partial_\alpha H_{k-\varepsilon e_\beta t}\widetilde{R}^\varepsilon_k(t)\right)\end{aligned}$$

since

$$\begin{aligned}\mathrm{Tr}\left(\frac{d}{dt}(\partial_\alpha H_{k-\varepsilon e_\beta t})\,\widetilde{\mathcal{U}}^\varepsilon_{\beta,k}(t)\ (iL_k^+\partial_\beta\gamma_k^0)\,\widetilde{\mathcal{U}}^\varepsilon_{\beta,k}(t)^*\right) &= -\varepsilon\,\mathrm{Tr}\left(\partial_{k_\alpha k_\beta} H_{k-\varepsilon e_\beta t}\widetilde{\mathcal{U}}^\varepsilon_{\beta,k}(t)\ (iL_k^+\partial_\beta\gamma_k^0)\,\widetilde{\mathcal{U}}^\varepsilon_{\beta,k}(t)^*\right) \\ &= -\varepsilon e_\alpha\cdot e_\beta\,\mathrm{Tr}\left(\widetilde{\mathcal{U}}^\varepsilon_{\beta,k}(t)\ (iL_k^+\partial_\beta\gamma_k^0)\,\widetilde{\mathcal{U}}^\varepsilon_{\beta,k}(t)^*\right) \\ &= -\varepsilon e_\alpha\cdot e_\beta\,\mathrm{Tr}\left(iL_k^+\partial_\beta\gamma_k^0\right) = 0,\end{aligned}$$

where we have used the fact that $\partial_{k_\alpha k_\beta} H_k = -e_\alpha \cdot e_\beta$ and the off-diagonal character of $iL_k^+ \partial_\beta \gamma_k^0$. Hence, using the bounds from Proposition 4.5.1, we obtain

$$\begin{aligned}\omega^\varepsilon(t) &= \frac{1}{t}\int_{\mathcal{B}} \mathrm{Tr}\left(\partial_\alpha H_{k-\varepsilon e_\beta t}\left(\widetilde{\mathcal{U}}^\varepsilon_{\beta,k}(t)\ (iL_k^+\partial_\beta\gamma_k^0)\widetilde{\mathcal{U}}^\varepsilon_{\beta,k}(t)^*\right)\right) dk + \frac{1}{t}\int_0^t dt' \int_{\mathcal{B}} \mathrm{Tr}\left(\partial_\alpha H_{k-\varepsilon e_\beta t'}\widetilde{R}^\varepsilon_k(t')\right) dk \\ &= O\left(\left(\frac{1}{t}+\varepsilon\right)e^{\eta\varepsilon t}\right).\end{aligned}$$

The result follows.

## 4.7 Metals

We prove the two assertions of Theorem 4.2.8 in sequence.

### 4.7.1 Linear response

We prove the first assertion of Theorem 4.2.8: We first note that, for $\varepsilon > 0$ small enough and $t \le \frac{1}{\varepsilon}\varepsilon^\theta$, the function $k \mapsto \lambda_{N_k+1,k-\varepsilon e_\beta t} - \lambda_{N_k,k-\varepsilon e_\beta t}$ is bounded away from zero, and therefore so is $g_k(\varepsilon t)$. We can therefore apply Corollary 4.5.5 on each $B_N$ to obtain

$$\begin{aligned} j^\varepsilon_{\alpha,\beta}(t) = (2\pi)^{-d}\sum_{N\in\mathbb{N}}\Bigg(&-\int_{B_N}\mathrm{Tr}\big(\partial_\alpha H_{k-\varepsilon e_\beta t}P_{N,k-\varepsilon e_\beta t}\big)dk \\ &-i\varepsilon\int_{B_N}\mathrm{Tr}\Big(\partial_\alpha H_{k-\varepsilon e_\beta t}L^+_{k-\varepsilon e_\beta t}\partial_\beta P_{N,k-\varepsilon e_\beta t}\Big)dk \\ &+i\varepsilon\int_{B_N}\mathrm{Tr}\Big(\partial_\alpha H_{k-\varepsilon e_\beta t}\widetilde{\mathcal{U}}^\varepsilon_{\beta,k}(t)\ L_k^+\partial_\beta P_{N,k}\widetilde{\mathcal{U}}^\varepsilon_{\beta,k}(t)^*\Big)dk\Bigg) \\ &+O\left(\varepsilon^2 t e^{\eta\varepsilon t}\right)\end{aligned} \tag{4.81}$$

and so

$$j^\varepsilon_{\alpha,\beta}(t) = -(2\pi)^{-d}\sum_{N\in\mathbb{N}}\int_{B_N}\mathrm{Tr}\big(\partial_\alpha H_{k-\varepsilon e_\beta t}P_{N,k-\varepsilon e_\beta t}\big)dk + O(\varepsilon^{(1+\theta)}\exp\left(\eta\varepsilon^\theta\right)) \tag{4.82}$$

when $t \le \frac{1}{\varepsilon}\varepsilon^\theta$. In contrast to the case of insulators however, the adiabatic term

$$-(2\pi)^{-d}\sum_{N\in\mathbb{N}}\int_{\mathcal{B}_N}\partial_\alpha\,\mathrm{Tr}\big(H_{k-\varepsilon e_\beta t}P_{N,k-\varepsilon e_\beta t}\big)dk = \varepsilon t(2\pi)^{-d}\sum_{N\in\mathbb{N}}\int_{\mathcal{B}_N}\partial_\alpha\partial_\beta\left(\mathrm{Tr}(H_kP_{N,k})\right)dk + O(\varepsilon^2t^2)$$

has a non-zero first-order contribution (the zeroth-order term vanishes by (4.43)). The proportionality factor is computed by the Stokes formula as

$$\begin{aligned}\sum_{N\in\mathbb{N}^*}\int_{B_N}\partial_\alpha\partial_\beta\,\mathrm{Tr}\big(H_k\gamma_k^0\big)dk &= \sum_{N\in\mathbb{N}^*}\int_{B_N}\partial_\alpha\partial_\beta\sum_{n=1}^N\lambda_{n,k} = \sum_{N\in\mathbb{N}^*}\left(\int_{\mathcal{S}_N}-\int_{\mathcal{S}_{N-1}}\right)\partial_\alpha\sum_{n=1}^N\lambda_{n,k}(ds\cdot e_\beta) \\ &= \sum_{N\in\mathbb{N}^*}\int_{\mathcal{S}_N}\partial_\alpha\lambda_{N,k}(ds\cdot e_\beta) = (2\pi)^dD_{\alpha,\beta}\end{aligned} \tag{4.83}$$

and the result follows.

### 4.7.2 Bloch oscillations

Under the assumptions of the second assertion, $N_k$ is either $N_{\rm met}$ or $N_{\rm met}-1$, and in both cases

$$\lambda_{N_k+1,k-\varepsilon e_\beta t} - \lambda_{N_k,k-\varepsilon e_\beta t}$$

is bounded away from zero uniformly in $k$,$t$. We can therefore apply Corollary 4.5.5 and obtain

$$j^\varepsilon_{\alpha,\beta}(t) = -(2\pi)^{-d} \sum_{N\in\mathbb{N}} \int_{B_N} \big(\partial_\alpha \operatorname{Tr}\big(H_{k-\varepsilon e_\beta t} P_{N_k,k-\varepsilon e_\beta t}\big)\big)\, dk + O((\varepsilon+\varepsilon^2 t)\mathrm{e}^{\eta\varepsilon t}).$$

From the decomposition

$$P_{N_k,k-\varepsilon e_\beta t} = P_{N_{\rm met}-1,k-\varepsilon e_\beta t} + \mathbb{1}(\lambda_{N_{\rm met},k} \le \mu_{\rm F}) |u_{N_{\rm met},k-\varepsilon e_\beta t}\rangle\langle u_{N_{\rm met},k-\varepsilon e_\beta t}|$$

and since $k \mapsto P_{N_{\rm met}-1,k-\varepsilon e_\beta t}$ is smooth and $\mathcal{R}^*$-periodic, we have

$$\begin{aligned} j^\varepsilon_{\alpha,\beta}(t) &= -(2\pi)^{-d} \int_{\mathcal{B}} \mathbb{1}(\lambda_{N_{\rm met},k} \le \mu_{\rm F}) \langle u_{N_{\rm met},k-\varepsilon e_\beta t} | \partial_\alpha H_{k-\varepsilon e_\beta t} | u_{N_{\rm met},k-\varepsilon e_\beta t}\rangle dk + O((\varepsilon+\varepsilon^2 t)\mathrm{e}^{\eta\varepsilon t}) \\ &= -(2\pi)^{-d} \int_{\mathcal{B}} \mathbb{1}(\lambda_{N_{\rm met},k} \le \mu_{\rm F}) \partial_\alpha \lambda_{N_{\rm met},k-\varepsilon e_\beta t} dk + O((\varepsilon+\varepsilon^2 t)\mathrm{e}^{\eta\varepsilon t}), \end{aligned}$$

which concludes the proof.

## 4.8 Semi-metals

We prove here Theorem 4.2.10. We decompose the integral defining $j^\varepsilon_{\alpha,\beta}(t)$ into several parts depending whether one integrates far from the Dirac points or not.

We introduce a small parameter $\delta > 0$ controlling the size of the neighborhood of the Dirac points, which is independent of $t, \varepsilon$. We decompose $\mathcal{B}$ as the disjoint union

$$\mathcal{B} = \mathcal{B}^\delta_{\rm out} \cup (\cup_{i\in\mathcal{I}} \mathcal{B}^\delta_i)$$

with

$$\mathcal{B}^\delta_i = B(k_i, \delta),$$

where $\delta > 0$ is small enough so that

$$\mathcal{B}^\delta_{\rm out} \subset \{k \in \mathcal{B},\ \lambda_{N_{\rm sm},k} \le \mu_F - c\delta\}$$

for some constant $c > 0$. Note that this decomposition is time-reversal symmetric in the sense that

$$-\mathcal{B}^\delta_{\rm out} = \mathcal{B}^\delta_{\rm out} \quad \text{and} \quad -(\cup_{i\in\mathcal{I}} \mathcal{B}^\delta_i) = (\cup_{i\in\mathcal{I}} \mathcal{B}^\delta_i).$$

We work in the regime $\varepsilon t \ll \delta \ll 1$, $\varepsilon \ll \delta \ll 1$.

In the following analysis, we first treat the regions $\mathcal{B}^\delta_{\rm out}$, where we will use adiabatic theory with a non-zero gap larger than a constant times $\delta$. In the sets $\mathcal{B}^\delta_i$, where the gap closes, we study the structure of the Taylor expansion of the Hamiltonian $H_k$ close to the Dirac points and construct two-band reduced Hamiltonians $H^R_{i,k}$. Then, we use the linear response Proposition 4.5.7, reducing successively from the Hamiltonian $H$ to the reduced Hamiltonian $H^R_{i,k}$, and finally to the Dirac Hamiltonian

$$H^D_k = \begin{pmatrix} 0 & k_1 - ik_2 \\ k_1 + ik_2 & 0 \end{pmatrix}$$

for which we can explicitly compute the current. Adding the contributions, we will obtain

$$\sigma_{\alpha,\beta} := \lim_{t\to\infty} \lim_{\varepsilon\to 0} \frac{1}{\varepsilon t} \int_0^t j^\varepsilon_{\alpha,\beta}(t')dt' = \frac{|\mathcal{I}|}{16} e_\alpha \cdot e_\beta + O(\delta)$$

Finally, we will pass to the limit $\delta \to 0$.

### 4.8.1 Far from the Dirac points

We set

$$j^{\varepsilon,\mathrm{out}}_{\alpha,\beta}(t') := -\frac{1}{4\pi^2}\int_{\mathcal{B}^\delta_{\mathrm{out}}} \mathrm{Tr}\left(\partial_\alpha H_k \widetilde{\mathcal{U}}^\varepsilon_{\beta,k}(t')\,\gamma^0_k\,\widetilde{\mathcal{U}}^\varepsilon_{\beta,k}(t')^*\right)\,dk.$$

Let $k \in \mathcal{B}^\delta_{\mathrm{out}}$. In the regime we consider, $\gamma^0_{k-\varepsilon e_\beta t} = P_{N_{\mathrm{sm}},k-\varepsilon e_\beta t}$ is gapped with a gap larger than a constant times $\delta$. Applying the analysis of the previous sections, we obtain that

$$\begin{aligned}-\mathrm{Tr}\left(\partial_\alpha H_k \widetilde{\mathcal{U}}^\varepsilon_{\beta,k}(t)\,\gamma^0_k\,\widetilde{\mathcal{U}}^\varepsilon_{\beta,k}(t)^*\right)&\\ = -\partial_\alpha\left(\mathrm{Tr}\Big(H_{k-\varepsilon e_\beta t}\gamma^0_{k-\varepsilon e_\beta t}\Big)\right) - i\varepsilon\,\mathrm{Tr}\Big(\partial_\alpha H_{k-\varepsilon e_\beta t} L^+_{k-\varepsilon e_\beta t}\partial_\beta\gamma^0_{k-\varepsilon e_\beta t}\Big)&\\ + i\varepsilon\,\mathrm{Tr}\Big(\partial_\alpha H_{k-\varepsilon e_\beta t}\widetilde{\mathcal{U}}^\varepsilon_{\beta,k}(t)\left(L^+_k\partial_\beta\gamma^0_k\right)\widetilde{\mathcal{U}}^\varepsilon_{\beta,k}(t)^*\Big) + O\left(\varepsilon^2 t\delta^{-6}\right).&\end{aligned}$$

We treat each term separately.

- For the first (adiabatic) term, we have

$$\begin{aligned}-\partial_\alpha\,\mathrm{Tr}\Big(H_{k-\varepsilon e_\beta t}\gamma^0_{k-\varepsilon e_\beta t}\Big) = -\partial_\alpha\,\mathrm{Tr}\big(H_k\gamma^0_k\big) + \varepsilon t\partial_\alpha\partial_\beta\,\mathrm{Tr}\big(H_k\gamma^0_k\big)&\\ + O\left(\varepsilon^2 t^2\delta^{-4}\right).&\end{aligned}$$

  By time-reversal symmetry, the first term vanishes when integrated on $\mathcal{B}^\delta_{\mathrm{out}}$. Using Stokes formula for the second term as in the metallic case, we get

$$\int_{\mathcal{B}^\delta_{\mathrm{out}}} -\partial_\alpha\left(\mathrm{Tr}\Big(H_{k-\varepsilon e_\beta t}\gamma^0_{k-\varepsilon e_\beta t}\Big)\right)dk = \varepsilon t\sum_{n\le N_{\mathrm{sm}}}\int_{\partial\mathcal{B}^\delta_{\mathrm{in}}}\partial_\alpha\lambda_{n,k}(ds\cdot e_\beta) + O\left(\varepsilon^2 t^2\delta^{-4}\right) \quad (4.84)$$

- For the second (static) term we similarly expand in $\varepsilon$

$$\begin{aligned}-i\varepsilon\int_{\mathcal{B}^\delta_{\mathrm{out}}}\mathrm{Tr}\Big(\partial_\alpha H_{k-\varepsilon e_\beta t}L^+_{k-\varepsilon e_\beta t}\partial_\beta\gamma^0_{k-\varepsilon e_\beta t}\Big)dk &= -i\varepsilon\int_{\mathcal{B}^\delta_{\mathrm{out}}}\mathrm{Tr}\left(\gamma^0_k[\partial_\alpha\gamma^0_k,\partial_\beta\gamma^0_k]\right)dk + O(\varepsilon^2 t\delta^{-6})\\ &= O(\varepsilon^2 t\delta^{-6}),\end{aligned}$$

  where we used the fact that the function $k\mapsto \mathrm{Tr}\left(\gamma^0_k[\partial_\alpha\gamma^0_k,\partial_\beta\gamma^0_k]\right)$ is odd.

- For the third (oscillatory) term, we use the same arguments as in the insulating case, and obtain

$$\frac{1}{t}\int_0^t dt'\int_{\mathcal{B}^\delta_{\mathrm{out}}} i\varepsilon\,\mathrm{Tr}\Big(\partial_\alpha H_{k-\varepsilon e_\beta t'}\widetilde{\mathcal{U}}^\varepsilon_{\beta,k}(t')\left(L^+_k\partial_\beta\gamma^0_k\right)\widetilde{\mathcal{U}}^\varepsilon_{\beta,k}(t')^*\Big)dk = O\left(\varepsilon\delta^{-6}\left(\frac{1}{t}+\varepsilon\right)\right).$$

We are left with

$$\begin{aligned}\frac{1}{t}\int_0^t j^{\varepsilon,\mathrm{out}}_{\alpha,\beta}(t')\,dt' =& \frac{\varepsilon}{4\pi^2 t}\int_0^t t'dt'\sum_{n\le N_{\mathrm{sm}}}\int_{\partial\mathcal{B}^\delta_{\mathrm{in}}}\partial_\alpha\lambda_{n,k}(ds\cdot e_\beta) + O\left(\frac{\varepsilon}{\delta^6}\left(\frac{1}{t}+\varepsilon(1+t^2)\right)\right)\\ =& \frac{\varepsilon t}{2\pi^2}\sum_{n\le N_{\mathrm{sm}}}\int_{\partial\mathcal{B}^\delta_{\mathrm{in}}}\partial_\alpha\lambda_{n,k}(ds\cdot e_\beta) + O\left(\frac{\varepsilon}{\delta^6}\left(\frac{1}{t}+\varepsilon(1+t^2)\right)\right). \quad (4.85)\end{aligned}$$

### 4.8.2 Close to Dirac points: reduction to the 2-band case

We set

$$j^{\varepsilon,\mathrm{in}}_{\alpha,\beta}(t) := -\frac{1}{4\pi^2}\sum_{i\in\mathcal{I}}\int_{\mathcal{B}^\delta_{\mathrm{in}}} \mathrm{Tr}\left(\partial_\alpha H_k \widetilde{\mathcal{U}}^\varepsilon_{\beta,k}(t)\,\gamma^0_k\,\widetilde{\mathcal{U}}^\varepsilon_{\beta,k}(t)^*\right) dk. \tag{4.86}$$

Using the linear response Proposition 4.5.7, we have for almost all $k\in\mathcal{B}^\delta_{\mathrm{in}}$ and all $\varepsilon, t\geq 0$,

$$\begin{aligned}-\mathrm{Tr}\left(\partial_\alpha H_{k-\varepsilon e_\beta t}\widetilde{\mathcal{U}}^\varepsilon_{\beta,k}(t)\,\gamma^0_k\,\widetilde{\mathcal{U}}^\varepsilon_{\beta,k}(t)^*\right) =& -\partial_\alpha \mathrm{Tr}\left(H_k\gamma^0_k\right) + \varepsilon t\partial_\alpha\partial_\beta\left(\mathrm{Tr}\big(H_k\gamma^0_k\big)\right)\\ &- i\varepsilon\,\mathrm{Tr}\big(\partial_\alpha H_k(e^{-itL_k}-1)L_k^+\partial_\beta\gamma^0_k\big) + O(\varepsilon^2t^2).\end{aligned}$$

Using (4.72), the equality $\mathrm{Tr}\,(H_k\gamma^0_k) = \sum_{n=1}^{N_{\mathrm{sm}}}\lambda_{n,k}$ and Assumption 4.2.5, it is easily seen that the left-hand side, as well as the first and fourth terms of the right-hand side of that equation, are bounded uniformly in $k$ and therefore integrable on $\mathcal{B}^\delta_i$. Besides, for $k\in\mathcal{B}^\delta_{\mathrm{in}}$, the second term is bounded by a constant multiple of $(1/|k-k_i|)$ as $k\to k_i$, and is therefore integrable. It follows that the third term is also integrable on $\mathcal{B}^\delta_i$.

We treat the three leading terms of the right-hand side in sequence.

- The first term vanishes when integrated on the time-reversal symmetric set $\cup_{i\in\mathcal{I}}\mathcal{B}^\delta_i$.
- For the second, arguing as in the metallic case, we get

  $$\int_{\mathcal{B}^\delta_i}\varepsilon t\partial_{\alpha\beta}\left(\mathrm{Tr}\big(H_k\gamma^0_k\big)\right)dk = -\varepsilon t\sum_{n\leq N_{\mathrm{sm}}}\int_{\partial\mathcal{B}^\delta_i}\partial_\alpha\lambda_{n,k}(ds\cdot e_\beta),$$

  so that the corresponding term in (4.86) cancels the contribution (4.85) from $\mathcal{B}^\delta_{\mathrm{out}}$.
- For the third term, we use

  $$\begin{aligned}&\mathrm{Tr}\big(\partial_\alpha H_k(e^{-itL_k}-1)L_k^+\partial_\beta\gamma^0_k\big) = \mathrm{Tr}\big(\partial_\alpha H_k(e^{-itL_k}-1)(L_k^+)^2[\gamma^0_k,\partial_\beta H_k]\big)\\ &= \sum_{n\leq N_{\mathrm{sm}}}\sum_{m>N_{\mathrm{sm}}}(e^{-it(\lambda_{n,k}-\lambda_{m,k})}-1)\frac{\langle u_{n,k},\partial_\beta H_k u_{m,k}\rangle\langle u_{m,k},\partial_\alpha H_k u_{n,k}\rangle}{(\lambda_{m,k}-\lambda_{n,k})^2} - \text{c.c.}\end{aligned}$$

  with the sum converging from the asymptotics (4.90).

  When $n\neq N_{\mathrm{sm}}$ or $m\neq N_{\mathrm{sm}}+1$, the denominators in that equation are bounded from below independently of $\delta$. The constant term vanishes when integrated over the time-reversal symmetric set $\cup_{i\in\mathcal{I}}\mathcal{B}^\delta_i$, and the oscillatory term can be treated using the formula

  $$\frac{1}{t}\int_0^t e^{-i\omega t'}dt' = \frac{e^{-i\omega t}-1}{-i\omega t}$$

  with $\omega = \lambda_{n,k}-\lambda_{m,k}$ bounded away from zero independently of $\delta$.

Putting all the results of the previous two sections together, we get that

$$\begin{aligned}\frac{1}{t}\int_0^t j^\varepsilon_{\alpha,\beta}(t')dt' &= \frac{1}{t}\int_0^t j^{\varepsilon,\mathrm{out}}_{\alpha,\beta}(t')dt' + \frac{1}{t}\int_0^t j^{\varepsilon,\mathrm{in}}_{\alpha,\beta}(t')dt'\\ &= -\frac{i\varepsilon}{4\pi^2 t}\sum_{i\in\mathcal{I}}\int_0^t dt'\int_{\mathcal{B}^\delta_i}(e^{-it'(\lambda_{N_{\mathrm{sm}},k}-\lambda_{N_{\mathrm{sm}}+1,k})}-1)\\ &\qquad\times\frac{\langle u_{N_{\mathrm{sm}},k},\partial_\beta H_k u_{N_{\mathrm{sm}}+1,k}\rangle\langle u_{N_{\mathrm{sm}}+1,k},\partial_\alpha H_k u_{N_{\mathrm{sm}},k}\rangle}{(\lambda_{N_{\mathrm{sm}}+1,k}-\lambda_{N_{\mathrm{sm}},k})^2}dk - \text{c.c.}\\ &\quad + O\left(\varepsilon^2\delta^{-6}(1+t^2)+\varepsilon\delta^{-6}t^{-1}+\varepsilon^2t^3(1+t^3)\right).\end{aligned}$$

At this stage of the proof, only two modes are involved in the formula giving the current, namely the two modes that cross at the Fermi level. Everything happens as for a two-band model that we now study. We write for short

$$\frac{1}{t}\int_0^t \frac{j^\varepsilon_{\alpha,\beta}(t')}{\varepsilon}\,dt' = -\frac{i}{4\pi^2 t}\sum_{i\in\mathcal{I}}\int_0^t I^{R,i}_{\alpha,\beta}(t')\,dt' + O\left(\varepsilon\delta^{-6}(1+t^2)+\delta^{-6}t^{-1}+\varepsilon t^3(1+t^3)\right),$$

with

$$I^{R,i}_{\alpha,\beta}(t) = \int_{\mathcal{B}_i^\delta}(e^{-it(\lambda_{N_{\rm sm},k}-\lambda_{N_{\rm sm}+1,k})}-1)\frac{\langle u_{N_{\rm sm},k},\partial_\beta H_k u_{N_{\rm sm}+1,k}\rangle\langle u_{N_{\rm sm}+1,k},\partial_\alpha H_k u_{N_{\rm sm},k}\rangle}{(\lambda_{N_{\rm sm}+1,k}-\lambda_{N_{\rm sm},k})^2}\,dk - \text{c.c.}.$$

### 4.8.3 Close to the Dirac points: the local model

We now are interested in the computation of $I^{R,i}_{\alpha,\beta}(t)$. In the following, we drop the index $i$ and assume without loss of generality that $k_i = 0$.

Hypothesis (4.32) implies that, for $k$ small enough, the Bloch Hamiltonian $H_k$ has exactly two eigenvalues (counting multiplicities) close to $\mu_{\rm F}$. Consider an arbitrary orthonormal basis $(v_0, w_0)$ of $\mathrm{Ran}(P_{N_{\rm sm}+1,0} - P_{N_{\rm sm}-1,0})$. For all $k$ small enough, we can construct an orthonormal basis $(v_k, w_k)$ of $\mathrm{Ran}(P_{N_{\rm sm}+1,k} - P_{N_{\rm sm}-1,k})$ by Löwdin orthonormalization of $((P_{N_{\rm sm}+1,k} - P_{N_{\rm sm}-1,k})v_0, (P_{N_{\rm sm}+1,k} - P_{N_{\rm sm}-1,k})w_0)$, and set

$$H_k^R = [v_k|w_k]^* H_k [v_k|w_k] = \begin{pmatrix} \langle v_k, H_k v_k\rangle & \langle v_k, H_k w_k\rangle \\ \langle w_k, H_k v_k\rangle & \langle w_k, H_k w_k\rangle \end{pmatrix}.$$

It follows that the reduced Hamiltonian

$$H_k\Big|_{\mathrm{Ran}(P_{N_{\rm sm}+1,k}-P_{N_{\rm sm}-1,k})}$$

is equivalent through a unitary transform that depends analytically on $k$ to the reduced $2\times 2$ Hamiltonian

$$H_k^R = \sum_{p=0}^{3} b^p(k)\sigma_p, \tag{4.87}$$

where

$$\sigma_0 = \mathrm{Id}_{\mathbb{C}^2},\quad \sigma_1 = \begin{pmatrix} 0 & 1 \\ 1 & 0 \end{pmatrix},\quad \sigma_2 = \begin{pmatrix} 0 & -i \\ i & 0 \end{pmatrix},\quad \sigma_3 = \begin{pmatrix} 1 & 0 \\ 0 & -1 \end{pmatrix}$$

are the Pauli matrices, and $(b^p)_{p=0,1,2,3}$ are real-valued analytic functions of $k$ in a neighborhood of 0.

The matrix $H_k^R$ has eigenvalues

$$\lambda_\pm(k) = b^0(k) \pm \sqrt{\sum_{i=1}^{3} b^p(k)^2}.$$

It follows that

$$b^0(k) = \mu_F + O(|k|^2),\quad b^p(k) = v_F\langle q^p, k\rangle + O(|k|^2),\quad p = 1,2,3,$$

where the $(q^p)_{p=1,2,3}$ are the lines of a $3\times 2$ matrix $Q$ with orthogonal columns, so that

$$H_k^R = \mu_F + v_F(Qk)\cdot\sigma + O(|k|^2). \tag{4.88}$$

Let $R \in \mathrm{SO}(3)$ be a rotation matrix that maps $\mathrm{Ran}(Q)$ to $\mathrm{Span}(e_1^0, e_2^0)$, where $(e_1^0, e_2^0, e_3^0)$ is the canonical basis of $\mathbb{R}^3$. Let $U$ be one of its associated $2 \times 2$ unitary matrices through the two-to-one $\mathrm{SU}(2) \to \mathrm{SO}(3)$ mapping, so that [20]

$$R_{pq} = \frac{1}{2} \mathrm{Tr}(\sigma_p U \sigma_q U^*).$$

It follows that

$$\begin{aligned} \mathrm{Tr}\big(\sigma_3 U H_k^R U^*\big) &= v_F \sum_{q=1}^{3} (Qk)_q \,\mathrm{Tr}(\sigma_3 U \sigma_q U^*) + O(|k|^2) \\ &= 2 v_F \sum_{q=1}^{3} \langle e_3^0, RQk\rangle + O(|k|^2) \\ &= O(|k|^2). \end{aligned}$$

Up to a unitary transform, we can therefore assume $Q$ to be a $2 \times 2$ matrix in (4.88).

### 4.8.4 The two-band case: reduction to the Dirac Hamiltonian

**Reduction to $H_k^R$** For $k \neq 0$, let $\lambda_{\pm,k}^R$ be the larger and smaller eigenvalues of $H_k^R$ respectively, and $u_{\pm,k}^R$ associated orthonormal eigenvectors in $\mathbb{C}^2$. We have $\lambda_{-,k}^R = \lambda_{N_{\mathrm{sm}},k}, \lambda_{+,k}^R = \lambda_{N_{\mathrm{sm}}+1,k}$, and

$$[v_k|w_k] u_{+,k}^R = e^{i\theta_+(k)} u_{N_{\mathrm{sm}}+1,k}, \qquad [v_k|w_k] u_{-,k}^R = e^{i\theta_-(k)} u_{N_{\mathrm{sm}},k}$$

for some phases $\theta_\pm(k) \in \mathbb{R}$. We have

$$\begin{aligned} \partial_\alpha H_k^R &= [v_k|w_k]^* \partial_\alpha H_k [v_k|w_k] + \partial_\alpha [v_k|w_k]^* [v_k|w_k] H_k^R + H_k^R [v_k|w_k]^* \partial_\alpha [v_k|w_k] \\ &= [v_k|w_k]^* \partial_\alpha H_k [v_k|w_k] + O(|k|) \end{aligned}$$

where we have used for the first line that $H_k$ commutes with $P_{N_{\mathrm{sm}}+1,k} - P_{N_{\mathrm{sm}},k} = [v_k|w_k][v_k|w_k]^*$, and for the second that $H_k^R = \mu_F \mathrm{Id}_2 + O(|k|)$ and $\partial_\alpha \Big( [v_k|w_k]^* [v_k|w_k] \Big) = \partial_\alpha \mathrm{Id}_2 = 0$. We therefore obtain

$$\begin{aligned} \langle u_{+,k}^R, \partial_\alpha H_k^R u_{-,k}^R \rangle &= e^{-i(\theta_+(k) - \theta_-(k))} \langle u_{N_{\mathrm{sm}}+1,k}, \partial_\alpha H_k u_{N_{\mathrm{sm}},k} \rangle + O(|k|) \\ \langle u_{-,k}^R, \partial_\beta H_k^R u_{+,k}^R \rangle &= e^{+i(\theta_+(k) - \theta_-(k))} \langle u_{N_{\mathrm{sm}},k}, \partial_\beta H_k u_{N_{\mathrm{sm}}+1,k} \rangle + O(|k|). \end{aligned}$$

Since $(\lambda_{-,k}^R - \lambda_{+,k}^R)$ is bounded from below by a constant multiple of $|k|$, it follows that

$$I_{\alpha,\beta}^R(\delta, t) = \int_{B(0,\delta)} (e^{-it(\lambda_{-,k}^R - \lambda_{+,k}^R)} - 1) \frac{\langle u_{-,k}^R, \partial_\beta H_k^R u_{+,k}^R \rangle \langle u_{+,k}^R, \partial_\alpha H_k^R u_{-,k}^R \rangle}{(\lambda_{+,k}^R - \lambda_{-,k}^R)^2} dk - \text{c.c.} + O(\delta). \quad (4.89)$$

**Reduction to $H_k^D$** By standard results of perturbation theory [51] applied to $H_k^R = \mu_F + v_F (Qk) \cdot \sigma + O(|k|^2)$ with gap greater than a constant multiple of $|k|$,

$$\lambda_{\pm,k}^R = \lambda_{\pm,k}^Q + O(|k|^2) \;\text{ and }\; u_{\pm,k}^R = u_{\pm,k}^Q + O(|k|)$$

where the superscript $Q$ refers to eigenvalues and appropriately chosen orthonormal eigenvectors of the Hamiltonian

$$H_k^Q = v_F (Qk) \cdot \sigma.$$

It follows that

$$I^R_{\alpha,\beta}(\delta,t) = I^Q_{\alpha,\beta}(\delta,t) + O(\delta),$$

where $I^R_{\alpha,\beta}(\delta,t)$ is defined similarly to (4.89) as

$$I^Q_{\alpha,\beta}(\delta,t) = \int_{B(0,\delta)} (e^{-it(\lambda^Q_{-,k}-\lambda^Q_{+,k})} - 1) \frac{\langle u^Q_{-,k}, \partial_\beta H^Q_k u^Q_{+,k}\rangle \langle u^Q_{+,k}, \partial_\alpha H^Q_k u^Q_{-,k}\rangle}{(\lambda^Q_{+,k}-\lambda^Q_{-,k})^2} dk - \text{c.c.}.$$

We perform the change of variable $k' = Qk$ (recall that $Q$ is orthogonal) and obtain

$$I^Q_{\alpha,\beta}(\delta,t) = e_\beta^T\, I^D(\delta,t) e_\alpha,$$

where the coefficients $I^D_{ij}(\delta,t)$ of the $2\times 2$ matrix $I^D(\delta,t)$ are given by

$$I^D_{ij}(\delta,t) = \int_{B(0,\delta)} (e^{-it(\lambda^D_{-,k}-\lambda^D_{+,k})} - 1) \frac{\langle u^D_{-,k}, \partial_{k_j} H^D_k u^D_{+,k}\rangle \langle u^D_{+,k}, \partial_{k_i} H^D_k u^D_{-,k}\rangle}{(\lambda^D_{+,k}-\lambda^D_{-,k})^2} dk - \text{c.c.}$$

and the superscript $D$ refers to the Dirac Hamiltonian

$$H^D_k = v_F k\cdot\sigma.$$

**The Dirac Hamiltonian $H^D_k$** We finish by computing $I^D(\delta,t)$ explicitly. Let $k = r(\cos\theta,\sin\theta)$. We have

$$\lambda^D_{\pm,k} = \pm v_F r,\quad u^D_{+,k} = \frac{1}{\sqrt{2}}\begin{pmatrix}1\\ e^{i\theta}\end{pmatrix} \text{ and } u^D_{-,k} = \frac{1}{\sqrt{2}}\begin{pmatrix}-e^{-i\theta}\\ 1\end{pmatrix}.$$

By an explicit calculation, we obtain

$$\int_0^{2\pi} (e^{-it(\lambda^D_{-,k}-\lambda^D_{+,k})} - 1) \frac{\langle u^D_{-,k}, \partial_{k_i} H^D_k u^D_{+,k}\rangle \langle u^D_{+,k}, \partial_{k_j} H^D_k u^D_{-,k}\rangle}{(\lambda^D_{+,k}-\lambda^D_{-,k})^2}\, d\theta - \text{c.c.} = i\pi \frac{1}{2r^2}\sin(2v_F r t)\delta_{ij}.$$

It follows that

$$\begin{aligned}\frac{1}{t}\int_0^t I^D_{ij}(\delta,t')\,dt' &= \frac{i\pi}{2}\delta_{ij}\frac{1}{t}\int_0^t\int_0^\delta \frac{\sin(2v_F r t')}{r}\,dr\,dt' = \frac{i\pi}{4t}\delta_{ij}\int_0^\delta \frac{1-\cos(2v_F r t)}{v_F r^2}\,dr\\ &= \frac{i\pi}{4}\delta_{ij}\int_0^{\delta v_F t}\frac{1-\cos(2r')}{(r')^2}\,dr' = \frac{i\pi^2}{4}\delta_{ij} + O\left((\delta t)^{-1}\right).\end{aligned}$$

We finally get by summing all the estimates

$$\frac{1}{t}\int_0^t \frac{j^\varepsilon_{\alpha,\beta}(t')}{\varepsilon}\,dt' = \frac{|\mathcal{I}|}{16} e_\alpha\cdot e_\beta + O\left(\delta + \varepsilon t^3(1+t^3) + \frac{1}{\delta^6}\left(\frac{1}{t} + \varepsilon(1+t)^2\right)\right),$$

hence the result.

## 4.9 Proofs of classical results

### 4.9.1 Proof of self-adjointness of $H$

Recall that we consider the Hamiltonian $H = \frac{1}{2}(-i\nabla + \mathcal{A})^2 + V$, for $\mathcal{A}\in L^4_{\text{per}}(\mathbb{R}^d,\mathbb{C})$, $V\in L^2_{\text{per}}(\mathbb{R}^d,\mathbb{C})$. $\Omega$ denotes the unit cell of the $\mathcal{R}-$periodic functions $V,\mathcal{A}$, and let $\widetilde{\Omega}$ denote a

domain with Lipschitz boundary and compact closure which contains $\Omega$ strictly (for instance, if $\Omega = [-1,1)^d, \widetilde{\Omega} = [-2,2)^d$).

Let $\chi$ be a smooth partition function, which is 1 on $\Omega$, 0 outside $\widetilde{\Omega}$, and transitions smoothly in $\widetilde{\Omega} \cap \Omega^c$, so that for all $x \in \mathbb{R}^d$, $0 \leq \chi(x) \leq 1$.

For any $R \in \mathcal{R}$, and $x \in R^d$, let $\chi_R(x) = \chi(x - R)$ and $\Omega_R = \Omega + R$, $\widetilde{\Omega}_R = \widetilde{\Omega} + R$.

First, note that $H$ acts on $f \in H^2(\mathbb{R}^d, \mathbb{C})$ as

$$Hf = -\frac{1}{2}\Delta f + \mathcal{A} \cdot (-i\nabla f) + \frac{1}{2}\mathcal{A}^2 f + Vf.$$

We first bound $\|Vf\|_{L^2(\mathbb{R}^d,\mathbb{C})}$ by considering separately each unit cell, and then summing over the lattice. By Hölder's inequality, which is licit since $f$ is in $H^2(\mathbb{R}^d, \mathbb{C}) \subset \mathcal{C}^0(\mathbb{R}^d, \mathbb{C})$, and $\chi_R$ has compact support, hence $f\chi_R$ is $L^\infty(\mathbb{R}^d, \mathbb{C})$, we obtain

$$\|Vf\|_{L^2(\Omega_R,\mathbb{C})} \leq \|(V\chi_R)(f\chi_R)\|_{L^2(\mathbb{R}^d,\mathbb{C})} \leq \|V\chi_R V\|_{L^2(\mathbb{R}^d,\mathbb{C})} \|f\chi_R\|_{L^\infty(\mathbb{R}^d,\mathbb{C})},$$

And by Fourier transform, and Cauchy-Schwarz, for $\frac{d}{2} < \beta < 2$, we have

$$\begin{aligned}
\|f\chi_R\|_{L^\infty(\mathbb{R}^d,\mathbb{C})} &\leq (2\pi)^{-d/2} \int_{\mathbb{R}^d} |\widehat{(f\chi_R)}(\xi)| d\xi \\
&\leq (2\pi)^{-d/2} \left( \int_{\mathbb{R}^d} (1 + |\xi|^2)^\beta |\widehat{(f\chi_R)}(\xi)| d\xi \right)^{\frac{1}{2}} \left( \int_{\mathbb{R}^d} \frac{1}{(1+|\xi|^2)^\beta} d\xi \right)^{\frac{1}{2}}
\end{aligned}$$

Moreover, for any $\varepsilon > 0$, there exists $C_\varepsilon$ such that

$$(1 + |\xi|^2)^\beta \leq \varepsilon (1 + |\xi|^2)^2 + C_\varepsilon.$$

Hence, for any $\varepsilon$, there exists another constant $C_\varepsilon$ (denoted the same for convenience), such that

$$\|f\chi_R\|_{L^\infty(\mathbb{R}^d,\mathbb{C})} \leq \varepsilon \|\Delta(\chi_R f)\|_{L^2(\mathbb{R}^d,\mathbb{C})} + C_\varepsilon \|\chi_R f\|_{L^2(\mathbb{R}^d,\mathbb{C})}.$$

It follows from $\Delta(\chi_R f) = \chi_R \Delta f + 2\nabla f \cdot \nabla \chi_R + f \Delta \chi_R$ that

$$\begin{aligned}
\|Vf\|_{L^2(\Omega_R,\mathbb{C})} \leq \|V\chi\|_{L^2(\Omega,\mathbb{C})} \Big( &\varepsilon \|\chi\|_{L^\infty(\mathbb{R}^d,\mathbb{C})} \|\Delta f\|_{L^2(\widetilde{\Omega},\mathbb{C})} + 2\varepsilon \|\nabla\chi\|_{L^\infty(\mathbb{R}^d,\mathbb{C})} \|\nabla f\|_{L^2(\widetilde{\Omega},\mathbb{C})} \\
&+ (C_\varepsilon + \|\Delta\chi\|_{L^\infty(\mathbb{R}^d,\mathbb{C})}) \|f\|_{L^2(\widetilde{\Omega}_R,\mathbb{C})} \Big).
\end{aligned}$$

Hence, the global squared norm is controlled as follows

$$\begin{aligned}
\int_{\mathbb{R}^d} V(x)^2 |f(x)|^2 dx &\leq \sum_{R \in \mathcal{R}} \left( \varepsilon^2 \int_{\widetilde{\Omega}} |\Delta f|^2 + C\varepsilon^2 \int_{\widetilde{\Omega}} |\nabla f|^2 + C \int_{\widetilde{\Omega}} |f|^2 \right) \\
&\leq \frac{|\widetilde{\Omega}|}{|\Omega|} \left( \varepsilon^2 \int_{\mathbb{R}^d} |\Delta f|^2 + C\varepsilon^2 \int_{\mathbb{R}^d} |\nabla f|^2 + C \int_{\mathbb{R}^d} |f|^2 \right).
\end{aligned}$$

From which we obtain that

$$\|Vf\|_{L^2(\mathbb{R}^d,\mathbb{C})} \leq \varepsilon \|\Delta f\|_{L^2(\mathbb{R}^d,\mathbb{C})} + C_\varepsilon \|f\|_{L^2(\mathbb{R}^d,\mathbb{C})}.$$

The term $\frac{1}{2}\mathcal{A}^2$ is treated exactly the same, since it is also $L^2_{\text{per}}(\mathbb{R}^d, \mathbb{C})$.

Finally, it remains to control the term $\mathcal{A} \cdot \nabla f$. With the same partition argument, we start by controlling the norm on $\Omega_R$,

$$\begin{aligned}
\|\mathcal{A} \cdot (-i\nabla f)\|_{L^2(\Omega_R,\mathbb{C})} &\leq \|\chi_R \mathcal{A} \cdot (-i\nabla(\chi_R f))\|_{L^2(\mathbb{R}^d,\mathbb{C})} \\
&\leq \|\chi_R^2 \mathcal{A} \cdot (-i\nabla f)\|_{L^2(\mathbb{R}^d,\mathbb{C})} + \|(\chi_R \mathcal{A}) \cdot (-i\nabla\chi_R) f\|_{L^2(\mathbb{R}^d,\mathbb{C})}.
\end{aligned}$$

By Cauchy-Schwarz, and periodicity of $\mathcal{A}$, the second term is controlled as follows

$$\| (\chi_R \mathcal{A}) \cdot (-i\nabla \chi_R) f\|_{L^2(\mathbb{R}^d,\mathbb{C})} \leq \|\chi \mathcal{A}\|_{L^2(\mathbb{R}^d,\mathbb{C})} \|\nabla \chi\|_{L^2(\mathbb{R}^d,\mathbb{C})} \|\chi_R f\|_{L^2(\mathbb{R}^d,\mathbb{C})},$$

where $\|\chi\mathcal{A}\|_{L^2(\mathbb{R}^d,\mathbb{C})}$ is bounded since $\mathcal{A}$ is in $L^4_{\text{per}}(\mathbb{R}^d,\mathbb{C})$, and hence $\chi\mathcal{A}$ is in $L^2(\mathbb{R}^d,\mathbb{C})$, and $\chi$ is smooth with compact support, hence $\nabla\chi$ is trivially in $L^2(\mathbb{R}^d,\mathbb{C})$.

To bound the first term,

$$\begin{aligned}
\|\chi_R \mathcal{A} \cdot (-i\nabla f)\chi_R\|^2_{L^2(\widetilde{\Omega}_R,\mathbb{C})} &= \int_{\widetilde{\Omega}_R} (\chi_R \mathcal{A} \cdot (-i\nabla f)\chi_R)^2 \\
&\leq \int_{\mathbb{R}^d} |\chi_R \mathcal{A}|^2 |\nabla f \chi_R|^2 \\
&\leq \sqrt{\int_{\mathbb{R}^d} |\chi_R \mathcal{A}|^4} \sqrt{\int_{\mathbb{R}^d} |\chi_R \nabla f|^4}
\end{aligned}$$

By the continuous Sobolev embedding, for $d \leq 3$, $H^1(\mathbb{R}^d,\mathbb{C}) \hookrightarrow L^6(\mathbb{R}^d,\mathbb{C})$, and in particular, $\nabla f$ is in $L^4(\mathbb{R}^d,\mathbb{C})$. Moreover, with the Hausdorff-Young inequality,

$$\begin{aligned}
\|\nabla f \chi_R\|_{L^4(\mathbb{R}^d,\mathbb{C})} &\leq C_1 \|\widehat{(\nabla f \chi_R)}\|_{L^{\frac{4}{3}}(\mathbb{R}^d,\mathbb{C})} \\
&\leq C_2 \|\widehat{(\nabla f \chi_R)}\|_{L^2(\mathbb{R}^d,\mathbb{C})} \\
&\leq C_2 \| (\nabla f \chi_R) \|_{L^2(\mathbb{R}^d,\mathbb{C})} \\
&\leq C_2 \|\nabla f\|_{L^2(\widetilde{\Omega}_R,\mathbb{C})}.
\end{aligned}$$

Hence, by summing over all $R \in \mathcal{R}$, we obtain

$$\begin{aligned}
\|\mathcal{A} \cdot (-i\nabla f)\|_{L^2(\mathbb{R}^d,\mathbb{C})} \leq \frac{|\widetilde{\Omega}_R|}{|\Omega_R|} \big( &\|\chi\mathcal{A}\|_{L^2(\mathbb{R}^d,\mathbb{C})} \|\nabla\chi\|_{L^2(\mathbb{R}^d,\mathbb{C})} \|f\|_{L^2(\mathbb{R}^d,\mathbb{C})} \\
&+ C_2 \, \|\chi\mathcal{A}\|_{L^4(\mathbb{R}^d,\mathbb{C})} \|\nabla f\|_{L^2(\mathbb{R}^d,\mathbb{C})} \big).
\end{aligned}$$

Using the Parseval's formula, and $\forall \varepsilon > 0, \xi, \;\; |\xi|^2 \leq \varepsilon^2 |\xi|^4 + \frac{1}{4\varepsilon^2}$, we have that

$$\begin{aligned}
\|\nabla f\|^2_{L^2(\mathbb{R}^d,\mathbb{C})} &= \int_{\mathbb{R}^d} |\xi|^2 |\widehat{f}(\xi)|^2 \, d\xi \\
&\leq \varepsilon^2 \int_{\mathbb{R}^d} |\xi|^4 |\widehat{f}(\xi)|^2 \, d\xi + \frac{1}{4\varepsilon^2} \int_{\mathbb{R}^d} |\widehat{f}(\xi)|^2 \, d\xi.
\end{aligned}$$

Hence,

$$\|\nabla f\|_{L^2(\mathbb{R}^d,\mathbb{C})} \leq \varepsilon \|\Delta f\|_{L^2(\mathbb{R}^d,\mathbb{C})} + \frac{1}{2\varepsilon} \|f\|_{L^2(\mathbb{R}^d,\mathbb{C})}.$$

It follows that for any $\varepsilon > 0$, there exists $C_\varepsilon > 0$ such that

$$\|\mathcal{A} \cdot (-i\nabla f)\|_{L^2(\mathbb{R}^d,\mathbb{C})} \leq \varepsilon \|\Delta f\|_{L^2(\mathbb{R}^d,\mathbb{C})} + C_\varepsilon \|f\|_{L^2(\mathbb{R}^d,\mathbb{C})},$$

which concludes the proof.

### 4.9.2 Asymptotic behavior of eigenvalues of the Hamiltonian

To bound the $\lambda_{n,k}$, we can see $H_k$ as a perturbation of the Laplacian with periodic boundary conditions by a $-\Delta$-bounded operator, that is, for $u \in H^2_{\text{per}}$,

$$\|(-\Delta - H_k)u\|_{L^2_{\text{per}}} \leq a\| - \Delta u\|_{L^2_{\text{per}}} + b\|u\|_{L^2_{\text{per}}},$$

we obtain on the quadratic forms

$$\int_\Omega u(-\Delta - H_k)u \leq a\int_\Omega |\nabla u|^2 + b\int_\Omega |u|^2,$$

hence, by the min-max characterization of eigenvalues, we obtain

$$|\lambda_{n,k} - \omega_n| \leq a\omega_n + b,$$

where $\omega_n$ is the $n$-th eigenvalue of $-\Delta$ on $L^2_{\rm per}$. To determine the asymptotic behavior of the $\omega_n$, a counting argument suffices. On a cubic periodic domain $[0,a]^d$, the eigenvectors are products of plane-waves with frequencies that are integer multiples of the fundamental $f_0 = \frac{1}{a}$. For $m_1, \dots, m_d \in \mathbb{N}$, the eigenvector $x \mapsto \exp\left(i2\pi \sum_{i=1}^d m_i f_0 x_i\right)$ has Laplacian $(2\pi f_0)^2 \sum_{i=1}^d m_i^2$. Counting the number of eigenvectors with kinetic energy below $R^2$ therefore amounts to counting the number of points of a cubic lattice with lattice parameter $f_0$ inside the sphere of radius $R$. The asymptotics for large $R$ are

$$\mathrm{Rank}\left(\mathbb{1}(-\Delta \leq R^2)\right) \sim C_0 R^d,$$

where $C_0$ depends on $f_0$ only. Hence $\omega_n \sim C_1 n^{d/2}$, and there exists $\underline{C_1}, \overline{C_1} \in \mathbb{R}$, and $\underline{C_2}, \overline{C_2} > 0$ such that

$$\underline{C_1} + \underline{C_2} n^{2/d} \leq \lambda_{n,k} \leq \overline{C_1} + \overline{C_2} n^{2/d}. \tag{4.90}$$

This argument can be generalized to any domain, by decomposing it into small cubes. See e.g. [86] for more precise estimates.

## 4.10 Proofs of two technical lemmata

### 4.10.1 Proof of Lemma 4.4.1

*Proof.* We replicate the proof of the Faris-Lavine Theorem given in [85], replacing the Laplacian by $\frac{1}{2}(-i\nabla + \mathcal{A})^2$. It consists in verifying the following two hypotheses of [85, Theorem X.37]. Let $A = \frac{1}{2}(-i\nabla + \mathcal{A})^2 + W + V$ and $N = A + 2c|x|^2 + b$, where $b \in \mathbb{R}$ will be specified below:

$$\textit{there exists } h, \textit{ such that for any } \phi \in \mathcal{C}, \quad \|A\phi\| \leq h\|N\phi\|; \tag{4.91}$$

$$\textit{for some } \ell, \textit{ for any } \phi \in \mathcal{C}, \quad |(A\phi, N\phi) - (N\phi, A\phi)| \leq \ell \|N^{\frac{1}{2}}\phi\|^2. \tag{4.92}$$

By hypothesis *3* in Lemma 4.4.1 and the conditions on $W$, it is possible to choose $b$ so that $N \geq 1$. As quadratic forms on $\mathcal{C}$,

$$\begin{aligned} N^2 &= (A+b)^2 + 2c|x|^2(A+b) + 2c(A+b)|x|^2 + 4c^2x^4 \\ &= (A+b)^2 + 4c\sum_{j=1}^d x_j(A+b+c|x|^2)x_j + 2c\sum_{j=1}^d [x_j,[x_j,A]] \\ N^2 &= (A+b)^2 + 4c\sum_{j=1}^d x_j(A+b+c|x|^2)x_j - 2cd, \end{aligned}$$

where we have used $\nabla \cdot \mathcal{A} = 0$, and $[x_j,[x_j,(-i\nabla+\mathcal{A})^2]] = [x_j,[x_j,-\Delta]] = 2$. Hypotheses *1* and *3* guarantee that $A + b + c|x|^2$ is bounded below. Hence, increasing the value of $b$ if necessary to make this operator positive, we have

$$\|(A+b)\phi\|^2_{L^2} \leq \|N\phi\|^2_{L^2} + 4cd\|\phi\|^2_{L^2},$$

which proves (4.91).

For (4.92), we observe that

$$\pm i[A,N] = \pm 2c(x\cdot(-i\nabla+\mathcal{A}) + (-i\nabla+\mathcal{A})\cdot x) \leq 2c\left((-i\nabla+\mathcal{A})^2 + |x|^2\right) \leq \ell N,$$

where we have used

$$(-i\nabla+\mathcal{A})^2 + |x|^2 \pm (x\cdot(-i\nabla+\mathcal{A}) + (-i\nabla+\mathcal{A})\cdot x) = (-i\nabla+\mathcal{A}\pm x)^2 \geq 0$$

and

$$N = \left(\frac{a}{2}(-i\nabla+\mathcal{A})^2 + V\right) + (W + c|x|^2) + \frac{1-a}{2}(-i\nabla+\mathcal{A})^2 + c|x|^2 + b \geq \ell^{-1}((-i\nabla+\mathcal{A})^2 + |x|^2),$$

where $\ell^{-1} = \min(c, \frac{1-a}{2}) > 0$ and where $b$ is chosen so that

$$b - f + \min\,\sigma\left(\frac{a}{2}(-i\nabla+\mathcal{A})^2 + V\right) \geq 0.$$

This proves (4.92). Hence $A$ is essentially self-adjoint on $\mathcal{C}$. □

### 4.10.2 Proof of Lemma 4.4.2

*Proof.* By the Kato-Rellich theorem, for any $0 \leq t \leq T$, $H(t)$ is self-adjoint on $L^2_{\text{per}}$ with domain $H^2_{\text{per}}$, and bounded below. We will show that there exists $\mu > 0$ so that the graph norm of $(H(t)+\mu)$ for any $0 \leq t \leq T$ is equivalent to the $H^2_{\text{per}}$-norm. This will prove Lemma 4.4.2 by Proposition 2.1 in [95] (see also Theorem X.70 in [85]).

We have for any $\mu > 0$, $0 \leq t \leq T$ and $\phi \in H^2_{\text{per}}$,

$$\|(H(t)+\mu)\phi\|_{L^2_{\text{per}}} \leq (1+a)\|H_0\phi\|_{L^2_{\text{per}}} + (b+\mu)\|\phi\|_{L^2_{\text{per}}} \leq (1+a+b+\mu)\|\phi\|_{H^2_{\text{per}}},$$

and so the graph norm is controlled by the $H^2_{\text{per}}$-norm.

For the other inequality, we relate the resolvent of $H(t)$ to that of $H_0$ by a bounded operator, with bounded inverse. Notice that, for any $\mu > 0$, since $H_0$ is positive,

$$\forall\ 0 \leq t \leq T, \quad (H(t)+\mu) = (1 + H_1(t)(H_0+\mu)^{-1})(H_0+\mu).$$

Furthermore,

$$\forall\ 0 \leq t \leq T, \quad \|H_1(t)(H_0+\mu)^{-1}\| \leq a\|H_0(H_0+\mu)^{-1}\| + b\|(H_0+\mu)^{-1}\| \leq a + \frac{b}{\mu}.$$

and so, for $\mu > \frac{b}{1-a}$, the operator $1 + H_1(t)(H_0+\mu)^{-1}$ is bounded and invertible with bounded inverse in $L^2_{\text{per}}$. Therefore $(H(t)+\mu)^{-1}$ is bounded from $L^2_{\text{per}}$ to $H^2_{\text{per}}$, which means there exists $C > 0$ such that, for any $\phi \in H^2_{\text{per}}$ and $0 \leq t \leq T$,

$$\|\phi\|_{H^2_{\text{per}}} = \|(H(t)+\mu)^{-1}(H(t)+\mu)\phi\|_{H^2_{\text{per}}} \leq C\|(H(t)+\mu)\phi\|_{L^2_{\text{per}}},$$

which concludes the proof. □

# Bibliography


[1] A diagram of the first brillouin zone of a face-centred cubic (fcc) lattice, with points of high symmetry marked. https://commons.wikimedia.org/wiki/File:Brillouin_Zone_(1st,_FCC).svg.

[2] Graphene. https://commons.wikimedia.org/wiki/File:Graphen.jpg.

[3] Microscopic structure of a halite (mineral) crystal. (purple is sodium ion, green is chlorine ion). there is cubic symmetry in the atoms' arrangement. https://commons.wikimedia.org/w/index.php?curid=702423.

[4] Schematics of calculated band structure of crystalline si. https://commons.wikimedia.org/wiki/File:Band_structure_Si_schematic.svg.

[5] S. Bachmann, W. De Roeck, and M. Fraas. The adiabatic theorem and linear response theory for extended quantum systems. *Communications in Mathematical Physics*, 361(3):997–1027, 2018.

[6] A. Bakhta, E. Cancès, P. Cazeaux, S. Fang, and E. Kaxiras. Compression of wannier functions into gaussian-type orbitals, 2017.

[7] J. Bellissard, A. van Elst, and H. Schulz-Baldes. The noncommutative geometry of the quantum Hall effect. *Journal of Mathematical Physics*, 35(10):5373–5451, 1994.

[8] J. Bezanson, A. Edelman, S. Karpinski, and V. B. Shah. Julia: A fresh approach to numerical computing. *SIAM review*, 59(1):65–98, 2017.

[9] J.-M. Bouclet, F. Germinet, A. Klein, and J. H. Schenker. Linear response theory for magnetic Schrödinger operators in disordered media. *Journal of Functional Analysis*, 226(2):301–372, 2005.

[10] C. Brouder, G. Panati, M. Calandra, C. Mourougane, and N. Marzari. Exponential Localization of Wannier Functions in Insulators. *Phys. Rev. Lett.*, 98(4), 2007.

[11] C. Brouder, G. Panati, M. Calandra, C. Mourougane, and N. Marzari. Exponential Localization of Wannier Functions in Insulators. *Phys. Rev. Lett.*, 98(4), 2007.

[12] E. Cancès, V. Ehrlacher, D. Gontier, A. Levitt, and D. Lombardi. Numerical quadrature in the Brillouin zone for periodic Schrödinger operators. *Numerische Mathematik*, in press.

[13] É. Cancès, A. Levitt, G. Panati, and G. Stoltz. Robust determination of maximally localized Wannier functions. *Phys. Rev. B*, 95(7):075114, 2017.

[14] Yuan Cao, Valla Fatemi, Shiang Fang, Kenji Watanabe, Takashi Taniguchi, Efthimios Kaxiras, and Pablo Jarillo-Herrero. Unconventional superconductivity in magic-angle graphene superlattices. *Nature*, 556(7699):43–50, 2018.

[15] S. Carr, D. Massatt, S. Fang, P. Cazeaux, M. Luskin, and E. Kaxiras. Twistronics: Manipulating the electronic properties of two-dimensional layered structures through their twist angle. *Phys. Rev. B*, 95:075420, Feb 2017.

[16] Y. Colin de Verdière. Sur les singularités de van Hove génériques. *Colloque en mémoire de Edmond Combet (Lyon, octobre 1989), Mémoire de la SMF 46*, pages 99–109, 1991.

[17] H. Cornean, D. Gontier, A. Levitt, and D. Monaco. Localised Wannier functions in metallic systems. *arXiv e-prints*, page arXiv:1712.07954, December 2017.

[18] H.D. Cornean, I. Herbst, and Gh. Nenciu. On the construction of composite Wannier functions. In *Ann. Henri Poincaré*, volume 17, pages 3361–3398. Springer, 2016.

[19] H.D. Cornean and D. Monaco. On the construction of Wannier functions in topological insulators: the 3D case. *Ann. Henri Poincaré*, 18:3863–3902, 2017.

[20] J.F. Cornwell. *Group Theory in Physics.* Number vol. 2 in Group Theory in Physics. Academic Press, 1984.

[21] J.F. Cornwell. *Group Theory in Physics*, volume 1 of *Techniques of Physics.* Academic Press, San Diego, 1997.

[22] A. Damle, L. Lin, and L. Ying. Compressed representation of kohn–sham orbitals via selected columns of the density matrix. *J. Chem. Theory Comput.*, 11(4):1463–1469, 2015.

[23] A. Damle, L. Lin, and L. Ying. Scdm-k: Localized orbitals for solids via selected columns of the density matrix. *J. Comput. Phys.*, 334:1–15, 2017.

[24] S. Das Sarma, S. Adam, E. H. Hwang, and E. Rossi. Electronic transport in two-dimensional graphene. *Rev. Mod. Phys.*, 83:407–470, 2011.

[25] G. De Nittis and M. Lein. *Linear Response Theory – An Analytic-Algebraic Approach.* Springer Briefs in Mathematical Physics 21. Springer, 2017.

[26] J. des Cloizeaux. Analytical properties of n-dimensional energy bands and Wannier functions. *Phys. Rev.*, 135(3A):A698, 1964.

[27] J. des Cloizeaux. Energy bands and projection operators in a crystal: Analytic and asymptotic properties. *Phys. Rev.*, 135(3A):A685, 1964.

[28] R.A. Evarestov and V.P. Smirnov. *Site Symmetry in Crystals: Theory and Applications.* Springer Series in Solid-State Sciences. Springer Berlin Heidelberg, 1997.

[29] C. Fefferman and M. Weinstein. Honeycomb lattice potentials and Dirac points. *Journal of the American Mathematical Society*, 25(4):1169–1220, 2012.

[30] C. Fermanian Kammerer and P. Gérard. Mesures semi-classiques et croisements de mode. *Bulletin de la SMF*, 130:123–168, 2002.

[31] C. Fermanian Kammerer and C. Lasser. Single switch surface hopping for molecular dynamics with transitions. *The Journal of chemical physics*, 128:144–102, 2008.

[32] C. Fermanian Kammerer and C. Lasser. An Egorov theorem for avoided crossings of eigenvalue surfaces. *Communications in Mathematical Physics*, 353(3):1011–1057, 2017.

[33] C. Fermanian Kammerer and F. Méhats. A kinetic model for the transport of electrons in a graphene layer. *Journal of Computational Physics*, 327:450 – 483, 2016.

[34] D. Fiorenza, D. Monaco, and G. Panati. $\mathbb{Z}_2$ invariants of topological insulators as geometric obstructions. *Comm. Math. Phys.*, 343(3):1115–1157, 2016.

[35] D. Fiorenza, D. Monaco, and G. Panati. Construction of real-valued localized composite Wannier functions for insulators. In *Ann. Henri Poincaré*, volume 17, pages 63–97, 2016.

[36] D. Fiorenza, D. Monaco, and G. Panati. $\mathbb{Z}^2$ invariants of topological insulators as geometric obstructions. *Comm. Math. Phys.*, 343(3):1115–1157, 2016.

[37] L. Fu, Ch.L. Kane, and E.J. Mele. Topological insulators in three dimensions. *Phys. Rev. Lett.*, 98(10):106803, 2007.

[38] D. Gall. Electron mean free path in elemental metals. *Journal of Applied Physics*, 119(8):085101, 2016.

[39] A. Geim and I. Grigorieva. Van der waals heterostructures. *Nature*, 499:419–425, 2013.

[40] P. Giannozzi, O. Baseggio, P. Bonfà, D. Brunato, R. Car, I. Carnimeo, C. Cavazzoni, S. de Gironcoli, P. Delugas, F. Ferrari Ruffino, A. Ferretti, N. Marzari, I. Timrov, A. Urru, and S. Baroni. Quantum espresso toward the exascale. *The Journal of Chemical Physics*, 152(15):154105, 2020.

[41] P. Giannozzi, Baroni S., S. Bonini, M Calandra, R. Car, C Cavazzoni, D. Ceresoli, G.L. Chiarotti, M. Cococcioni, I. Dabo, A. Dal Corso, S. de Gironcoli, S. Fabris, G. Fratesi, R. Gebauer, U. Gerstmann, C. Gougoussis, A. Kokalj, M. Lazzeri, L. Martin-Samos, N. Marzari, F. Mauri, R. Mazzarello, S. Paolini, A. Pasquarello, L. Paulatto, C. Sbraccia, S. Scandolo, G. Sclauzero, A.P. Seitsonen, A. Smogunov, P. Umari, and R.M. Wentzcovitch. Quantum espresso: a modular and open-source software project for quantum simulations of materials. *J. Phys. Condens. Matter*, 21(39):395502, 2009.

[42] A. Giuliani, V. Mastropietro, and M. Porta. Universality of conductivity in interacting graphene. *Communications in Mathematical Physics*, 311(2):317–355, 2012.

[43] G.A. Hagedorn. Molecular propagation through electron energy level crossings. *Memoirs of the AMS*, 111(536), 1994.

[44] G.A. Hagedorn and A. Joye. Molecular propagation through small avoided crossings of electron energy levels. *Reviews in Mathematical Physics*, 11, 1997.

[45] G.A. Hagedorn and A. Joye. Landau-Zener transitions through small electronic eigenvalue gaps in the Born-Oppenheimer approximation. *Annales de l'I.H.P. Physique théorique*, 68(1):85–134, 1998.

[46] F. D. M. Haldane. Model for a quantum Hall effect without landau levels: Condensed-matter realization of the" parity anomaly". *Physical Review Letters*, 61(18):2015, 1988.

[47] B. Hall and B.C. Hall. *Lie Groups, Lie Algebras, and Representations: An Elementary Introduction*. Graduate Texts in Mathematics. Springer, 2003.

[48] B.C. Hall. *Quantum Theory for Mathematicians*. Graduate Texts in Mathematics. Springer New York, 2013.

[49] C.L. Kane and E.J. Mele. $\mathbb{Z}_2$ topological order and the quantum spin Hall effect. *Phys. Rev. Lett.*, 95:146802, 2005.

[50] T. KATO. On the perturbation theory of closed linear operators. *J. Math. Soc. Japan*, 4(3-4):323–337, 12 1952.

[51] T. Kato. *Perturbation Theory for Linear Operators*, volume 132. (Springer-Verlag Berlin Heidelberg New York, 1966.

[52] R.D. King-Smith and D. Vanderbilt. Theory of polarization of crystalline solids. *Phys. Rev. B*, 47(3):1651, 1993.

[53] K. v. Klitzing, G. Dorda, and M. Pepper. New method for high-accuracy determination of the fine-structure constant based on quantized hall resistance. *Phys. Rev. Lett.*, 45:494–497, Aug 1980.

[54] W. Kohn. Analytic properties of Bloch waves and Wannier functions. *Phys. Rev.*, 115(4):809, 1959.

[55] W. Kohn and L. J. Sham. Self-consistent equations including exchange and correlation effects. *Phys. Rev.*, 140:A1133–A1138, Nov 1965.

[56] G. Kresse and J. Furthmüller. Efficient iterative schemes for ab initio total-energy calculations using a plane-wave basis set. *Phys. Rev. B*, 54:11169–11186, Oct 1996.

[57] R. Kubo. Statistical-mechanical theory of irreversible processes. I. general theory and simple applications to magnetic and conduction problems. *Journal of the Physical Society of Japan*, 12(6):570–586, 1957.

[58] P. Kuchment. An overview of periodic elliptic operators. *Bull. Amer. Math. Soc. (N.S.)*, 53(3):343–414, 2016.

[59] R. B. Laughlin. Quantized Hall conductivity in two dimensions. *Phys. Rev. Lett.*, 23(10):5632–5633, May 1981.

[60] H. Leinfelder and C.G. Simader. Schrödinger operators with singular magnetic vector potentials. *Mathematische Zeitschrift*, 176(1):1–19, 1981.

[61] K. Leo, P.H. Bolivar, F. Brüggemann, R. Schwedler, and K. Köhler. Observation of Bloch oscillations in a semiconductor superlattice. *Solid State Communications*, 84(10):943–946, 1992.

[62] E. H. Lieb. *Density Functionals for Coulomb Systems*, pages 269–303. Springer Berlin Heidelberg, Berlin, Heidelberg, 2002.

[63] L. Lin. Private communication, 2018.

[64] W.C. Lu, C.-Zh. Wang, T.-L. Chan, K. Ruedenberg, and K.M. Ho. Representation of electronic structures in crystals in terms of highly localized quasiatomic minimal basis orbitals. *Phys. Rev. B*, 70(4):041101, 2004.

[65] G. Marcelli, G. Panati, and C. Tauber. Spin conductance and spin conductivity in topological insulators: Analysis of Kubo-like terms. *Annales Henri Poincaré*, 2019.

[66] N. Marzari, A.A. Mostofi, J.R. Yates, I. Souza, and D. Vanderbilt. Maximally localized Wannier functions: Theory and applications. *Rev. Mod. Phys.*, 84(4):1419, 2012.

[67] N. Marzari and D. Vanderbilt. Maximally localized generalized wannier functions for composite energy bands. *Phys. Rev. B*, 56:12847–12865, 1997.

[68] H.P. McKean and E. Trubowitz. Hill's operator and hyperelliptic function theory in the presence of infinitely many branch points. *Comm. Pure Appl. Math.*, 29(2):143–226, 1976.

[69] K. Momma and F. Izumi. *VESTA3* for three-dimensional visualization of crystal, volumetric and morphology data. *J. Appl. Crystallogr.*, 44(6):1272–1276, 2011.

[70] D. Monaco. Chern and fu–kane–mele invariants as topological obstructions. In *Advances in Quantum Mechanics*, pages 201–222. Springer, 2017.

[71] D. Monaco, G. Panati, A. Pisante, and S. Teufel. Optimal decay of wannier functions in chern and quantum hall insulators. *Communications in Mathematical Physics*, 359(1):61–100, 2018.

[72] D. Monaco and S. Teufel. Adiabatic currents for interacting electrons on a lattice. *Reviews in Mathematical Physics*, 2017.

[73] A.A. Mostofi, J.R. Yates, G. Pizzi, Y.-S. Lee, I. Souza, D. Vanderbilt, and N. Marzari. An updated version of wannier90: A tool for obtaining maximally-localised wannier functions. *Comput. Phys. Commun.*, 185(8):2309–2310, 2014.

[74] J.I. Mustafa, S. Coh, M.L. Cohen, and S.G. Louie. Automated construction of maximally localized wannier functions: Optimized projection functions method. *Phys. Rev. B*, 92(16):165134, 2015.

[75] J.I. Mustafa, S. Coh, M.L Cohen, and S.G. Louie. Automated construction of maximally localized Wannier functions for bands with nontrivial topology. *Physical Review B*, 94(12):125151, 2016.

[76] G. Nenciu. Existence of the exponentially localised Wannier functions. *Comm. Math. Phys.*, 91(1):81–85, 1983.

[77] G. Nenciu. Dynamics of band electrons in electric and magnetic fields: rigorous justification of the effective hamiltonians. *Rev. Mod. Phys.*, 63:91–127, Jan 1991.

[78] G. Panati. Triviality of Bloch and Bloch–Dirac bundles. 8(5):995–1011, 2007.

[79] G. Panati and A. Pisante. Bloch Bundles, Marzari-Vanderbilt Functional and Maximally Localized Wannier Functions. *Communications in Mathematical Physics*, 322:835–875, September 2013.

[80] G. Panati and A. Pisante. Bloch bundles, Marzari-Vanderbilt functional and maximally localized Wannier functions. *Comm. Math. Phys.*, 322:835–875, 2013.

[81] G. Panati, H. Spohn, and S. Teufel. Effective dynamics for Bloch electrons: Peierls substitution and beyond. *Communications in Mathematical Physics*, 242(3):547–578, 2003.

[82] G Pizzi, V. Vitale, R. Arita, S. Blügel, F. Freimuth, G. Géranton, M. Gibertini, D. Gresch, C. Johnson, T. Koretsune, J. Ibañez-Azpiroz, J.-M. Lee, H.and Lihm, D. Marchand, A. Marrazzo, Y. Mokrousov, J.I. Mustafa, Y. Nohara, Y. Nomura, L. Paulatto, S. Poncé, T. Ponweiser, J. Qiao, F. Thöle, S.S. Tsirkin, M. Wierzbowska, N. Marzari, D. Vanderbilt, I. Souza, A.A. Mostofi, and J.R. Yates. Wannier90 as a community code: new features and applications. *Journal of Physics: Condensed Matter*, 32(16):165902, jan 2020.

[83] C. Rackauckas and Q. Nie. `DifferentialEquations.jl`–a performant and feature-rich ecosystem for solving differential equations in Julia. *Journal of Open Research Software*, 5(1), 2017.

[84] M. Reed and B. Simon. *I: Functional Analysis*. Elsevier, 1972.

[85] M. Reed and B. Simon. *II. Fourier analysis, self-adjointness*. Elsevier, 1975.

[86] M. Reed and B. Simon. *IV: Analysis of Operators*. Elsevier, 1978.

[87] R. Sakuma. Symmetry-adapted wannier functions in the maximal localization procedure. *Phys. Rev. B*, 87:235109, Jun 2013.

[88] B. Simon. Holonomy, the quantum adiabatic theorem, and Berry's phase. *Physical Review Letters*, 51(24):2167, 1983.

[89] A.A. Soluyanov and D. Vanderbilt. Wannier representation of $F_2$ topological insulators. *Phys. Rev. B*, 83:035108, 2011.

[90] A.A. Soluyanov and D. Vanderbilt. Smooth gauge for topological insulators. *Phys. Rev. B*, 85:115415, 2012.

[91] I. Souza, N. Marzari, and D. Vanderbilt. Maximally localized wannier functions for entangled energy bands. *Phys. Rev. B*, 65:035109, Dec 2001.

[92] Q. Sun. Libcint: An efficient general integral library for gaussian basis functions. *Journal of Computational Chemistry*, 36:1664–1671, 2015.

[93] S. Sun, T.C. Berkelbach, N.S. Blunt, G.H. Booth, S. Guo, Z. Li, J. Liu, J.D. McClain, E.R. Sayfutyarova, S. Sharma, S Wouters, and G. Kin-Lic Chan. Pyscf: the python-based simulations of chemistry framework, 2017.

[94] M. Tahir, O. Pinaud, and H. Chen. Emergent flat band lattices in spatially periodic magnetic fields. *arXiv e-prints*, page arXiv:1808.10046, Aug 2018.

[95] S. Teufel. *Adiabatic Perturbation Theory in Quantum Dynamics*. Lecture Notes in Mathematics. Springer Berlin Heidelberg, 2003.

[96] S. Teufel. Non-equilibrium almost-stationary states and linear response for gapped quantum systems. *Communications in Mathematical Physics*, 2019.

[97] D.J. Thouless, M. Kohmoto, M. P. Nightingale, and M. den Nijs. Quantized Hall conductance in a two-dimensional periodic potential. *Physical Review Letters*, 49(6):405, 1982.

[98] G. Tritsaris, S. Shirodkar, E. Kaxiras, P. Cazeaux, M. Luskin, P. Plechac, and E. Cances. Perturbation theory for weakly coupled two-dimensional layers. *Journal of Materials Research*, 31:1–8, 03 2016.

[99] J.C. Tully. Perspective: Nonadiabatic dynamics theory. *The Journal of Chemical Physics*, 137:22A301, 2012.

[100] J.C. Tully and R.K. Preston. Trajectory surface hopping approach to nonadiabatic molecular collisions: The reaction of $H^+$ with $D_2$. *Chemical Physics*, 55:562–572, 1971.

[101] G. H. Wannier. The structure of electronic excitation levels in insulating crystals. *Phys. Rev.*, 52:191–197, Aug 1937.

[102] H. Weyl. *The Classical Groups: Their Invariants and Representations*. Princeton mathematical series. Princeton University Press, 1939.

[103] H. Weyl. *The Theory of Groups and Quantum Mechanics*. Dover Books on Mathematics. Dover Publications, 1950.

[104] C.H. Wilcox. Theory of Bloch waves. *J. Anal. Math.*, 33:146–167, 1978.

[105] G.W. Winkler, A.A. Soluyanov, and M. Troyer. Smooth gauge and wannier functions for topological band structures in arbitrary dimensions. *Phys. Rev. B*, 93:035453, 2016.

[106] X. Wu, A. Selloni, and R. Car. Order-n implementation of exact exchange in extended insulating systems. *Phys. Rev. B*, 79(8):085102, 2009.

[107] J. R. Yates, X. Wang, D. Vanderbilt, and I. Souza. Spectral and Fermi surface properties from Wannier interpolation. *Phys. Rev. B*, 75(19):195121, may 2007.

[108] J.R. Yates, X. Wang, D. Vanderbilt, and I. Souza. Spectral and Fermi surface properties from Wannier interpolation. *Phys. Rev. B*, 75(19):195121, 2007.

[109] C. Zener. A theory of the electrical breakdown of solid dielectrics. *Proceedings of the Royal Society of London. Series A*, 145(855):523–529, 1934.